

University of Alberta
Department of Civil Engineering



Structural Engineering Report No. 168

ERECTION ANALYSIS OF
CABLE-STAYED BRIDGES

by
Zabihollah Behin
and
David W. Murray

September 1990

Structural Engineering Report No. 168

**ERECTION ANALYSIS OF
CABLE-STAYED BRIDGES**

by

Zabihollah Behin

and

David W. Murray

Department of Civil Engineering

University of Alberta

Edmonton, Alberta

Canada

T6G 2G7

September 1990

ABSTRACT

Erection analysis is an essential and integral part of the design of cable-stayed bridges. The purpose of it is to generate sufficient information to make an effective monitoring of the shape and internal force distribution of each partial structure possible. This begins with specifying a desirable geometry and distribution of internal moments in the girder of the completed bridge. Then, in a 'backward' solution each unit of the bridge is disassembled, in the reverse order of the proposed erection plan, in order to obtain the geometric configuration and internal force distribution of the partial structure at each stage of erection.

The computer code, called CASBA, generates sufficient information to define the 'unstressed' (initial) shape of each bridge element. With the use of these 'unstressed' configurations and the careful monitoring of the geometry and force distribution of every partial structure, the specified reference configuration will be achieved at the completion of erection.

CASBA takes into consideration the cable nonlinearity and $P-\Delta$ effects in its erection analysis. It allows for on-site variations in the erection plan by permitting a restart from any previous stage of disassembly. The results, in terms of the geometry and internal force distribution of each of the partial structures, can be viewed on the video screen of a computer and/or be studied from the nodal displacements and member-end forces in the output file. The code has been designed to run on any standard PC-AT with 640 KB of RAM.

ACKNOWLEDGEMENT

This report is the thesis arising from the research work of Zabihollah Behin, carried out under the supervision of Dr. D. W. Murray, and submitted in partial fulfillment of the requirements for a Ph. D. degree in Civil Engineering from the University of Alberta. The thesis was defended on August 20, 1990, before an examination committee consisting of : Dr. R. A. Dorton, Dr. D. W. Murray, Dr. A. E. Elwi, Dr. T. M. Hruday and Dr. W. Lipsett.

The author acknowledges the support of the Natural Sciences and Engineering Research Council of Canada, whose financial support through operating grant OGP 0005307 made this work possible.

TABLE OF CONTENTS

Abstract	
Acknowledgement	
Table of Contents	
List of Tables	
List of Figures	
List of Symbols	
	Page
Chapter 1 : Introduction	
1.1 Cable-Stayed Bridges	1
1.2 History of Cable-Stayed Bridges	2
1.3 Methods of Erection	4
1.4 Structural Complexities of Cantilever Method	6
1.5 Research Objectives	7
1.6 Solution Considerations	8
1.7 The Reference Configuration	11
1.8 Backward and Forward Solutions for a Fixed Ended Beam ..	13
1.9 Forward Analysis vs. Backward Analysis	14
Chapter 2 : Literature Review	
2.1 Behaviour of Cables	21
2.2 Analysis and Erection of Cable-Stayed Bridges	24
2.3 State-of-the-Art	26
2.4 Relation of Current Project to State-of-the-Art	27
Chapter 3 : Cables	
3.1 Types of Cables for Cable-Stayed Bridges	31
3.2 Mechanical Properties of Cables	33
3.3 The Catenary Cable	36

3.4	Cable Stiffness Matrix	40
3.5	Cable Forces in the Reference Configuration	43
3.6	Cable Nonlinearity	47

Chapter 4 : Development of the Linear Routines

4.1	Introduction.	58
4.2	An Overview of the Solution Technique	59
4.3	Substructure Types	62
4.4	Substructural Numbering	64
4.5	Global Numbering System	69
4.6	Systems of Coordinates and Sign Conventions	72
4.7	The Reference Configuration	73
4.7.1	The 'Work Point' Line	73
4.7.2	Determination of the Reference Configuration Moments	74
4.7.3	The 'Tie-Down' Cables.	76
4.8	Assembly and Reduction	77
4.9	Load Vector Operations	81
4.10	Backsubstitution	81

Chapter 5 : Erection Analysis

5.1	Introduction	95
5.2	Strategy for Dealing with Loading Effects During Erection	96
5.2.1	Strategy for Dealing with Loading Effects During Erection Analysis	96
5.2.2	Schematic Treatment of Load Reduction and Backsubstitution	97
5.3	Erection Variations	98
5.4	Cable Adjustments	99
5.5	Girder Variations	101
5.6	Bracing	103

5.7	Changes in Girder-Tower Connection	103
5.8	Graphics Capability	104
Chapter 6 : Nonlinearities		
6.1	Introduction	112
6.2	Cable Nonlinearity	113
6.3	P- Δ Effect	116
6.4	Major Sources of Nonlinearity in Cable-Stayed Beidges	119
Chapter 7 : The Program and Its Applications		
7.1	Introduction	125
7.2	The Program Structure	125
7.3	Input/Output Arrangements	129
7.4	Data Management Schemes	130
7.5	Graphics Facilities	133
7.6	A Typical Application Example	133
7.6.1	Preparation of Input Data	134
7.6.2	Live Load Analysis	136
7.6.3	Comments on Graphical Output.	136
7.7	Application to Special Cable-Stayed Bridges	138
Chapter 8: Summary, Conclusions and Recommendations		
8.1	Summary and Conclusions	199
8.2	Recommendations	201
References		205
Appenddix A : User's Manual		
A.1	Introduction	209
A.2	MAIN.DAT	209
A.3	ERECT.DAT	212
A.4	OUTPUT	218
A.5	PRINT.PLT	218

A.6	Hardware Requirements	219
A.7	Software Requirements	219
A.8	System Configuration	220
A.9	Source Code Alteration	220
Appendix B : Catenary Equations of a Cable Element		
B.1	The Inextensible Cable	222
B.2	The Elastic Cable	226
Appendix C : Treatment of Variations in Centroidal Axis		229

LIST OF TABLES

Table	Page:
1.1 Basic Deflection Solutions	16
1.2 Backward (Disassembly) Solution	17
1.3 Forward (Assembly) Solution	18
3.1 An Example of Fatigue Life Computations	49
3.2 Typical Cable Properties	50
4.1 Substructure Types	83
4.2 The Sequential Assembly and Reduction Scheme	84
4.3 Numerical Values of Array INDEX.	85
7.1 Array IST(IS)	140
7.2 Nodal Coordinates and Bending Moments for Reference Configuration	141
7.3 Member Properties and Load Specifications	144
7.4 Member Capacities	146
7.5 Assembly Procedure	148
7.6 Disassembly Procedure	148
7.7 DATA Statements for Substructure Modification	149
C.1 Centroidal Axis Variation	231
D.1 List of Subroutines	234

LIST OF FIGURES

Figures	Page:
1.1 Cable Supported Bridges	19
1.2 Backward and Forward Solutions	20
1.3 Reference Configuration	20
2.1 Types of Deck Anchorage	30
3.1 Stress-Strain Diagram for a Wire	51
3.2 Catenary Cable Element	52
3.3 Flowchart for Computation of H , V_B and L_0 for a Catenary Cable	53
3.4 Flowchart for Computation of H , V_B , V_A , and Stiffness Matrix Coefficients for a Catenary Cable	54
3.5 Computation of Cable Forces in the Reference Configuration	55
3.6 Flowchart of Subroutine DLBM	56
3.7 Variation of Effective Modulus of Elasticity of a Cable with Its Tensile Stress	57
4.1 Flowchart of Linear Analysis	86
4.2 Global Nodal and Member Numbering.	87
4.3 Substructure Types	88
4.4 Flowchart of Subroutine NUMBER	89
4.5 Systems of Coordinates	90
4.6 Specified Bending Moment for Reference Configuration . .	91
4.7 Simplified Structure for Approximate Computation of Tie-Down Forces	92
4.8 Schematic Matrix Reduction and Load Vector Processing . .	92-A
4.9 Flowchart of Subroutine REDUCE	93
4.10 Flowchart of Subroutine BACSUB	94

5.1	Force Increment in Cables	104-A
5.2	Girder Forces Due to Removal of Substructure SS	104-A
5.3	Flowchart of Subroutine CABLES	105
5.4	Uncoupling of the Girder	106
5.5	Erection Loads in Backward Analysis	106
5.6	Flowchart of Subroutine UNCOUP	107
5.7	Flowchart of Subroutine DECK	108
5.8	Bracing	109
5.9	Flowchart of Subroutine BRACG.	110
5.10	Change in Girder-Tower Connection	109
5.11	Flowchart of Subroutine DTBC	111
6.1	Distribution of Cable Forces Due to Point Loads	120
6.2	Flowchart of EQCHEC.	121
6.3	Load-Displacement Curve of a SDOF Cable.	122
6.4	An Example of P- Δ Effects.	123
6.5	Steps in Nonlinear Erection Analysis	124
7.1	The Program Structure.	150
7.2	External Storage Scheme	151
7.3	Typical Application	152
7.4	Nodal and Member Numbering.	153
7.5	Specified Internal Bending Moment Distribution for Girder	154
7.6	MAIN.DAT File	155
7.7	ERECT.DAT File	158
7.8	OUTPUT File.	160
7.9	Reference Configuration	176
7.10	Topping Removal	178
7.11	Deck-Tower Jack Installation.	180

7.12	Installation of Bracing Sets	182
7.13	Derricks on the Girder	184
7.14	Ungrouting of PC Deck (Members No. 1-5)	186
7.15	Removal of PC Deck (Members No. 1-5).	188
7.16	Uncoupling of the Girder	190
7.17	Removing Member No. 1.	192
7.18	Ungrouting PC Deck (Member No. 23)	194
7.19	Removal of PC Deck (Member No. 23)	196
7.20	Removal of Cable No. 60	198
B.1	Catenary Cable Element	228
C.1	Central Axis Variation	232

LIST OF SYMBOLS

General

{}	Column vector
[]	Matrix
[] ^T	Transposed matrix
AF	Axial force
BM	Bending moment
C _n	Configuration number n
DOF	Degree of freedom
FIN	Front interboundary degree(s) of freedom of a substructure
II	Member number (within a substructure)
INN	Internal degree(s) of freedom of a substructure
IS	Substructure's sequential number in assembly
ISF	Maximum number of substructures on each side of a bridge
ISYM	Symmetry flag
JN	J-end nodal number of a member
JS	Substructure type
KN	K-end nodal number of a member, Kilo-Newton
LHS	Left hand side
LR	Left hand side/right hand side flag
M	Meter
mm	Millimeter
N	Newton
PS	Partial structure

RHS	Right hand side
SDOF	Single degree of freedom
SH	Shear force
SS	Substructure
<u>Scalars</u>	
a	Length, horizontal projection of a cable element
a_{ij}	Stiffness matrix coefficient
b	Length; vertical projection of a cable element
dx	Differential of x
dy	Differential of y
E	Modulus of Elasticity
E_c	Effective modulus of elasticity of a cable
H	Horizontal component of a cable force
L	Length
L_0	Unstressed length
M	Bending moment
N	Axial force; number of cycles
P	Point load
q	Uniformly distributed load
s	b/a ; length of an arc
T	Cable tension
V	Shear force, vertical component of a cable force
w	Unit weight of a cable
x,y	Local system of coordinates
X,Y	Global system of coordinates

Matrices

[A]	Global stiffness matrix of a substructure
[AA]	Reduced stiffness matrix of a partial structure
[K]	Global stiffness matrix
{r}	Global displacement vector
{R}	Global applied load vector

Arrays

ANP(I)	Angle of point load I with axis X
E(IS,I1)	Modulus of elasticity of member I1 in substructure IS
INDEX(JS,1)	Number of condensable DOF in substructure type JS
INDEX(JS,2)	First dummy DOF in substructure type JS
INDEX(JS,3)	Last dummy DOF in substructure type JS
INDEX(JS,4)	Last DOF in substructure type JS
IST(IS)	Type of substructure IS
JEN(JS,I1)	J-end nodal number of member I1 of substructure type JS
KEN(JS,I1)	K-end nodal number of member I1 of substructure type JS
MNTR(IS,I1)	Global member number of member I1 of substructure IS
NNTR(IS,JN)	Global nodal number of joint JN of substructure IS
NSE(JS)	Number of members in substructure type JS
NSJ(JS)	Number of nodes in substructure type JS
PL(IS,I1,I)	Point load number I on member I1 of substructure IS
QA(IS,I1)	Cross-sectional area of member I1 of substructure IS
QI(IS,I1)	Moment of inertia of member I1 of substructure IS
QM(IS,I1)	Specified bending moment at J-end of member I1 of

substructure IS

RA(N) Nth reduced stiffness coefficient in linear array

XCO(IS,I) X-coordinate of node I of substructure IS

YCO(IS,I) Y-coordinate of node I of substructure IS

XU(IS,I) Displacement I of substructure IS

Greek

α Angle of a girder segment with X-axis; nondimensionalized distance; stiffness coefficient of a catenary cable element

δ Increment; cable stiffness coefficient

Δ Deflection; increment

ϵ Strain; error limit

ϕ Angle of a cable element cord with X-axis

γ Cable density, cable stiffness coefficient

θ Cable stiffness coefficient

CHAPTER 1 : INTRODUCTION

1.1 Cable-Stayed Bridges

The superstructure of a cable-stayed bridge consists of a deck supported by continuous girders which are stiffened by inclined stays passing over or attached to vertical towers. The basic difference between a suspension bridge, Fig. 1.1a, and a cable-stayed bridge, Fig. 1.1b, is that in the latter all the cables are directly supported by the towers, while in the former the main cables receive the loads through a large number of smaller hangers and transfer them to the towers and the ground anchorages. This variation in the cable arrangements has significant structural and erectional implications. For instance, the deck in a cable-stayed bridge is normally subjected to a large compressive force which is absent in the case of a suspension bridge unless it is self-anchored.

Investigations by some authors and designers indicate that cable-stayed bridges are superior to suspension bridges, not only from the structural and economical points of view, but their erection is also significantly faster and easier (Leonhardt and Zellner, 1970; Troitsky 1988.) Indeed, for a certain range of crossing spans (say 200-500 m.) a cable-stayed bridge would be a logical choice. More recently, cable-stayed bridges have been economically used for spans as small as 27 m (Walther, et al. 1988), and have been proposed for spans as long as 2000 m (Scordelis, 1989).

Structurally, a cable-stayed bridge is stiffer than a suspension bridge of similar span. This increase in stiffness becomes very significant in the case of heavy unsymmetrical loads (such as railway loading). Furthermore, it has been found (Leonhardt and Zellner, 1970) that cable-stayed bridges have greater system dampings and are, therefore, more stable against wind-induced vibrations. For a more detailed comparative study of these two cable-supported systems reference should be made to Leonhardt and Zellner (1970), Troitsky (1988); and Podolny and Scalzi (1986).

1.2 History of Cable-Stayed Bridges

The historical review of cable-stayed bridges has been well-documented by several authors, such as, Leonhardt and Zellner (1970), Troitsky (1988) and Walther et al. (1988). A brief summary, drawn primarily from these references, is given below.

The idea of supporting horizontal beams by stay ties connected to vertical supports is very old. A primitive example of this type of structure is the hanging footpaths of the tropical forests in South East Asia, South America and Africa. It consists of a flexible footpath connected to tall trees on the sides of a deep valley by strong ropes.

A more advanced version of this system of bridging was used by a Venetian engineer, Faustus Verantius in 1617 (Troitsky 1988). His bridge consisted of a wooden deck supported by several chain stays which were fixed to two massive masonry side towers. In 1784, Immanuel Loscher, a German carpenter, built a wooden bridge over a river near Fribourg in Germany with wooden stays and towers. His bridge was 32 m. long (Troitsky 1988).

The first predecessor of modern cable-stayed bridges was constructed by two British engineers, Redpath and Brown, in 1817. Soon after, many similar pedestrian cable-stayed bridges were erected in Europe and the United States. Unfortunately, a considerable number of these bridges failed a few years after their construction.

In 1830, Navier, the famous French scientist and engineer, prepared a report on the collapse of these bridges and the reliability of the ones which were still standing. His recommendation was that suspension bridges were stronger and more reliable than cable-stayed bridges. However, it is very likely that the real cause of collapse of the cable-stayed bridges was a combination of poor design, loose and sagging stays, and high wind vibrations (Troitsky, 1988).

Navier's report served as an impetus to the development of suspension bridges in the remaining decades of the nineteenth century. Very few bridges using stay stiffeners were built during this period. However, with the invention of locomotives in the second half of the nineteenth century, suspension bridges did not adequately meet the challenges of the trains with heavy unsymmetrical loads.

In 1938, F. Dischinger, a German engineer, rediscovered the important role of stay cables in reducing large deflections of suspension bridges under unsymmetrical loads. Dischinger's ingenuity lies in his realization for the first time that for a stay cable to be fully effective it must be completely stretched and tight. The greater the length of the cable, the more critical becomes its tightness. Soon after the publication of Dischinger's studies in 1949, several cable-stayed bridges were proposed for major crossings in Germany and a few other European countries. The first modern cable-stayed bridge based on the newly-developed concept was

constructed by a German contractor in Sweden in 1955 (Troitsky, 1988). The first cable-stayed bridge in Germany was completed in 1958. The history of cable-stayed bridges will always remain associated with the name of Professor Fritz Leonhardt who has been actively involved with the design, construction and promotion of cable-stayed bridges since 1952.

The development of cable stayed bridges in North America started very late in comparison with Europe, and their use has not been fully explored. In 1972 there were only six cable-stayed bridges in North America; five of them in Canada. At that time the total number of the cable-stayed bridges in the world was forty-three, with thirteen of them in Germany. By 1977, the total number was sixty-two; with nineteen in Germany, eighteen in Japan, six in the United States, five in France and five in Canada. In 1985, the number of completed cable-stayed bridges in the United States was seven, with another six under construction, four in the design stage and four under study.

The Annacis bridge completed in 1986 in Vancouver, with its central span of 465 m. is presently the longest cable-stayed bridge in the world. This bridge is now called the Alex Fraser Bridge.

1.3 Methods of Erection

In any large structure, fabrication and erection are of primary importance and should be taken into consideration in the initial stages of design development.

Fabrication and erection have significant bearing on the following aspects of a large structure:

- Total cost;

- Constructional safety;
- Final configuration;
- Construction time;
- Locked-in stresses;
- Bidding and contractor selection; and,
- Ease of construction.

In the case of the Annacis cable-stayed bridge the designers concluded (Taylor and Torrejon,1987) that simplicity of shape and connections, combined with the modular usage of high strength elements contributed significantly to the low cost and ease of construction of the bridge.

Under normal circumstances, the designer would recommend a method of erection and the contractor would be free to either adopt that method or to propose an alternative to be approved by the consulting engineers. Erection methods of cable-stayed bridges are far from standardized and depend largely on the experience and ingenuity of the contractor. However, on a very broad basis, the erection procedures can be divided into the following three categories.

a) Staging Method

In this method the deck is first erected on a number of temporary and permanent piers sufficient to support its dead load. Then, the deck is jacked up at the piers to a predetermined geometry. Next, the towers are erected on the permanent piers and the cables are installed. Finally, the jacks are released and the deck takes its projected profile. This method is both accurate and simple. It can also be economical if the deck is not too high. Its final practicality will depend on whether the temporary piers can be erected without interference with the traffic under the bridge.

b) Push-out Method

This technique has application to box girder bridges. It consists of pushing out the completed deck over a number of rolling supports from the abutments. On a number of occasions this method has been used to erect cable-stayed bridges in Europe (Podolny and Scalzi, 1986b.) Its major application is in the case of city overpasses where the traffic underneath cannot be interrupted.

c) Cantilever Method

This is the easiest and the most widely used method of erection for cable-stayed bridges. It was successfully used for the erection of Stromsund bridge, the first modern cable-stayed bridge, built in Sweden in 1955. It consists of cantilevering appropriate lengths of girder extensions from the part of the deck already completed, installing the cables, and completing the deck between the extended girders. In order to keep the partial structure in balance, the extensions have to be done on either side of the tower on an alternate basis. Derricks and other material handling equipment will be moving on the completed portion of the deck during the course of erection. Temporary ballast loading and/or bracing of the deck and the towers are used to counter-balance the weight of the derricks and to control undesirable large deflections.

1.4 Structural Complexities of Cantilever Method

During the course of free cantilevering the partial structure will go through a large number of geometric and force configurations which are totally different from the final configuration of the completed bridge. The

partial structures are substantially more flexible and less stable than the complete structure. These factors have to be taken into consideration if overstressing, excessive distortions, and unacceptable locked-in stresses are to be avoided.

Clearly, a well-defined and detailed erection procedure must be prepared and adhered to in order to be able to analyse and predict the configuration of the partial structure at each stage of erection. Moreover, the erection plan and analysis must ensure that the completed bridge will assume the geometric and force configuration, under its dead load, for which the bridge was designed. If such an erection plan and detailed analysis is combined with, and supported by, a continuous system of monitoring and adjustment of the partial structures, then the result will be a cable-stayed bridge which conforms with the design specifications not only upon completion but also at all stages of its construction.

1.5 Research Objectives

The general objective of the work contained herein is to develop a versatile microcomputer based program which is suitable for the analysis of a cable-stayed bridge in its completed and partially assembled configurations, as it is being erected by the cantilever method. It is envisaged that such a program would be used in both the design and construction phases of the bridge. In the latter case the computer could be located on site so that the project engineer could assess the effects of variations in erection procedure as construction progresses.

The program should have the following capabilities.

- 1 The program should be capable of analysing for the conditions cited

above with sufficient graphical capabilities to display the results of its analyses.

2. The program should be able to correctly predict the evolution of a sequence of partial structures to arrive at a final structure under its dead load.
3. The program should be capable of dealing with major nonlinearities which may exist in either the partial structures or the completed bridge.
4. The program should allow the user to move either forward or backward in the partial structure analysis. This feature will facilitate the study of changes in the erection plan, which may have to be modified during erection should unforeseen circumstances dictate that this is desirable.
5. The program should provide for the implementation of all common means used for the stabilization and control of deflections in the partial structures.

1.6 Solution Considerations

There are three aspects of structural analysis of a cable-stayed bridge which require special attention. These are:

a) Nonlinearities

Two types of nonlinearities have been considered to be of significance in the analysis of cable-stayed bridges. These are:

- i- Geometrical nonlinearity of the cables which is particularly important in the erection analysis in the vicinity of the elements which are being erected. This is due to the fact that the

geometrical nonlinearity of a cable increases rapidly when its internal tension falls below a certain limit.

-ii-Second-order (P-Δ) effects in the towers and the deck.

In order to take these nonlinearities into consideration, the program has been based on an updated incremental Lagrangian formulation which allows for the geometrical nonlinearity by incremental loading and iteration, and takes care of the (P-Δ) effects by updating the geometry of the structure.

b) Backward and Forward Solutions

Fig. 1.2 shows a load-deflection diagram for a nonlinear system with displacement vector $\{r\}$ and external force vector $\{R\}$. Each intermediate configuration of the system under a load vector $\{R_B\}$ is defined by a displacement vector $\{r_B\}$ which, provided an incremental linear performance is assumed, may be obtained from

$$\{r_B\} = \{r_A\} + [K_A]^{-1} (\{R_B\} - \{R_A\}) \quad [1.1]$$

or, alternatively, from

$$\{r_B\} = \{r_C\} + [K_C]^{-1} (\{R_B\} - \{R_C\}) \quad [1.2]$$

Equation [1.1] represents a 'forward' solution in which the previous configuration C_A has been used as the reference configuration. On the other hand, [1.2] represents a 'backward' solution which is based on a more advanced configuration C_C as its reference configuration. Whether to choose a 'forward' or a 'backward' solution in solving a structural problem would

mainly depend on the problem specifications. If a more advanced configuration of the structure is specified, such as C_c , the most obvious choice would be a backward solution. On the other hand, if the structure's initial configuration is specified (or is readily known), a 'forward' solution is more conventional.

c) Structural Changes During Erection:

Structural changes during erection affect the stiffness matrix as well as the load vectors of the partial structures. In order to take these changes into consideration, these matrices have to be updated each time the partial structure is changed. Assuming that at erection stage (n) the member (m) is to be added to configuration C_{n-1} to arrive at C_n , the following relationships may be written in a 'forward' solution.

$$[K]_n = [K]_{n-1} + [\delta K]_m \quad [1.4]$$

$$\{r\}_n = \{r\}_{n-1} + [K]_n^{-1} \{\delta R\}_m \quad [1.5]$$

where,

$[\delta K]_m$ is the contribution of member m to the stiffness matrix [K], and;

$\{\delta R\}_m$ is the fixed-ended force vector in member m after its connection to the structure. (It is assumed that the only change in loading is due to the erection of member m and that these forces are applied through this member.).

The corresponding backward solution will be obtained by disassembling member m+1 from configuration C_{n+1} in order to arrive at C_n . The following

equations are applicable.

$$[K]_n = [K]_{n+1} - [\delta K_{m+1}] \quad [1.6]$$

$$\{r\}_n = \{r\}_{n+1} + [K]_n^{-1} \{\delta R_{m+1}\} \quad [1.7]$$

in which $[\delta K_{m+1}]$ is the contribution of member $m+1$ to the stiffness matrix $[K]$, and $\{\delta R_{m+1}\}$ is the reverse of the end-force vector in member $m+1$ in configuration C_{n+1} .

1.7 The Reference Configuration

A cable-stayed bridge is a highly indeterminate structure. Cable forces and cable initial lengths can be used as two sets of variables to control the girder geometry and its internal force distribution. In the present work, it is assumed that the designer will use these variables to specify the geometry and the internal force distribution in the completed bridge under its dead load at normal temperature. This specified configuration of the bridge is referred to as the 'reference configuration'.

The vertical component of the cable force is principally fixed by the length of girder and the uniformly distributed dead load which it supports. However, near the abutments and the middle of the central span bending moment distribution is not repetitive in successive girder spans. In general the designer can specify independently a force and a geometric reference configuration for the completed bridge. Once the moments and axial forces

for the reference configuration are determined, the configurations of the partial structures during a cantilever erection procedure which are consistent with the reference configuration, may be computed by a disassembly procedure. That is, by removing the segments of the bridge in reverse order to the manner in which they were assembled. Such a computational procedure will be referred to as a 'backward' analysis.

A complication in this procedure is that in a partial structure the cables become substantially nonlinear when their tension is reduced due to the removal of the nearby segments. Consequently, predicting the precise configuration that the bridge should assume in any stage of erection is not a simple task.

It is argued, herein, that a backward procedure is not a necessity for the computation of the initial shapes of members. As will be demonstrated in the example of Section 1.8 the same results are equally obtainable from a 'forward' analysis. The latter terminology is used to describe an analysis which follows the deflected shapes of the resulting partial structures as the bridge is assembled in the same manner as it is erected.

Whatever procedure is used to determine the initial shape and length of individual elements, it is very important to ensure that the elements are fabricated according to these initial dimensions, as otherwise, major discrepancies from the desired geometry and internal force distribution may arise during and after the erection of the bridge. Obviously, the greatest attention should be given to the marking and cutting of the cable elements to their unstressed lengths, as these are the principal determinants of the bridge geometry.

1.8 Backward and Forward Solutions for a Fixed Ended Beam

To illustrate the superposition of deflections in a simple structure, the partial structure configurations of a three segment fixed ended beam erected by the cantilever method are examined in this Section. It is assumed that the beam material remains linear elastic at all times. The selected reference configuration is that the beam be perfectly straight after its erection by the cantilever method. This reference configuration and the reactive forces for the beam are shown in Fig. 1.3.

The backward solution of this beam is shown in Table 1.2. The reference configuration is designated as B_0 . Removal of the right fixed-ended reactions produces partial structure B_1 , with deflected shape Y_1^b . Successive removal of segments produces partial structures B_2 , B_3 , and B_4 with deformations designated as Y_2^b , Y_3^b , and Y_4^b . These shapes are obtained by the superposition of the deflections produced by the partial loadings as tabulated in Table 1.1. The computation of the shapes for the partial structures in the backward solution is shown in the lower part of Table 1.2. The unloaded segment of each of the configurations B_2 to B_4 represents a shape (called the initial shape) according to which that segment should be cambered during fabrication. With these initial shapes, and provided that the joining end tangents are colinear at the time of erection by the cantilever method, the resulting completed beam will be perfectly straight.

That the above statement is true may be verified by assembling segments with the initial shapes of the unloaded segments of configurations B_2 to B_4 and then applying the end forces of configuration B_1 to arrive at configuration B_0 .

The configurations of the partial structures for the forward solution are given in Table 1.3. The solution begins with the initial configuration of the beam under zero internal force resultants. In general, this initial configuration should be obtained by integrating the curvatures associated with negative of the specified final bending moment distribution in order to obtain the deflections. Clearly, if these deflections are superimposed on the reference configuration the initial configuration of the beam will be obtained.

In the particular case of this example in which the specified bending moment diagram is identical with the 'normal' bending moment diagram of the beam under its weight, the desired stress-free initial shape can be obtained by simply applying the load $-w$ to the reference configuration. According to Table 1.1 this is $-Y_1$ which has been used in Table 3.1 as the initial configuration. The other partial structures configurations are simply obtained by linear combination of the deflected shapes in Table 1.1.

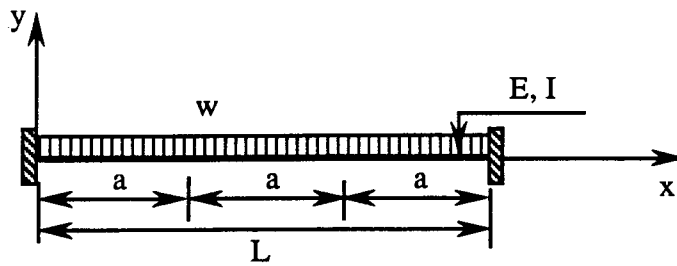
From a comparison of Table 1.2 and Table 1.3, and as demonstrated in Fig. 1.2, an identical configuration is obtained for each partial structure regardless of the method of solution. This is, of course, to be expected since linear equations are used throughout.

1.9 Forward Analysis vs. Backward Analysis

As demonstrated in Section 1.8, in the case of a linear elastic structure a backward analysis from a specified reference configuration is not a requirement for obtaining an initial configuration from which assembly should begin. With the type of nonlinearities which are considered in the erection analysis of cable-stayed bridges a unique solution for each partial structure should be obtained regardless of whether a backward or a

forward analysis is carried out.

However, due to the fact that for the case of a cable-stayed bridge the specified configuration is the completed reference configuration and that a forward analysis begins with more pronounced nonlinearities in the cables, the formulation of the computer program developed herein, and designated as CASBA, is based on a backward analysis.

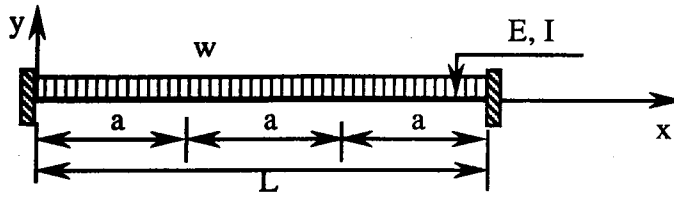


Define:

$$\begin{cases} Y = Ely \\ \alpha = x/a \end{cases}$$

Case	Loading	Deflected Shape
1		$Y_1 = -\frac{\alpha^2 (3-\alpha)^2}{24} wa^4 \quad 0 \leq \alpha \leq 3$
2		$Y_2 = -\frac{\alpha^2 (\alpha - 12\alpha + 54)}{24} wa^4 \quad 0 \leq \alpha \leq 3$
3		$Y_3 = -\frac{\alpha^2 (15 - 2\alpha)}{12} wa^4 \quad 2 \leq \alpha \leq 3$ $Y_3 = -\frac{(\alpha^4 - 12\alpha^3 + 54\alpha^2 - 32\alpha + 16)}{24} wa^4$
4		$Y_4 = -\frac{\alpha^2 (9 - 2\alpha)}{12} wa^4 \quad 1 \leq \alpha \leq 2$ $Y_4 = -\frac{(\alpha^4 - 8\alpha^3 + 24\alpha^2 - 4\alpha + 6)}{24} wa^4$
5		$Y_5 = -\frac{\alpha^2 (\alpha^2 - 4\alpha + 6)}{24} wa^4 \quad 0 \leq \alpha \leq 1$ $Y_5 = -\frac{4\alpha - 1}{24}$
6		$Y_6 = \frac{\alpha^2 (9 - \alpha)}{6} wa^3$
7		$Y_7 = \frac{\alpha^2}{2} Ma^2$

Table 1.1 Basic Deflection Solutions



Define:
 $Y = EIy$
 $\alpha = x/a$

Case	Loading	Deflected Shape
B_0		$Y_0^b = 0$ (Reference Configuration)
B_1		$Y_1^b = \frac{\alpha^2(2\alpha - 15)}{8} wa^4 \quad 0 \leq \alpha \leq 3$
B_2		$Y_2^b = \frac{\alpha^2(2\alpha - 15)}{24} wa^4 \quad 0 \leq \alpha \leq 2$ $Y_2^b = \frac{\alpha^4 - 6\alpha^3 + 9\alpha^2 - 32\alpha + 16}{24} wa^4 \quad 2 \leq \alpha \leq 3$
B_3		$Y_3^b = -\frac{\alpha^2(3 - 2\alpha)}{24} wa^4 \quad 0 \leq \alpha \leq 1$ $Y_3^b = -\frac{(\alpha^4 - 6\alpha^3 + 9\alpha^2 - 4\alpha + 1)}{24} wa^4 \quad 1 \leq \alpha \leq 2$
B_4		$Y_4^b = \frac{\alpha^2(\alpha - 3)}{24} wa^4 \quad 0 \leq \alpha \leq 1$

COMPUTATIONS:

(Y_1, Y_2, \dots, Y_7 from Table 1.1.)

$Y_0^b = 0$ (Reference Configuration)

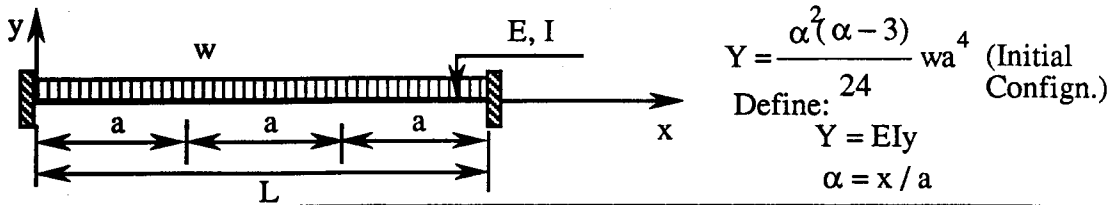
$$Y_1^b = Y_0^b - Y_6 + Y_7 = 0 - \alpha^2(9 - \alpha)(3wa/2)a^3/6 + \alpha^2(3wa^2/4)a^2/2 \quad 0 \leq \alpha \leq 3$$

$$Y_2^b = Y_1^b - Y_3 = \frac{\alpha^2(2\alpha - 15)wa^4}{8} + \begin{cases} \alpha^2(15 - 2\alpha)wa^4/12 & 0 \leq \alpha \leq 2 \\ (\alpha^4 - 12\alpha^3 + 54\alpha^2 - 32\alpha + 16)wa^4/24 & 2 \leq \alpha \leq 3 \end{cases}$$

$$Y_3^b = Y_2^b - Y_4 = \frac{\alpha^2(2\alpha - 15)wa^4}{24} + \begin{cases} \alpha^2(9 - 2\alpha)wa^4/12 & 0 \leq \alpha \leq 1 \\ (\alpha^4 - 8\alpha^3 + 24\alpha^2 - 4\alpha + 1)wa^4/24 & 1 \leq \alpha \leq 2 \end{cases}$$

$$Y_4^b = Y_3^b - Y_5 = \alpha^2(3 - 2\alpha)wa^4/24 + \alpha^2(\alpha^2 - 4\alpha + 6)wa^4/24 \quad 0 \leq \alpha \leq 1$$

Table 1.2 Backward (Disassembly) Solution



Case	Loading	Deflected Shape
F_0		$Y_0^f = \frac{\alpha^2(\alpha-3)}{24} wa^4 \quad 0 \leq \alpha \leq 1$
F_1		$Y_1^f = -\frac{\alpha^2(3-2\alpha)}{24} wa^4 \quad 0 \leq \alpha \leq 1$ $Y_1^b = -\frac{(\alpha^4 - 6\alpha^3 + 9\alpha^2 - 4\alpha + 1)}{24} wa^4 \quad 1 \leq \alpha \leq 2$
F_2		$Y_2^f = \frac{\alpha^2(2\alpha-15)}{24} wa^4 \quad 0 \leq \alpha \leq 2$ $Y_2^f = \frac{\alpha^4 - 6\alpha^3 + 9\alpha^2 - 32\alpha + 16}{24} wa^4 \quad 2 \leq \alpha \leq 3$
F_3		$Y_3^f = \frac{\alpha^2(2\alpha-15)}{8} wa^4 \quad 0 \leq \alpha \leq 3$
F_4		$Y_4^f = 0 \quad (\text{Reference Configuration})$

COMPUTATIONS:

(Y_1, Y_2, \dots, Y_7 from Table 1.1.)

$Y_0^f = Y$ (Initial Configuration) NOTE THAT: $F_0 \equiv B_4, F_1 \equiv B_3, F_2 \equiv B_2, F_3 \equiv B_1, F_4 \equiv B_0$

$$Y_1^f = Y + Y_5 = \left[\frac{\alpha^2(3-\alpha)^2}{24} - \frac{\alpha^2(\alpha^2 - 4\alpha + 6)}{24} \right] wa^4 \quad 0 \leq \alpha \leq 1$$

$$Y_1^f = Y + Y_5 = \left[\frac{\alpha^2(3-\alpha)^2}{24} - \frac{(4\alpha-1)}{24} \right] wa^4 \quad 1 \leq \alpha \leq 2$$

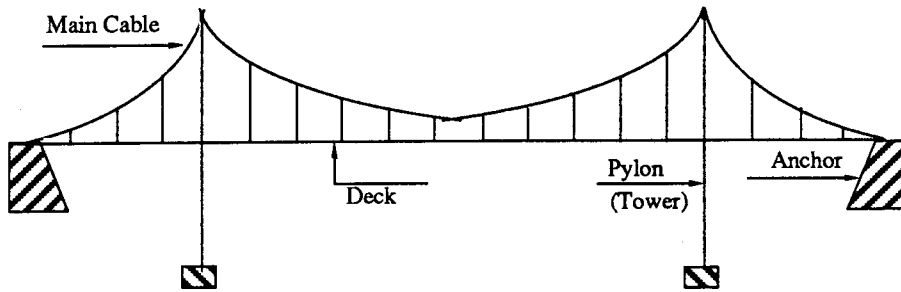
$$Y_2^f = Y + Y_2 - Y_3 = wa^4 \left[\frac{\alpha^2(3-\alpha)^2 - \alpha^2(\alpha^2 - 12\alpha + 54) + 2\alpha^2(15-2\alpha)}{24} \right] \quad 0 \leq \alpha \leq 2$$

$$Y_2^f = Y + Y_2 - Y_3 = wa^4 \left[\frac{\alpha^2(3-\alpha)^2 - \alpha(\alpha^4 - 12\alpha^3 + 54\alpha^2 - 32\alpha + 16)}{24} \right] \quad 2 \leq \alpha \leq 3$$

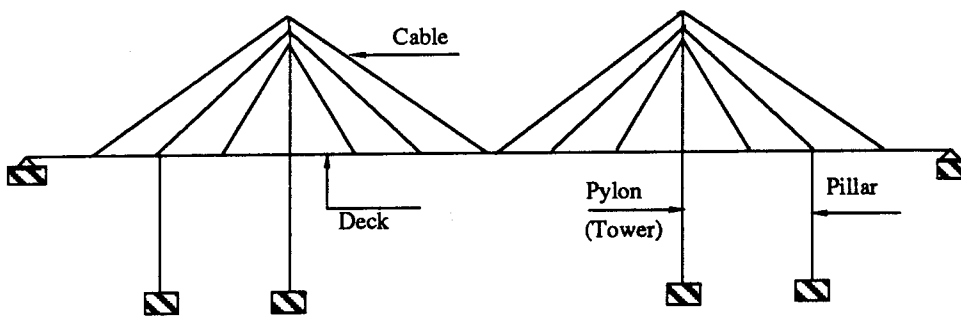
$$Y_3^f = Y + Y_2 = wa^4 \left[\frac{\alpha^2(3-\alpha)^2 - \alpha^2(\alpha^2 - 12\alpha + 54)}{24} \right] \quad 0 \leq \alpha \leq 3$$

$$Y_4^f = Y_3^f + Y_6 + Y_7 = \left[\frac{\alpha^2(2\alpha-15)}{8} + 3\alpha^2 \left(\frac{9-\alpha}{12} - \frac{3\alpha^2}{8} \right) \right] wa^4$$

Table 1.3 Forward (Assembly) Solution



a) A Suspension Bridge



b) A Cable-Stayed Bridge

Figure. 1.1

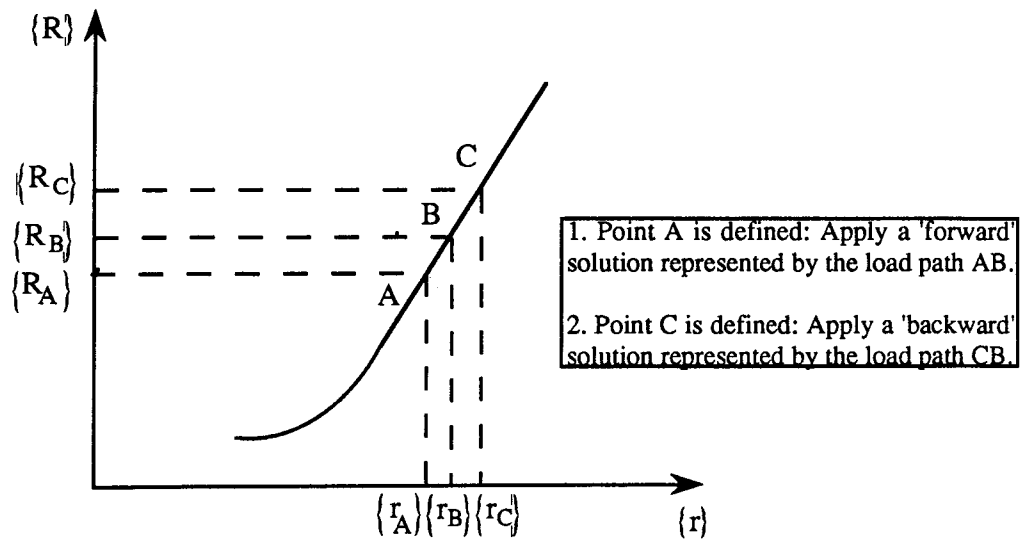
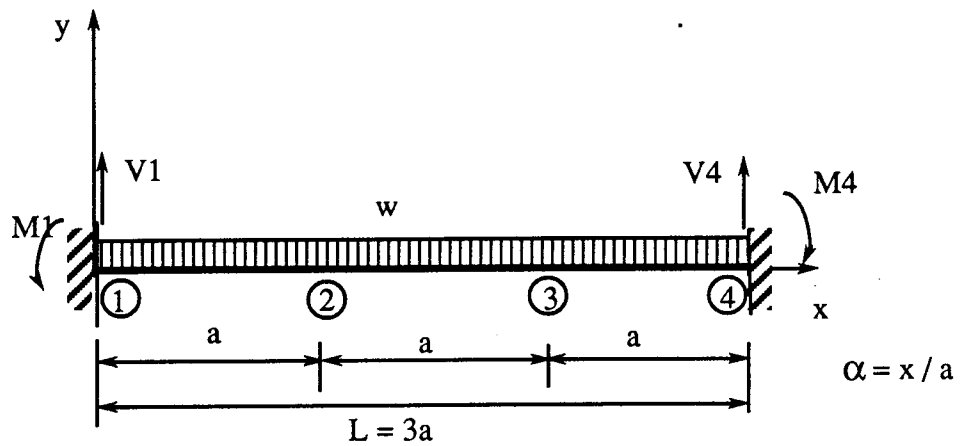


Figure 1.2 Backward and Forward Solutions



Reference (specified) configuration::

$$y=0.0$$

$$M1 = 3wa^2/4$$

$$M4 = -3wa^2/4$$

$$V1 = V4 = 3wa / 2$$

Figure 1.3

CHAPTER 2 : LITERATURE REVIEW

2.1 Behaviour of Cables

The catenary solution of a free cable dates back to 1691 and is attributed to James Bernouilli and a group of scientists working under his supervision (Pugsley, 1956). The English version of the solution was published by David Gregory in 1697.

Till the middle of the nineteenth century the main concern of the workers in this field was to find analytical expressions for cable shapes under typical loadings. Another important concern at that time was the safe strength of a cable with a given size and material.

In 1794, Fuss, a Russian scientist, developed the theory of the parabolic cable while he was working on the Neva Bridge at Leningrad. In England, David Gilbert, the then President of the Royal Society, developed the theory of a chain with uniform stress along its length (Pugsley, 1956).

Towards the middle of the nineteenth century and with the invention of heavy train locomotives, the deflection of cable-supported bridges became increasingly critical. Many engineers and scientists in the United States and Europe were anxiously looking for a solution to the large deflection of these bridges.

Rankine (1858 and 1863) proposed the use of heavy stiffening girders in order to distribute heavy concentrated loads over a larger section of the catenary cables. In the United States, Roebling was designing the Niagara Falls Bridge around this time. In a letter to the bridge company he proposed to increase the weight of the deck in order to make the cables

less flexible. His letter reads (Pugsley, 1956):

"Although the question of applying the principle of suspension to railroad bridges has been disposed of in the negative by Mr. Robert Stephenson.... Any span with fifteen hundred feet, with the usual deflection, can be made perfectly safe for the support of railroad trains as well as common travel...."

After the completion and successful testing of the bridge he commented (Roebing, 1855):

"Weight is a most essential condition, where stiffness is a great object...."

Up to this stage no one was yet able to calculate the deflections of a cable under concentrated moving loads.

In 1862, an unknown author referred to the nonlinear deflection of cables and gave an approximate method for its calculation (Pugsley, 1956).

J. Melan (1888) was the first engineer to formulate the nonlinear theory of cables and to apply it to the deflection calculation of a catenary cable under moving loads. A revised edition of his work was published in 1906.

Later, Carstraphen (1919 and 1920) worked out the analytical relationship for the deflection of a cable under evenly-spaced loads. Steinman (1922) translated the work of J. Melan from German and developed its application to suspension bridges.

In Europe, Keifer (1915), Pigeand (1924) and Walmsley (1924) continued their works on the development of the relationships between the length, the tension and the sag of a cable supporting various types of loads. Dischinger (1949) studied inclined stays and was the first one to discover the importance of high tensile stress in reducing large deflections of the stay.

In the 1960's and the early part of the 1970's, there was a great surge in cable studies and, therefore, in the number of publications related to this subject. It was thought that cable-supported structures were both economical and aesthetic and, therefore, the public demand for them would sharply increase. However, lack of widespread knowledge about the analysis and erection of this type of structure has not yet allowed the full realization of this expectation (Buchhaoldt, 1985).

In order to generalize and simplify cable solutions, Michalos and Brinstiel (1960) and Jennings (1962) proposed numerical analysis of the problem. Their proposal proved to be highly instrumental to the development of nonlinear analysis of structures with large deflections in general, and that of a cable in particular. Later, O'Brien and Francis (1964) applied an alternative numerical procedure to make the solution more expeditious and applicable to 'rolling' loads.

Tung and Kudder (1968) proposed a much simpler solution for inclined cables under their weight and end forces which is based on an equivalent straight tie. A similar method was developed in Germany at about the same time. The practical implication of this method is the replacement of the geometrical nonlinearity of a cable with an equivalent hypothetical material nonlinearity represented by a modified modulus of elasticity.

Many other authors and investigators have used a variety of other

numerical techniques for different applications. Among them, is the use of the perturbation technique by Buchanan (1970).

The dynamic analysis of cables has been investigated by many researches, such as, Dominguez and Smith (1972) and Syed Amjad Ali (1986). However, dynamic analysis is specifically excluded from this work.

2.2 Analysis and Erection of Cable-Stayed Bridges

In the first half of the nineteenth century a number of cable-stayed bridges with spans of less than 50 m. were built by bridge contractors who relied solely upon their experience and intuition. For about a century no other cable stayed bridge was constructed because of the belief that they were unsafe and inferior to suspension bridges (Pugsley, 1956).

Dischinger (1949) was the first engineer who ventured to re-examine the use of cable-stayed bridges and to make recommendations for their successful design and erection. As previously mentioned, his conclusion was that nonlinear, large deflections of the deck could be prevented by subjecting the inclined cables to high tensile stresses. The early development of the theory of modern cable-stayed bridges took place exclusively in Germany soon after the World War II. The first few publications in the German technical literature were in the form of general reports on the constructional aspects and economy of the cable-stayed bridges built in this period.

Gimsing (1966) presented one of the first papers on cable-stayed bridges at a bridge symposium in Lisbon. In this paper he differentiated between the three systems of decking which may lead to self-anchored, partially-anchored or fully-anchored cable-stayed bridges, depending on the location of the expansion joints. (See Fig. 2.1).

Smith (1967) formulated an analytical method suitable for computer analysis of single-plane cable-stayed bridges. Later, he published a modified version of his formulation for application to double-plane bridges (Smith, 1968). In his matrix formulation both forces and displacements are used to arrive at a mixed solution.

Taylor (1969) set out the general requirements for design and construction of cable-stayed bridges and favoured their construction in Canada as medium span bridges. His paper was probably the first introduction of cable-stayed bridges in the North American technical literature.

In Japan, Okauchi, Yabe and Audo (1967) were among the first investigators to study cable-stayed bridges.

Leonhardt and Zellner (1970) presented a comprehensive paper on the development of cable-stayed bridges at a Canadian Structural Engineering Conference in Toronto. In this paper the superiority of cable-stayed bridges over suspension bridges for spans as large as 1300 m was demonstrated.

In the United States, Podolny and Fleming (1971) were among the first investigators in this field. Podolny (1971) used the stiffness method combined with an iterative procedure to study the effects of the cable nonlinearities. Tang (1971) applied the transfer matrix method to the linear and nonlinear analyses of cable-stayed bridges.

Troitsky and Lazar (1971) used the flexibility method coupled with an iterative procedure to study the same nonlinearities. They verified the accuracy of their analysis by testing a model.

Douglass, et al (1972) applied the concept of load balancing developed by Lin (1961) in order to adjust the deck and tower bending moment

distribution.

Baron and Lien (1971 and 1973) and Kajita and Cheung (1973) developed a three dimensional analysis to allow for lateral rigidity and torsion of the deck. Baron and Lien considered dynamic effects as well.

A Task Committee (1977) of ASCE prepared tentative recommendations for cable-stayed bridges and a Subcommittee of ASCE (1977) provided a chronological bibliography and data on cable-stayed bridges.

Khalil, et al (1983) developed a time-dependent analysis of precast cable-stayed bridges with due consideration to shrinkage and creep in concrete, and relaxation in prestressing steel.

Hegab (1985) developed an iterative procedure based on the potential energy of the stayed-girder which could be used for both linear and nonlinear analysis.

Taylor (1986) described the economy and technical achievements of the Annacis bridge as the longest cable-stayed bridge in the world.

As far as the erection and construction details of cable-stayed bridges are concerned, Podolny and Scalzi (1976, 1987); Troitsky (1977, 1988); Gimsing (1983); and Walther, et al (1988) have contributed immensely to the documentation of cable-stayed bridges in the world.

2.3 State-of-the-art

The early cable-stayed bridges, built in Germany or elsewhere after World War II, had a limited number of cable stays and could, therefore, be analysed, with sufficient accuracy, as a continuous beam or truss resting on a number of flexible supports.

As the spans became longer and the erection methods improved, it was possible to use a larger number of cable stays which would enhance both

the economy and appearance of cable-stayed bridges. Some modern cable-stayed bridges have more than fifty cables in their central span. This increase in the number of cables requires special attention during design and erection.

As far as the analysis and design are concerned, a larger number of cables means a shallower girder with a larger main span/depth ratio. Clearly, this lack of stiffness has a very significant effect on the dynamic behaviour of the deck under loads.

Recent developments in the field of cable-stayed bridges are necessarily directed at the solution of the above problems. Because of the complexity of the structure and its large degree of indeterminacy, the analysis and design have been computerized. On the other hand, control of construction during the erection of such sensitive and flexible structures makes it desirable to have computer programs which can rapidly respond to questions posed by the site engineer in order to determine the effect of possible adjustments to the erection procedure.

Fujisau and Tomo (1985), and Taylor and Torrejan (1987) refer to some of the complexities involved in the design and erection of these flexible modern cable-stayed bridges..

Waldner and Kulick (1988) explain how a spreadsheet program with graphical capability was used to adjust the cables in the course of the erection of the Quincy Bay-View Bridge in the United States.

2-4 Relation of Current Project to State-of-the Art

As mentioned by Gimsing (1983, pg. 242) and Walther, et al (1988, pg. 121), the most direct method of finding forces and geometry of a partial structure at each stage of erection is to use the 'backward' solution which

is based on the disassembly of the complete bridge with a specified geometry and system of forces. This method can provide the following information at any time during erection.

1. The length and tension for any of the cables.
2. The geometry of the deck and its forces.
3. The geometry of the pylons and pillars and their forces.

Based on the above information, the initial (zero load) configuration of all the cables and the other flexural elements of the bridge can be computed. In this way it is possible to proceed with the erection of a bridge with elements which have definite initial shapes which will lead to the final configuration of the bridge if they are assembled with the cable forces appropriate for each partial structure.

The other alternative of using approximate lengths and tensions for the cables and re-adjusting them in order to arrive at an acceptable shape and system of forces in the deck and towers, seems to be more suitable for bridges with a limited number of cables. Whatever method of analysis is selected, it is imperative that a detailed erection procedure is adopted and the geometric and force configurations for each stage of erection corresponding to a particular partial structure are obtained. At the time of erection the proposed erection procedure should be closely followed and the geometry and cable forces should be checked against the computed values in order to assess whether the completed structure will attain the form and internal load distributions specified by the designer.

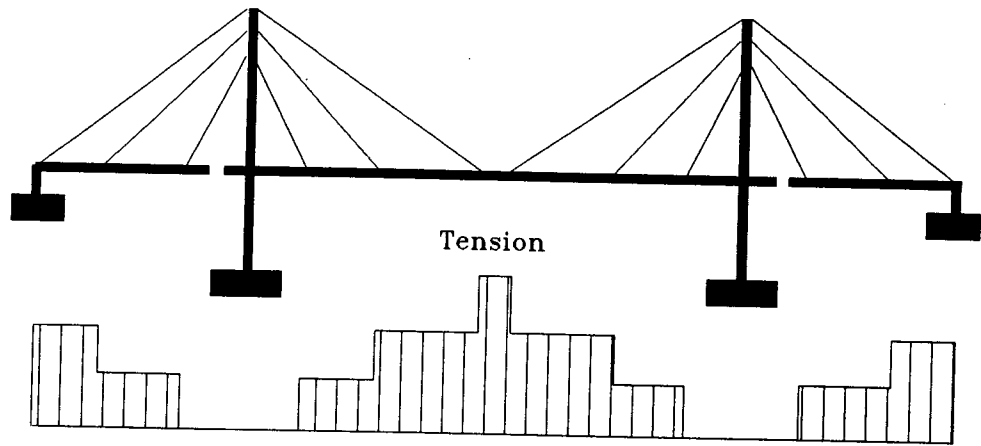
The present work is based on the 'backward' solution but enhanced by many computational tools in order to allow for possible on-site erection modifications. For instance, the restart file stores all the information required to return to any previous erection stage from which an alternative

erection procedure may be adopted.

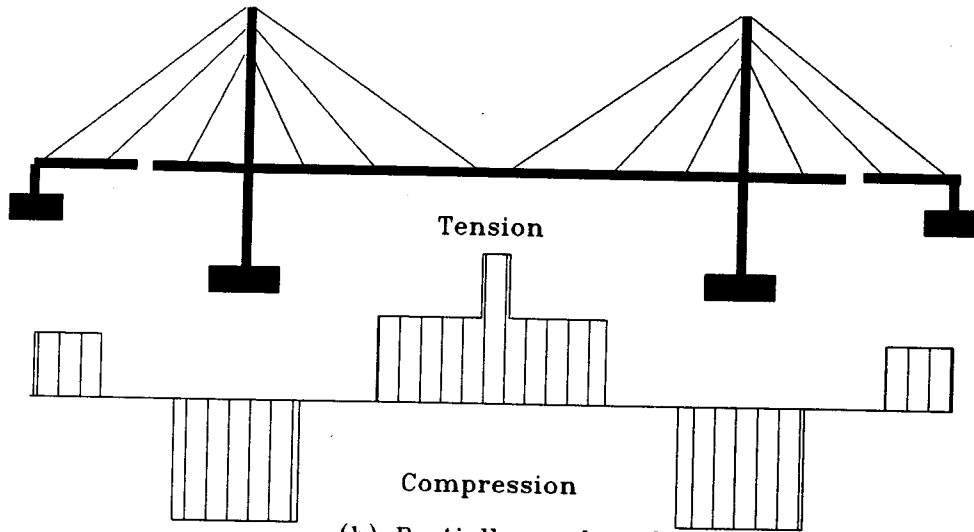
Because many cable-stayed bridges have been built using the cantilever erection procedure, computations of the nature of those which are the subject of this work must obviously have been carried out by a large number of different engineering and contracting organizations. However, the author is aware of only one special purpose program specifically tailored for erection analysis of such bridges. This program is that of DRC Consultants, New York, N.Y. It does not appear to have the versatility of the program developed herein.

A cable-stayed bridge program of general applicability has also been developed by Buckland and Taylor, of Vancouver, B. C. Such programs are proprietary and are not generally available to the profession at large, except through their purchase as a consulting service.

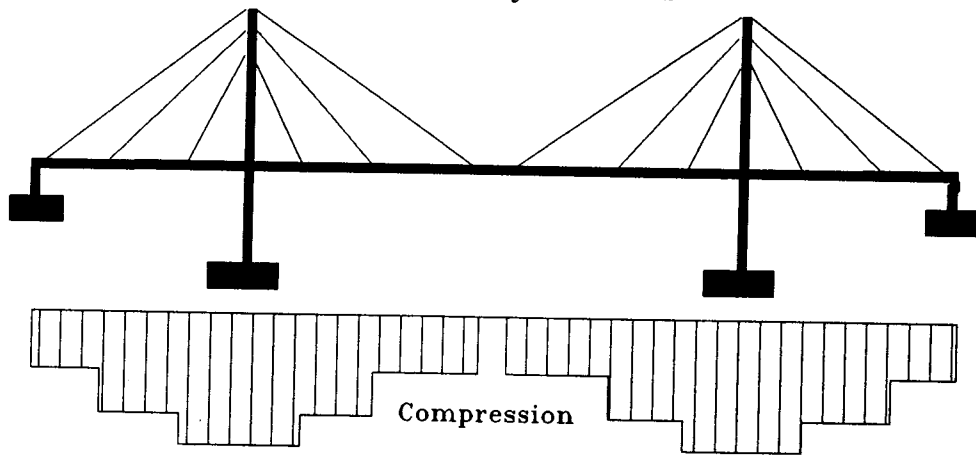
The author did not find any reference to the strategies used in the above programs in the technical literature. While, the concept of frontal solution of structures is well known, the author is not aware of its application in a systematic way to achieve the objectives set out in this work.



(a) Fully anchored



(b) Partially anchored



(c) Self anchored

Figure 2.1 Types of Deck Anchorage

CHAPTER 3 : CABLES

3.1. Types of Cables for Cable-Stayed Bridges

The majority of the existing cable-stayed bridges are supported by locked-coil strands with diameters from 40mm to 120 mm. Until recently, the German Specifications required the use of this type of strand because of its satisfactory corrosion resistance and high modulus of elasticity. Locked-coil strands are made of a central core of helically-wound (or parallel) wires and outer layers of wedge or S-shaped wires which provide an effective cover for the inner core. Some of the most important advantages of this type of strands are as follows (Podolny and Scalzi, 1986):

1. They are very flexible and can, therefore, be easily reeled or unreeled without permanent damage to the strand.
2. Because of their high density and compactness (almost 100% for the outer layers which constitute 84% of the cross-section), their connections and fittings are smaller and lighter.
3. Only a few of the outer layers have to be galvanized. The rest of the cross-section is filled-up with red lead which provides an acceptable corrosion resistance at a very low cost.
4. Their modulus of elasticity is about 190 000 MPa, or about 95% of that of the constituent wires.
5. Individual wires contact one another over a large area and are, therefore, subjected to minimal contact stresses and the resulting

danger of indentation.

However, locked-coil strands are not commonly used in North America and a more recent type of strand which is being used increasingly in the construction of cable-stayed bridges, is the parallel-wire strand. It was first used in 1965 for the main cables of a suspension bridge (Gimsing, 1983). Subsequently, a large number of tests in the United States proved the satisfactory performance of this type of cable in reeling and unreeling (Durkee, 1966), and since then it has been used increasingly in various types of structures, including cable-stayed bridges. Among its advantages are, simplicity of fabrication, and higher strength and modulus of elasticity (virtually equal to those of the constituent wires).

However, in order to achieve an acceptable level of corrosion resistance, all the wires have to be galvanized and encased in a plastic or a flexible steel pipe, which in turn is filled up with a suitable mortar after the erection of the cable or wax before erection. Steel pipes reduce flexibility of the cable, while plastic jackets are easily damaged during erection.

A recent report of Watson and Stafford (1988) indicates that regardless of the type of cable used, the problem of cable corrosion in cable-stayed bridges is far from being solved satisfactorily. With the possibility of a brittle type of progressive collapse in cable-stayed bridges, the combination of corrosion and fatigue seems to be one of the most challenging problems facing the future development of this type of bridge. One advantage of using multiple stays in a bridge is that it is possible to replace any of the stays if necessary.

3.2. Mechanical Properties of Cables

a) Stress-Strain Diagram

Fig. 3.1 shows a typical stress-strain diagram for the type of wires used in the fabrication of cables. The most important characteristics of this diagram are:

Minimum guaranteed tensile strength :	1600 MPa
Modulus of elasticity:	205000 MPa
Limit of proportionality:	1250 MPa
Ultimate strain:	1.4%

Typically, the strength values are 5 - 6 times greater and the strain values are 5 - 6 times smaller than the corresponding values for ordinary structural steel. The modest plastic deformation before rupture is a sign of a very limited tolerance for redistribution of loads among the cables, should one of them snap due to excessive stress or a combination of fatigue and corrosion.

The limit of proportionality is of great significance in the fatigue design of cables. It has been established that irreversible plastic deformations have cumulative effects on the reduction of the fatigue strength of a material and must, therefore, be avoided under service loads (Gimsing, 1983).

The mechanical properties of a cable or a strand are somewhat different from those of its constituent wires. For instance, the modulus of elasticity of a short piece of cable is adversely affected by its void ratio and the pitch of its spiral winding. In order to minimize this type of loss in property, cables are prestretched to about 55% of their rated breaking strength at the factory. This process will remove most of the plastic deformation at working stress levels and increase the effective

modulus of elasticity.

As for the ultimate tensile strength of a cable, the spiral winding of the wires leads to substantial contact stresses between the wires which can cause plastic deformation and necking. The smaller the pitch the greater will be the tensile strength reduction due to this effect. Table 3.1 compares the mechanical properties of three different types of cables which are fabricated from the same type of wires.

The mechanical properties of a long unsupported cable are also affected by its sag and will be dealt with in Section 3.3.

b) Fatigue Strength

The long-term strength of a cable under fluctuating loads is a function of a large number of parameters, such as, its chemical composition, details of its joints and connections, its mechanical properties, and the type of loads and environmental agents to which it is subjected. Due to the complex nature of these influencing parameters, the fatigue strength of a cable cannot be established with the same degree of accuracy as its ultimate tensile strength. A study of existing cable structures indicates that a combination of poor connections, corrosion and fluctuating loads would certainly cause breakage in individual wires in a progressive manner and would eventually lead to the collapse of the whole cable within a limited number of years (Phoenix, et al., 1986.) In most cases lower end sockets are found to deteriorate at a faster rate due to the accumulation of water from the upper sections of the cable.

Cable fatigue is a more serious problem in the case of railway bridges or roadway bridges with light steel decks. This is due to higher stress amplitudes.

Birkenmaier and Narayan (1982) studied the performance of parallel-wire strands under repeated loading and recommended the following equations for the applicable Wöhler curve.

$$\text{Log } \Delta\sigma = - \frac{1}{4.5} \text{Log } N + 3.710 \quad N \leq 10^6 \quad [3.1]$$

$$\text{Log } \Delta\sigma = - \frac{1}{8} \text{Log } N + 3.127 \quad N > 10^6 \quad [3.2]$$

Where:

$\Delta\sigma$ is the permissible stress range, and;

N is the maximum number of cycles.

Equations [3.1] and [3.2] are approximate in nature and should be used with caution. The European Codes recommend that the stress range for a bridge be limited to $\Delta\sigma = 218$ MPa, which corresponds to 2×10^6 cycles (Gimsing, 1983).

To estimate the life expectancy of the cables in a multi-stay bridge, a number of actual service load cases with average intensities and high frequencies of occurrence are used to calculate the range of stress variations in the cables. Then, these stress variations with their corresponding frequencies are compared to the values from the Wöhler curve in order to arrive at a reasonable life expectancy for the cables. Table 3.2, in which N has been computed from [3.1] and [3.2] for various stress ranges, shows an example of this type of computation.

c) Relaxation

Cable relaxation becomes many times more significant when the tensile

stress due to permanent loads exceed 50% of the ultimate tensile strength (Gimsing, 1983). It is therefore advisable to ensure that the cable stresses due to dead load is limited to a maximum of $0.45f_u$.

3.3. The Catenary Cable

The problem of a suspended cable subjected to its weight and any other type of static forces has been accurately solved by O'Brien (1967) and a number of other investigators. Using the notations of Fig. 3.2a, the basic equations of a catenary are derived in Appendix B and cable can be summarized as follows.

$$L = \frac{a}{\lambda} \sqrt{s^2 \lambda^2 + \sinh^2 \lambda} \quad [3.3]$$

$$V_B = \frac{w}{2} (b \coth \lambda + L) \quad [3.4]$$

$$V_A = \frac{w}{2} (b \coth \lambda - L) \quad [3.5]$$

$$H = V_B / \sinh (\phi - 2\lambda) \quad [3.6]$$

$$y = \frac{2H}{w} \sinh \lambda \sinh (\phi - \lambda) \quad [3.7]$$

$$\begin{aligned} \Delta L &= L - L_0 \\ &= \frac{HL^2}{aAE} \left[\lambda \coth \lambda - \frac{a^2}{2L^2} \left(\frac{\sinh 2\lambda}{2\lambda} - 1 \right) \right] \end{aligned} \quad [3.8]$$

where:

$$s = b / a \quad [3.9]$$

$$\lambda = wa / 2H \quad [3.10]$$

$$\phi = \lambda + \sinh^{-1} \frac{s\lambda}{\sinh \lambda} \quad [3.11]$$

$$w = \gamma A$$

[3.12]

The above set of equations contain nine basic variables which are listed below.

- L_0 The unstressed length
- a The horizontal distance between the two ends
- b The vertical distance between the two ends
- γ The weight per unit length (density)
- A The cross-sectional area
- E The modulus of elasticity of a short piece of the cable
- V_A The vertical component of the lower end tension
- V_B The vertical component of the upper end tension
- H The horizontal component of the end tensions

In order to solve a catenary problem, six of the above variables must be specified before the other three can be found by solving these equations. Moreover, the solution is usually numerical and iterative as it involves the evaluation of a number of hyperbolic functions.

As for the application of the above equations to a cable-stayed bridge, one of the following two algorithms may be used, depending on the situation.

a) Algorithm 1 This is for the case of the reference configuration where the following particulars of the cables are known.

- End coordinates: From which a and b can be calculated.
- Cross-sectional area, A .
- Modulus of elasticity for the straight cable, E .
- Weight per unit length, w .

-Vertical reaction at the point of attachment to the girder, V_A .

In this case the following algorithm can be used to compute the other three variables, namely: the horizontal reaction, H ; the vertical reaction at the tower, V_B ; and the unstressed length, L_0 .

1. $s = b / a$
2. $H_p = (V_A + \frac{\gamma A a \sqrt{1 + s^2}}{2}) / s$ (Parabolic approximation. See, for example, Odenhausen, 1965.)
3. $\lambda_0 = w a / 2H_p$
4. $\lambda = \lambda_0$
5. $H = w a / 2\lambda$
6. $L = \frac{a}{\lambda} \sqrt{s^2 \lambda^2 + \sinh^2 \lambda}$
7. $\lambda_n = \coth^{-1} \left(\frac{2V_A}{wb} + \frac{L}{b} \right)$
8. $\Delta\lambda = \lambda - \lambda_n$
9. $\lambda = \lambda_n$
10. If $\Delta\lambda < \text{error limit}$, go to 10. Otherwise, go to 5.
11. $\Delta L \cong \frac{HL^2}{aAE} \left[\lambda \coth \lambda - \frac{1}{2} \left(\frac{a}{L} \right)^2 \left(\frac{\sinh 2\lambda}{2\lambda} - 1 \right) \right]$
12. $L_0 = L - \Delta L$
13. $V_B = wL_0 - V_A$

A flowchart of this algorithm is shown in Fig.3.3.

b) Algorithm 2 This is for situation in which a , b , w , E , A and L_0 are given. The following algorithm may be used to obtain the other three variables, V_A , V_B , and H .

1. $s = b / a$
2. $H_p = (V_A + \frac{\gamma A a \sqrt{1 + s^2}}{2}) / s$ (Parabolic approximate
3. $\lambda_0 = w a / 2H_p$ solution. See note on p. 8.)
4. $\lambda = \lambda_0$
5. $H = w a / 2\lambda$
6. $\Delta L = \frac{HL_0^2}{aAE} \left[\lambda \coth \lambda - \frac{1}{2} \left(\frac{a}{L_0} \right)^2 \left(\frac{\sinh 2\lambda}{2\lambda} - 1 \right) \right]$
7. $L = L_0 + \Delta L$
8. $\lambda_n = \sinh^{-1} \left(\lambda \sqrt{\frac{L^2 - b^2}{2}} \right)$
9. $\Delta \lambda = \lambda - \lambda_n$
10. $\lambda = \lambda_n$
11. If $\Delta \lambda < \text{error limit}$, go to 12. Otherwise, go to 5.
12. $\phi = \lambda + \sinh^{-1} \frac{s\lambda}{\sinh \lambda}$
13. $V_B = H \sinh (\phi - 2\lambda)$
14. $V_A = wL_0 - V_B$

In either case the cable end tensions can be calculated from:

$$T_A = \sqrt{H^2 + V_B^2} \quad [3.13]$$

$$T_B = \sqrt{H^2 + V_A^2} \quad [3.14]$$

The flowchart of Fig. 3.4 is for the numerical computation of an incremental cable stiffness matrix using the exact catenary equations and determining stiffness coefficients as the change in end forces produced by increments in the coordinates of the end points. The algorithm above is the inner loop for this process.

3.4 Cable Stiffness Matrix

Equations [3.3] through [3.14] show that V_A , V_B and H are transcendental implicit functions of a , b , L_0 , E , A , and w . For a given catenary cable for which L_0 , E , A , and w are known constants, it should, therefore, be possible to find the partial derivatives of V_A , V_B , and H with respect to a and b and to use them as stiffness coefficients in the cable stiffness matrix.

However, due to the nonlinearity of the relationships, and the fact that the catenary problem has to be solved numerically prior to the computations for the stiffness matrix (the stiffness is dependent on the cable tension T), it was decided to form the stiffness matrix numerically. To this end, a and b are incremented independently, and the corresponding increments of V and H are computed by solving the catenary problem, using Algorithm 2 of Section 3.3, for each increment. The matrix incremental equations of equilibrium for the cable ends after the application of these displacements may be shown as (Fig. 3.2b):

$$\begin{Bmatrix} \Delta V \\ \Delta H \end{Bmatrix} = \begin{bmatrix} \frac{\Delta V}{\Delta b} & \frac{\Delta V}{\Delta a} \\ \frac{\Delta H}{\Delta b} & \frac{\Delta H}{\Delta a} \end{bmatrix} \begin{Bmatrix} \Delta b \\ \Delta a \end{Bmatrix} \quad [3.15]$$

Using a transformation matrix $[T]$, [3.15] can be written in terms of the global displacement vector $\{\Delta r\}$ containing the six degrees of freedom shown

in Fig. 3.2a, as

$$\begin{Bmatrix} \Delta V \\ \Delta H \end{Bmatrix} = \begin{bmatrix} \frac{\Delta V}{\Delta b} & \frac{\Delta V}{\Delta a} \\ \frac{\Delta H}{\Delta b} & \frac{\Delta H}{\Delta a} \end{bmatrix} [T] \{\Delta r\} \quad [3.16]$$

in which,

$$[T] = \begin{bmatrix} 0 & -1 & 0 & 0 & 1 & 0 \\ 0 & 0 & -1 & 0 & 0 & 1 \end{bmatrix} \quad [3.17]$$

Similarly the global force vector $\{\Delta R\}$ is related to ΔV and ΔH through

$$\{\Delta R\} = [T]^T \begin{Bmatrix} \Delta V \\ \Delta H \end{Bmatrix} \quad [3.18]$$

Substituting [3.16] in [3.18] yields

$$\{\Delta R\} = [T]^T \begin{bmatrix} \frac{\Delta V}{\Delta b} & \frac{\Delta V}{\Delta a} \\ \frac{\Delta H}{\Delta b} & \frac{\Delta H}{\Delta a} \end{bmatrix} [T] \{\Delta r\} \quad [3.19]$$

in which the stiffness matrix [K] for the cable is represented by

$$[K] = [T]^T \begin{bmatrix} \frac{\Delta V}{\Delta b} & -\frac{\Delta V}{\Delta a} \\ \frac{\Delta H}{\Delta b} & -\frac{\Delta H}{\Delta a} \end{bmatrix} [T] = \begin{matrix} & \begin{matrix} 1 & 2 & 3 & 4 & 5 & 6 \end{matrix} \\ \begin{matrix} 1 \\ 2 \\ 3 \\ 4 \\ 5 \\ 6 \end{matrix} & \begin{bmatrix} 0 & 0 & 0 & 0 & 0 & 0 \\ 0 & \gamma & \delta & 0 & -\gamma & -\delta \\ 0 & \beta & \alpha & 0 & -\beta & -\alpha \\ 0 & 0 & 0 & 0 & 0 & 0 \\ 0 & -\gamma & -\delta & 0 & \gamma & \delta \\ 0 & -\beta & -\alpha & 0 & \beta & \alpha \end{bmatrix} \end{matrix} \quad [3.20]$$

where:

$$\alpha = \frac{\Delta H}{\Delta a} \qquad \beta = \frac{\Delta H}{\Delta b}$$

$$\delta = \frac{\Delta V}{\Delta a} \qquad \gamma = \frac{\Delta V}{\Delta b}$$

It is to be noted that, in general, a numerical solution gives β slightly different from δ , which means, the stiffness matrix is asymmetric. However, this difference decreases sharply with the reduction of cable sag and for all practical purposes a symmetric stiffness matrix with the following formulation may be used.

$$[K] = \begin{matrix} & \begin{matrix} 1 & 2 & 3 & 4 & 5 & 6 \end{matrix} \\ \begin{matrix} 1 \\ 2 \\ 3 \\ 4 \\ 5 \\ 6 \end{matrix} & \begin{bmatrix} 0 & 0 & 0 & 0 & 0 & 0 \\ 0 & \gamma & \delta & 0 & -\gamma & -\delta \\ 0 & \delta & \alpha & 0 & -\delta & -\alpha \\ 0 & 0 & 0 & 0 & 0 & 0 \\ 0 & -\gamma & -\delta & 0 & \gamma & \delta \\ 0 & -\delta & -\alpha & 0 & \delta & \alpha \end{bmatrix} \end{matrix} \quad [3.21]$$

Fig. 3.4 shows a flowchart for the computation of the stiffness matrix for a catenary cable.

3.5 Cable Forces in the Reference Configuration

Section 1.7 demonstrates that it is possible to specify independently the geometric configuration and the internal force system for a cable-stayed bridge under its dead load. This gives the designer considerable freedom to select a desirable geometry combined with an optimal force distribution (i.e. bending moments distribution) in the girders. Moreover, when this is done, a cable-stayed bridge with a high degree of indeterminacy is reduced to a determinate system from which the cable forces are computed from simple static equations. These cable forces plus the dead load are then reapplied to the structure as the first load case to compute the actual internal forces in all the elements.

Figure 3.5 shows the centroidal axes of simulated girder segments of a cable-stayed bridge between nodes $i-1$ and $i+1$. The uniformly distributed load of q_1 represents dead load per unit length of the girder measured along its centroidal axis. Cable tensions are shown by T_1 and form angle ϕ_1 with the horizontal direction. The girder is assumed to be composed of a number of straight segments making angle α_1 with the global X axis. Using the notation of Fig. 3.5., equilibrium of joint i requires

$$T_1 \sin \phi_1 = V_{1,i-1} + V_{1,i+1} \quad [3.22]$$

$$T_1 \cos \phi_1 = -H_{1,i-1} + H_1 \quad [3.23]$$

Summing moments about node $i + 1$

$$-\Delta X_1 V_{1,i+1} + q_1 L_1 \frac{\Delta X_1}{2} + H_1 \Delta Y_1 + M_1 - M_{i+1} = 0 \quad [3.24]$$

from which

$$V_{1,i+1} = q_1 L_1 / 2 + H_1 \tan \alpha_1 + \frac{M_1 - M_{i+1}}{L_1 \cos \alpha_1} \quad [3.25]$$

Summing moments about node $i - 1$

$$\Delta X_{1-1} V_{1,i-1} - q_{1-1} L_{1-1} \frac{\Delta X_{1-1}}{2} + H_{1-1} \Delta Y_{1-1} + M_{1-1} - M_1 = 0 \quad [3.26]$$

from which

$$V_{1,i-1} = q_{1-1} L_{1-1} / 2 + \frac{M_1 - M_{1-1}}{L_{1-1} \cos \alpha_{1-1}} - H_{1-1} \tan \alpha_{1-1} \quad [3.27]$$

Substituting [3.25] and [3.27] into [3.22] and solving for T_1 yields

$$T_1 = \frac{1}{\sin \phi_1} \left\{ \frac{q_{1-1} L_{1-1} + q_1 L_1}{2} + \frac{M_1 - M_{1-1}}{L_{1-1} \cos \alpha_{1-1}} + \frac{M_1 - M_{i+1}}{L_1 \cos \alpha_1} + H_1 \tan \alpha_1 - H_{1-1} \tan \alpha_{1-1} \right\} \quad [3.28]$$

And from [3.23], after substituting T_1 from [3.28] and solving for H_{1-1}

$$H_{i-1} = H_i \frac{\tan \alpha_i - \tan \phi_i}{\tan \alpha_{i-1} - \tan \phi_i} + \frac{1}{\tan \alpha_{i-1} - \tan \phi_i} \left[\frac{q_{i-1} L_{i-1} + q_i L_i}{2} + \frac{M_i - M_{i-1}}{L_{i-1} \cos \alpha_{i-1}} + \frac{M_i - M_{i+1}}{L_i \cos \alpha_i} \right] \quad [3.29]$$

Now H_{i-1} can be substituted in [3.28] to find

$$T_i = \left[\left(\frac{q_{i-1} L_{i-1} + q_i L_i}{2} + \frac{M_i - M_{i-1}}{L_{i-1} \cos \alpha_{i-1}} + \frac{M_i - M_{i+1}}{L_i \cos \alpha_i} \right) \left(\frac{\tan \phi_i}{\tan \phi_i - \tan \alpha_{i-1}} \right) + H_i \frac{\tan \phi_i (\tan \alpha_i - \tan \alpha_{i-1})}{\tan \phi_i - \tan \alpha_{i-1}} \right] \left(\frac{1}{\sin \phi_i} \right) \quad [3.30]$$

Equation [3.30] can be used to compute the tension in the cable attached to the girder at node i , provided that the moments at nodes $i-1$, i and $i+1$ are known.

The term in [3.30] containing the horizontal force H_i requires more explanation. In a major highway the angle α which represents the road gradient, and its variation which represents the curvature of the vertical connecting curves are subject to regulatory restrictions depending on the design speed of the highway. For a design speed of 100 km/hr, the Roads and Transportation Association of Canada, RTAC (1986), recommends a maximum gradient of 5% and a parabolic connection curve of 700 m for the case of a crest vertical curve which is shown in Fig. 3.5a. For such a curve, the average change of angle per unit length is

$$\Delta\alpha \cong 10\% / 700 = 1.5 * 10^{-4} \text{ (1/ m)} \quad [3.31]$$

Assuming an average cable spacing of 10 m (9 m in the Annacis Bridge) along the girders

$$\tan \alpha_1 - \tan \alpha_{1-1} \cong 1.5 * 10^{-4} * 10 \cong 0.0015 \quad [3.32]$$

It is reasonable to assume that the critical combination of the horizontal force H and the angle α , which represents the vertical curvature of the girder will occur in the first quarter of the central span where there is a substantial amount of axial force and a moderate amount of vertical curvature. Assuming H to be in the order of $6T_1$ and $\sin \phi_1 \cong 0.6$ the critical magnitude of the term containing H_1 in [3.30] may be estimated from

$$0.0015 * 6 T_1 / 0.6 \cong 0.015 T_1 \quad [3.33]$$

Knowing that H_1 is maximum near the towers where $\sin \phi_1 \cong 1$, it can be concluded that the contribution of this term to the cable forces is about 1.5% of the cable tension under worst conditions. If a bridge is horizontal or its slope is constant, this term will completely vanish. In the majority of cable-stayed bridges the contribution of this term to cable forces would be less than 1% and is, therefore, neglected in the computations. This approximation has no effect on the actual internal force computations in the reference configuration because the computed T_1 from [3.30] are applied to the bridge as external forces to produce the reference configuration bending moments. Therefore, after applying the forces T_1 to the bridge, the

actual values of moments are computed for the precise reference configuration to which other configurations are referred.

Neglecting the effect of the horizontal force H, [3.30] becomes

$$T_1 = \left(\frac{q_{1-1}L_{1-1} + q_1L_1}{2} + \frac{M_1 - M_{1-1}}{L_{1-1} \cos \alpha_{1-1}} + \frac{M_1 - M_{1+1}}{L_1 \cos \alpha_1} \right) \frac{1}{\sin(\phi_1 - \alpha_1)}$$

[3.34]

Subroutine DLBM of Fig. 3-6 uses the term in large brackets of [3.34] to compute the vertical girder reactions at the cable ends shown by RM. These vertical reactions are then multiplied by the remaining term of [3.34] to obtain the cable forces.

Once cable forces are found, Algorithm 1 of Section 3.3 is used to find the unstressed cable length L_0 .

3.6 Cable Nonlinearity

A very good approximation for the effective modulus of elasticity of a catenary cable is (Leonhardt and Zellner, 1970)

$$E_c = \frac{E}{1 + \frac{E \gamma^2 a^2}{12 \sigma^3}}$$

[3.35]

where σ is the cable tensile stress.

Using the representative values of

$$E = 180000 \text{ MPa}$$

$$\gamma = 0.000078 \text{ N / mm}^3$$

$$a = 250000 \text{ mm (Slightly greater than the horizontal projection of the longest cable in the Annacis Bridge.)}$$

in [3.35] results in

$$E_c / E = \frac{1}{1 + \frac{5703750}{\sigma^3}} \quad [3.36]$$

Equation [3.36] is plotted as a function of σ in Fig. 3.7.

As Fig. 3.7 shows, at a tensile stress of 460 MPa the cable has an effective modulus of approximately 95% of its maximum modulus of elasticity, E . Considering that most cable stayed-bridges are designed for cable stresses of the order of $0.45f_u \cong 750$ MPa (See Section 3.2c) under their service load, it follows that the geometrical nonlinearity of the cables may be disregarded in the analysis of the reference configuration of the bridge and in the live load analysis.

Conversely, during erection cables are subjected to fluctuating tensile stresses which may change from zero to their material limit of proportionality. Consequently, their effective modulus of elasticity may also change from zero to its maximum value of E . This means that there is a greater degree of geometrical nonlinearity in the performance of the cables in the partial structures, while the bridge is being erected, than in the completed bridge.

To account for this nonlinearity, the erection part of the program uses an iterative procedure based on the updating of the cables' tensions and their stiffness matrices in order to achieve joint equilibrium. A complete account of the special provisions for this nonlinearity, as well as the other types of nonlinearities considered in the program, is presented in Chapter 6.

Table 3.1 Typical Cables Properties

PROPERTY \ TYPE OF CABLE	PARALLEL BARS 26 - 16 MM	PARALLEL WIRES 128 - 7 MM	PARALLEL STRANDS (OF TWISTED WIRES) 27 - 17 MM	LOCKED-COIL CABLE (DIFFERENT SIZES)
ULTIMATE TENSILE STRENGTH (MPa)	1500	1670	1770 - 1870	1000 - 1300
0.2% PROOF STRESS (MPa)	1350	1470	1570 - 1670	-
MODULUS OF ELASTICITY (MPa)	210000	205000	190000 - 200000	160000 - 165000
FAILURE LOAD (KN)	7624	7487	7634	7310
SERVICE LOAD @ 45% OF ULTIMATE (KN)	3431	3369	3435	3290

(*) Adapted from Rene Walther, et al. (1988)

Table 3.2 An Example of Fatigue Life Computations

Load Case Number	Estimated Frequency Per Year	Computed Stress Range (MPa)	Total Permissible Frequency	Estimated Life (Year)
1	25000	200	4000000	160
2	40000	150	40000000	1000
3	200000	125	174000000	870
4	20000	220	1900000	95
5	1000	300	155000	155
6	450000	100	100000000	2300

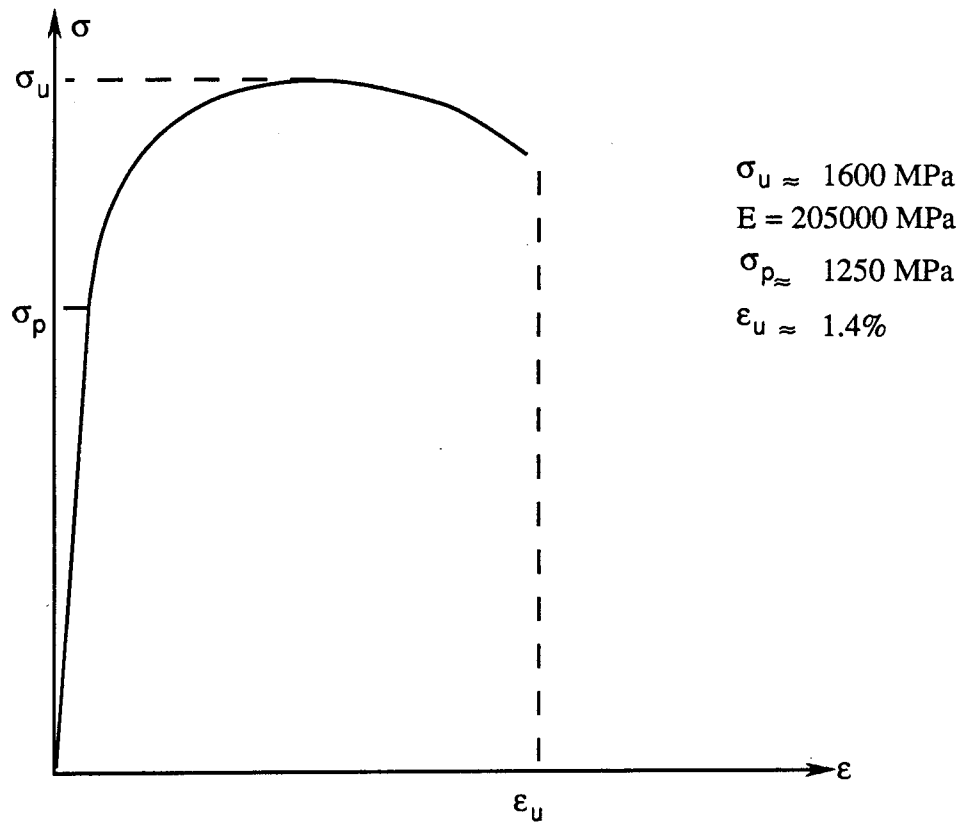
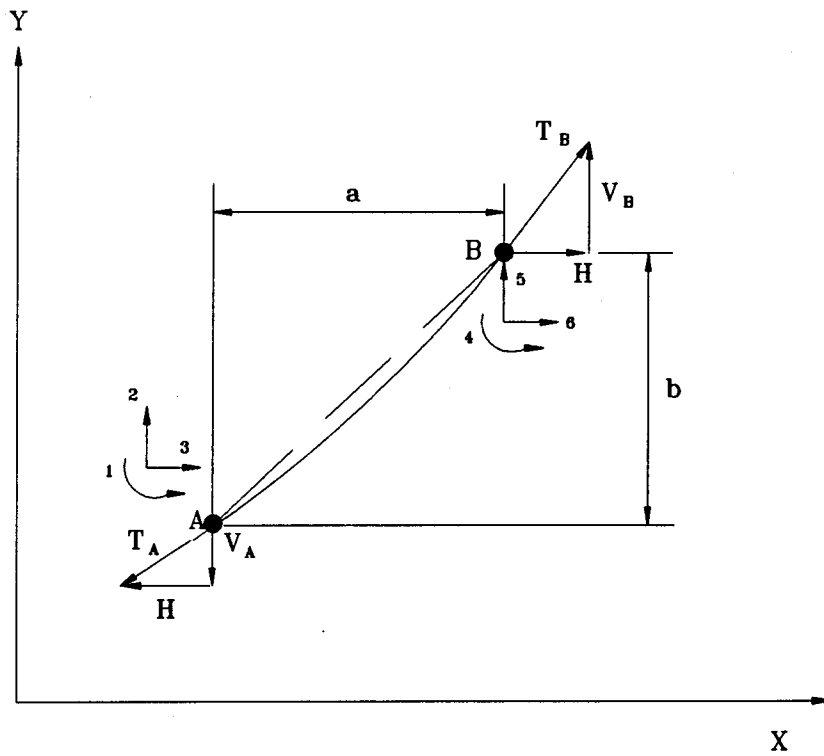
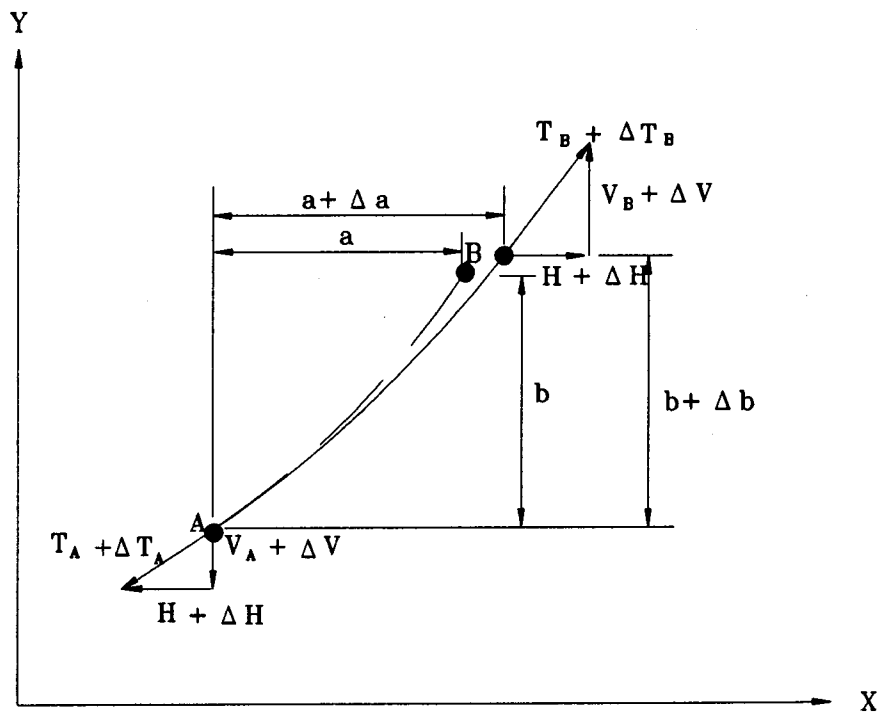


Figure 3.1 Stress-Strain Diagram for a Wire



(a) A cable element with 6 DOF



(b) Same cable element subjected to Δa & Δb

Figure 3.2 A Catenary Cable Element

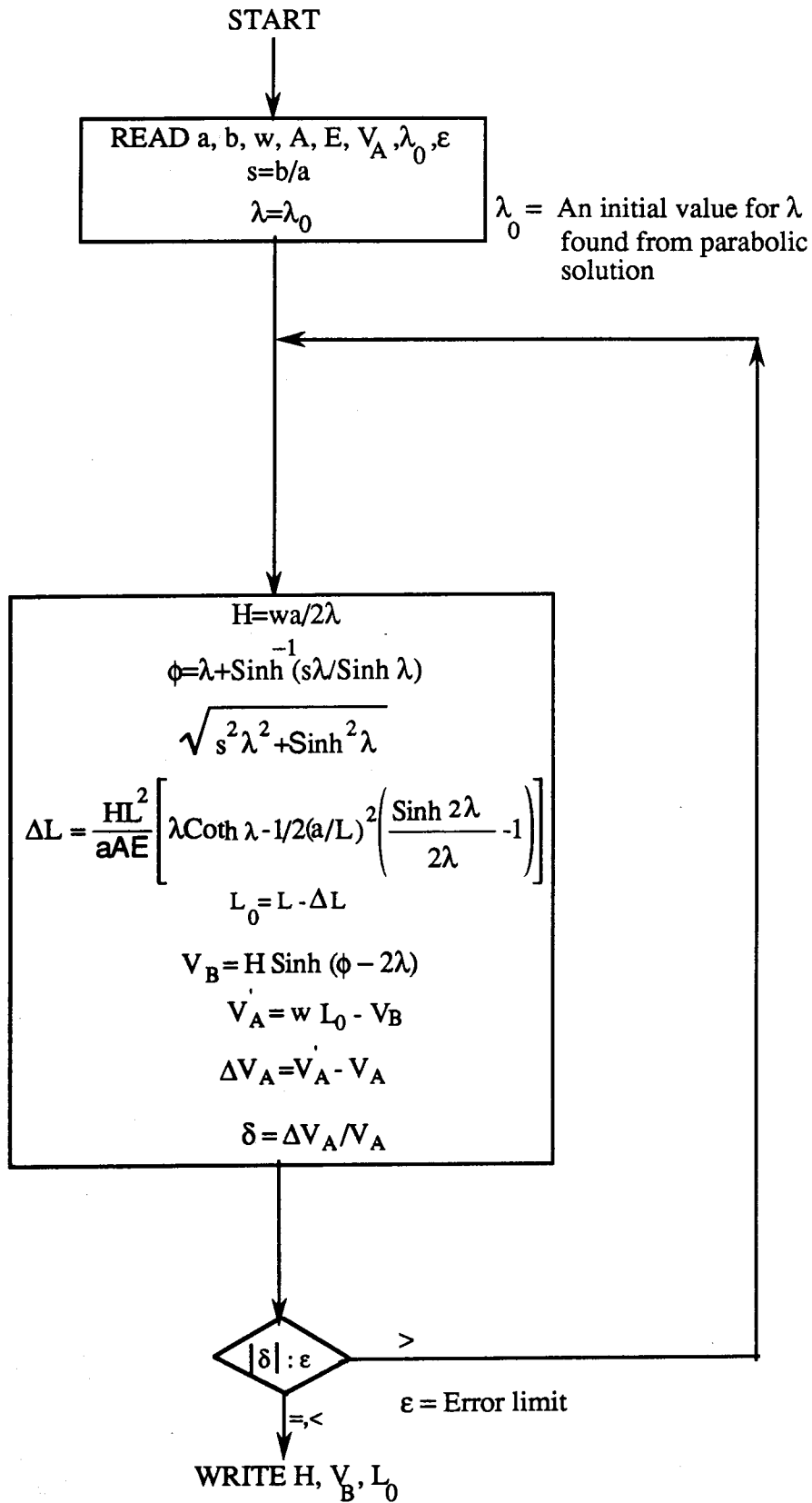


Figure 3.3 Flow Chart for Computation of H, V_B and L_0 for a Catenary Cable

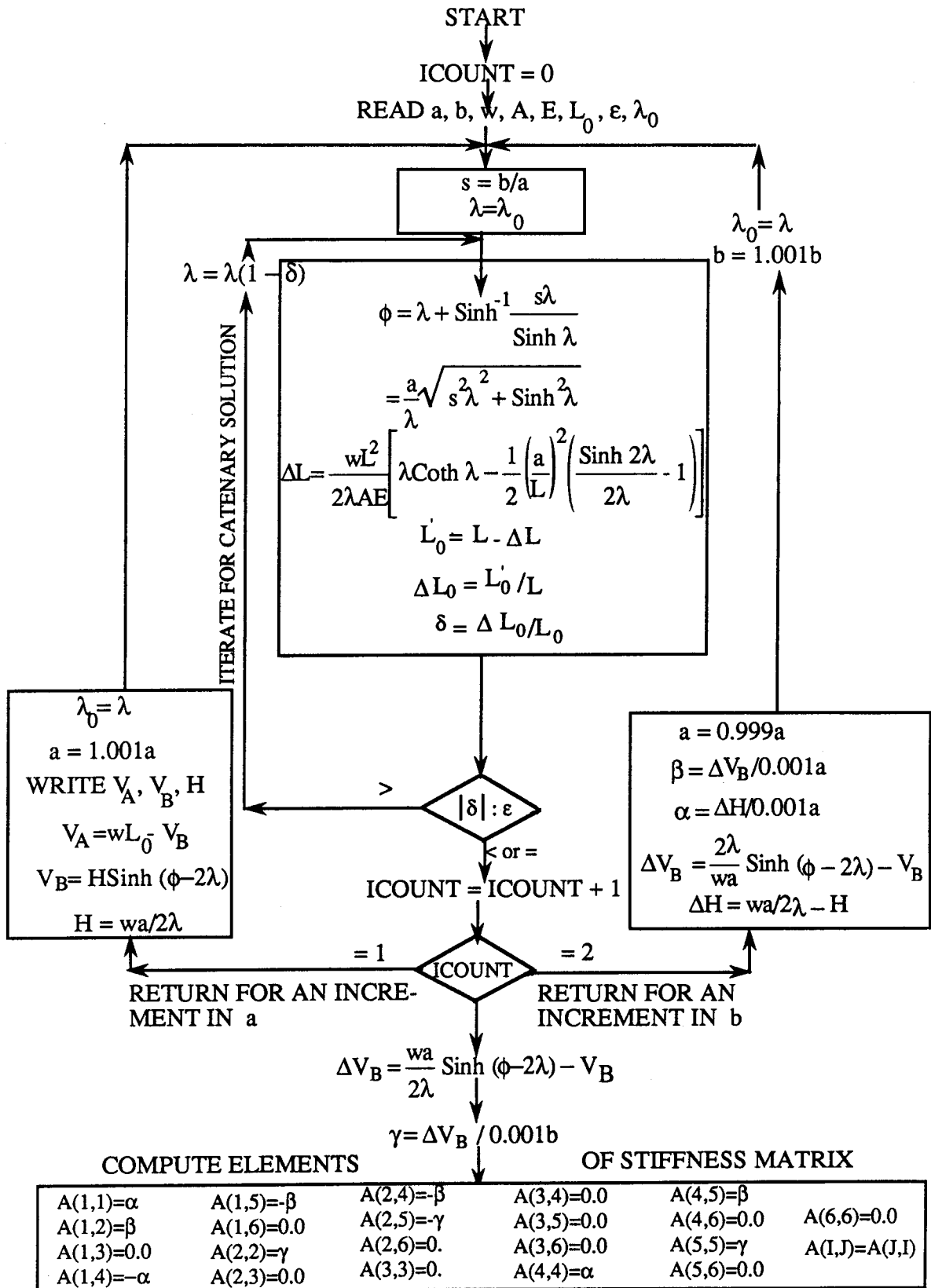
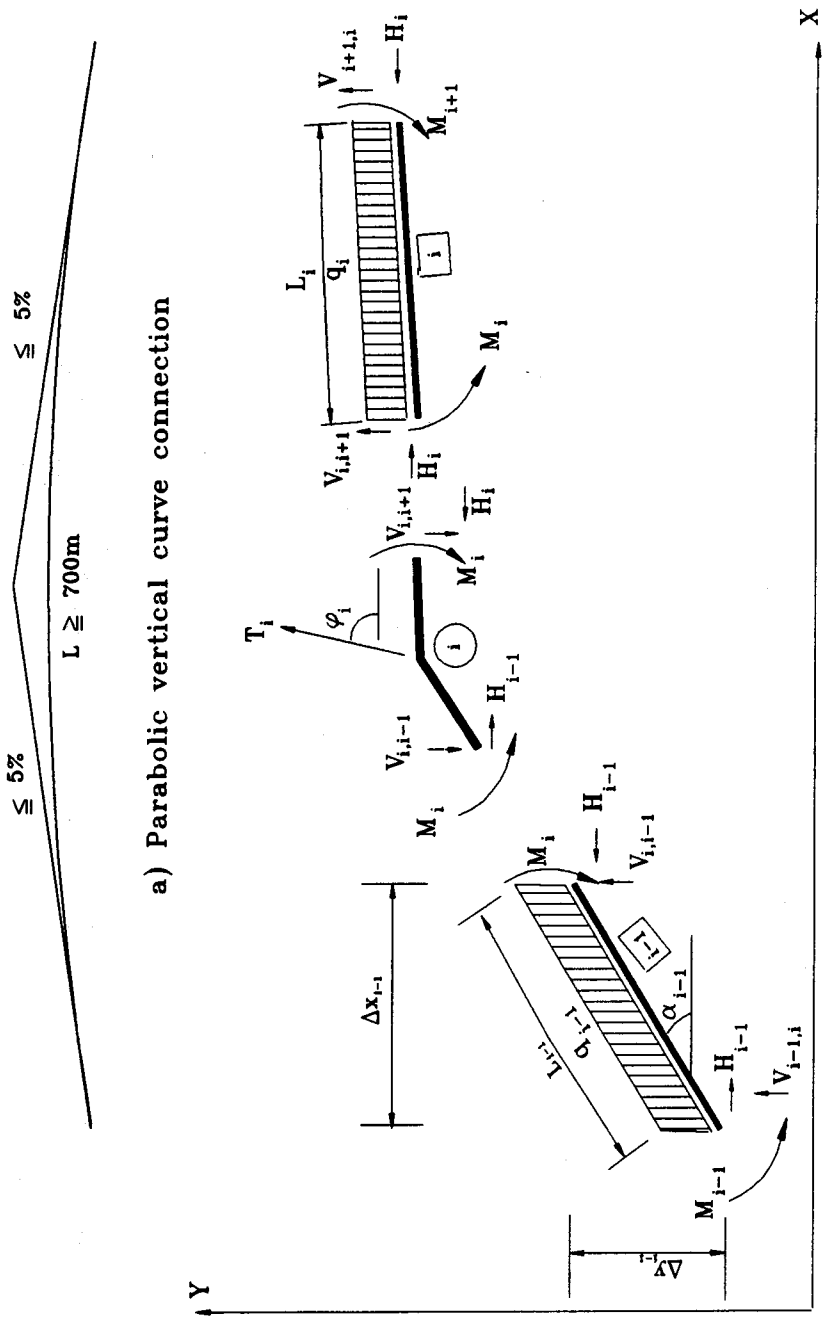


Figure 3.4 Flow Chart for Computation of H, V_B, V_A, & Stiffness Matrix Coefficients for a Catenary Cable



b) Cable force at node i

Figure 3.5 Computation of Cable Forces in the Reference Configuration

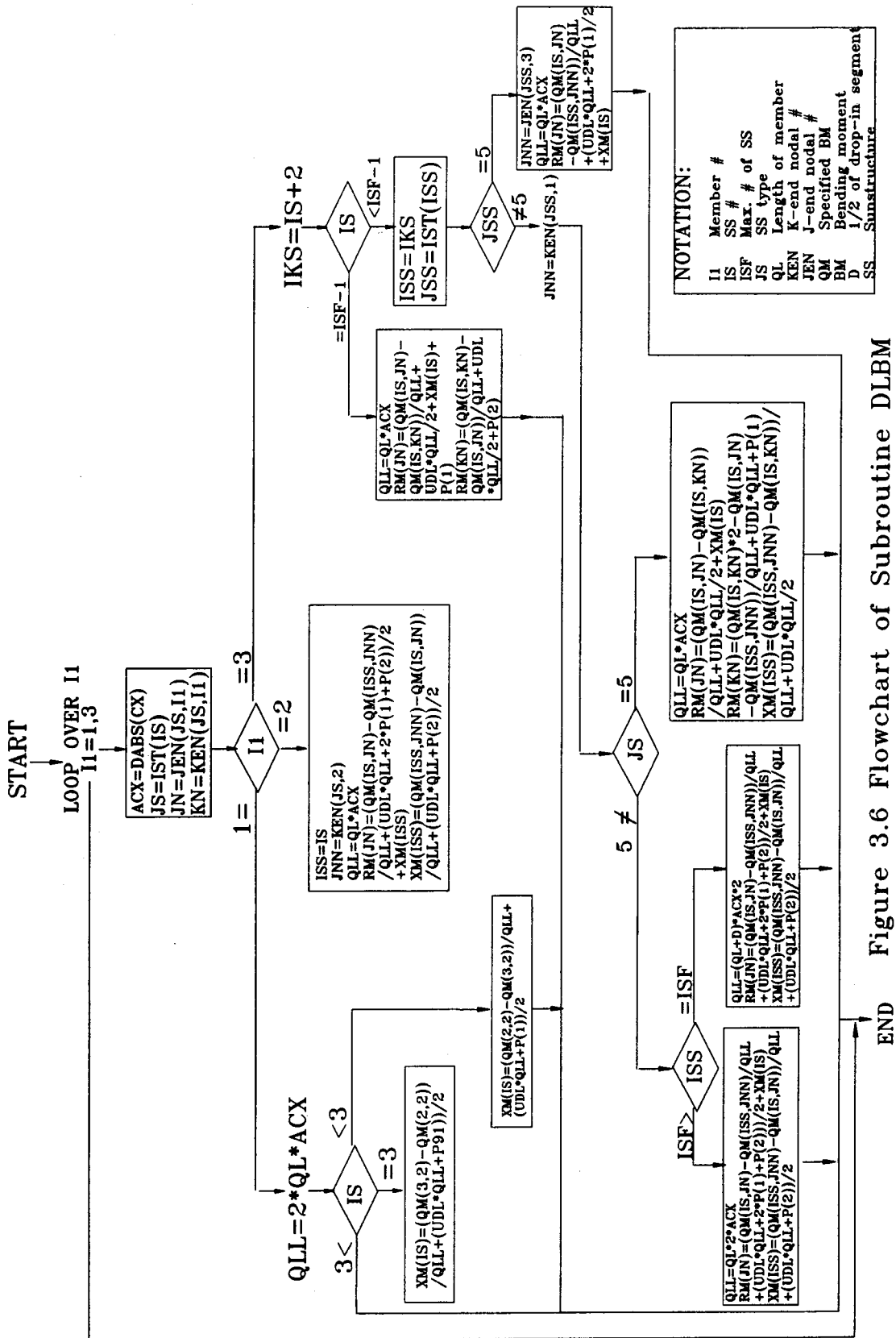


Figure 3.6 Flowchart of Subroutine DLBM

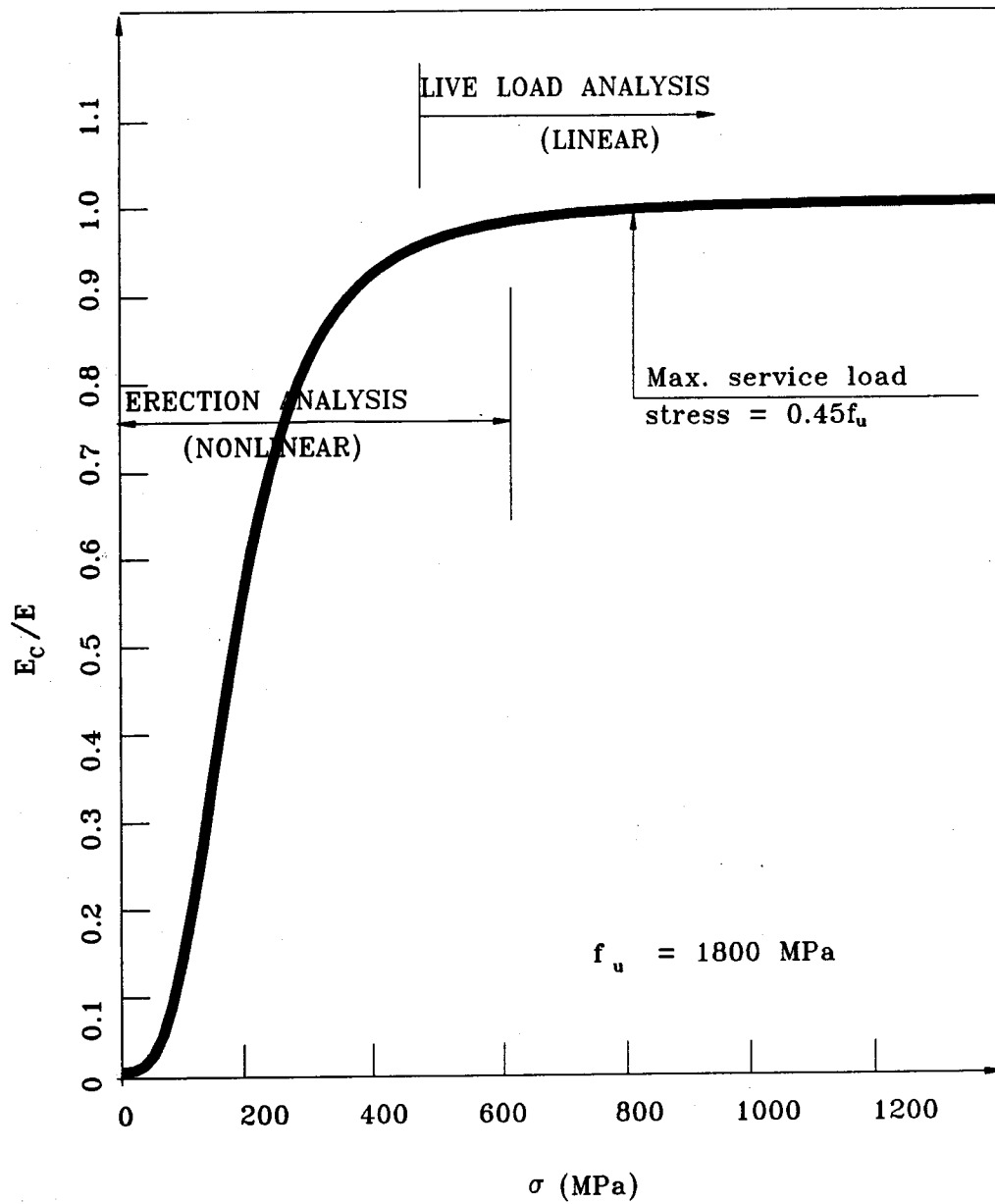


Figure 3.7 Variation of Effective Modulus of Elasticity of a Cable with its Tensile Stress

CHAPTER 4 : DEVELOPMENT OF THE LINEAR ROUTINES

4.1 Introduction

Any structural analysis program is built around a central unit, a core, which handles the linear analysis of the problem and produces the basic values, such as joint displacements, used by other complementary sections of the program. This central unit occupies a substantial space in the computer memory and is used repeatedly. Therefore, its efficiency in terms of memory requirements and CPU time is of great importance to the overall efficiency of the whole program.

Normally, it is possible to adopt a standard linear analysis package and incorporate it into a more elaborate program without sacrificing too much efficiency. Occasionally, severe hardware limitations may dictate a specially designed linear routine which, for instance, uses less computer memory but more CPU time.

The program developed in this study has been called CASBA, which is an acronym for CAble Stayed Bridge Aalysis. In the case of CASBA an attempt has been made to design a special linear analysis routine which would satisfy the following requirements.

1. It would take advantage of the modular components of cable-stayed bridges.
2. It would efficiently handle the continuously changing shape of the sequential partial structures which must be analysed during the erection of a cable-stayed bridge.

3. Its computer memory requirements would be minimal so that the complete program with its graphics facilities may be run on an AT microcomputer.
4. It would easily assess the effects of variations in cable lengths, addition or deletion of bracing sets, placement of counterweights, etc., at any stage of the erection process.

The present Chapter deals, in some detail, with the development of this basic unit and with its major subroutines as they are set out in Fig. 4.1.

4.2 An Overview of The Solution Technique

In CASBA the three basic operations of assembly, reduction and backsubstitution of the joint equations of equilibrium are based on the combined principles of the frontal and the substructure techniques. The frontal solution technique (Irons, 1970; Hinton and Owens, 1977) is a very effective means of forming and solving the matrix equations of structural problems, especially when core storage is restricted. Unlike banded-matrix solutions, which are nodal numbering dependent, frontal solutions use the prescribed order of members as the main index of their operations. Therefore, new members may be added to an existing structure without renumbering, provided that the prescribed order of the members already in place is not altered. Both of these two features are highly beneficial for the erection analysis of a cable-stayed bridge by a microcomputer in which a series of partial structures are analysed under memory restriction.

In the standard frontal technique members are assembled one at a time into the stiffness matrix according to a prescribed order. A relatively elaborate scheme, called the prefront process, determines when a degree of

freedom is ready for elimination and how the new degrees of freedom are linked to the ones already in the active array. This rigorous housekeeping arrangement is suitable for a general finite element or frame program where structures of arbitrary shape and a large number of elements of various shapes are assembled into the structural stiffness matrix.

In the special case of a cable-stayed bridge which has modular units and simple connectivity, a simpler procedure performing the same functions as the prefront can be devised. The method consists of identifying a small number of substructure types with a fixed pattern of numbering, which are assembled one at a time and according to a prescribed order to make the partial structures and, finally, the complete structure. Here, the condensable degrees of freedom will be known a priori by the substructure type and the connectivity will become automatic by the repetition of a simple nodal numbering system. Section 4.3 will deal with these substructure types and their automatic linking arrangement. It is to be noted that the technique is equally applicable to any structure for which a limited number of substructure types can be identified and a nodal numbering system with the requirements laid down in Section 4.4 can be devised.

The matrix formulation of substructure analysis with a variety of algorithms for computer implementation has been presented by many authors. Elwi and Murray (1985) use the Cholesky method for the partial decomposition of the resulting submatrices stored in skyline form. In the present work the Gaussian elimination technique has been employed to decompose the matrices of each partial structure and the reduced coefficients are then stored in a linear array identified with the sequential number of the partial structure. The following matrix equations

are the symbolic representation of the basic operations involved in this solution procedure (Gallagher,1975).

Denoting the structural stiffness matrix by $[A]$, the nodal displacements by $\{r\}$, and the applied forces by $\{R\}$ the equilibrium equations are written in the form

$$\begin{bmatrix} [A]_{CC} & [A]_{CF} \\ [A]_{FC} & [A]_{FF} \end{bmatrix} \begin{Bmatrix} \{r\}_C \\ \{r\}_F \end{Bmatrix} = \begin{Bmatrix} \{R\}_C \\ \{R\}_F \end{Bmatrix} \quad [4.1]$$

in which the 'condensable' degrees of freedom are denoted by the subscript C and the front interboundary degrees of freedom are denoted by the subscript F. (See Section 4.4 for a precise definition of these terms.)

Solving the upper partition for $\{r\}_C$ yields

$$\{r\}_C = [A]_{CC}^{-1} (\{R\}_C - [A]_{CF} \{r\}_F) \quad [4.2]$$

Substituting [4.2] into the lower partition of [4.1] yields

$$([A]_{FF} - [A]_{FC} [A]_{CC}^{-1} [A]_{CF}) \{r\}_F = \{R\}_F - [A]_{FC} [A]_{CC}^{-1} \{R\}_C \quad [4.3]$$

Defining the new stiffness matrix as

$$[\bar{A}]_{FF} = [A]_{FF} - [A]_{FC} [A]_{CC}^{-1} [A]_{CF} \quad [4.4]$$

and the new load vector as

$$\{\bar{R}\}_F = \{R\}_F - [A]_{FC} [A]_{CC}^{-1} \{R\}_C \quad [4.5]$$

[4.3] becomes

$$[\bar{A}]_{FF} \{r\}_F = \{\bar{R}\}_F \quad [4.6]$$

in which $\{\bar{R}\}_F$ is the load vector associated with the front interboundary degrees of freedom, and $[\bar{A}]_{FF}$ is the effective stiffness matrix for these degrees of freedom.

It can be shown (see, for instance, Elwi and Murray, 1985) that the stiffness matrix and load vector in [4.6] are identical with those formed by a partial reduction, in which elimination is carried out only for the pivots in $[A]_{CC}$. Consequently, the matrix $[\bar{A}]_{FF}$ is the matrix retained in the active array subsequent to the partial reduction.

4.3 Substructure Types

Using substructures to assemble the stiffness matrix of a cable-stayed bridge has the following two advantages:

- a) The assembly corresponds to the actual erection sequence of the bridge.
- b) It provides all the reduced matrices which are required for backsubstitution in the analysis of the partial structures which occur during disassembly from a specified reference configuration.

However, the standard substructure analysis requires that the user specify each of the sets of global and substructural numbering, and an array to link the two together, a type of manual work which may not suit a user oriented program. In order to solve this problem and to devise a

mechanism by which the frontal solution may be implemented without the prefront process, a limited number of substructure types can be defined which depict the shape of all the substructures required to assemble a standard cable-stayed bridge. The five substructure types which are required are shown in Table 4.1.

An illustration of how these substructure types are assembled into partial structures is shown in Table 4.2. The link between each substructure to be assembled into the bridge and its substructure type is provided by the array $IST(IS)$, in which IS is the substructure's sequential identity number and $IST(IS)$ is its substructure type. As an example, $IST(3) = 2$ indicates that the third substructure to be assembled, in the sequence illustrated in Table 4.2, has the topology of substructure type 2, identified by $JS = 2$ in Tables 4.1 and 4.2.

A substructural numbering system has been designed for each substructure type which determines the condensable degrees of freedom for this type and provides for the automatic linkage between an existing partial structure and the substructure being assembled.

As far as the user is concerned, his only interaction with the substructure types is in terms of the preparation of the input data for the array $IST(IS)$, which is an array of about 25 integers for a very large cable-stayed bridge. The program uses a defined pattern of numbering, as illustrated in Tables 4.1 and 4.2, for each of the five substructure types. Through subroutine $NUMBER$, it then works out the relationships between these substructural numbering schemes and the global numbering system. Details of subroutine $NUMBER$ are discussed in Section 4.5.

Section 4.4 contains more information about each of the necessary arrays. Tables 4.1, 4.2 and 4.3 show the numerical values of the arrays for

the five substructure types required for assembly of a standard cable-stayed bridge.

4.4 Substructural Numbering

Since a standard Gaussian elimination technique is used to reduce the degrees of freedom within a substructure, the member numbering system (shown by the numbers in the squares of Table 4.1), is of no importance and is simply selected in an arbitrary sequence. Conversely, the nodal numbering system is particularly important because of the automatic linkage requirement. The substructure nodal numbering system is governed by the order in which the nodes are eliminated from the working array (i.e. active stiffness matrix) in high speed storage. Since each node has three degrees of freedom, each nodal number is associated with 3 X 3 submatrices which can be identified with the nodal number. As indicated in Section 4.2, one of the basic requirements in allocating nodal numbers to the nodes in a substructure type is that these numbers must identify with the sequential position in the working array to which the submatrix of the node will be added at the time of assembly of the substructure. After the substructure is assembled into the active array, the array is reduced by Gaussian elimination (partially triangularized) to eliminate degrees of freedom associated with the nodes for which all attaching members have been assembled. The coefficients are shifted in the array as each equation becomes the pivot so that the pivot element is always in position (1,1) of the array. Thus the active nodal number associated with a node reduces by one upon completion of the elimination for the degrees of freedom as each node which is condensed out.

Since some of the nodes in the partial structure are 'condensed out'

(and will be referred to as condensable nodes) while others must be retained in the active stiffness matrix because additional elements will be attached to them prior to their elimination, it is necessary to provide this control information to the equation solver.

To facilitate the description of the process we use the following terminology and notation.

- a) Front interboundary nodes (FIN's) are those nodes of the partial structure which must be retained as active nodes in the working array because additional members have yet to be attached to them.
- b) Rear interboundary nodes (RIN's) are those nodes of the partial structure to which the interboundary nodes of the substructure currently being assembled attach. Because, with one exception, no more than two substructures share any particular node, RIN's become condensable immediately after the assembly of the current substructure is completed.
- c) Internal nodes (INN's) are nodes of the partial structure which are neither FIN's nor RIN's. (These nodes appear in only one substructure and are condensable immediately after assembly of the substructure.)

Consequently, the number of condensable nodes in a partial structure, immediately after assembly of the current substructure, is

$$N = RIN + INN \quad [4.7]$$

The condensable nodes are indicated in Tables 4.1 and 4.2 by black dots, while the FIN's are indicated by black squares.

To describe the way the substructure nodal numbering is determined consider the sequence of assembly and reduction shown in Table 4.2. Any substructure shown in column A is assembled to the previous partial

structure of column C to obtain a new unreduced partial structure shown in column B. Condensable nodes are then eliminated to give the new partial structure in column C. The nodal numbers shown in the circles are the active numbers associated with their positions in the assembled array at the appropriate stage identified by column A, B or C. (In the following, SS, UPS and RPS will be used as abbreviations to denote substructure, unreduced partial structure, and reduced partial structure, respectively).

The only nodes retained as active in the RPS's of column C are those to which elements of subsequent substructures attach. By definition these are the front interboundary nodes (i.e. FIN's). The FIN's for a RPS in column C are obvious from the nodal connectivity required by subsequent structures. However, their numbering is not. The following procedure can be used to establish the numbering.

The sequence of substructure assembly is indicated by the values of IS in Table 4.2. Let us first focus on the RPS in column C for IS = 3 (hereinafter, this, and similar structures in Table 4.2, will be referred to by a tabular position designation such as C3). Three FIN's with active nodal numbers 1, 2 and 5 are shown in C3. The leftmost node has the nodal number 5, rather than 3, because this node remains an FIN for the subsequent RPS C4, and will not be condensed out until after the four condensable nodes of the UPS B4. Therefore, the minimum nodal number for the leftmost node in C3 is 5.

Having established nodal numbers for the FIN's of the RPS in C3 one can now identify the active nodes in the UPS of B3 which consist of the the FIN's of C3 augmented by the nodes of SS A3. There are 5 of these which are condensed out in going from UPS B3 to RPS C3. Hence, the nodal numbers of the FIN's of the UPS B3 become:

$$1 + 5 = 6$$

$$2 + 5 = 7$$

$$5 + 5 = 10$$

The ordering of the condensable nodes is not important in B3, except to note that nodes 1, 4 and 5 are not only nodes arising from SS A3 but are also FIN's of RPS C2. The nodes of the RPS C2 which are in common with those of UPS B3, must have the same nodal numbers as in UPS B3 and SS A3, because the addition of the stiffness of SS A3 to the stiffness of RPS B2 must produce the correct stiffness for UPS B3. In ordering the nodal numbers for RPS C2 it is noted that node 1 is not only a FIN of RPS C2 but is also a FIN of RPS C1. Consequently, it is given the lowest nodal number in C2 and hence in B3.

With the numbering of the active FIN's in C2 now established, the total set of active nodes in the UPS B2 is obtained by augmenting the nodes in the RPS C2 by the number of nodes condensed out in going from UPS B2 to RPS C2, which is 3. Consequently, the nodal numbers of the FIN's of C2 (i.e. 1, 4, 5, 6, 7) are incremented by 3 to obtain the nodal numbers of B2 (i.e. 4, 7, 8, 9, 10). The condensable nodes in B2 are then given the numbers 1, 2, 3.

The substructure nodal numbers, which appear in column A of Table 4.2, are given the same numbers as those appearing in the UPS's of column B. Consequently, we have identified, by working through the above illustration, the SS nodal numbering system for the substructures in rows 2 and 3 of Table 4.2. These have been defined as substructure types JS = 1 and JS = 2 in Table 4.1. Table 4.1 summarizes all substructure types

necessary to assemble a complete cable-stayed bridge of the type contemplated. (Note that only five different SS types are required.) By identifying the substructure nodes with global nodes, whose co-ordinates are arbitrary, the spatial configuration of the substructure varies, and hence left and right handed substructures are unnecessary.

Column D of Table 4.2 indicates the way the active nodal numbers for the nodes of the UPS's change to those of the RPS's during the process of reduction of equations. It is apparent from the nodal numbers indicated in Column D, that there are empty spaces ('gaps') left in the active stiffness matrix which will be filled in by INN's upon assembly of the subsequent substructure. The algorithm which carries out the partial reduction associated with the condensable degrees of freedom should recognize this fact and skip over the associated zero rows and columns. Since the nodal numbers in Column B of Table 4.2 are identical to those of the substructures in Column A, it is apparent that these gaps are a characteristic of the substructure type. The characteristics of the stiffness matrices for the five types of substructures shown in Tables 4.1 and 4.2, that are necessary in assembly and reduction, are shown in the array of Table 4.3, which is designated as INDEX(JS,I).

The definition of the elements of the arrays used in the computer code which define the order of substructure assembly, and all the characteristics of the substructures necessary to form and assemble their stiffness matrix, and carry out the partial reduction for the partial structures, is as follows.

1. $IST(IS) = JS$: Substructure type for substructure number IS.
2. $INDEX(JS,1)$: Number of condensable degrees of freedom in partial structure IS. (Table 4.3)

3. INDEX(JS,2) : Beginning of 'gap' in the nodal degrees of freedom of partial structure IS. (Table 4.3)
4. INDEX(JS,3) : End of 'gap' in the nodal degrees of freedom of partial structure IS. (Table 4.3)
5. INDEX(JS,4) : Last degree of freedom in partial structure IS. (Table 4.3)
6. JEN(JS,I1) : J-end nodal number for member I1 of substructure type JS. (Table 4.1)
7. KEN(JS,I1) : K-end nodal number for member I1 of substructure type JS. (Table 4.1)
8. NSE(JS) : Number of members in substructure type JS. (Table 4.1)
9. NSJ(JS) : Number of nodes in substructure type JS. (Table 4.1)

4.5 Global Numbering System

The global numbering system is the medium through which the user communicates with the program. All input, output and graphical displays are defined in terms of this numbering system, which consists of similar nodal and member numbering for each 'half' of the bridge. (Note that the bridge need not be symmetric). Figure 4.2 shows the member and nodal numbering systems which are adopted for one 'half' of the bridge. The relationship between the systems of substructural and global numbering is provided by subroutine NUMBER. For the proper conversion of one system to the other it is crucially important that the systems of member and nodal global numbering patterns indicated in Fig. 4.2 are exactly followed.

Note that the substructure numbering begins with the bottom tower segment with IS = 1 (See also Fig. 4.3) and increments sequentially with

the substructures on alternate sides of the tower. The global nodal and member numbering for the girder start at the 'centreline' and continue sequentially to the land side pier. The base of the pier is given the next nodal number, and the sequence of nodal numbers then progresses up the tower. Similarly the pier receives the first member number after the girder is completed, and member numbers then progress up the tower. The member numbers for cables follow, beginning with the longest cable on the water side and progressing to the longest cable on the land side.

In order to demonstrate a typical example of some of the operations which subroutine NUMBER performs, the conversion from the substructure numbering system to the global numbering system for the nodes and members of the substructures with odd IS numbers (i.e.- the ones on the land side of the tower) is considered here, except for the last of these substructures (IS = 9) which is of a different substructure type (JS = 5). Note that ISF signifies the total number of substructures to assemble one 'half' of the bridge, whereas IS designates the sequence number of the particular substructure under consideration. The substructures are separated for easy identification in Fig. 4.3, where their sequence numbers, IS, and type numbers, JS, are shown. Excluding the centre drop-in span and the base of the tower, there are (ISF / 2 - 1) substructures on each side of the tower. The number of girder nodes on the water side is

$$N_w = 3 (ISF / 2 - 1) + 2 \quad [4.8]$$

and the number of girder nodes on the land side is

$$N_L = 3 (ISF / 2 - 1) \quad [4.9]$$

The nodal number of the leftmost node of substructure IS on the land side is

$$N = N_w + 3 \left(\frac{IS - 3}{2} \right) \quad [4.10]$$

Recognizing that this nodal number is the number of the JEN node of member $II = 1$ of substructure IS (See Table 4.1), we may use [4.10] to write the J end global nodal numbers for $1 \leq II \leq 3$ as

$$NNTR(IS, JN) = N_w + 3 \left(\frac{IS - 3}{2} \right) + II - 1 \quad [4.11]$$

Substituting for N_w from [4.8], [4.11] becomes

$$NNTR(IS, JN) = 1.5 ISF + 1.5 IS + II - 6.5, \quad 1 \leq II \leq 3 \quad [4.12]$$

This equation links the J node of member II of substructure IS (which is of substructure type JS) to the associated global node number. Similar equations can be derived for the cable and tower nodes, and for the other types of substructures, and are evaluated by subroutine NUMBER. The JEN and KEN nodal numbers (Table 4.1) may, therefore, be linked to their global numbers and the results are stored in array NNTR.

For global member numbers, note that in Fig. 4.2 the global JEN nodal number for member II is the same as the global number of the member. Therefore, a procedure similar to that developed above, for identifying substructure joint numbers with a global joint number, may be developed for member numbers. The global member numbers are stored in the array

MNTR(IS,I1).

A flowchart for subroutine NUMBER is shown in Fig. 4.4. The equations necessary to compute the nodal and member numbers for all types of substructures are shown therein.

Section 7.6.1 contains more information about the global numbering system but note that:

- a) it is necessary that the input data specify the coordinates associated with the reference configuration location of each global node; and ,
- b) the numbering of substructures must begin at the tower and sequentially identify the order in which the substructures are to be assembled in the manner illustrated in Fig. 4.3.

4.6 Systems of Co-ordinates and Sign Conventions

The two systems of co-ordinates defined below have been used for the forces, displacements and other linear dimensions in CASBA.

a) The Local (Member) Coordinates

The ends of the centroidal axis of each member are denoted by the letters J and K, with J designating the left end (with respect to the viewer) of girder elements and the lower end of tower elements. The axis JK, with its origin at J, is selected as the x-coordinate of the member. The y-coordinate is oriented 90° counterclockwise from the x-axis and in the vertical plane which passes through JK. Its positive direction is given by the right hand rule when the positive z-axis points towards the viewer. Fig. 4.5a shows the local coordinates of member I1.

It is to be noted that all member-end forces in CASBA are output in the member co-ordinates, so that they can be used in stress computations without any transformation.

b) The Global System of Co-ordinates

The global system of coordinates for CASBA is shown in Fig. 4.5b. The Y-axis is positive in a vertically upward direction passing through the centre of the closing girder segment. The X-axis may be selected to be any horizontal axis in the plane of the structure which is positive when directed towards the right of the viewer. In Fig. 4.5b, this axis is selected to pass through the centroid of the cross-section at the midpoint of the closing girder segment, but this is not essential.

c) Sign Conventions

1. All positive angles are measured counterclockwise from the positive X-axis.
2. All external loads are defined by their absolute magnitudes and the positive angles to their vector orientation.
3. Member end forces are defined as positive in the direction of positive axes, and by the right hand rule, in both the global and local coordinate systems.
4. Internal stress resultants are defined in the local coordinate system, in the conventional manner for shearing force and bending moment, and are positive if:
 - i) axial force is tensile,
 - ii) pairs of shearing forces produce clockwise moment,
 - iii) bending moments produce compression for positive values of y .

4.7 The Reference Configuration

4.7.1 The 'Work Point Line'

Linear analysis in CASBA begins with the reference configuration. As discussed in Chapters 1 and 3, the designer is permitted to specify both

the geometry and the bending moment distribution for the girder under the bridge dead load. The present version of CASBA requires that the girder geometry be specified in terms of the coordinates of the centroidal axes of its constituent members. However, it is realized that describing the reference geometry in terms of the top flange of the girders may be more desirable. The latter forms a continuous and smooth line, called the 'work point line'. Its use as a reference line for geometry would facilitate the regular checking of coordinates during erection and is, therefore, preferable.

4.7.2 Determination of the Reference Configuration Moments

The girder geometry is normally fixed by the geometrical requirements of the highway which is supported by the bridge. On the other hand, the specified bending moment distribution in the reference configuration can be selected to minimize the combined bending moments under dead load and live loads in order to achieve greater economy. The process of selection of a desirable bending moment distribution for the reference configuration is essentially iterative and includes the following steps (Gimsing, 1983, p. 240).

1. Compute the girder dead load by using suitable preliminary cross-sections. Assume an arbitrary distribution of dead load moment in each span for positive and negative moment, such that in the designer's judgement, when combined with the estimated total axial force and live load moment envelopes it will produce acceptable stress conditions in the top and bottom flanges (Fig. 4.6a).
2. Estimate the cable sizes and carry out an analysis of the total bridge to determine moment envelopes for live load which, in combination with

the dead load moments estimated in 1, produce the total moments of Fig. 4.6b and the axial forces of Fig. 4.6c.

3. From an interaction diagram for the cross-section (Fig. 4.6d) and using the axial forces of Fig. 4.6c, determine the net bending moment capacities as shown in Fig. 4.6e.
4. Superimpose the moment capacities of Fig. 4.6e onto the moment envelopes of Fig. 4.6b, to obtain Fig. 4.6f.

The illustration in Fig. 4.6f indicates that the envelope of total negative moments exceeds the negative moment capacity of the cross-section from A to B. However, this can be eliminated by translating both the positive and negative dead load moment distributions over this region in the positive direction, providing that the sum of the absolute values of the envelopes over this region (Fig. 4.6b) does not exceed the sum of the absolute values of the capacities (Fig. 4.6e)

5. Add the moment ordinates, associated with the shaded area in Fig. 4.6f to the dead load moments in Fig. 4.6a to obtain a new and more desirable specified dead load moment distribution.
6. Repeat the process from step 2 until the moment envelopes in Fig. 4.6f fall inside the capacity envelopes.

Upon completion of the above iterative process a desirable distribution of dead load moment for the reference configuration will have been determined. This distribution of dead load moment forms the starting point for the disassembly procedure for erection analysis.

The following comments are relevant to the above procedure.

- a) As discussed in Sections 1.7 and 1.8, the reference configuration moments may be adjusted arbitrarily by varying the shapes of the

unstressed elements. Therefore, the designer is free to move the ordinates in Fig. 4.6a at will, provided that the absolute values of the difference in ordinates between the two lines in the figure remains constant and equal to the simple span moment.

- b) If the sum of the ordinates for moment capacities in Step 4, above, is less than the sum of the ordinates for the moment envelopes, it is apparent that the cross-section must be increased. Similarly, if the capacity sum is greater than the envelope sum the cross-section may be decreased.

4.7.3 The 'Tie-Down' Cables

The bending moment distribution in the towers is mainly dominated by the tie-down forces in the back-stays which connect the top of the towers to the side piers. The tie-down force at the base of the tower can be estimated by assuming zero internal forces at the centre of the drop-in segment of the main girder and applying the equations of equilibrium to the simplified structure of Fig. 4.7. The value computed from this computation should only be used as a guide for the final selection of the force. Obviously, if the tie-down force in the reference configuration increased, a moment must be provided at the base of the tower and the compressive stresses on the land side of the tower increase. This is a situation which may not be desirable for reinforced concrete towers due to the long term creep implications. On the other hand, if the tie-down forces are not sufficiently large, the towers may bend substantially toward the centre of the span under the influence of combined dead and live loads and this may cause overstressing of the water face of the towers. Gimsing (1983) points out that, if the tie-down force is not sufficient, the back-stay stress

could reduce to zero for live load in the side span and this would result in an unstable structure.

In order to arrive at a desirable specified value for the tie-down force, the designer must rely on his past experience of dealing with similar bridges, as well as trial runs of the program for the combined effects of the dead load and selected live loads. To obtain a more complete picture of possible moment variation in the towers the trial runs should be conducted for a range of tie-down forces.

4.8 Assembly and Reduction

a) Overview of Assembly and Reduction

The three operations of assembly, reduction and backsubstitution of the equilibrium equations are performed using the substructural numbering system in which the nodal numbers correspond to their sequential position in the active stiffness matrix array, as discussed in Section 4.4. A typical cycle of assembly and reduction for a new partial structure which is to be formed by adding substructure number IS (with substructure type JS = IST(IS)) to an existing partial structure consists of the following operations:

- 1) The stiffness matrix of each member of the substructure is formed in the member coordinates and transformed to the global coordinates. The initial stiffness of the cables is computed using the tensile forces in the reference configuration.
- 2) The transformed member stiffness matrices are assembled to form the substructure stiffness matrix using the nodal numbers identified in Table 4.1.
- 3) The substructure stiffness matrix is assembled to the existing partial structure stiffness matrix in the active array to form the stiffness

matrix of the new partial structure as indicated in Table 4.2.

- 4) All the condensable degrees of freedom in the newly-formed stiffness matrix are eliminated to obtain the reduced matrix of the newly formed partial structure. To carry out this elimination the information from the array INDEX(JS,I) of Table 4.3 is required. INDEX(JS,1) contains the upper limit of the condensable degrees of freedom for the partial structure, while INDEX(JS,2) and INDEX(JS,3) are the beginning and the end of the dummy degrees of freedom, respectively. INDEX(JS,4) is the highest degree of freedom in the active array corresponding to the partial structure.
- 5) The reduced coefficients are then stored in a linear array for subsequent transferal to the backing storage.

To better illustrate the flow of operations it is useful to look at the process in schematic form.

It will be assumed that the active stiffness matrix for an 'unreduced' partial structure (URPS), such as those shown in Column B of Table 4.2, may be represented by the partitioning shown in Fig. 4.8a, in which the upper partition contains the condensable nodes. The schematic form of the stiffness matrix after triangularization for the condensable nodes is indicated for the 'partially reduced' partial structure (PRPS) in Fig. 4.8b. Of course, if the coefficients are shifted during the triangularization process, the only coefficients remaining in the active array are those associated with the noncondensable nodes. This matrix, in substructure analysis terminology, would be that for the 'condensed' partial structure (CPS), and would occupy the position shown in Fig. 4.8c. Completion of the reduction of the condensed partial structure matrix results in the reduced condensed partial structure (RCPS) matrix of Fig.

4.8d.

Assuming the next substructure has index $j=i+1$, this substructure matrix adds directly to matrix D' of Fig. 4.8 to yield the matrix in Fig. 4.8e. Figures 4.8f to 4.8h are a schematic representation of the continuation of the process described above for partial structure j . The matrices stored on disk for future use are identified in the square brackets, [], in Fig. 4.8.

b) Operations in Assembly and Reduction

The successful performance of the above operations depends largely on the transfer of data between the global and substructural numbering systems. The following step-by-step procedure demonstrates how the basic information is transferred from one system to the other.

1. Determine substructure type, $JS = IST(IS)$.
2. Determine number of nodes for JS, $NJ = NSJ(JS)$. (Table 4.1)
3. Determine number of members for JS, $I1 = NSE(JS)$. (Table 4.1)

**** LOOP OVER NUMBER OF MEMBERS (I1) OF THE SUBSTRUCTURE

4. J-end of member, $JN = JEN(JS,I1)$. (Table 4.1)
5. K-end of member, $KN = KEN(JS,I1)$. (Table 4.1)
6. Co-ordinates of each node from $XCO(IS,JN)$, $YCO(IS,JN)$,....
7. Cross-sectional properties of element $E(IS,I1)$, $QA(IS,I1)$,...

(Note that in the first run of the program the substructure nodal and member numbering for IS is converted into the global numbering system through the subroutine NUMBER, as has been discussed in Section 4.5. This subroutine also prepares the arrays $NNTR(IS,JN)$ and $MNTR(IS,I1)$. Arrays such as $XCO(IS,JN)$, $YCO(IS,JN)$, $E(IS,I1)$, etc... are formed directly at the time the input data is read.

8. Form member stiffness matrix in member co-ordinates system.

9. Transform member stiffness matrix to global co-ordinate orientation.

10. Assemble member stiffness matrices to form substructure stiffness matrix.

**** END THE LOOP OVER NUMBER OF MEMBERS.

11. Add substructure stiffness matrix [A] to reduced partial structure stiffness matrix [AA] in the active array (This is done by adding together the coefficients with the same indices. See Section 4.4).

12. Use INDEX(JS,1) to determine which degrees of freedom are condensable after assembly.

**** LOOP OVER THE CONDENSABLE DEGREES OF FREEDOM UP TO INDEX(JS,1).

13. Reduce each condensable degree of freedom by using the following Gaussian elimination algorithm, shift the reduced coefficients by one vertical and one horizontal position during the reduction procedure, and place the coefficients of the pivotal row into a linear array prior to transfer to backing storage. The algorithm for the reduction of the active array may be expressed as

$$a_{i-1,j-1} = a_{ij} - \frac{a_{im} a_{mj}}{a_{mm}} \quad [4.9]$$

where:

$i = m + 1, \dots, n$ is the row number.

$j = i, \dots, n$ is the column number.

$m = 1, \dots, \text{INDEX(JS,1)}$ is the pivotal row number.

n is the total number of degrees of freedom for the substructure, i.e. INDEX(JS,4).

14. Zero the vacated positions in the active array.

**** END THE LOOP OVER THE CONDENSABLE DEGREES OF FREEDOM.

At the end of the above procedure a reduced stiffness matrix corresponding to the FIN degrees of freedom of the new partial structure remains in the active array. This will be used for the forward assembly of the next sequential substructure by simply returning to step 1.

c) Operations to Fully Reduce Partial Structure Matrix

While the reduction process for the sequential erection of substructures has just been described in Section 4.7b, it also is necessary to treat any partial structure as a complete structure if one wishes to determine stresses and deflections for it during the erection process. Consequently, the reduction process is continued for the FIN's but without disturbing the active matrix remaining at the end of Step 14. This requires that the matrix obtained at the end of Step 14 be reproduced elsewhere and the elimination for the pivot rows associated with the degrees of freedom between INDEX(JS,1)+1 and INDEX(JS,4) be completed. This results in the matrix D'' of Fig. 4.8 which is also placed in backing storage so that a complete analysis of this partial structure can be carried out at any subsequent time.

Consequently the process described in Section 4.7b is followed by the following step.

**** LOOP OVER THE FRONT INTERBOUNDARY DOF's.

15. Repeat step # 13

**** END THE LOOP OVER THE FRONT INTERBOUNDARY DOF's.

By this time the linear backing storage array will contain about 400 reduced stiffness coefficients for each partial structure which are stored in a direct access external file with a record access label corresponding to IS.

Table 4.2 illustrates this method of assembly and elimination in a

schematic form. Fig. 4.9 shows a flowchart of subroutine REDUCE which performs the above operations. Figure 4.10 shows a flowchart for subroutine BACSUB which will be discussed in Chapter 5.

Assuming the process of reducing the stiffness matrix described above has been carried out for the 'half-bridge' shown in Fig. 4.2, the matrix H' of Fig. 4.8g is the 3X3 condensed stiffness matrix associated with node 1. If a similar procedure to that described above is carried out for the other 'half' of the bridge (note again that the bridge need not be symmetric), the addition of the two H' matrices yields the condensed stiffness matrix of the 'centre' joint in the completed bridge. The reduction of this combined H' matrix to H'' , and the processing of the load vector, as shown in Fig. 4.8h, produces the displacements of this centre joint which may then be used for backsubstitution in each 'half' of the bridge to yield the configuration of the total structure.

Table 4.1 Substructure Types

SUBSTRUCTURE TYPE	JS	NSE(JS)	NSJ(JS)	I1	JEN(JS,I1)	KEN(JS,I1)
	1	8	10	1	4	2
				2	2	3
				3	3	10
				4	3	8
				5	2	7
				6	1	7
				7	7	8
				8	9	8
	2	5	10	1	1	2
				2	2	3
				3	3	10
				4	3	5
				5	2	4
	3	8	11	1	2	3
				2	3	4
				3	4	11
				4	4	9
				5	3	8
				6	1	8
				7	8	9
				8	9	10
	4	7	10	1	2	1
				2	3	2
				3	4	3
				4	4	5
				5	5	6
				6	6	7
				7	4	10
	5	5	10	1	2	3
				2	1	2
				3	1	10
				4	10	5
				5	1	4

LEGENDS

- NODE #
- MEMBER #
- CONDENSABLE NODES
- FRONT INTERBOUNDARY NODES

JS : SUBSTRUCTURE TYPE
 NSE : # OF MEMBERS IN A SUBSTRUCTURE
 NSJ : # OF NODES IN A SUBSTRUCTURE
 JEN : J-END OF A MEMBER & KEN : K-END OF A MEM.
 I1 : MEMBER #

Table 4.2 The Sequential Assembly and Reduction Scheme

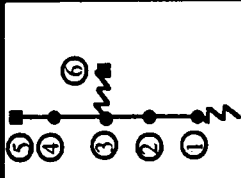
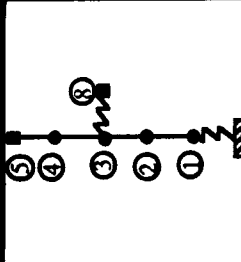
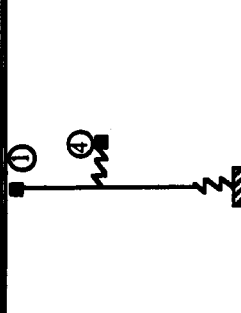
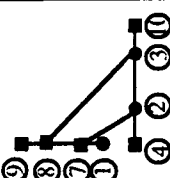
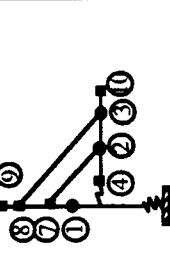
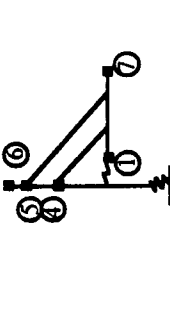
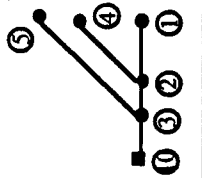
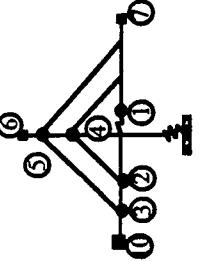
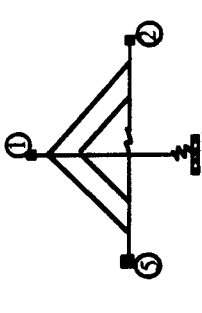
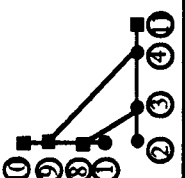
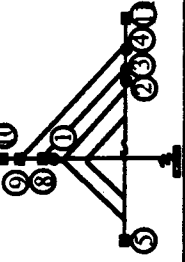
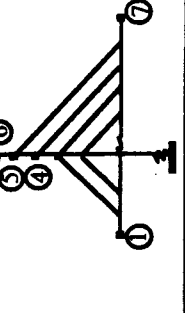
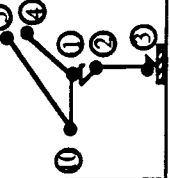
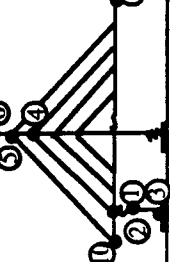
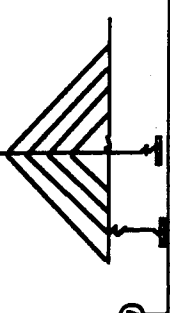
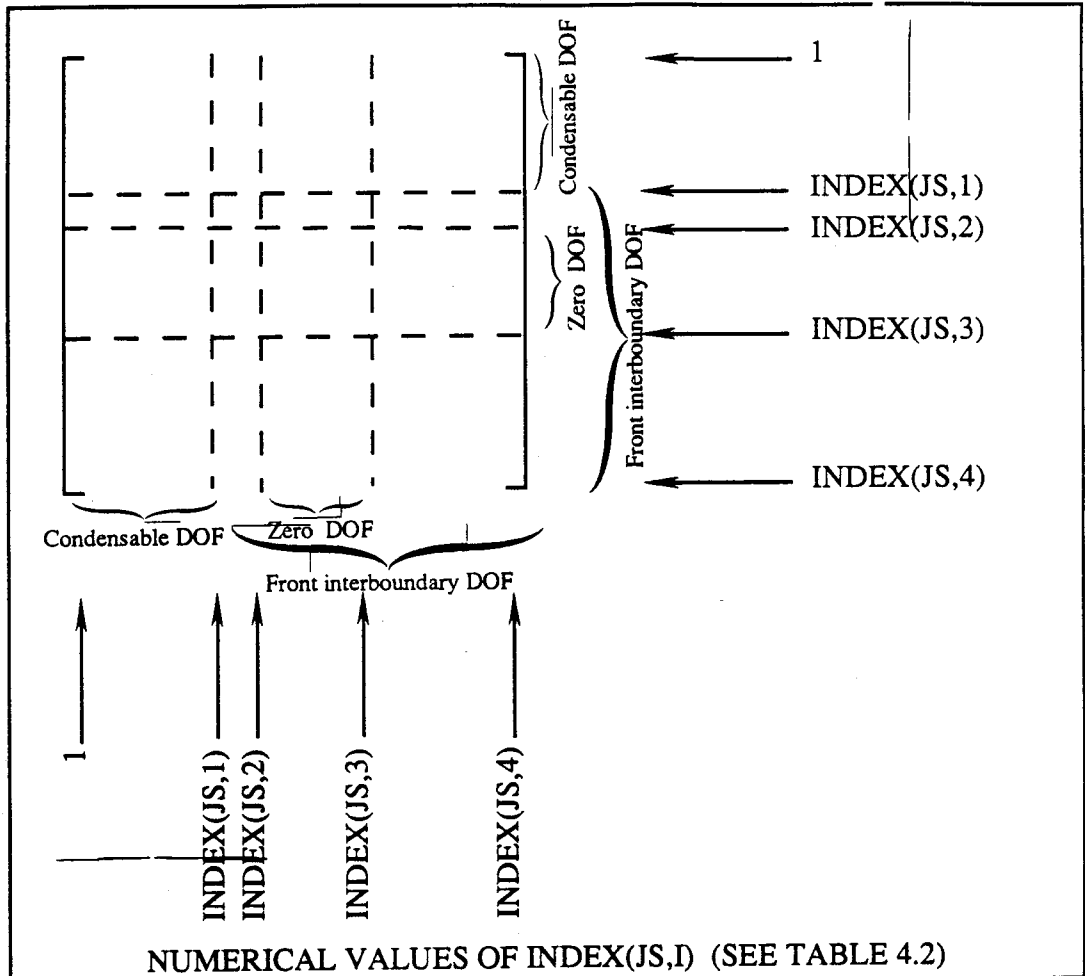
IS	COLUMN			D	
	A	B	C		
IS	JS	UNREDUCED PARTIAL STRUCTURE	REDUCED PARTIAL STRUCTURE	REDUCTION SCHEME	
1	4				UNREDUCED PARTIAL STRUCTURE: ① ② ③ ④ ⑤ ⑥ REDUCE ① & MOVE OTHERS ONE STEP DOWNWARD ① ② ③ ④ ⑤ ⑥ REPEAT ABOVE ① ② ③ ④ ⑤ ⑥ " " ① ② ③ ④ ⑤ ⑥ " " ① ② ③ ④ ⑤ ⑥ REDUCED PARTIAL STRUCTURE: ① ④
2	1				UNREDUCED PARTIAL STRUCTURE: ① ② ③ ④ ⑤ ⑥ ⑦ ⑧ ⑨ ⑩ ⑪ REDUCE ① & MOVE OTHERS DOWNWARD: ① ② ③ ④ ⑤ ⑥ ⑦ ⑧ ⑨ ⑩ ⑪ REPEAT ABOVE: ① ② ③ ④ ⑤ ⑥ ⑦ ⑧ ⑨ ⑩ ⑪ REDUCED PARTIAL STRUCTURE: ① ④ ⑤ ⑥ ⑦
3	2				UNREDUCED PARTIAL STRUCTURE: ① ② ③ ④ ⑤ ⑥ ⑦ ⑧ ⑨ ⑩ ⑪ REDUCE ① & MOVE OTHERS DOWNWARD: ① ② ③ ④ ⑤ ⑥ ⑦ ⑧ ⑨ ⑩ ⑪ REPEAT ABOVE: ① ② ③ ④ ⑤ ⑥ ⑦ ⑧ ⑨ ⑩ ⑪ REPEAT ABOVE: ① ② ③ ④ ⑤ ⑥ ⑦ ⑧ ⑨ ⑩ ⑪ REPEAT ABOVE: ① ② ③ ④ ⑤ ⑥ ⑦ ⑧ ⑨ ⑩ ⑪ REDUCED PARTIAL STRUCTURE: ① ② ③ ④ ⑤ ⑥ ⑦
4	3				UNREDUCED PARTIAL STRUCTURE: ① ② ③ ④ ⑤ ⑥ ⑦ ⑧ ⑨ ⑩ ⑪ REDUCE 1 & MOVE OTHERS DOWNWARD: ① ② ③ ④ ⑤ ⑥ ⑦ ⑧ ⑨ ⑩ ⑪ REPEAT ABOVE: ① ② ③ ④ ⑤ ⑥ ⑦ ⑧ ⑨ ⑩ ⑪ REPEAT ABOVE: ① ② ③ ④ ⑤ ⑥ ⑦ ⑧ ⑨ ⑩ ⑪ REDUCED PARTIAL STRUCTURE: ① ② ③ ④ ⑤ ⑥ ⑦
5	5				UNREDUCED PARTIAL STRUCTURE: ① ② ③ ④ ⑤ ⑥ ⑦ ⑧ ⑨ ⑩ ⑪ REDUCE 1 & MOVE OTHERS DOWNWARD: ① ② ③ ④ ⑤ ⑥ ⑦ ⑧ ⑨ ⑩ ⑪ REPEAT ABOVE: ① ② ③ ④ ⑤ ⑥ ⑦ ⑧ ⑨ ⑩ ⑪ REPEAT ABOVE: ① ② ③ ④ ⑤ ⑥ ⑦ ⑧ ⑨ ⑩ ⑪ REPEAT ABOVE: ① ② ③ ④ ⑤ ⑥ ⑦ ⑧ ⑨ ⑩ ⑪ REDUCED PARTIAL STRUCTURE: ① ② ③ ④ ⑤ ⑥ ⑦
LEGENDS IS: PARTIAL STRUCTURE # JS: SUBSTRUCTURE TYPE ● CONDENSABLE NODES ■ FRONT INTER-BOUNDARY NODES (FIN'S) ○ NODAL #					

Table 4.3



NUMERICAL VALUES OF INDEX(JS,I) (SEE TABLE 4.2)

JS \ I	1	2	3	4
1	9	13	18	30
2	15	22	27	30
3	12	16	21	33
4	18	22	27	30
5	15	22	27	30

STIFFNESS MATRIX FORMATION INPUT READING & REDUCTION
BACKSUBSTITUTION LOAD VECTOR FORMATION & REDUCTION

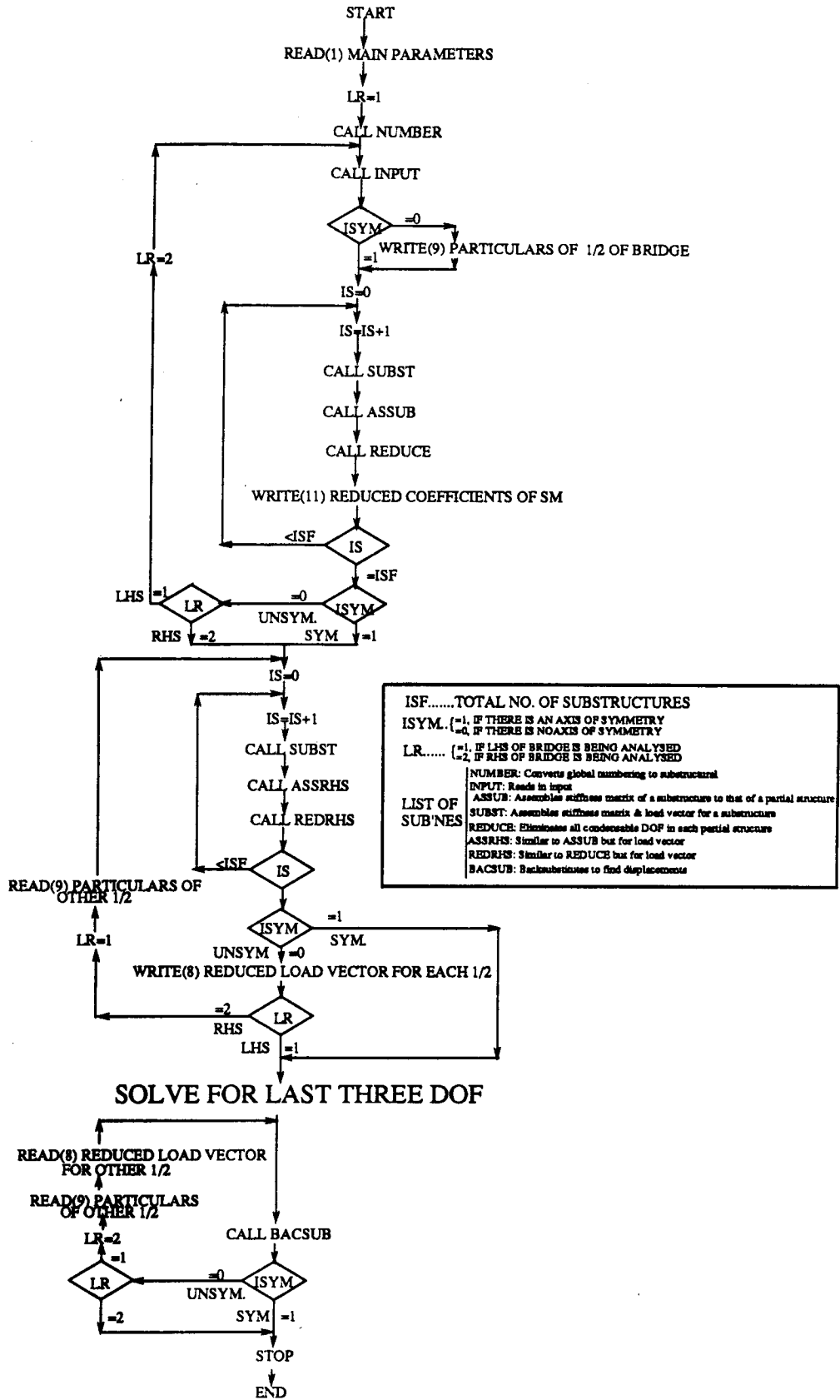


Figure 4.1 Flowchart of Linear Analysis

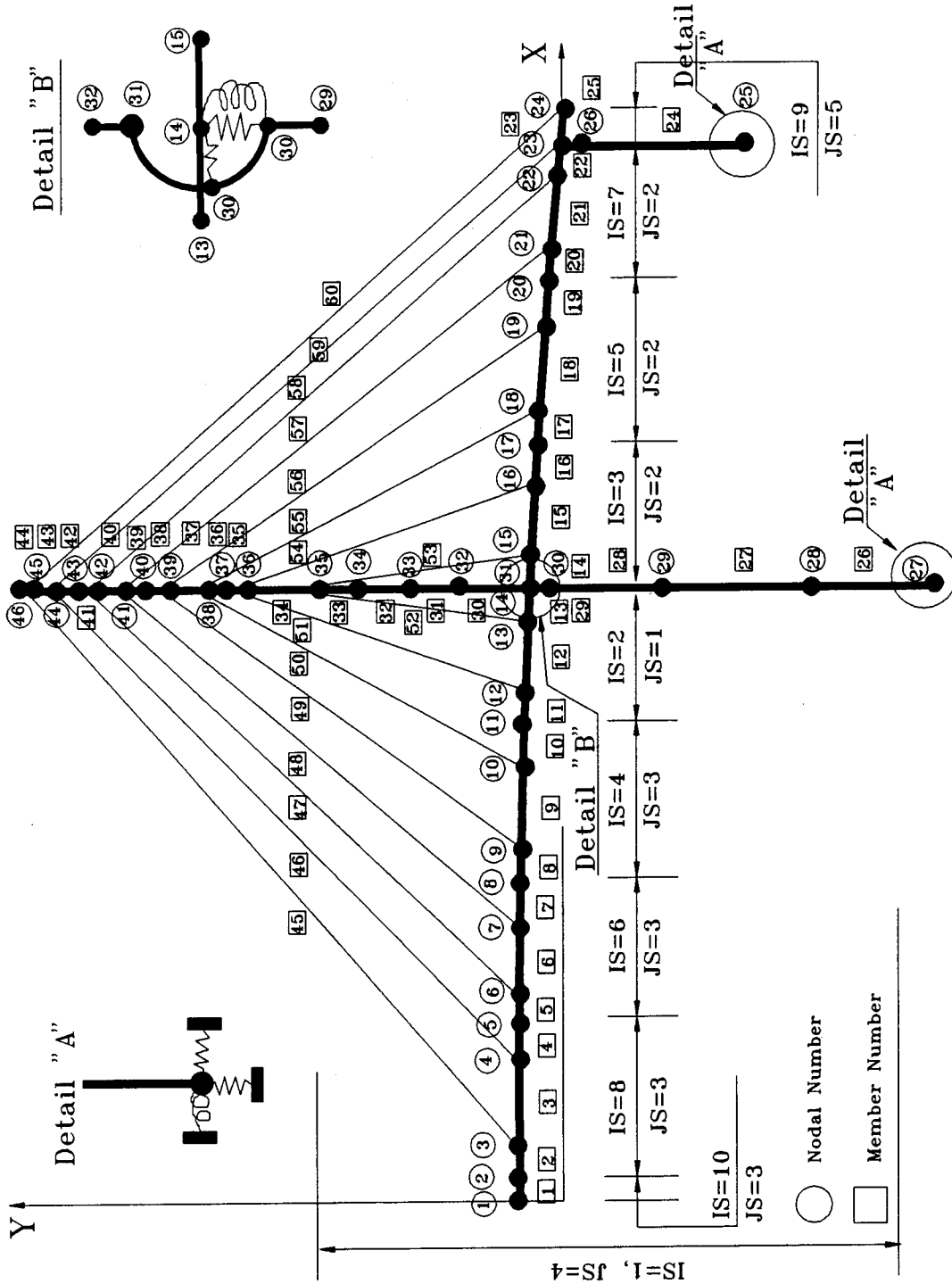


Figure 4.2 Global Nodal and Member Numbering

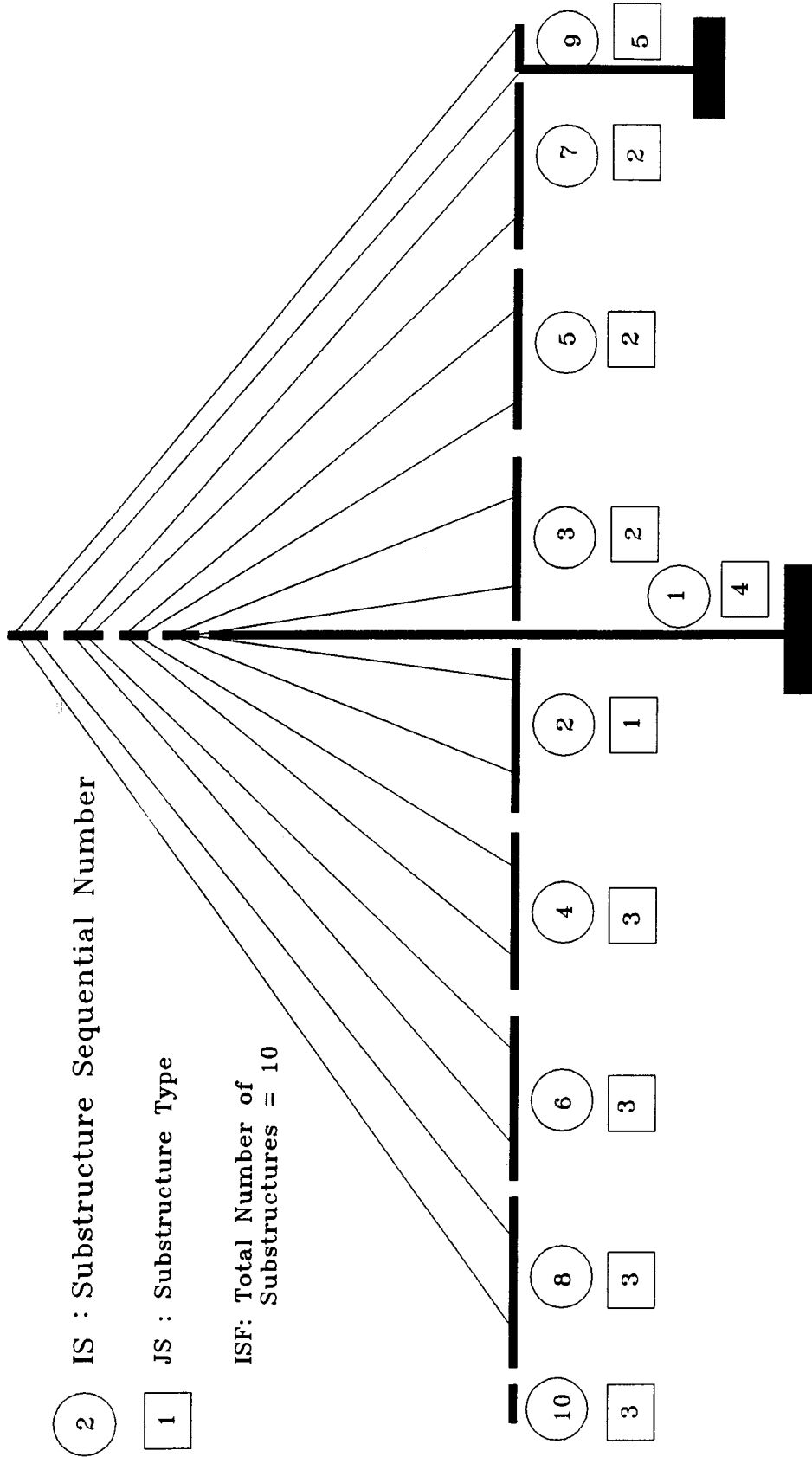


Figure 4.3 Substructure Types

SS: SUBSTRUCTURE
 IS: SS #
 JS: SS TYPE
 I1: MEMBER #
 IST: ARRAY OF SS TYPES
 ISF: TOTAL # OF SS's FOR EACH 'HALF'
 MNTR: GLOBAL MEMBER # FOR MEMBER I1 OF SS IS
 NNTR: GLOBAL NODAL # FOR NODE KN OF SS IS
 IDBR: J-END AND K-END NODAL 3's OF MEMBERS IN GLOBAL NUMBERS

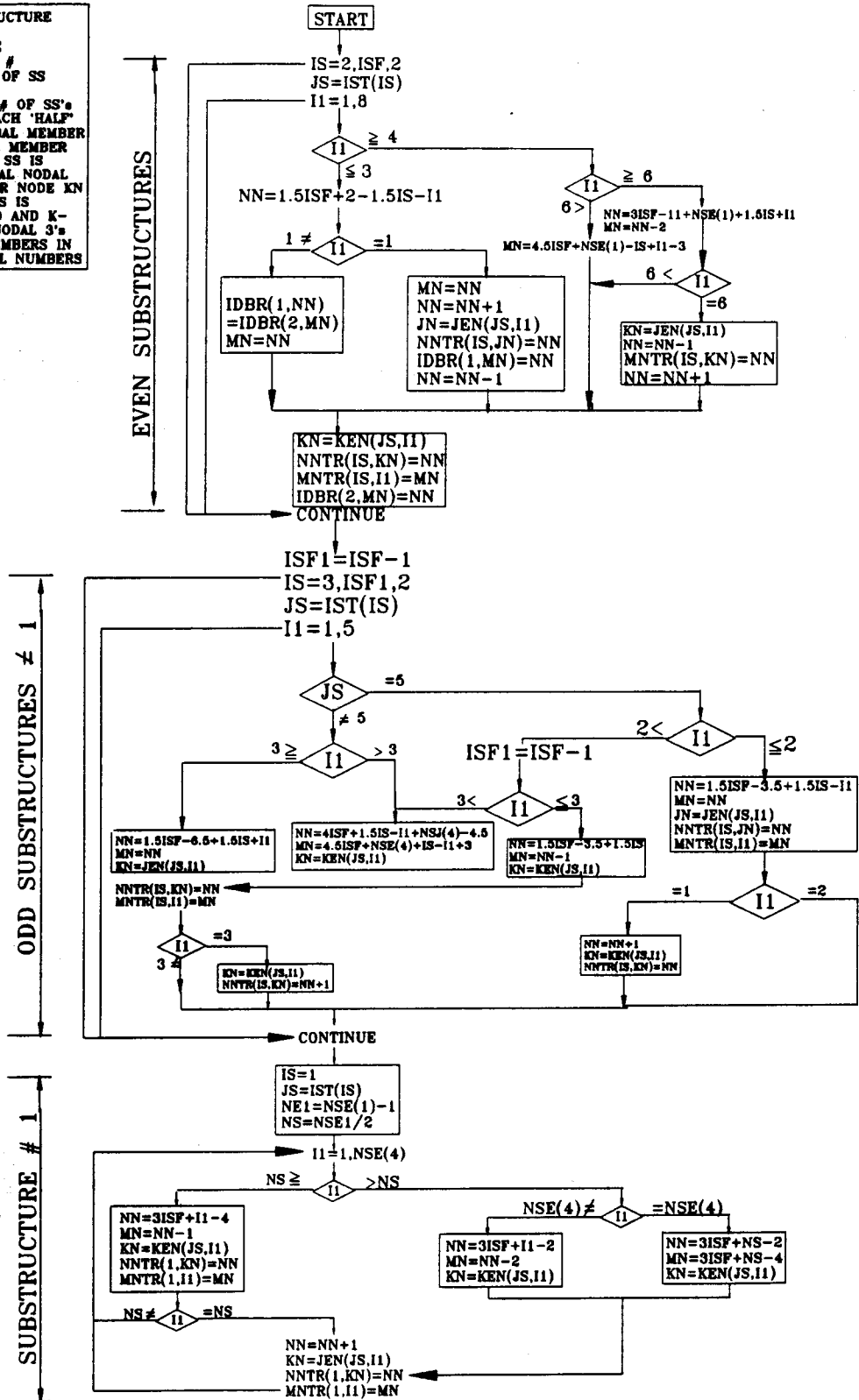
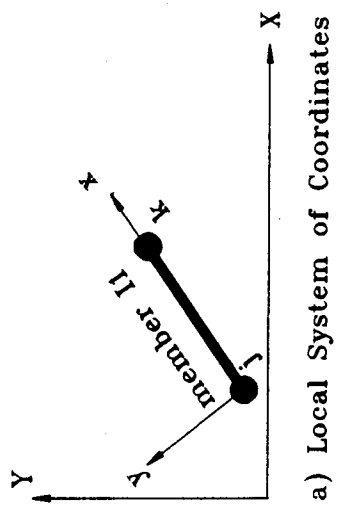
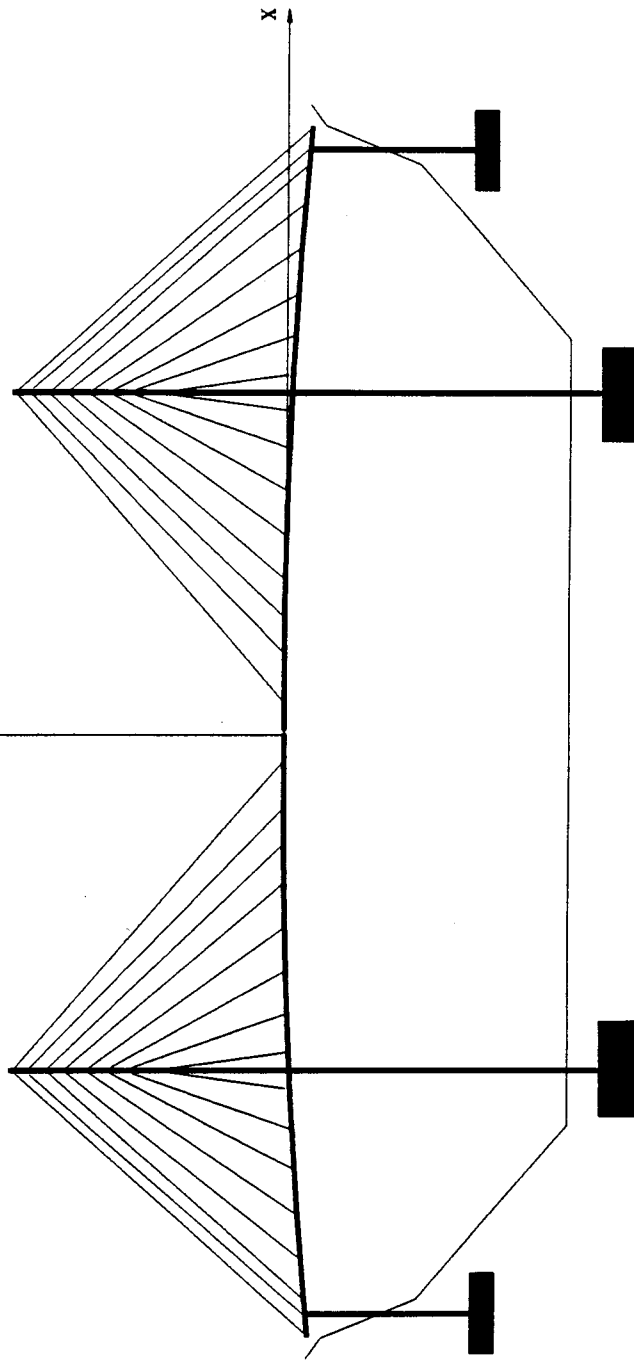


Figure 4.4 Flowchart of Subroutine NUMBER

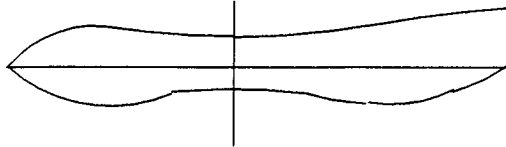
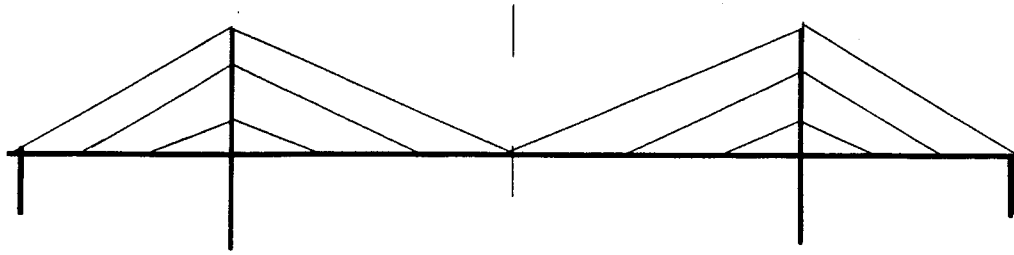


a) Local System of Coordinates

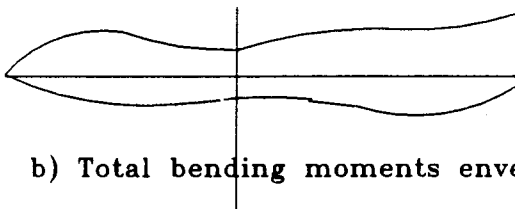


b) Global System of Coordinates

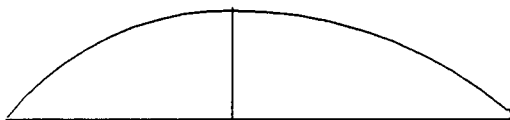
Figure 4.5 Systems of Coordinates



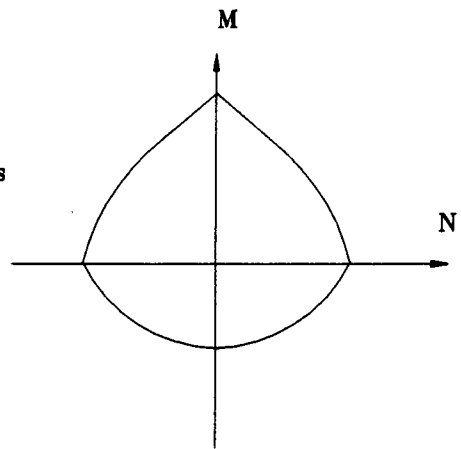
a) Specified dead load bending moment distribution



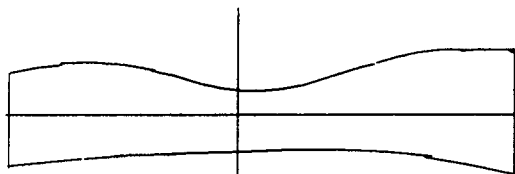
b) Total bending moments envelopes



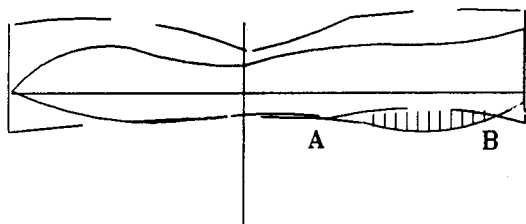
c) Total axial force diagram



(d) Interaction diagram

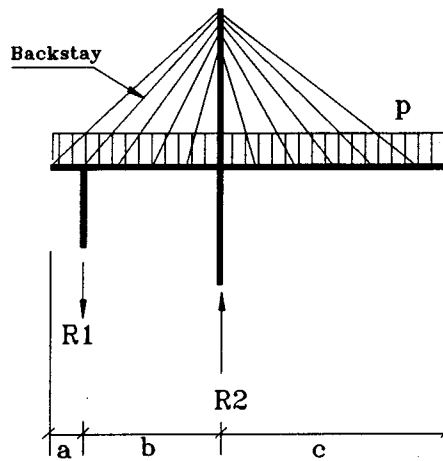


(e) Bending moment capacities



f) Superposition of e) onto b)

Fig. 4.6 Specified Bending Moment for Reference Configuration



Assumptions:

1. Roller support between girder and pier
2. Zero bending moment at tower base
3. Zero internal forces at centre of main span

Equations of Equilibrium:

$$-R1 + R2 - p(a + b + c) = 0$$

$$R1(b + c) - R2(c) + p[(a + b + c)^2] / 2 = 0$$

Figure 4.7 Simplified Structure for Approximate Computation of Tie-Down Force R1

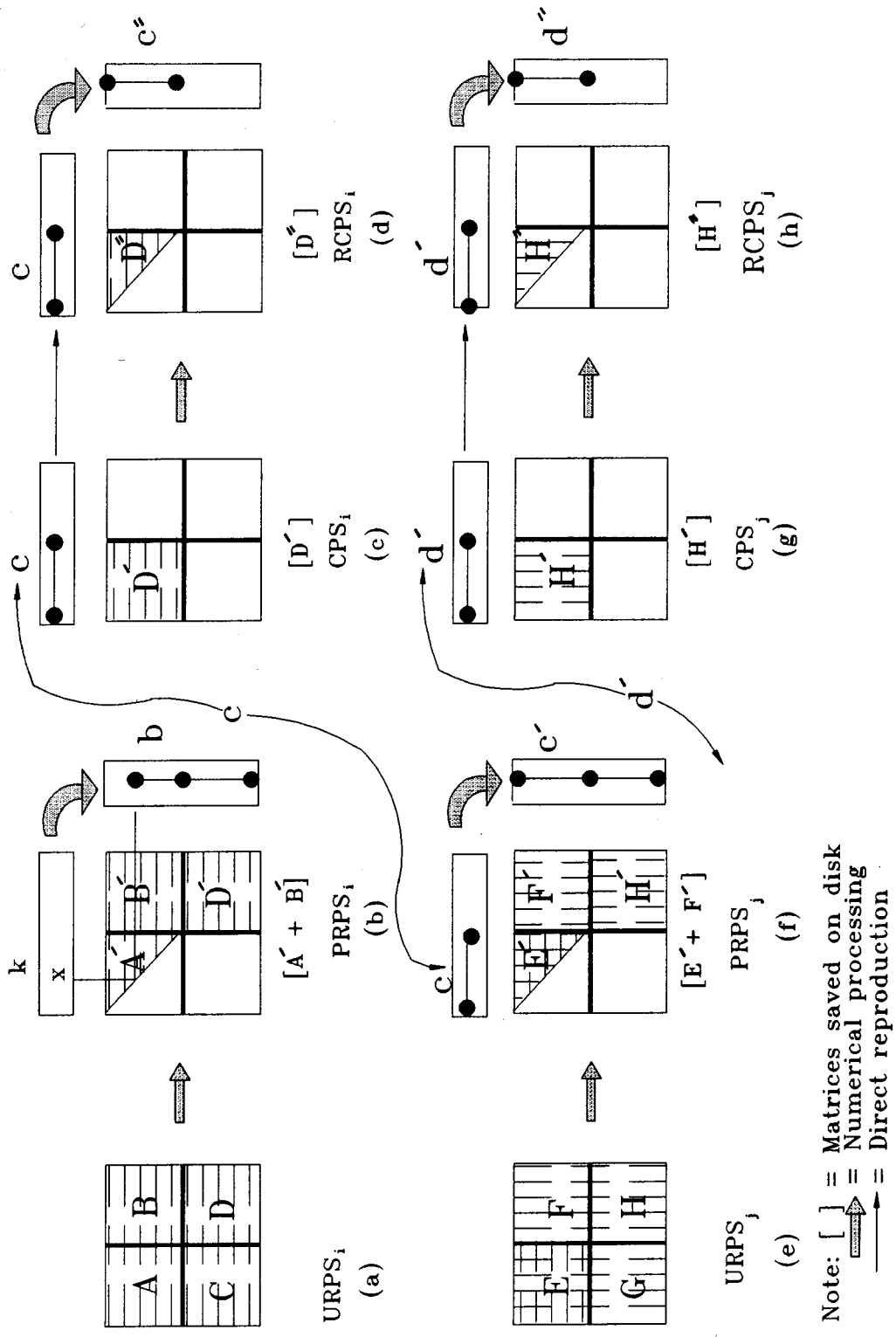


Figure 4.8 Schematic Matrix Reduction and Load Vector Processing

SUBROUTINE REDUCE

(FOR EACH NEW SUBSTRUCTURE ASSEMBLED)

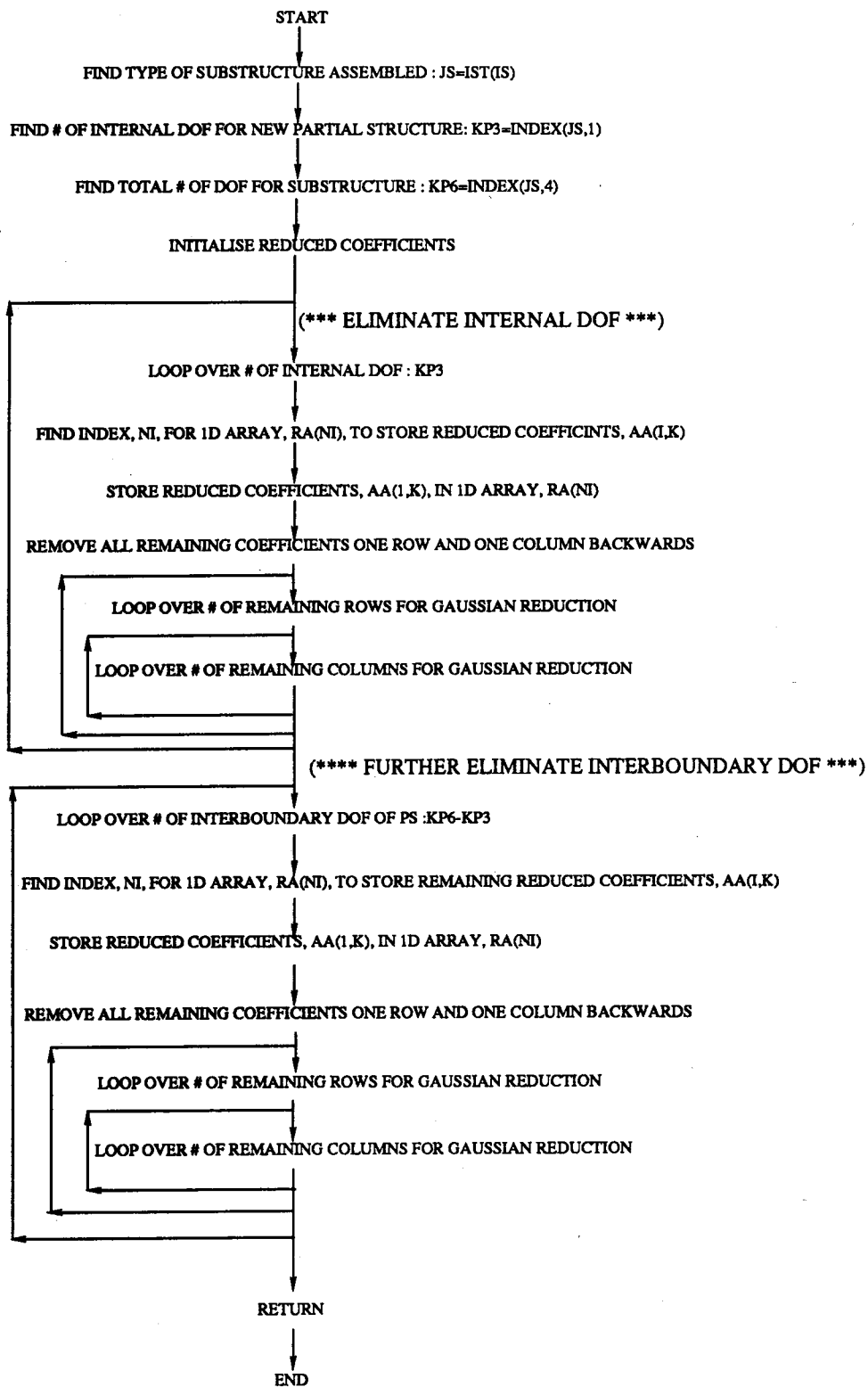


Figure 4.9 Flowchart of Subroutine REDUCE

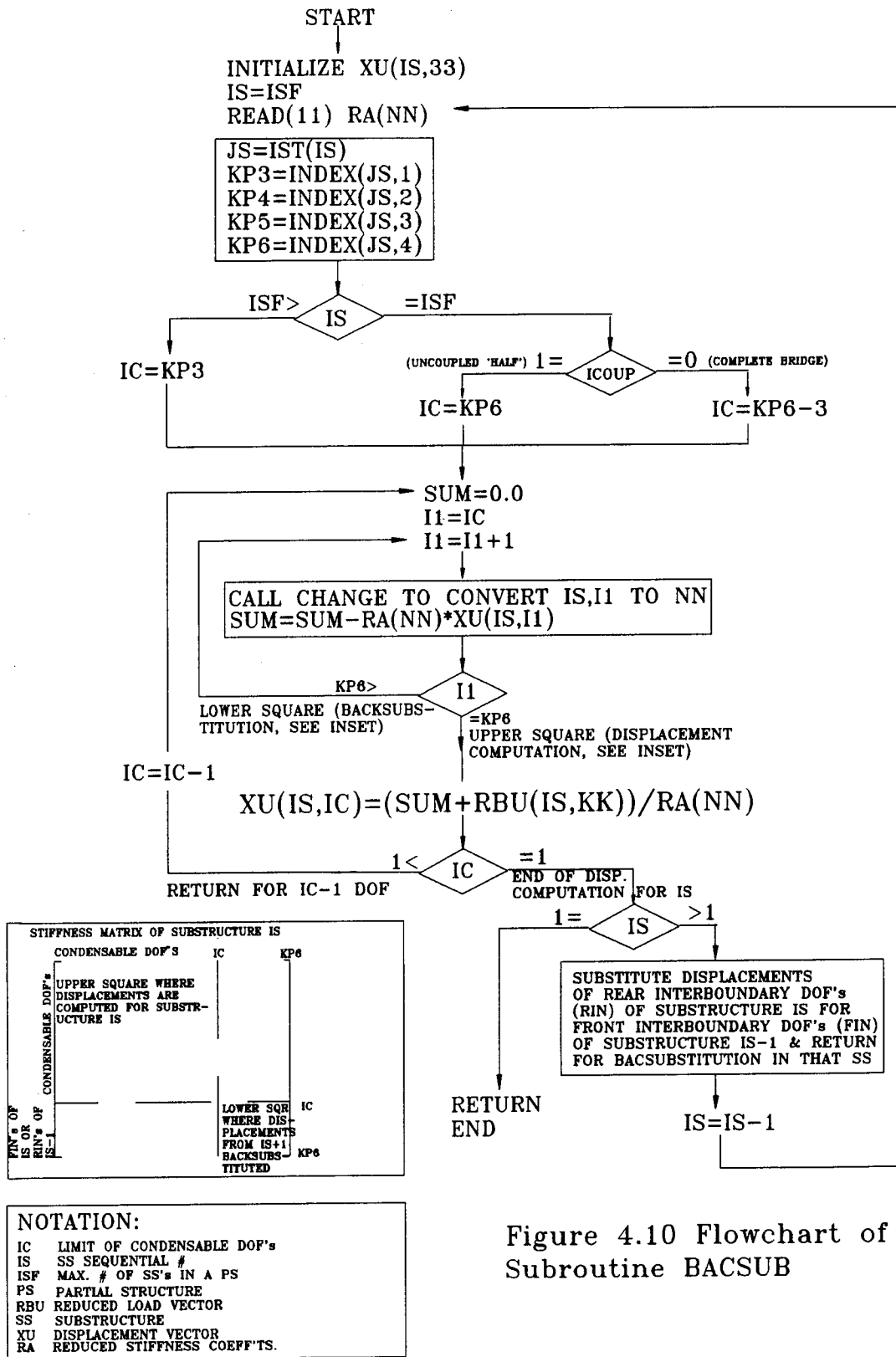


Figure 4.10 Flowchart of Subroutine BACSUB

CHAPTER FIVE: ERECTION ANALYSIS

5.1 Introduction

The task of ensuring the attainment of the specified force and geometric reference configurations for a very flexible and highly redundant structure such as a cable-stayed bridge is rather complex and involved. Nonlinear behaviour of the partial structures, their continuous structural changes, unforeseen erection variations, and geometric deviations or inaccuracies from the exact elemental shapes required to arrive at a specified configuration are some of the causes of the complexity.

In order to deal effectively with these erection problems, it was decided that CASBA should have features to account for:

1. geometric (length) changes of the cables and cross-sectional changes of the girder elements;
2. modifications in the erection procedure without having to re-run the program from the first erection step;
3. temporary bracing and changes in the support conditions at the deck and tower connections;
4. installation of jacks between the towers and the deck to control the relative movement of the two; and,
5. modifications in the cable forces.

In addition, graphical display of the geometric and force configurations for each partial structure is desirable so that the program may be used conveniently on site.

The following Sections will deal with each of these features in more detail and will discuss the basis for the operation of each function with

respect to erection analysis.

5.2 Load Reduction and Backsubstitution

5.2.1 Strategy for Dealing with Loading Effects During Erection Analysis

The erection analysis consists of a multiplicity of sequential load cases, many of which are temporary, acting on a structure of continually changing form. The basic strategy adopted to handle this situation is that any incremental loading is processed only once (i.e. for a single pass of reduction and backsubstitution). This will produce a set of incremental displacements and a distribution of incremental member-end forces which equilibrate the incremental load. The incremental displacements may be added to the previous coordinates to get updated joint coordinates and the incremental member-end forces may be added to the previously accumulated member-end forces to obtain the total member-end forces for the total loading including the present increment. If all external loads are transferred to the joints through the members, joint equilibrium may be checked by the summation of member-end forces at the joints and this summation should not include any of the externally applied loads.

The approach above has been used throughout CASBA and has the following implications.

- a) All loads are applied to members and never to the joints. (i.e. concentrated joint loads, if they occur, are treated as member loads at the end of the member.)
- b) Cumulative load vectors, and the effect of individual loads need not be retained in storage, since the current configuration always reflects the geometry and internal force distribution for the total

loading on the structure at a particular instant of time in the evolution of the structure. This greatly simplifies the data management associated with 'load combinations'.

- c) Corrections to the configuration may always be made by summing the internal forces at the joints to find the unbalanced forces, and applying these unbalanced forces to determine the incremental changes. This is the basis of the nonlinear analysis, presented in Chapter 6. Because 'exact' catenary equations may be used to evaluate cable-end forces the nonlinearity of cables can be properly accounted for. Because an updated geometric configuration may be used, P- Δ effects can be properly accounted for.

5.2.2 Schematic Treatment of Load Reduction and Backsubstitution

To illustrate the flow of the program for load reduction and backsubstitution we return to the schematic description of Fig. 4.8 of Section 4.8.

Suppose that a load is applied to a partial structure, in association with degree of freedom k of substructure i . The form of the unreduced load vector is indicated above the matrix in Fig. 4.8b. The form of the reduced load vector, after the matrix reduction indicated from Fig. 4.8a to Fig. 4.8b, is shown to the right of the matrix. This reduction can be carried out using the coefficients in A' and B' . The segment c of the reduced load vector should now be carried over as the effective load vector acting on partial structure j in Fig. 4.8f, and reduction by the matrix coefficients in this figure converts the right hand side to segment c' and d' . In this manner a load applied to degree of freedom k of substructure i fills in the right hand side for all subsequent partial structures. If j were, however,

the last substructure of the partial structure at the time of load application, the load vector would be processed into vector d'' of Fig. 4.8h, and backsubstitution could start using the coefficients of H'' . Backsubstitution then progresses back through the sequence of reduced matrices up to substructure 1, at which time displacement increments for all nodes in the entire partial structure, due to this particular applied load, are determined.

At this stage, the displacement increments due to this applied load are used: (1) to update the coordinates of all nodes; and (2) to compute increments in member end forces which are added to the previous end forces for all members. Hence a new 'current configuration' has been determined. Note, however, that it is necessary to know the last substructure in the current partial structure in order to determine when to terminate the load reduction and start the backsubstitution. In CASBA, this last substructure number in the current partial structure is designated as the control variable, ISF.

5.3 Erection Variations

Despite every effort to foresee all the problems and details of erection, sometimes unexpected variations in the erection scheme become unavoidable. In this type of situation the program is equipped with a restart file which allows it to find the revised configurations without having to restart from the reference configuration, i.e. without re-running the entire program. More precisely, if the variation occurs between erection steps m and n ($n > m$), the program can begin from configuration n and stop at configuration m in order to give the new configurations due to this variation. The restart file contains sufficient information for each

configuration of the bridge to enable it to restart at any desired configuration. Clearly, this accumulation of information exists only after the first complete run for erection analysis.

5.4 Cable Adjustments

As Section 1.8 shows, in a backward analysis it is possible to obtain accurate initial (unloaded) shapes for members of a bridge so that when they are erected on site according to a specific erection procedure the specified reference configuration is attained. Cables can be cut to any required unstressed length without difficulty, but to fabricate or cast flexural elements to cambered shapes is not convenient. In practice, towers and girders are either cast or erected as straight modular elements.

Provided that the girder is assembled by a large number of short elements, and the geometric and alignment inaccuracies are kept within acceptable limits, the deviations from the reference configuration will not be substantial. Minor departures which will occur in both the geometric and force configurations can be minimized by readjustment of cables already in place. Hence, one would like to be able to determine the effects of these cable adjustments at any stage of erection.

Another important application of the cable adjustment feature is when a proposed erection scheme causes overstressing of one of the elements such as a tower. In this case it may be possible for the designer to proceed with the same plan by adjusting some of the cables at strategic locations. However, this type of application may have to be done on the basis of trial-and-error and its success depends on the experience of the designer.

CASBA allows cable adjustments both in terms of force or length adjustments. It can also eliminate a cable completely, a feature which is

necessary for the backward disassembly of the bridge. These modifications are implemented by first, computing the forces which are required to effect the adjustment and then applying these forces to the structure in the direction of the affected cable and at its ends. As far as the stiffness matrix of the structure is concerned, three different cases may arise:

- a) If a cable tension is being adjusted, the cable area should not be represented in the stiffness matrix. This is done by putting the area of the cable equal to zero for this load case. The specified change in cable tension, ΔT , is then applied to the structure to determine the incremental changes, the area of the cable is restored to its original magnitude, and the unstressed length of the cable is reduced by $\Delta T * L / AE$. This procedure is demonstrated in Fig. 5.1.
- b) If a cable is being eliminated, the incremental changes are determined by applying as external loads its current member-end forces to the structure in which the area of the cable has been set to zero. In this case the area of the cable is removed from the stiffness matrix permanently.
- c) If a cable's length is being adjusted, the length adjustment is converted to an equivalent pair of colinear and opposite forces which are applied to the structure at the ends of the cable. In this case there is no change in the representation of the cable area in the stiffness matrix but L_0 is adjusted by the specified value.

These three procedures are implemented by subroutine CABLES with a flowchart in Fig.5.3.

Whenever a stiffness matrix modification is required, only that part of the stiffness matrix which is contributed to by the affected substructure is modified and added to the reduced stiffness matrix of the

previous partial structure which is present in backing storage. In this manner a considerable amount of computer effort will be saved by not reassembling and reducing the complete stiffness matrix.

5.5 Girder Variations

The girder goes through a large number of geometrical and load variations during erection. In a backward analysis, the girder is first uncoupled at the centreline of the bridge and then each half of it is disassembled by eliminating one substructure at a time.

a) Uncoupling of the Deck

In one of the early stages of disassembly the two halves of the bridge must be uncoupled at the centreline. This corresponds to a reversal of one of the final stages of erection when the two halves of the bridge are joined together at the centre. In order to uncouple the two parts each side of the bridge is treated as an independent partial structure. The internal forces at the connection are reduced to zero by applying the reverse of each side's internal forces to the end joint of the partial structures as external forces. Moreover, in this case, the shear and axial forces will be zero and the bending moment after removal of the deck will be very small. Fig. 5.4 shows the forces which should be applied to each half of the structure. A flowchart of subroutine UNCOUP which implements the uncoupling of the deck is shown in Fig. 5.6.

b) Erection Loads during Disassembly Analysis

Erection loads of the construction or material handling equipment must be applied to the girder as the process of disassembly continues. Because of the cumulative nature of the analysis, and the fact that the structure is analysed by a backward procedure, the loads to be applied should be

changed to the loads going from the later time to the earlier time. Two examples of this are:

- i- in a forward analysis when the derricks are finally removed from the deck their weights would be taken away from the structure by applying forces equal and opposite to the weight of the derricks at their final locations. In a backward analysis this procedure has to be reversed . That is, in the step corresponding to the removal of the derricks their weights are applied to the deck at their final positions before removal, as if they were being newly mounted at those locations.
- ii- In order to move load P from point A to point B, $-P$ should be applied at A and $+P$ at B.

Fig. 5.5 illustrates the procedure in ii.

Besides the above erection loads, whenever a girder segment is removed, its weight is taken away from the partial structure. This is done by applying the positive of the member end forces in the segment to be removed to the remaining partial structure at the point of disconnection.

Fig. 5.2 shows the girder loads due to a substructure removal.

c) Changes in Section Properties during Disassembly Analysis

In a composite deck when the concrete slab is removed, the cross-sectional properties, including the location of the neutral axis in the section, will change. The dislocation of the neutral axis in the affected segment of the girder has a limited effect on the redistribution of the local forces and will be discussed in Appendix C. The new cross-sectional properties replace the old ones at the time of modification and the stiffness matrix is reassembled and reduced for the affected substructure. Subroutine DECK handles all the above girder variations for CASBA. A flowchart of this subroutine appears in Fig. 5.7.

5.6 Bracing

CASBA allows up to five sets of bracing on each half of the bridge. Bracing is one of the most effective ways of stabilizing the girder and controlling stress distribution in the towers. Bracing may be installed, removed, or adjusted through the subroutine BRACG. Any substructure can have bracing connected to the k-end of its first member (see Fig. 5.8), provided that the total number of bracing sets for each half of the bridge does not exceed 5. Bracing is treated as an inclined spring which connects to the ground. Moreover, since the ground ends are assumed fixed and are not given a nodal number, their installation or removal does not affect the nodal numbering system. The default value for the spring coefficients is zero.

In order to incorporate the stiffness of a bracing set into the stiffness matrix of the structure, the global stiffness matrix is re-assembled from the partial structure where the brace is newly installed or removed. Fig. 5.8 illustrates the information required to install a new brace. Fig. 5.9 shows a flowchart for subroutine BRACG.

5.7 Changes in Girder-Tower Connection

During erection a hinged connection between the girder and the tower contributes substantially to the stabilization of what might otherwise be a very unstable partial structure (Fig. 5.10). However, after the completion of the bridge this type of connection is not desirable since temperature variations in the deck will introduce large horizontal forces at the connection with the flexible towers. In order to change the support conditions at the deck-tower connection, CASBA uses three spring elements

with stiffnesses linking the three global degrees of freedom (X, Y, and rotation) of the node in the tower and the node in the girder. The spring stiffnesses can be adjusted or eliminated whenever required. Moreover, it is also possible to introduce specified forces or relative displacements for any of these three elements. This provision allows for the jacking and relative movement of the deck and the tower during erection.

Subroutine DTBC with the flowchart of Fig. 5.11 deals with connection changes in CASBA.

5.8 Graphics Capability

The Graphical Kernel System (GKS) subroutines, with the additional library prepared by the Computer Graphics Group of the Pontificia Universidade Catolica do Rio de Janeiro (PUC) of Brazil, have been used to display and print the internal forces and the deflected shapes of the partial structures and the complete bridge. This graphics facility is expected to be especially useful for monitoring the erection procedure on site. It can also facilitate study of erection variations on site.

However, the graphics routine takes additional time for displaying and printing and whenever greater speed is required (such as during the preliminary design of a bridge) it should be opted out at the beginning of the run.

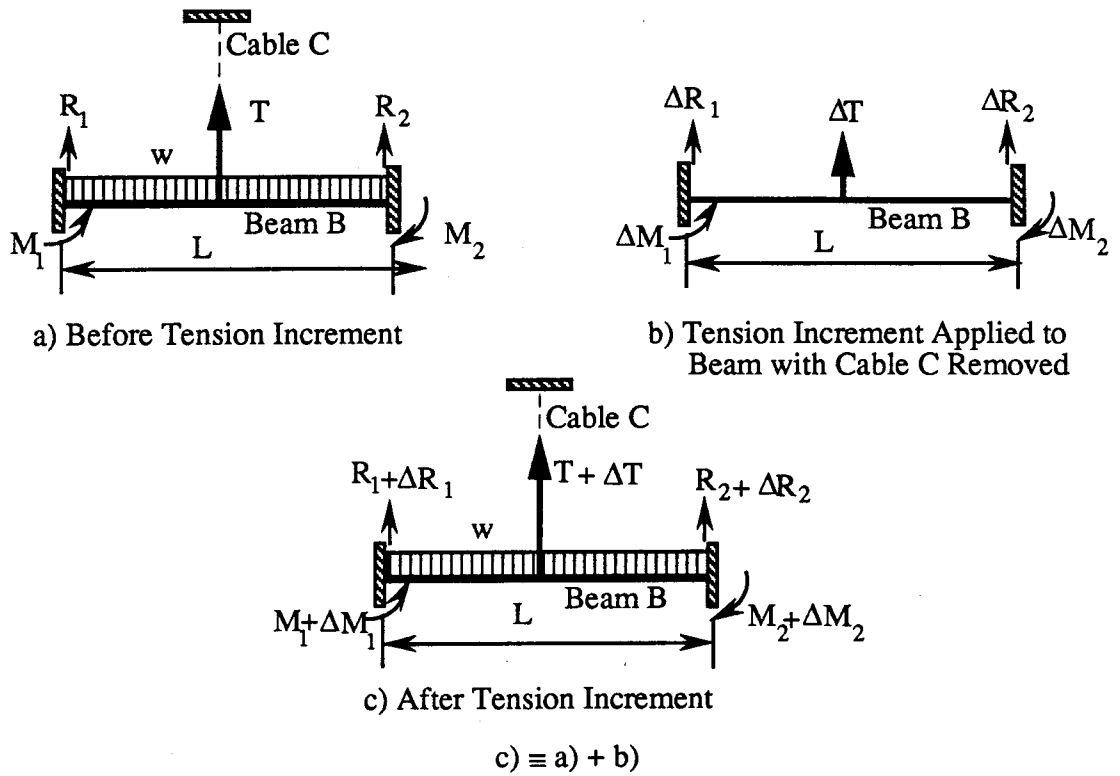


Fig. 5.1 Force Increment In Cables

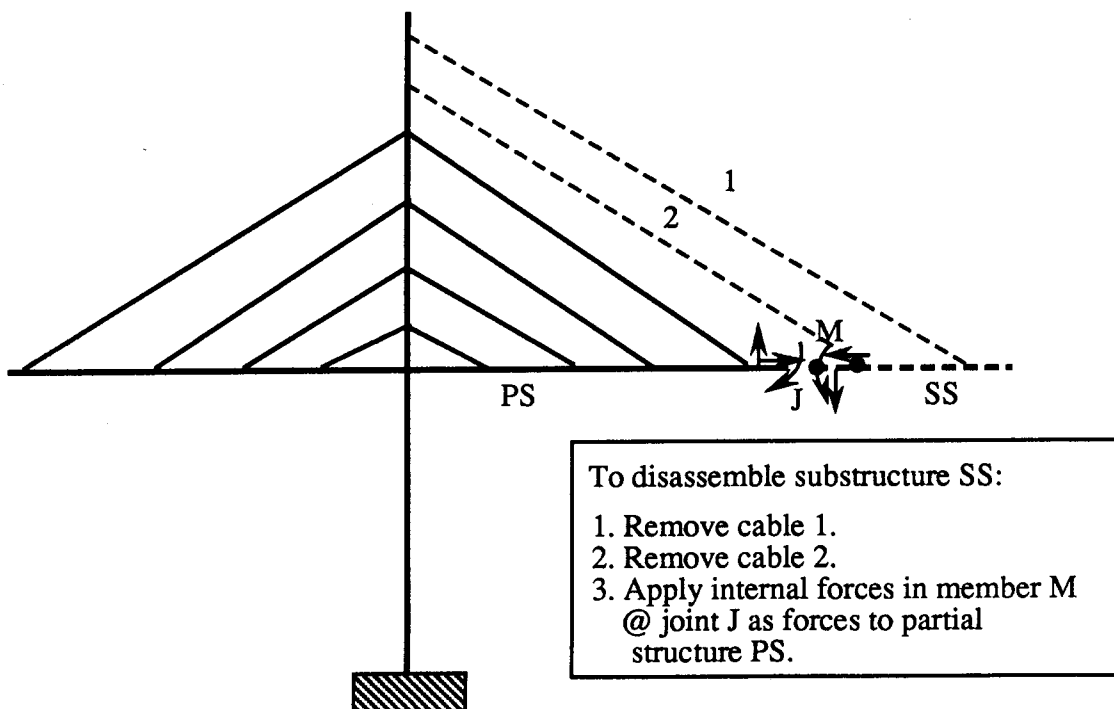
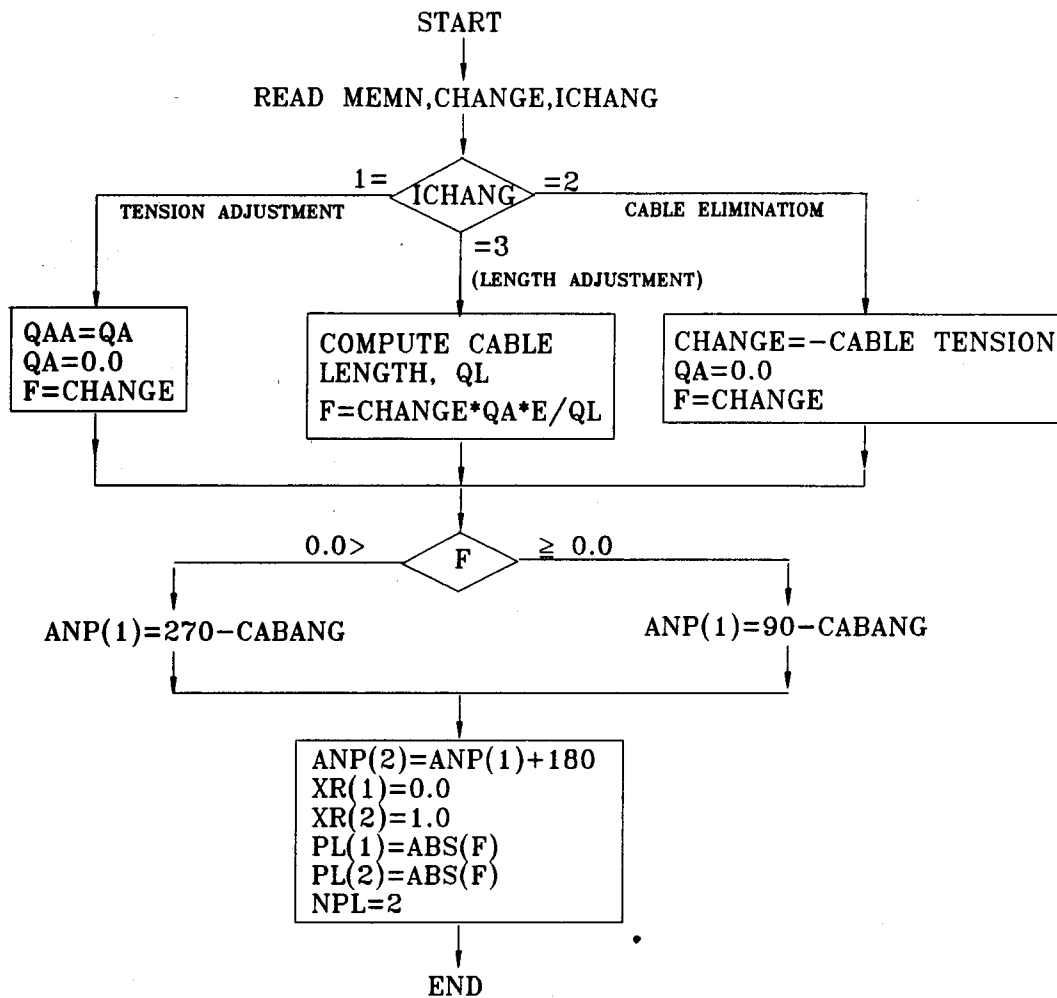


Figure 5.2 Girder Forces Due To Removal Of Substructure SS



NOTATION	
ANP	ANGLE BET. X-AXIS & EXTERNAL FORCE PL
E	MODULUS OF ELASTICITY
CABANG	SEE INSET
CHANGE	AMOUNT OF VARIATION IN CABLE FORCE/LENGTH
ICHANG	VARIATION CODE
PL	EXTERNAL POINT LOAD DUE TO CABLE VARIATION
QA	C.S. AREA OF CABLE
QAA	AUXILIARY ARRAY USED TO RECOVER QA AFTER TENSION ADJUSTMENT
NPL	# OF POINT LOADS
XR	NONDIMENSIONAL DISTANCE FROM J-END TO PL
F	CABLE FORCE VARIATION

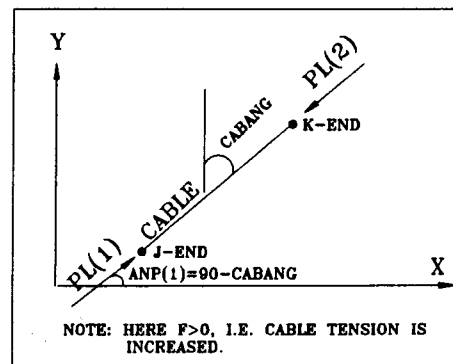


Figure 5.3 A Flowchart for Subroutine CABLES

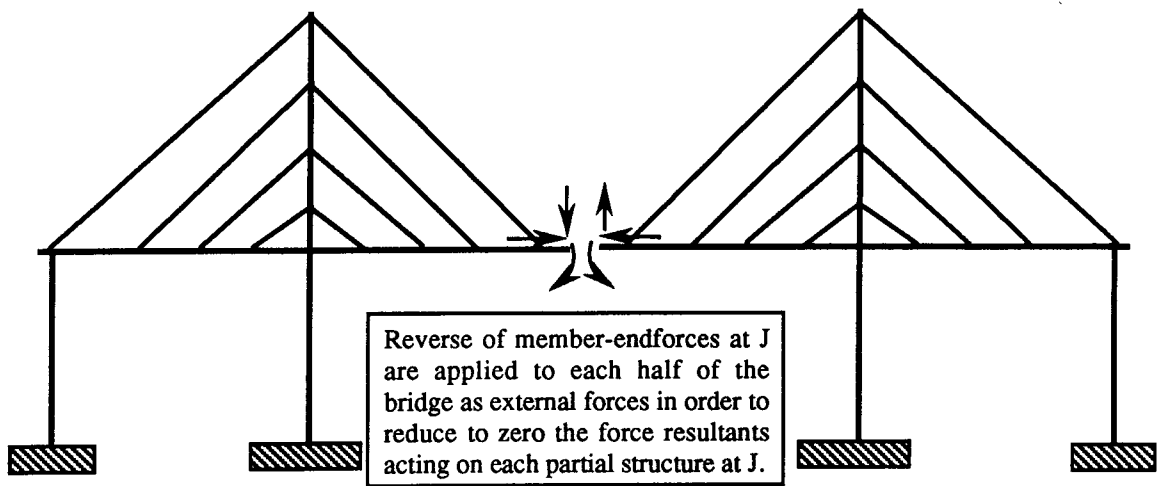


Figure 5.4 Uncoupling of the Girder

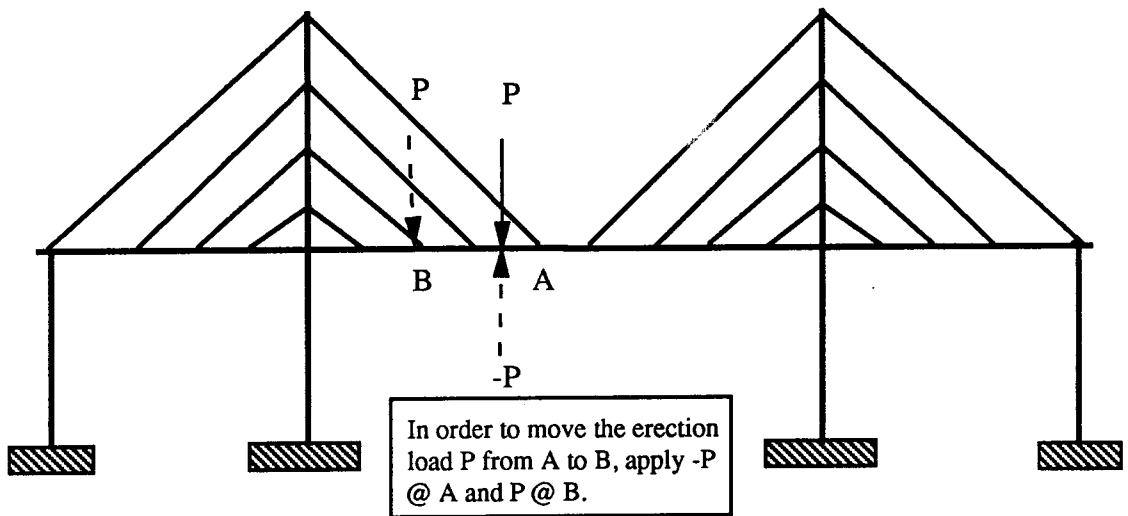
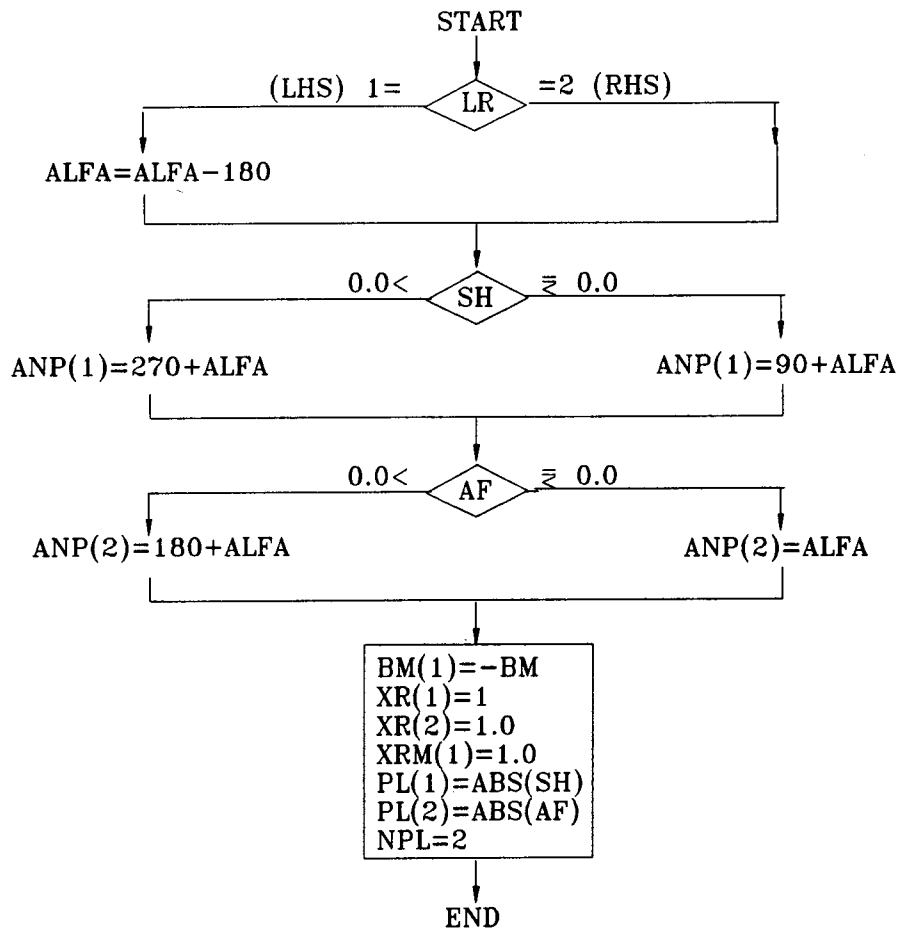


Figure 5.5 Erection Loads in Backward Analysis



NOTATION	
AF	AXIAL FORCE @ C OF DROP-IN SEGMENT
BM	BENDING MOMENT @ C OF DROP-IN SEGMENT
ANP	ANGLE BETWEEN X-AXIS & AN EXTERNAL POINT LOAD
ALFA	ANGLE BETWEEN X-AXIS & DROP-IN SEGMENT
PL	EXTERNAL POINT LOAD
BEM	EXTERNAL BENDING MOMENT
NP	# OF POINT LOADS
XR	NONDIMENSIONAL DISTANCE FROM J-END TO POINT LOAD
XRM	NONDIMENSIONAL DISTANCE FROM J-END TO EXTERNAL BENDING MOMENT

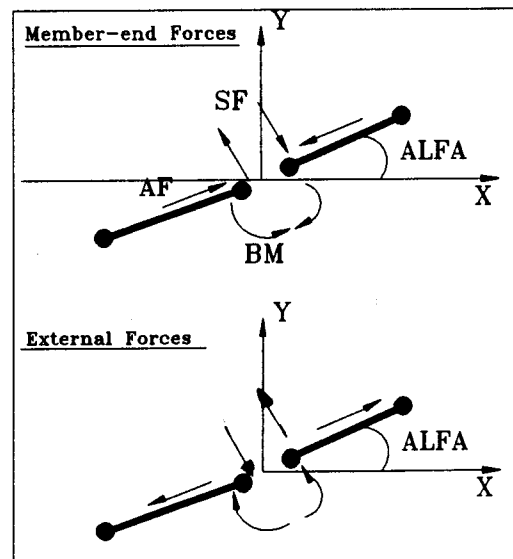
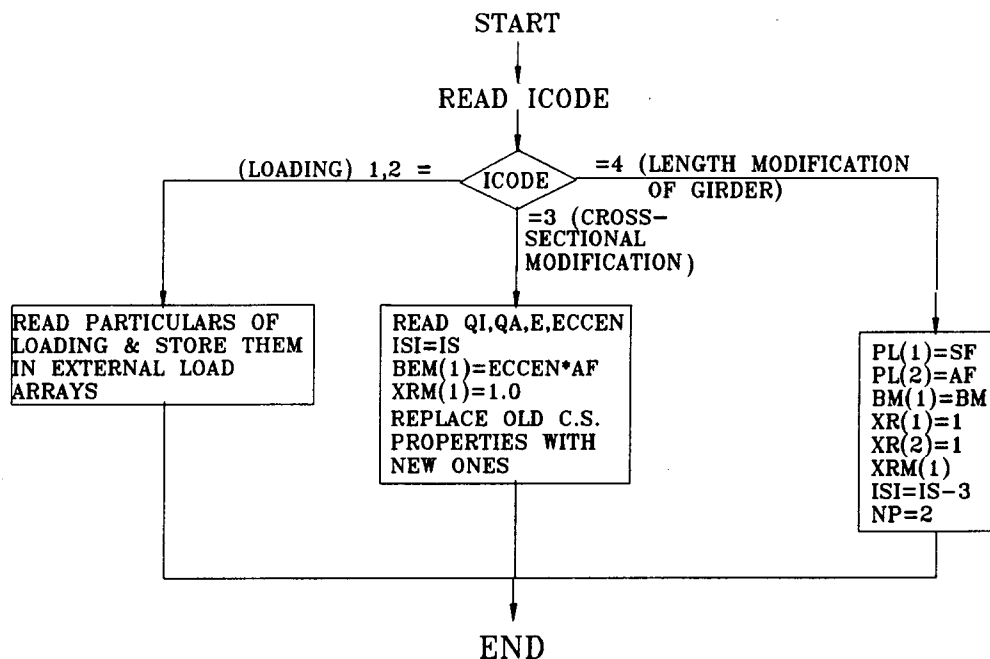


Figure 5.6 Flowchart of Subroutine UNCOUP



NOTATION	
AF	AXIAL FORCE IN MEMBER BEING DISASSEMBLED
BM	BENDING MOMENT IN MEMBER BEING DISASSEMBLED
SF	SHEAR FORCE IN MEMBER BEING DISASSEMBLED
PL	EXTERNAL FORCE APPLIED TO REMAINING PS AT BOUNDARY WITH SS BEING DISASSEMBLED
BEM	EXTERNAL BENDING MOMENTS APPLIED TO REMAINING PS AT BOUNDARY WITH SS BEING DISASSEMBLED
PS	PARTIAL STRUCTURE
SS	SUBSTRUCTURE
XR	NONDIMENSIONAL DISTANCE BETWEEN FORCES AND J-END OF MEMBERS
XRM	NONDIMENSIONAL DISTANCE BETWEEN POINT OF APPLICATION
QA	NEW CROSS-SECTIONAL AREA OF GIRDER ELEMENT
QI	NEW MOMENT OF INERTIA OF GIRDER ELEMENT
E	NEW MODULUS OF ELASTICITY
ECCEN	DISTANCE BETWEEN NEUTRAL AXES OF NEW AND OLD CROSS-SECTIONNS

Figure 5.7 A Flowchart of Subroutine DECK

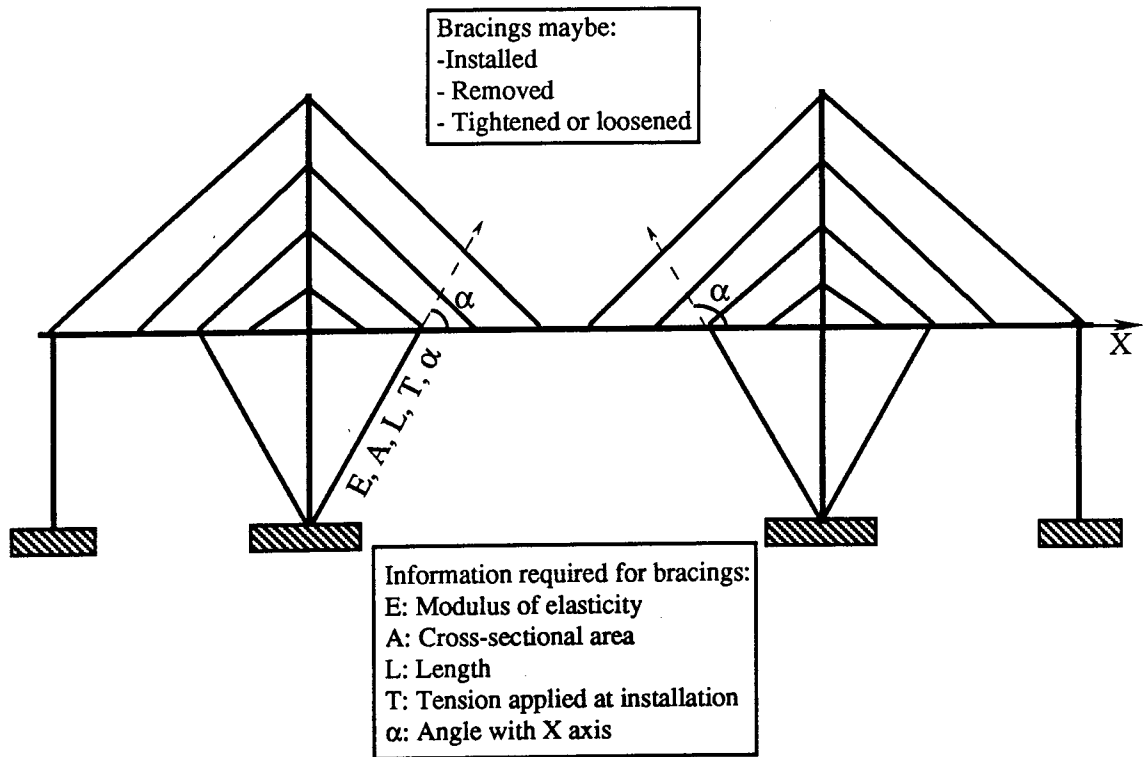


Figure 5.8 Bracing

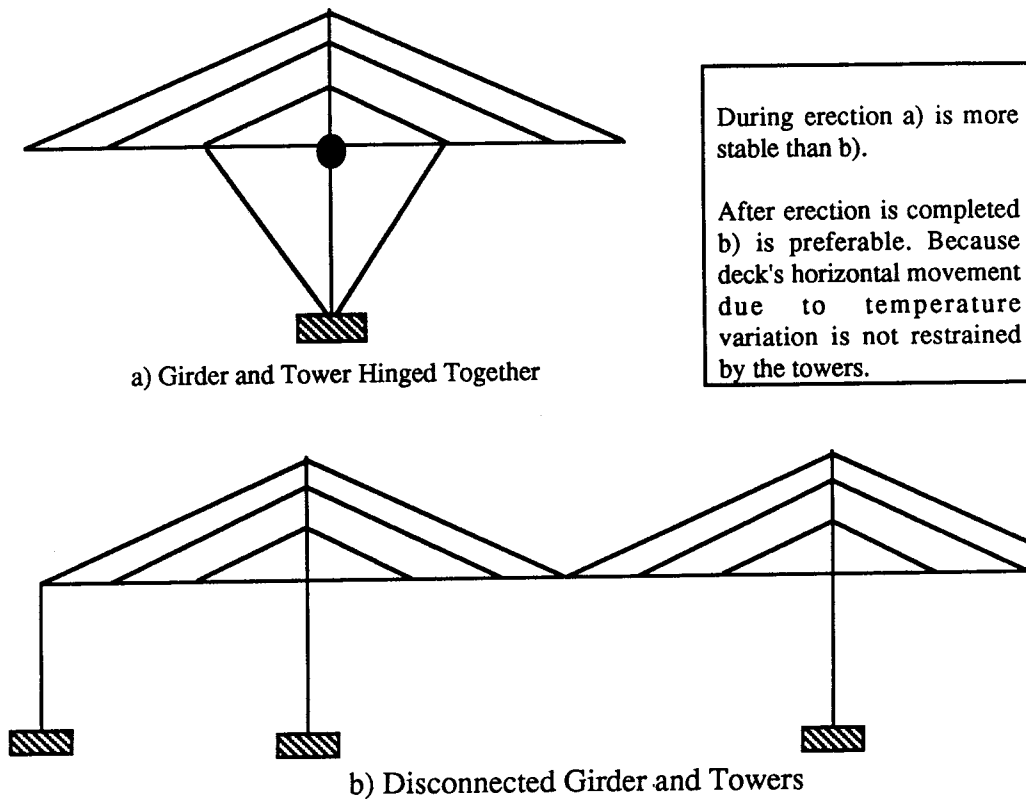
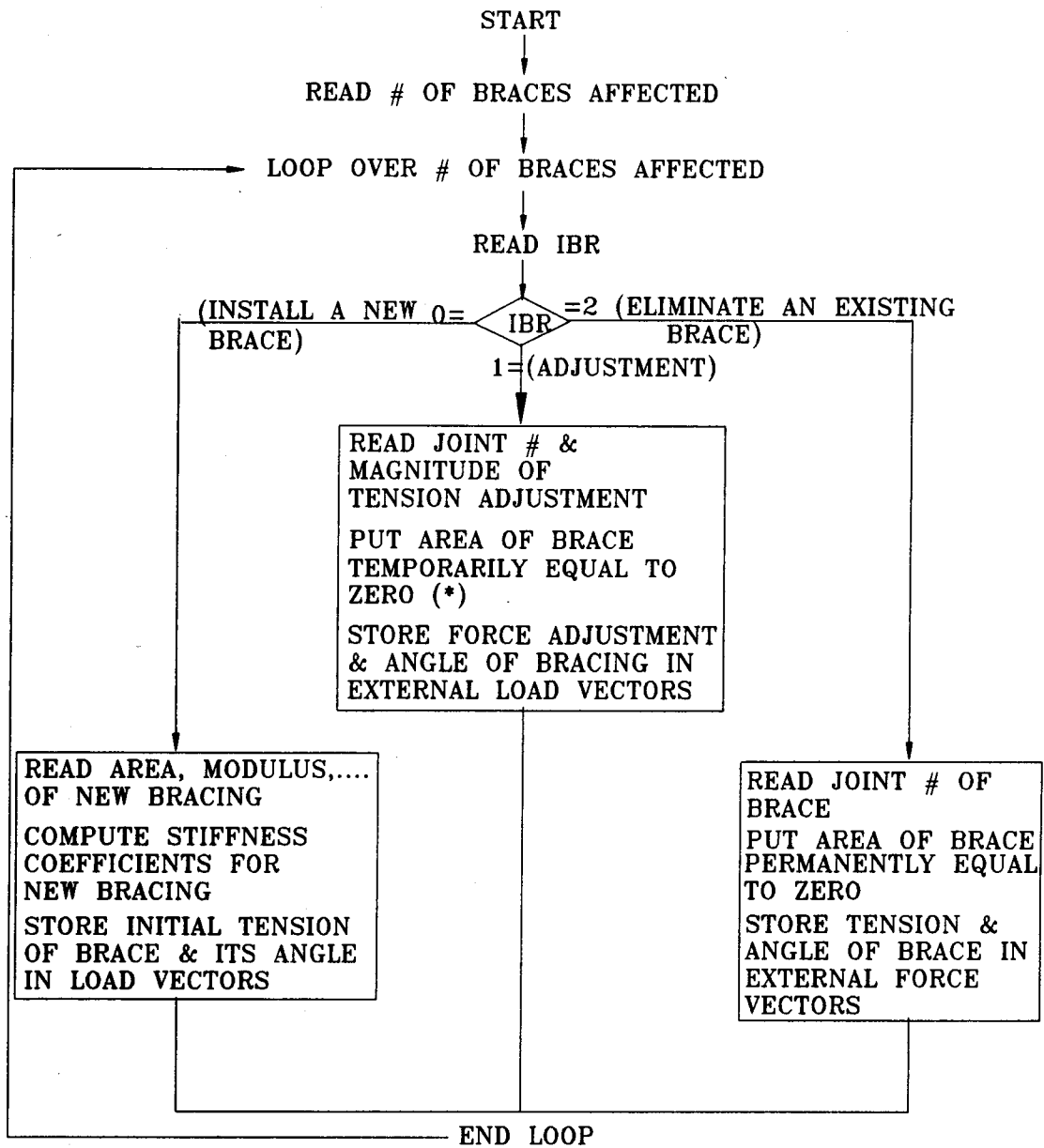


Figure 5. 10 Change in Girder-Tower Connection



(*) The area of the brace is stored in a temporary array and will be restored to its original value at the end of tension adjustment.

Figure 5.9 Flowchart of Subroutine BRACG

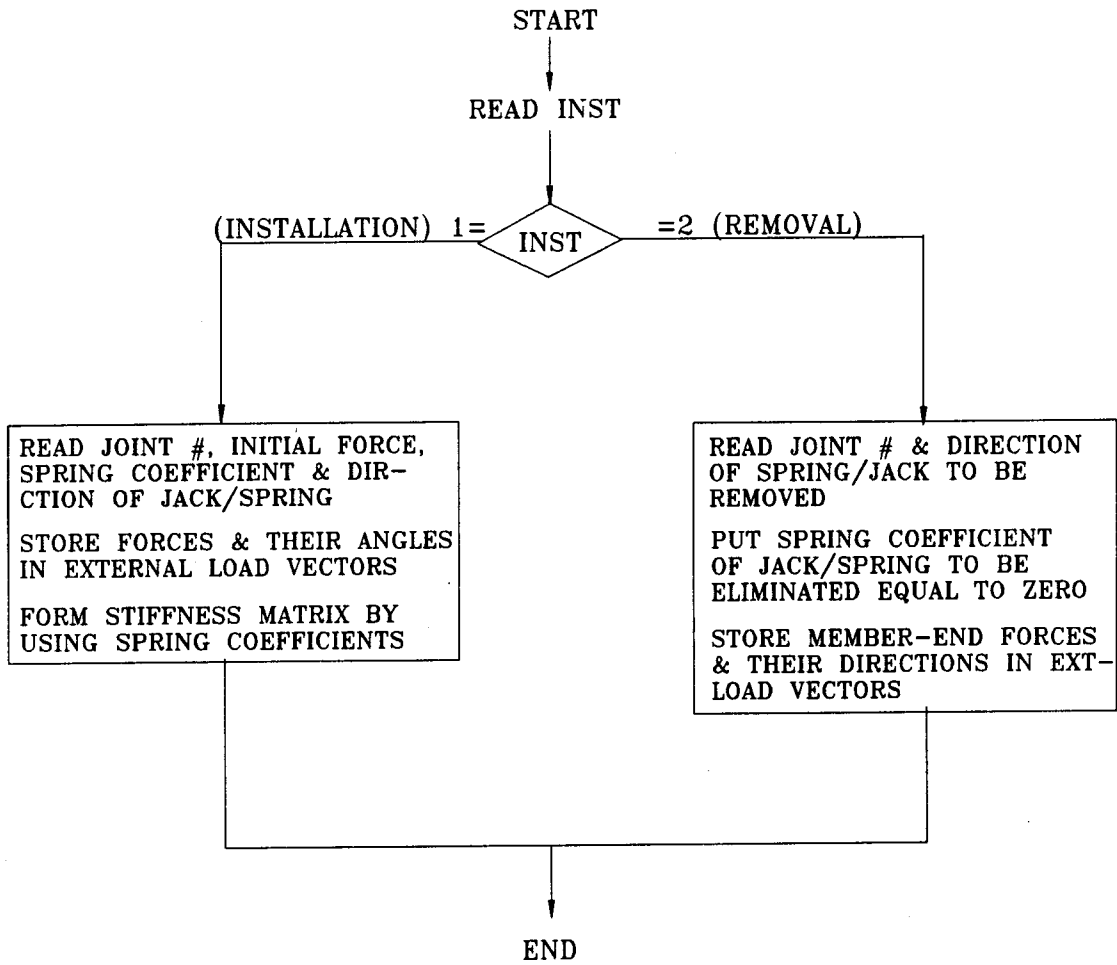


Figure 5.11 Flowchart of Subroutine DTBC

CHAPTER 6 : NONLINEARITIES

6.1 Introduction

Four sources of nonlinearity may affect the performance of a structure and cause its load-deflection path to deviate from a simple straight line.

These are:

- a. inelastic material behaviour (for instance, of reinforced concrete elements);
- b. large deflections (for instance, geometric nonlinearity of cable elements);
- c. inelastic strains (such as creep or shrinkage); and,
- d. stiffness changes produced by variations in the boundary conditions or alterations in structural configuration.

In the design and erection analysis of a cable-stayed bridge the last three items of the list are of more importance.

The term large deflections is used, herein, for the nonlinear behaviour of the cables and the (P- Δ) effects in the girder and the towers. Inelastic strains may play an important role in the case of in-situ reinforced concrete decks and towers. However, the present work does not cover this type of nonlinearity as the main application of the program is expected to be in the field of erection analysis of modular, precast elements in which most of the shrinkage strains have normally taken place and creep strains do not have time to accumulate. Stiffness changes exist in the erection analysis of cable-stayed bridges because the partial structures and their support conditions go through a large number of structural changes, as discussed in Chapter 5. The present Chapter treats

the nonlinear problem of large displacements in the cables of a cable-stayed bridge and P-Δ effects in the towers and girder.

6.2 Cable Nonlinearity

Since Dischinger discovered the importance of high tensile stress in the stays of a bridge in 1938, strands with a very high level of Guaranteed Ultimate Tensile Strength (GUTS) have become a permanent feature of cable-stayed bridges. GUTS of the order of 1700 - 1800 MPa with an allowable working stress of 750 - 850 MPa (if fatigue is not a major consideration) are quite normal. Assuming a live load to dead load ratio of 0.4, the average tensile stress under the dead load alone will become

$$750 / 1.4 = 540 \text{ MPa.}$$

The effective modulus of elasticity ratio for a cable with $E = 1800000$ MPA, $\gamma = 0.000078 \text{ N/mm}^3$, $a = 250000 \text{ mm}$ and at a tensile stress of 540 MPa is computed from [3.35] to be:

$$E_c / E = 1 / (1 + E \gamma^2 a^2 / 12 \sigma^3) = 0.965$$

This shows that a linear analysis of the reference configuration or any subsequent live load analysis will introduce less than 4% inaccuracy in the computations which is well within the normal level of inaccuracies encountered in structural analysis. Heavy unsymmetrical live loads tend to decrease the tensile stress of the cables attached to the side spans. However, as Fig. 6.1 indicates this has a marginal effect on the effective modulus of elasticity ratio of these cables, providing that the normal

limit of side span to central span ratio of 0.35 is observed.

On the other hand, cable nonlinearity may become an important factor during the course of erection between the time of installation of the cables and completion of the deck. During this period the cables may be subjected to a relatively large change in their tensile stress. Based on the above, CASBA analyses the reference configuration and the live load cases through its linear elastic routines, while for erection load cases (disassembly analysis) it takes into consideration the large deflection of the cables, the P- Δ effect of the girder and the towers, and the change in configuration of the partial structures during erection.

These nonlinear considerations can only be taken care of by an iterative procedure in which the joint equations of equilibrium are checked in every cycle of iteration in the deformed structural configuration and the unbalanced forces are reapplied to the joints until a reasonable convergence criterion is satisfied.

The detailed procedure includes the following steps.

1. In the formation of the stiffness matrix, each cable is replaced by its equivalent straight member with the effective modulus of elasticity given by [3.16]. Inaccuracies of the order of 5% may exist in the computed stiffness coefficients of the cables due to this approximation, but this is of no consequence as the exact catenary equations are used to check the equations of equilibrium.
2. After the displacement computations, the system's configuration is updated (subroutine UPDATE), and the horizontal and vertical cable forces at the cable ends are computed by using the catenary equations of Chapter 3 (subroutine CATENARY).
3. The joint equations of equilibrium at each cable end are formulated

and the unbalanced load vector is formed (subroutine UNBALF).

4. The average norm of the unbalanced forces is computed from:

$$ERR = \left\{ \left[\sum_{i=1}^n ((\delta X_i)^2 + (\delta Y_i)^2) \right]^{1/2} \right\} / n \quad [6.1]$$

in which

δX_i and δY_i are the X and Y projections of the unbalanced forces at joint i; and,

n is the total number of the cable ends in the structure,

5. The average norm of the member-end forces (the axial and shear forces) is computed from:

$$FNORM = \left\{ \left[\sum_{i=1}^N ((X_i)^2 + (Y_i)^2) \right]^{1/2} \right\} / N \quad [6.2]$$

where:

X_i and Y_i are the axial and shear member end forces in member i,

N is the total number of elements in the structure.

6. An error limit of $DLIMIT = 0.01 * FNORM$ is defined.
7. The equations of equilibrium are considered to be satisfied if ERR is found to be smaller than or equal to DLIMIT and the next load combination is initiated.
8. If ERR is found to be greater than DLIMIT the unbalanced forces are applied to the structure until the equilibrium criterion defined under 7 is satisfied. This iterative procedure is done according to the Newton-Raphson (N-R) procedure, i.e. by the complete updating of the stiffness matrix in each cycle of iteration. In this particular case, experience has shown that the computer time required for convergence

would be less than the time for the modified N-R procedure which uses a constant stiffness matrix.

Fig. 6.2 shows a flowchart of EQCHEC which checks the joint equilibrium in CASBA.

6.3 P- Δ Effect

The traditional methods of structural analysis are based on achieving equilibrium of the structure in its initial undeformed configuration. This is an acceptable approximation, providing that the deformations are very small, i.e. the theory of small deformations is applicable to the structure.

With the recent tendency toward flexible, slender structures with their combined elegance and economy, the above simplification has become the subject of increasing scrutiny. From the theoretical point of view, equations of equilibrium should be formulated on the basis of the deformed configuration, simply because equilibrium exists after a deformable body has gone through its deformations under the system of external forces.

Obviously, the main reason for using the initial configuration as the basis of equilibrium is that this configuration is readily available and can be used in a simple direct solution without any iteration. In mathematical terms, the formulation based on the equilibrium of the structure in its deformed configuration results in additional matrices, called geometric stiffness matrices, which are algebraically added to the stiffness matrix of the structure. Whether the geometric matrix of an element is positive definite or negative definite depends on the sign of the axial force in that element. Members in tension have positive definite geometric matrices, while members in compression have negative definite

geometric matrices.

Cables, as discussed in the first part of this Chapter, are examples of members in which the geometric matrix is positive. In fact, in the early part of loading it is the geometric matrix which is dominant, but gradually the material component becomes more significant and when the cable approaches a straight line the geometric component becomes a minor component of the stiffness matrix. This change of state is demonstrated by the load deflection curve of a single degree of freedom cable shown in Fig. 6.3.

On the other hand, girders and towers of a cable-stayed bridge may experience a considerable stiffness reduction due to their high compressive axial force. This interaction of deflections and internal stresses (forces) is referred to as the P- Δ effect.

In order to illustrate the P- Δ effect in a simple structure, and more specifically, in order to show the influence of the sign of the axial stresses, the simple example of Fig. 6.4 in which a pinned rigid bar with a horizontal spring attachment is subjected to the horizontal force H and the vertical force V is solved here. It is assumed that the spring will remain horizontal throughout the course of loading.

Assuming that the equations of equilibrium are written in the initial configuration, the stiffness coefficient of the system in the horizontal direction is computed from

$$H - K \Delta = 0 \quad [6.3]$$

$$\text{or } \Delta = H / K \quad [6.4]$$

where K is the spring coefficient.

As the horizontal component of the bar's axial force increases, the above relationship becomes less accurate. In order to formulate the equations of equilibrium accurately, they should be written with reference to the deformed configuration shown in Fig. 6.4b.

$$H + N \sin \alpha - K \Delta = 0 \quad [6.5]$$

or,

$$H + N \frac{\Delta}{L} - K\Delta = 0 \quad [6.6]$$

From which,

$$\Delta = H / (K - N / L) \quad [6.7]$$

Eq. [6.7] shows that the real stiffness of the system in the horizontal direction is $K - N / L$. This stiffness coefficient, which is composed of the material component K , and the geometric component $-N/L$, may be greater or smaller than K depending on the sign of N . Fig. 6.4c shows the three possible variations in load-displacement curves for the horizontal degree of freedom of the system depending on the sign of the axial force N . Note also that the $P-\Delta$ effect may be taken into consideration either by modifying the stiffness of the structure, or by modifying the forces applied to the structure by considering the components of the internal axial forces as supplements to the external forces (such as adding $N \Delta/L$ to H in [6.5]). Finally, the above example shows that by writing the equations of equilibrium in the deformed configuration the $P-\Delta$ effect is automatically taken care of.

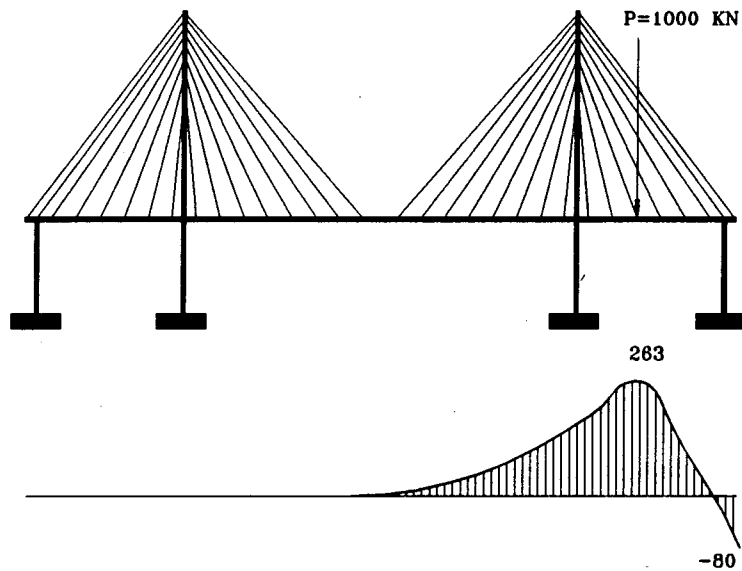
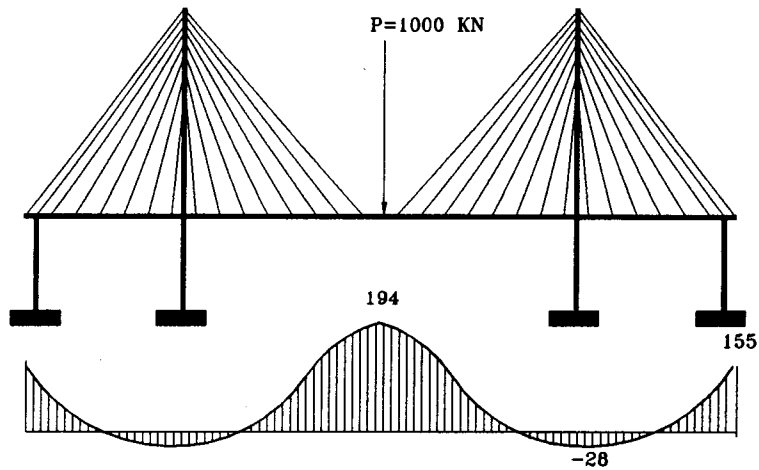
Figure 6.5 shows the procedure which has been used in CASBA to incorporate the $P-\Delta$ effect into the program. In each load step, or cycle of

iteration, the geometry of the structure is updated immediately after the computation of the displacements due to the applied loads. Then the internal forces in the new configurations are computed by applying the constitutive relationships (for example, the catenary equations for the cables) to the new configuration. Then the joint equations of equilibrium are checked in the deformed configuration and finally the unbalanced forces are computed and applied to the updated configuration of the structure until the convergence criterion is met.

6.4. Major Sources of Nonlinearity in Cable-Stayed Bridges

Provided that inelastic deformations are negligible, the major sources of nonlinearity in a cable-stayed bridge are confined to geometric nonlinearities. The geometric nonlinearity of the cables becomes insignificant as their tensile stress increases. It is suggested that for moderate central spans of up to 500 m whenever this tensile stress is in excess of 500 MPa this nonlinearity can be neglected.

The other important type of geometric nonlinearity which should be taken into consideration (especially for larger spans and axial forces), is the P- Δ effect. This may be handled simply by an iterative procedure which checks the equations of equilibrium in the updated configuration and reapplies the unbalanced forces to the deformed structure until the convergence criterion is met.



Assume:

$$\sigma_{DL+LL} = 750 \text{ Mpa} ; \quad \frac{LL}{DL} = 0.4$$

Then:

$$\sigma_{DL} = 750/1.4 = 540 \text{ MPa} ; \quad \sigma_{LL} = 210 \text{ MPa}$$

And for tension variation shown above

$$\Delta\sigma_{LL} < \frac{-80 * 210}{263} = -64$$

So reduced stress in anchor cable $> 540 - 64 = 476 \text{ MPa}$

Then from [3.35]: $\frac{E_c}{E} > 0.95$ (Compared with 0.965)

Fig. 6.1 Typical Distribution of Cable Forces Due to Point Loads

NOTATION:	
E	Modulus of a straight cable
EC	Effective modulus of a catenary cable
NC	Number of cables
TNM	Total number of members
TA	Cable tension @ A
TB	Cable tension @ B
TC	Average cable tension
AC	Cross-sectional area of a cable
DEN	Cable density
XA	Horizontal projection of a cable
YB	Vertical projection of a cable
LEQ	Equilibrium flag

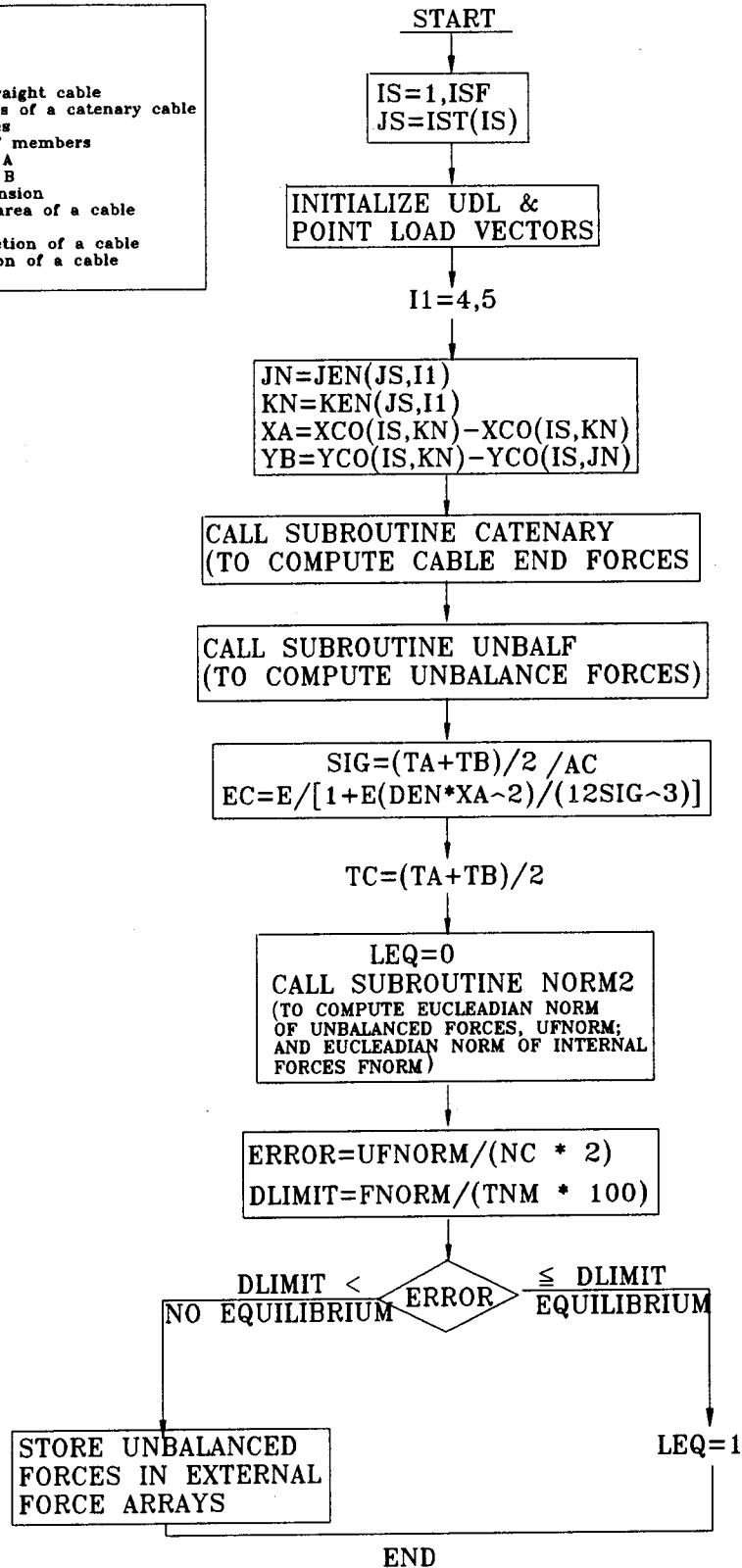


Figure 6.2 Flowchart of Subroutine EQCHEC

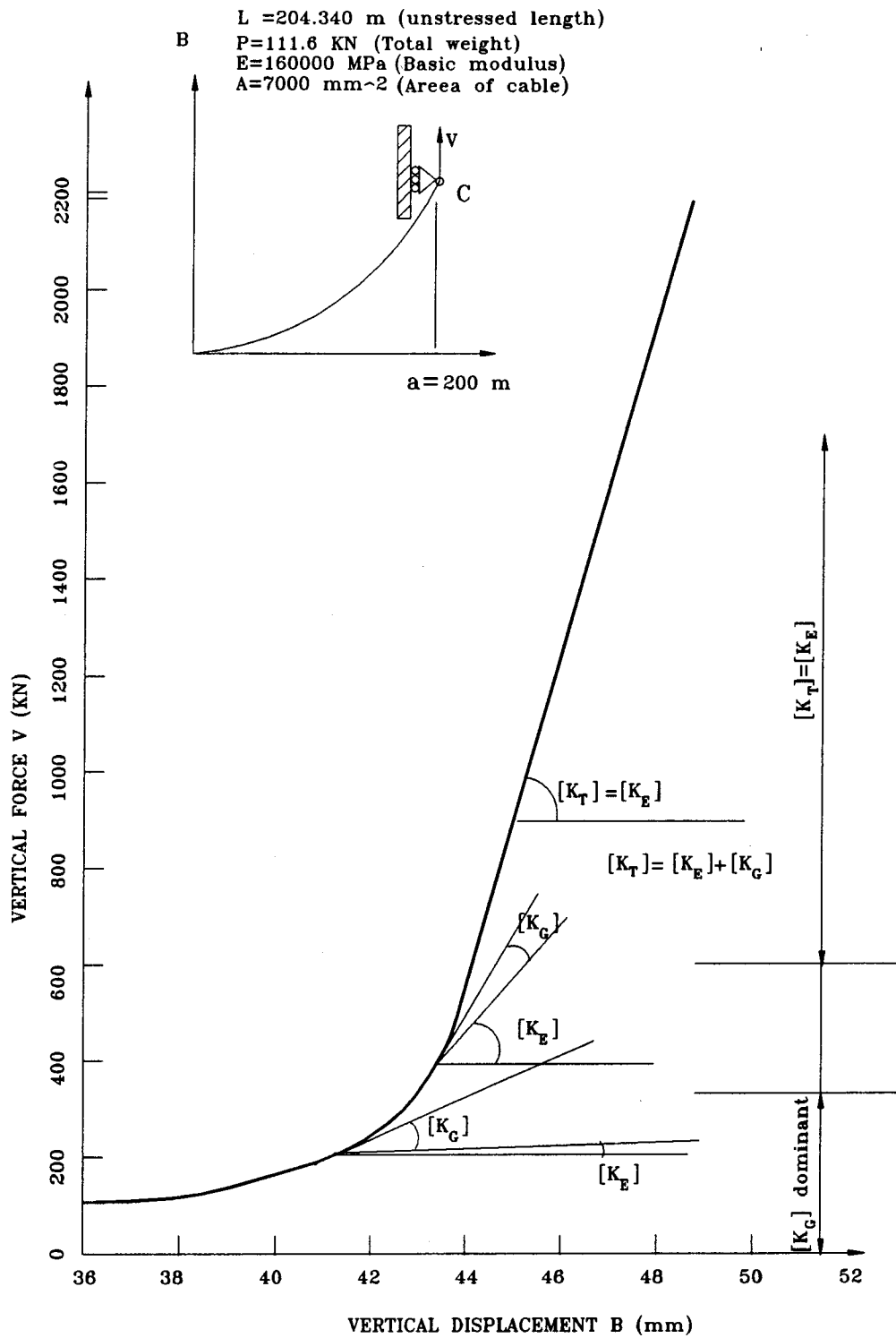
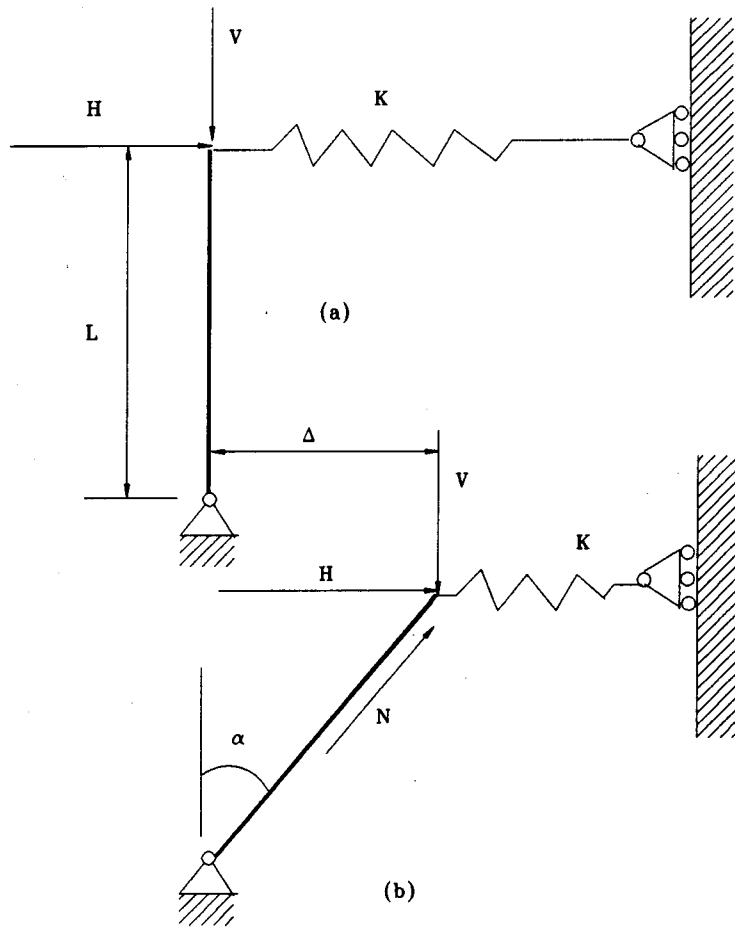


Figure 6.3 Load-Displacement Curve for a SDOF Cable



N positive
in compression

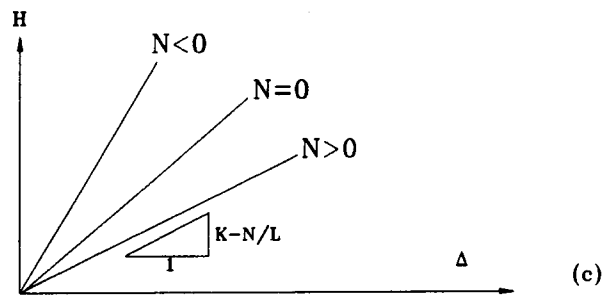


Fig. 6.4

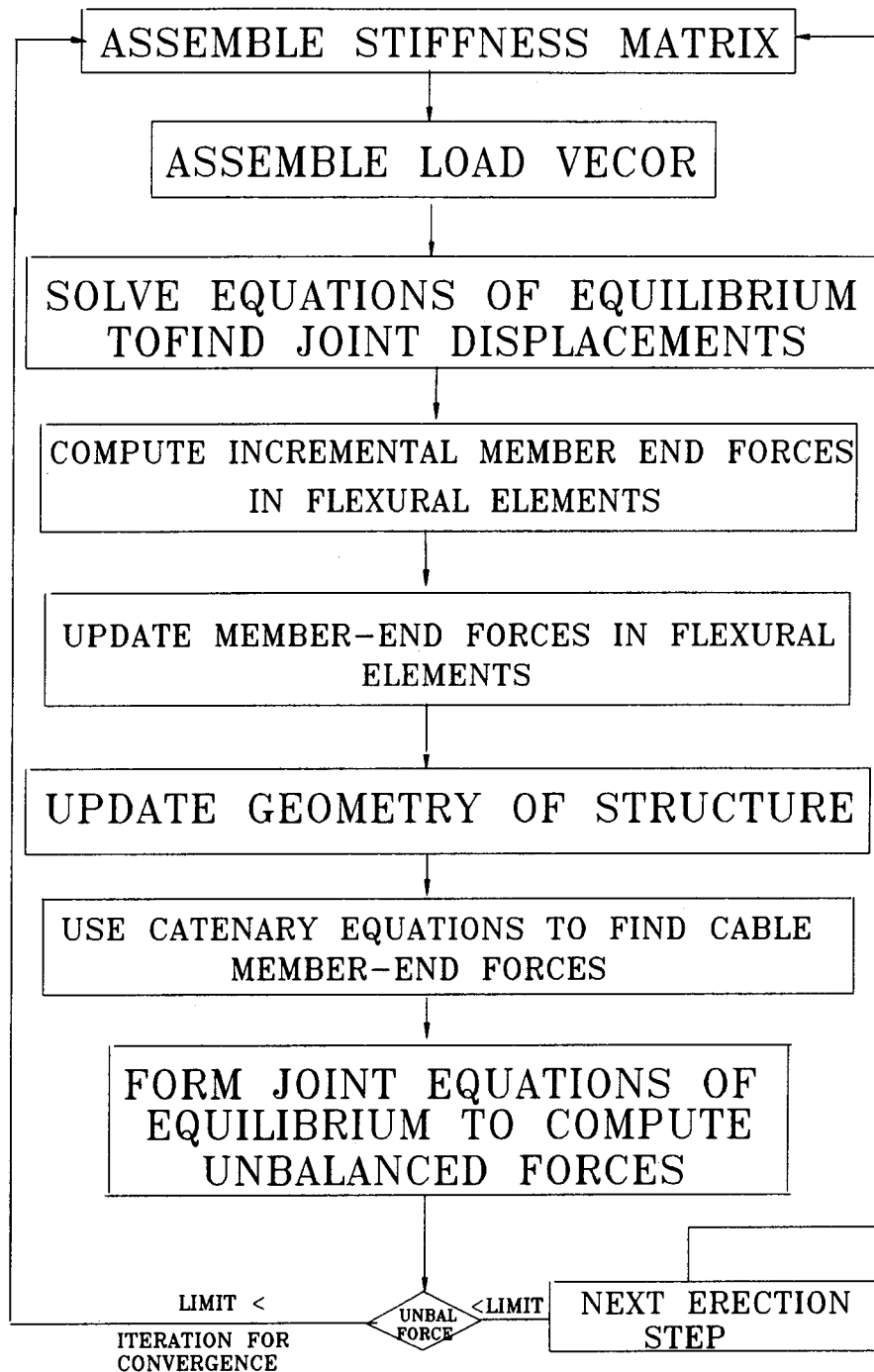


Figure 6.5 Steps in Nonlinear Erection Analysis

CHAPTER 7 : THE PROGRAM AND ITS APPLICATIONS

7.1 Introduction

Chapters 3 to 6 have dealt with the development of the major components of CASBA, such as the stiffness matrix, the load vector, the equation solver, the nonlinearities, and the erection procedures and loads.

The present Chapter describes CASBA and its applications as a whole program.

CASBA's typical application is in the field of erection analysis and design of three span, multi-cable-stayed bridges. It can also be applied to other types of cable-stayed bridges, or in fact, any type of framed structure providing appropriate modifications are made to the source code. In its typical application it considers geometric nonlinearities due to catenary cables as well as the P- Δ effect in the flexural elements.

7.2 The Program Structure

The main program uses a number of primary subroutines, each of which is responsible for a major task in the process of design or erection analysis of a cable-stayed bridge. More specific tasks within each primary subroutine are done through a number of auxiliary subroutines. A tree structure of the primary and the most important auxiliary subroutines is illustrated in Fig. 7.1.

The main program may be divided into the following segments.

Segment 1: Input Reading and Processing:

- (a) In this segment the specified nodal bending moments and the geometric and material properties of the reference configuration

are input through subroutine INPUT. This input is rearranged and stored in arrays with substructural numbering indices provided by auxiliary subroutines NUMBER and JKENDS.

- (b) Subroutine DLBM (for, dead load bending moment) then computes the cable forces associated with the specified bending moment distribution in the girder and prepares the load data for the application of these forces to the girder as external loads for the initial run of the program. This initial run determines all the member-end forces in the bridge consistent with the specified bending moments in its reference configuration.

Segment 2: Stiffness Matrix Formation and Reduction:

The primary subroutine SUBST (for, substructure) is an umbrella subroutine covering all the various operations required at the substructure level. As one of its assignments, it assembles the stiffness matrix of a substructure through the auxiliary subroutines MEMST (which prepares the member stiffness matrix) and ASSMEM (which transfers member stiffness matrices into the global coordinate directions and assembles them together). Subroutine ASSUB assembles the stiffness matrix of the substructure to the reduced stiffness matrix of a previous partial structure to produce an unreduced stiffness matrix for the newly formed partial structure. Subroutine REDUCE eliminates all the condensable degrees of freedom from this stiffness matrix. (These operations have all been discussed in Chapter 4.)

Segment 4: Load Vector Formation and Reduction:

Here, subroutine SUBST through the auxiliary subroutine MLOAD (for, member load), forms the member load vector, transforms it

to the global coordinate directions and assembles it into the substructure load vector. Subroutine ASSRHS (for, assemble right hand side) assembles this load vector to the reduced load vector of the previous partial structure and subroutine REDRHS reduces it by using the pivotal ratios obtained in subroutine REDUCE at the time of the associated stiffness matrix reduction. It is to be noted that subroutine LOAD which inputs the loading properties of each load case is activated only in the case of live load analysis. Erection loads are defined by the primary subroutine ERECT which will be discussed later.

Segment 4: Computation of Deformations and Member-end Forces:

The global nodal deformations are computed by the primary subroutine BACSUBST and are used in subroutine SUBST to compute the member-end forces of each member in the local coordinates.

Segment 5: Unstressed Cable Length Computation:

After the first run for the reference configuration the program computes the unstressed lengths of the cable elements through the primary subroutine ZEROL. This subroutine uses the auxiliary subroutine CATENARY to solve the catenary equations for the given end forces and coordinates in order to arrive at the cable stress and its current length from which the unstressed length is computed according to Section 3.5.

Segment 6: Nonlinear Considerations:

This segment of the program is used in erection analysis only. The primary subroutine UPDATE updates the geometric configuration of the structure by adding the incremental deflections to the previous configuration and subroutine EQCHEC uses this updated

configuration to check joint equilibrium through the auxiliary subroutines CATENARY (which computes the cable force components at the cable ends), UNBALF (which checks the joint equations of equilibrium and finds the horizontal and vertical components of the nodal unbalanced forces) and NORM2 (which computes the Euclidean norm of the unbalanced forces at the cable ends as well as the Euclidean norm of the axial and shear forces in the members). If the convergence criterion of Section 6.2 is satisfied, Segment 7 of the program will be activated; otherwise, iteration for convergence will begin by recomputing the entire stiffness matrix according to Segment 2.

Segment 7: Output Processing and Display:

The updated results obtained in Segment 6 are all in terms of arrays with substructure indices which are not convenient for direct consumption by the user. The auxiliary subroutines JOINID and MEMID convert these substructure indices into their equivalent global nodal and member numbers through the data generated by subroutine NUMBER of Segment 1. Moreover, subroutine MEMEND transfers the member-end forces from the member coordinates to the global coordinates in preparation for graphical display. Finally, the auxiliary subroutine GRAFIX uses a number of lower level subroutines to display the results graphically. The numerical output is written to an external file called OUTPUT . These results comprise the nodal deformations in the global coordinates and the member-end forces in the member co-ordinates.

Segment 8: Erection Data:

There are five auxiliary subroutines within the primary subroutine ERECT which are responsible for all the structural and load variations due to erection. These are:

- a) Subroutine DTBC which implements the variations at the deck-tower connections. These variations may be in terms of forces or spring coefficients assumed to connect the two parts of the structure together.
- b) Subroutine BRACG which can install, adjust or eliminate a bracing set during erection analysis.
- c) Subroutine UNCOUP which is used to uncouple the two 'halves' of the bridge as one of the early steps of the disassembly analysis.
- d) Subroutine CABLES which may be used to remove a cable element or adjust its length or its tension.
- e) Subroutine DECK which is responsible for implementation of a number of structural changes in, and the erection load application to, the girder of the bridge.

7.3 The Input / Output Arrangements

CASBA requires two sets of input data. The basic geometric and material properties of the reference configuration and the specified nodal bending moments are input through a file called MAIN.DAT. In the non-interactive mode of the program, the erection data is input through a different file called ERECT.DAT. If the interactive mode is selected, the erection data is input through the keyboard. The first option is faster but less flexible. The second option is slower but allows modifications in the erection plan if overstressing or some other types of problems are observed. In the same manner, the user has the option of receiving the numerical output in an

external file called OUTPUT, or having this file plus the graphical display on the screen from which a hard copy may be obtained at the end of the run. Again, the graphics mode provides a convenient means of identifying problems which may be encountered due to a proposed erection plan, but requires some extra computer processing time. At the beginning of a run the user will be asked to make one of the following choices relative to input/output facilities.

<u>ENTER</u>	<u>DISASSEMBLY INPUT</u>	<u>DISASSEMBLY OUTPUT</u>
1	KEYBOARD	GRAPHICS & FILE
2	KEYBOARD	FILE ONLY
3	FILE	GRAPHICS & FILE
4	FILE	FILE ONLY

Clearly, number 1 is the most interactive while number 4 is the fastest of the above choices. It is possible that users with previous experience in erection analysis of similar cable-stayed bridges may be able to use the non-interactive option (Mode 4), which is the fastest, without too much difficulty. Others may find it advisable to begin with Mode 1, and decrease the level of interaction with the program as they become more familiar with the consequences of each disassembly sequence.

Section 7.6 and the User's Manual of Appendix A contain more detailed information about the input and output files, including their formats and units of measurement.

7.4 Data Management Schemes

When the present work was initiated in 1986, the second generation of

microcomputers (PC-AT and compatibles) with their expanded high-speed storage and faster microprocessors were being introduced. At the same time, more advanced assemblers and linkers were being developed to make full use of these new hardware capacities and speed. All these positive developments encouraged the authors to tailor CASBA for execution on an AT microcomputer. At that time the only operating system which was widely available was DOS with a maximum net application handling capacity of about 550 KB. Knowing that the GKS graphics library requires close to 270 KB of RAM, it was soon realized that the size of the executable file of the program should be kept within 250 KB. This was a major constraint from the beginning of the present work. (However, with the most recent developments in the hardware and software technologies (1990), these restrictions are no longer necessary.) Nevertheless, the objective of the work remained to develop a program which could carry out the erection analysis on a microcomputer with very limited core memory.

With these restrictions in mind, the following steps have been taken in an effort to keep the high-speed memory requirements of the program to an acceptable limit without sacrificing too much of its speed.

1. Constructionally, each 'half' of the bridge is erected as an independent unit and then the two 'halves' are coupled together in the middle of the central span. The program has been designed for this cantilever construction method so that at any time during its execution only one 'half' of the bridge is active. This arrangement reduced the size of all the active arrays to 1/2 of what would be required for keeping the whole structure active at the same time. As Fig. 7.2 indicates, once the stiffness matrix for the left hand 'half' of the bridge is formed and reduced, the reduced coefficients and all other

data pertaining to this 'half' of the bridge are stored in an external direct-access file and are replaced by the data for the RHS of the structure which becomes active at this moment.

2. By adopting the substructural-frontal technique of assembly and reduction of the matrices it has been possible to keep the maximum size of the largest active array to 33×33 which corresponds to the maximum number of degrees of freedom in the substructure types. Moreover, the reduced coefficients of each partial structure (about 400 elements) are shifted to an external direct-access file upon the completion of the reduction procedure and their place in the internal memory is occupied by the coefficients of the next partial structure.

Figure. 7.2 shows more details of data transfer between the internal high-speed memory and external direct-access files. The two types of data which must be exchanged frequently are the current geometric and material properties of the partial structures and the current member-end forces. These are written into the external files designated by logical unit numbers 8 and 9. The data corresponding to each 'half' of the bridge is recorded under the record number associated with that 'half' (record number $REC = 1$ for the left hand 'half' and $REC = 2$ for the right hand 'half').

Another frequently used external file is the one designated by logical unit number 11. The reduced stiffness coefficients of each partial structure are written into a record number which is a function of both the sequential partial structure number (IS) and the particular 'half' to which the partial structure belongs ($LR = 1$ for the LHS and $LR = 2$ for the RHS). Finally, the external file designated as logical unit number 12 contains the complete record of each partial structure so that the program may restart from any

previously treated partial structure at any time. This file is written to by subroutine RESULTS, and it is read at the beginning of a restart run.

7.5 Graphics Facilities

The graphics facility of CASBA is intended to enable the user to decide readily whether or not a proposed live load arrangement, or erection step, is acceptable. This is particularly useful for erection analysis where the designer has to check the acceptability of a very large number of load and structural configurations with a reasonable level of accuracy (due to the temporary nature of erection configurations) in order to avoid serious overstressing of any segment of the structure.

Towards this end, the load-effect diagrams (deformations, bending moments, shear forces and axial forces) are displayed on the video screen together with their corresponding allowable magnitudes. Wherever the load-effect falls outside the boundary marked by the maximum allowable values for that particular load-effect, overstressing is implied. If this occurs the proposed loading or erection step can be amended by stopping the program and restarting it from a previous configuration.

The graphics package used to display the results is an implementation of the ANSI standard GKS subroutines prepared by the Computer Graphics Group of the Department of Civil Engineering of Pontificia Universidade Catolica de Janeiro in Brazil. The package allows for hard copies of the diagrams to be printed at the end of the execution of CASBA. The User's manual in Appendix A contains more information on the use of the graphics package.

7.6 A Typical Application Example

As a typical example, the step-by-step procedure for the application of

CASBA to the erection analysis of the cable-stayed bridge shown in Fig. 7.3 is illustrated here.

7.6.1 Preparation of Input Data

1. Specify the reference configuration for the girder by selecting a desirable bending moment distribution with specified magnitudes at the points of attachment of the cables to the girder under consideration (Fig.7.5). (See Section 4.7). In order to specify the value of the tie-down forces at the piers, an initial value of 2300 KN was estimated from the computations in Fig. 4.9. (See Section 4.7). Then the bending moments at the base of the towers corresponding to several trial values of the tie-down force have been computed by CASBA for the dead load of 136 KN/M and the live load of 60 KN/M. Finally, a tie-down force of 2800 KN was selected as one which was expected to produce acceptable tower bending moments due to combined dead and live load.
2. Assign global nodal and member numbering to each half of the bridge as in Fig. 7.4. (See Section 4.5). Note that the bridge symmetry has been disregarded in order to make the example more general.
3. List the maximum number of substructures for each 'half' of the bridge, NSS(LR), and the substructure type for each of these substructures, IST(IS) as in Table 7.1.
4. List the nodal co-ordinates from the specified geometric reference configuration and the specified member end bending moments at the points of attachment of the cables to the girder (Fig.7.5) in (Table 7.2. (Note that Fig. 7.5 shows the internal moments, while Table 7.2 contains the member J-end bending moments).
5. For each member determine, the geometric and material properties

(cross-sectional area, moment of inertia, and the modulus of elasticity), and the dead load in the reference configuration. These are listed in Table 7.3. The member capacities are then determined and listed as in Table 7.4.

6. Propose an erection plan and prepare the corresponding disassembly input data, by reversing the sequences and changing the signs of the erection loads. As an example, if the last step in the erection of a bridge is the application of the topping, in the disassembly analysis this would constitute the first load case or configuration (actually the second configuration because the first run corresponds to the reference configuration). For this load case the dead load of the topping will be applied to the girder in the upward direction, which implies the removal of the topping. Tables 7.5 and 7.6 show the final stages of the erection plan and the corresponding disassembly input data, respectively.
7. From the data in Tables 7.1 to 7.6 and according to the instructions in the User's Manual (Appendix A), prepare the two input files as shown in Figs. 7.6 and 7.7.
8. If the program is used in its interactive mode, then the second input file is not required. The values will be entered through the keyboard in response to the questions displayed on the video screen. Although an input file is not required, it would be useful, in any case, to organize the data for each disassembly step in the manner shown in Fig. 7.7.
9. After running the program and responding to all the screen questions, the output file should contain the results illustrated, in part, in Fig. 7.8.

If the graphics option is utilized, the load effect diagrams shown in Figs. 7.9 - 7.20 will be displayed on the screen one at a time. (Note that these Figures are directly 'captured' from the screen).

7.6.2 Live Load Analysis

At the end of the initial run for the reference configuration CASBA requires that the user specify whether the program is being run for live load or erection analysis. Due to the large number of individual load cases which may be involved in both erection and live load analyses, it is preferable to have an independent run for each of these two phases. Normally, live load analysis is much simpler and may be done prior to the erection analysis. If the proposed dimensions are found to be satisfactory under the critical load combinations, then the erection analysis of the bridge may begin in a separate run.

In the case of live load analysis only the MAIN.DAT file has to be prepared according to the instructions in Appendix A.

7.6.3 Comments on Graphical Output

- A. Figures 7.9 through 7.20 show the results of some of the basic operations in the final stages of erection (corresponding to the early stages of disassembly) of a cable-stayed bridge. They are designed to include the most important disassembly steps required in the backward solution adopted for CASBA. It is to be noted that for the complete disassembly of a bridge with the central span of about 450 m the number of operations will be in the order of 500 - 1000.
- B. Each Figure contains four parts.
Part (a) shows the reference configuration and the deflected shape of

one 'half' of the bridge in dotted and solid lines, respectively.

Part (b) contains the reference configuration (in dotted lines), the bending moment diagram (in solid lines) and the bending moment capacity of the members (in dashed lines).

Parts (c) and (d) are similar to Part (b) but for the shear force diagram and the axial force diagram, respectively. Note that in Part (d) the cable force and the bracing force (if any) are shown by vertical solid lines at their points of attachment to the girder. The associated capacities are shown by vertical dashed lines.

- C. Displacements are magnified by 50 times to make the deflected shapes more distinctive. Their magnitude may be estimated by comparison with the tower height, for instance. If the upper part of the tower is about 50 m, then it would represent about 1 m of deflection on the screen.
- D. Other effects may be estimated by comparison with their corresponding member capacities. In Figs. 7.9 to 7.20 the following figures show the approximate capacities of the members.

Bending moment capacity of girder elements	4000 KN.M
Shear force capacity of girder elements	1400 KN
Axial force capacity of girder elements	9500 KN
Bending moment capacity of tower at base	85000 KN.M
Shear force capacity of tower at base	9500 KN
Axial force capacity of tower at base	150000 KN

- D. Because of structural and loading symmetry, only left hand side drawings are reproduced here. If either of these two are asymmetric (i.e. ISYM=0), the program will display the diagrams for each side of the bridge separately.
- E. Wherever one of the load effects (mostly bending moment diagram;

occasionally axial force diagram) falls outside the upper boundary representing the corresponding member capacity, the implication is that the proposed disassembly operation (i.e. its corresponding erection operation) may cause overstressing of the member(s) over which the effect exceeds the capacity. This situation exists, for instance, in Fig. 7.15b, both in the girder and the tower. As one of the remedial measures, the designer may decide to restart the analysis from the previous stage and either adjust the forces in the existing braces or to install a new set of bracing, or to use favourable temporary loading on the girder.

7.7 Application to Special Cable-Stayed Bridges

The program can handle some variations from the typical example of a 'standard' type of bridge described in Section 7.6. Some of these special types can be implemented by manipulating the input files. Others may even require a few changes in the source code of the program. Making changes in the source code of any program is often tricky and must be done with utmost care and after preparing a backup copy of the original source code. However this type of modification is not needed under normal circumstances.

An example of the case where changes may be accommodated by simple alterations in the input files is the case of cable-stayed bridges with a large distance between cables. (Generally, these are an older type of cable-stayed bridge.) In this case it would be advisable to use substructure types with single cables. This variation can be handled by CASBA by putting the area of the second cable in every substructure equal to zero. Some cable-stayed bridges have a smaller number of cables in the side spans than in the central span. This type of arrangement can also be handled by putting

the second cable area equal to zero in some of the substructures in the side spans. Variations of this nature can easily be handled with a little ingenuity on the part of the analysts.

If the application problem cannot be handled by simple changes in the substructure types built into the program, then new substructure types should be designed according to the particular need. Designing new substructure types as discussed in Chapter 4 is a major task which can be done by trial and error only. Fortunately this type of alteration is not needed under normal circumstances. However, if the program is to be applied to a structure which is substantially different from a standard cable-stayed bridge, then the alteration of the substructure types may become unavoidable. Naturally, the first step is to design a set of new substructure types from which the proposed structure may be assembled. Then the nodal characteristics of these substructure types as set out in Tables 4.1 and 4.3 must be prepared and incorporated into the DATA statements shown in Table 7.7. If the maximum number of nodes in the substructure types is greater than 11, then all the array dimensions containing 33 must be changed to the maximum number of nodes multiplied by 3. These arrays are listed in the declaration statements in the beginning of the source code file ANALYSE1.FOR. Instructions for the recompilation and linking of the source codes are included in the User's Manual of Appendix A.

Table 7.1 Array IST(IS)

Sequential No. of Substructure (IS)	Substructure Type for LHS of Bridge IST(IS)	Substructure Type for RHS of Bridge IST(IS)
1	4	4
2	1	1
3	2	2
4	3	3
5	2	2
6	3	3
7	2	2
8	3	3
9	5	5
10	4	4

NSS(1) = 10, NSS(2) = 10

Table 7-2 Nodal Coordinates and Bending Moments for Reference Configuration

Nodal #	X-Coordinate (mm)	Y-Coordinate (mm)	Specific. BM X 10**9 (N.mm)
LHS of Bridge			
1	0	0	-
2	-500	0	-
3	-5000	0	-1.20
4	-14000	0	0.60
5	-18500	0	-
6	-23000	0	1.80
7	-32000	0	1.60
8	-36500	0	-
9	-41000	0	1.10
10	-50000	0	1.40
11	-54500	0	-
12	-59000	0	1.20
13	-68000	0	1.50
14	-72500	0	-
15	-77000	0	1.30
16	-86000	0	1.00
17	-90500	0	-
18	-95000	0	1.50
19	-104000	0	1.60
20	-108500	0	-
21	-113000	0	1.80
22	-122000	0	-0.80
23	-126500	0	-3.50
24	-131000	0	-
25	-126500	-30000	-
26	-126500	0	-
27	-72500	-50000	-
28	-72500	-49000	-
29	-72500	-15000	-
30	-72500	0	-
31	-72500	0	-
32	-72500	15000	-
33	-72500	30000	-
34	-72500	50000	-
35	-72500	51000	-
36	-72500	53000	-
37	-72500	54000	-
38	-72500	55000	-
39	-72500	57000	-
40	-72500	58000	-
41	-72500	59000	-
42	-72500	61000	-
43	-72500	62000	-

Table 7-2 (Contd...)

Nodal #	X-Coordinate (mm)	Y-Coordinate (mm)	Specifid. BM X 10**9 (N.mm)
44	-72500	63000	-
45	-72500	65000	-
46	-72500	66000	-
RHS of Bridge			
1	0	0	-
2	500	0	-
3	5000	0	-1.20
4	14000	0	0.60
5	18500	0	-
6	23000	0	1.80
7	32000	0	1.60
8	36500	0	-
9	41000	0	1.10
10	50000	0	1.40
11	54500	0	-
12	59000	0	1.20
13	68000	0	1.50
14	72500	0	-
15	77000	0	1.30
16	86000	0	1.00
17	90500	0	-
18	95000	0	1.50
19	104000	0	1.60
20	108500	0	-
21	113000	0	1.80
22	122000	0	-0.80
23	126500	0	-3.50
24	131000	0	-
25	126500	-30000	-
26	126500	0	-
27	72500	-50000	-
28	72500	-49000	-
29	72500	-15000	-
30	72500	0	-
31	72500	0	-
32	72500	15000	-
33	72500	30000	-
34	72500	50000	-
35	72500	51000	-
36	72500	53000	-
37	72500	54000	-
38	72500	55000	-
39	72500	57000	-
40	72500	58000	-

Table 7-2 (Contd...)

Nodal #	X-Coordinate (mm)	Y-Coordinate (mm)	Specifid. BM X 10**9 (N.mm)
41	72500	59000	-
42	72500	61000	-
43	72500	62000	-
44	72500	63000	-
45	72500	65000	-
46	72500	66000	-

Table 7-3 Member Properties and Load Specifications

Member Number	Moment of Inertia X10 ¹¹ (mm ⁴)	C.S. Area X10 ⁴ (mm ²)	Modulus of Elasticity X10 ⁴ (MPa)	Dead Load (N/mm)
LHS				
1	2.00	19.95	20.00	136.00
2	2.00	19.95	20.00	136.00
3	2.00	19.95	20.00	136.00
4	2.00	19.95	20.00	136.00
5	2.00	19.95	20.00	136.00
6	2.00	19.95	20.00	136.00
7	2.00	19.95	20.00	136.00
8	2.00	19.95	20.00	136.00
9	2.00	19.95	20.00	136.00
10	2.00	19.95	20.00	136.00
11	2.00	19.95	20.00	136.00
12	2.00	19.95	20.00	136.00
13	2.00	19.95	20.00	136.00
14	2.00	19.95	20.00	136.00
15	2.00	19.95	20.00	136.00
16	2.00	19.95	20.00	136.00
17	2.00	19.95	20.00	136.00
18	2.00	19.95	20.00	136.00
19	2.00	19.95	20.00	136.00
20	2.00	19.95	20.00	136.00
21	2.00	19.95	20.00	136.00
22	2.00	19.95	20.00	136.00
23	2.00	19.95	20.00	136.00
24	155.00	300.00	3.00	0.00
25	0.00	20000000.00	0.00	0.00
26	880.00	880.00	3.00	0.00
27	880.00	880.00	3.00	222.00
28	880.00	880.00	3.00	222.00
29	0.00	0.00	0.00	0.00
30	550.00	800.00	3.00	186.00
31	550.00	800.00	3.00	186.00
32	550.00	800.00	3.00	250.00
33	330.00	744.00	3.00	186.00
34	330.00	744.00	3.00	186.00
35	330.00	744.00	3.00	186.00
36	330.00	744.00	3.00	186.00
37	330.00	744.00	3.00	186.00
38	330.00	744.00	3.00	186.00
39	330.00	744.00	3.00	186.00
40	330.00	744.00	3.00	186.00
41	330.00	744.00	3.00	186.00
42	330.00	744.00	3.00	186.00
43	330.00	744.00	3.00	186.00
44	330.00	744.00	3.00	186.00

Fig. 7-3 (Contd...)

Member Number	Moment of Inertia (mm ⁴)	C.S. Area (mm ²)	Modulus of Elasticity (MPa)	Dead Load (N/mm)
45	0.00	0.30	16.00	0.00
46	0.00	0.30	16.00	0.00
47	0.00	0.30	16.00	0.00
48	0.00	0.30	16.00	0.00
49	0.00	0.30	16.00	0.00
50	0.00	0.30	16.00	0.00
52	0.00	0.30	16.00	0.00
53	0.00	0.30	16.00	0.00
54	0.00	0.30	16.00	0.00
55	0.00	0.30	16.00	0.00
56	0.00	0.30	16.00	0.00
57	0.00	0.30	16.00	0.00
58	0.00	0.30	16.00	0.00
59	0.00	0.30	16.00	0.00
60	0.00	0.30	16.00	0.00
RHS SAME AS LHS				

Table 7-4 Member Capacities

Member Number	BM Capacity X10 ¹⁰ (N mm)	SF Capacity X10 ⁶ (N)	AF Capacity X10 ⁶ (N)
LHS			
1	0.40	1.40	9.50
2	0.40	1.40	9.50
3	0.40	1.40	9.50
4	0.40	1.40	9.50
5	0.40	1.40	9.50
6	0.40	1.40	9.50
7	0.40	1.40	9.50
8	0.40	1.40	9.50
9	0.40	1.40	9.50
10	0.40	1.40	9.50
11	0.40	1.40	9.50
12	0.40	1.40	9.50
13	0.40	1.40	9.50
14	0.40	1.40	9.50
15	0.40	1.40	9.50
16	0.40	1.40	9.50
17	0.40	1.40	9.50
18	0.40	1.40	9.50
19	0.40	1.40	9.50
20	0.40	1.40	9.50
21	0.40	1.40	9.50
22	0.40	1.40	9.50
23	0.40	1.40	9.50
24	2.30	2.60	13.50
25	0.00	0.00	0.00
26	8.50	9.50	150.00
27	8.50	9.50	150.00
28	8.50	9.50	150.00
29	0.00	0.00	0.00
30	4.50	6.50	100.00
31	4.50	6.50	100.00
32	4.50	6.50	100.00
33	4.00	6.00	100.00
34	4.00	6.00	100.00
35	4.00	6.00	100.00
36	4.00	6.00	100.00
37	4.00	6.00	100.00
38	4.00	6.00	100.00
39	4.00	6.00	100.00
40	4.00	6.00	100.00
41	4.00	6.00	100.00
42	4.00	6.00	100.00
43	4.00	6.00	100.00
44	4.00	6.00	100.00
45	0.00	0.00	3.50

Table 7-4 (Contd...)

Member Number	BM Capacity X10 ⁹ (N mm)	SF Capacity X10 ⁶ (N)	AF Capacity X10 ⁶ (N)
46	0.00	0.00	3.50
47	0.00	0.00	3.50
48	0.00	0.00	3.50
49	0.00	0.00	3.50
50	0.00	0.00	3.50
51	0.00	0.00	3.50
52	0.00	0.00	3.50
53	0.00	0.00	3.50
54	0.00	0.00	3.50
55	0.00	0.00	3.50
56	0.00	0.00	3.50
57	0.00	0.00	3.50
58	0.00	0.00	3.50
59	0.00	0.00	3.50
60	0.00	0.00	3.50
RHS SAME AS LHS			

Table 7.5 Assembly Procedure

Step No.	Actions
N+1	Install cable # 60
N+2	Place PC deck blocks on member # 23
N+3	Grout PC deck blocks on member # 23
N+4	Install member # 1 (drop-in segment)
N+5	Apply coupling forces to drop-in segment and join two 'halves' together
N+6	Place PC deck blocks on members # 1-4
N+7	Grout PC deck blocks on members # 1-4
N+8	Remove derricks from deck
N+9	Remove braces @ nodes 10 & 18 of each 'half'
N+10	Release the horizontal jacks between towers and deck
N+11	Place wearing course on top of PC deck

Table 7.6 Disassembly Procedure

Step No.	Actions
1	Remove topping from PC deck
2	Install horizontal jacks between towers and deck
3	Install braces at nodes 10 & 18
4	Place derricks on deck
5	UngROUT PC blocks on members # 1-4
6	Remove PC blocks from members # 1-4
7	Uncouple girder at centre of drop-in panel
8	Remove member # 1 (drop-in segment)
9	UngROUT PC blocks on member # 23
10	Remove PC blocks from member # 23
11	Remove cable # 60

Table 7.7

a) DATA Statements

DATA INDEX /9,15,12,18,15,13,22,16,22,22,18,27,21,27,27,30, >30,33,30,30/ BLOCK DATA DATA NSJ/10,10,11,10,10/ DATA NSE/8,5,8,7,5/ DATA JEN/4,1,2,2,2,2,2,3,3,1,3,3,4,4,1,3,3,4,4,10,2,2,3,5,1, >1,0,1,6,0,7,0,8,4,0,8,0,9,0,0/ DATA KEN/2,2,3,1,3,3,3,4,2,2,10,10,11,3,10,8,5,9,5,5,7,4,8,6,4 >,7,0,8,7,0,8,0,9,10,0,9,0,10,0,0/
--

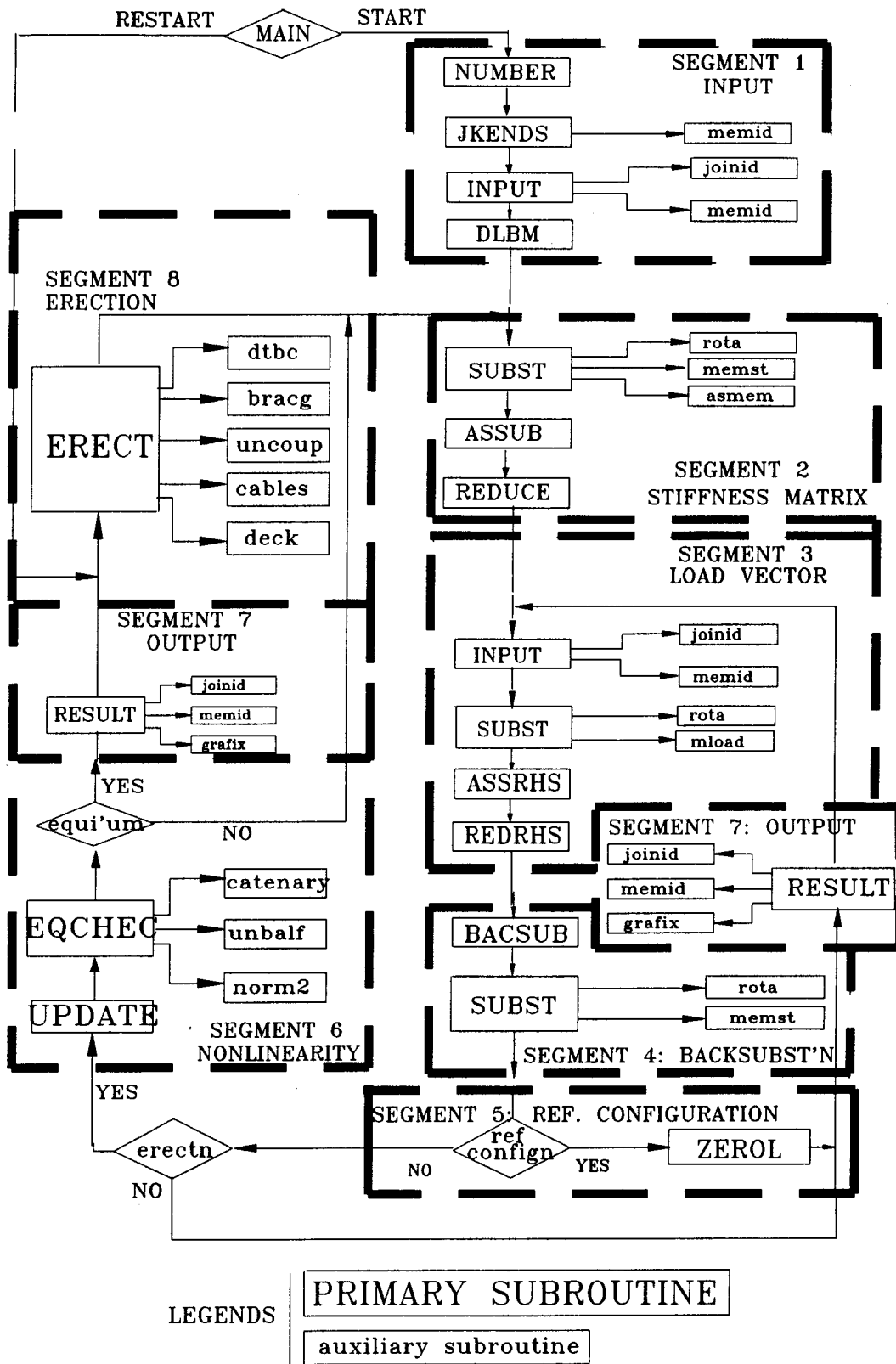
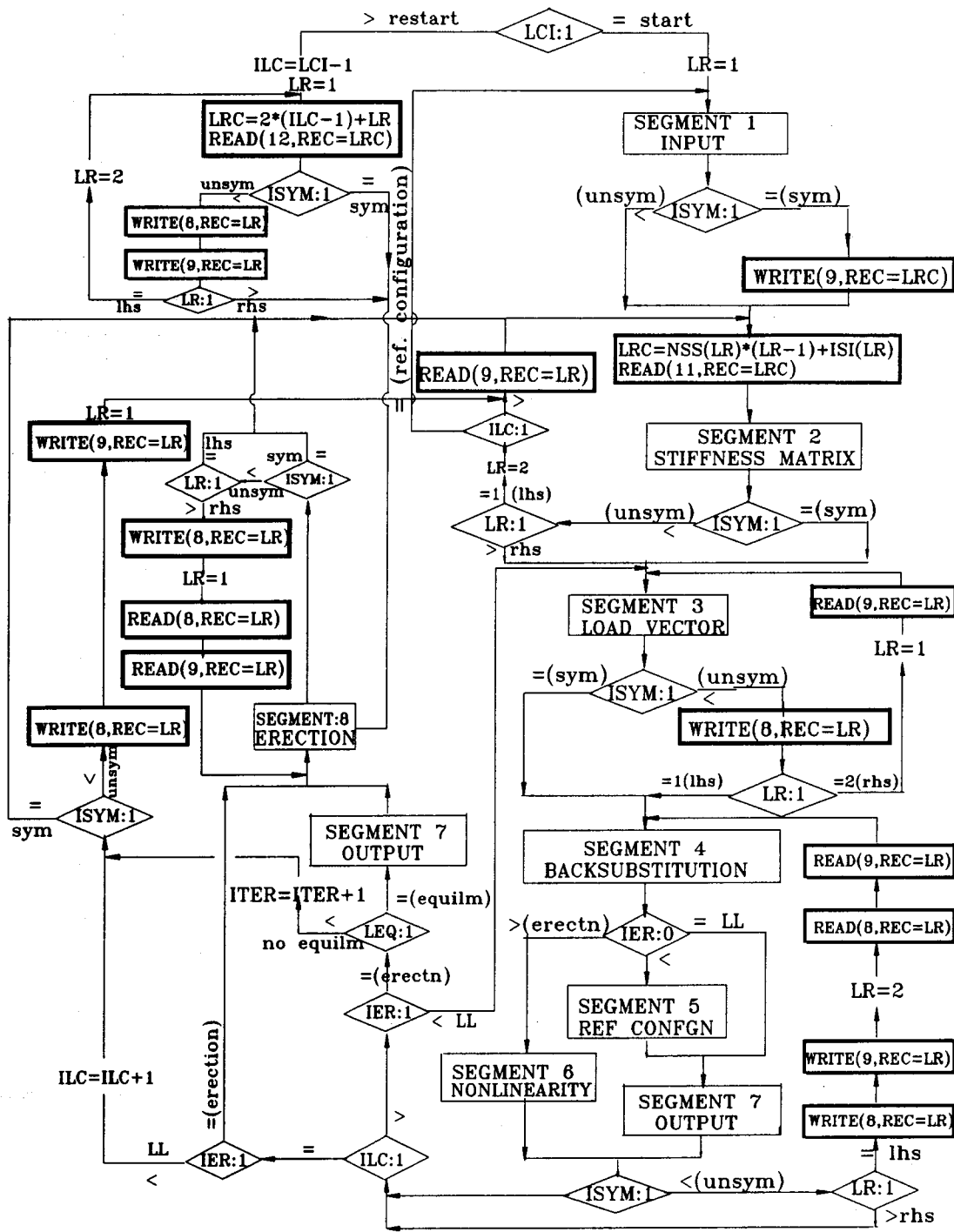


Figure 7.1 The Program Structure



LOGICAL #	VARIABLES
8	REDUCED LOAD VECTOR & UPDATED MEMBER-END FORCES
9	MATERIAL & GEOMETRIC SPECIFICATIONS OF MEMBERS & NODES
11	REDUCED STIFFNESS COEFFICIENTS OF EACH PARTIAL STRUCTURE
12	RESTART FILE CONTAINING UPDATED CONFIGURATION FOR EACH LOAD CASE

Figure 7.2 External Storage Scheme

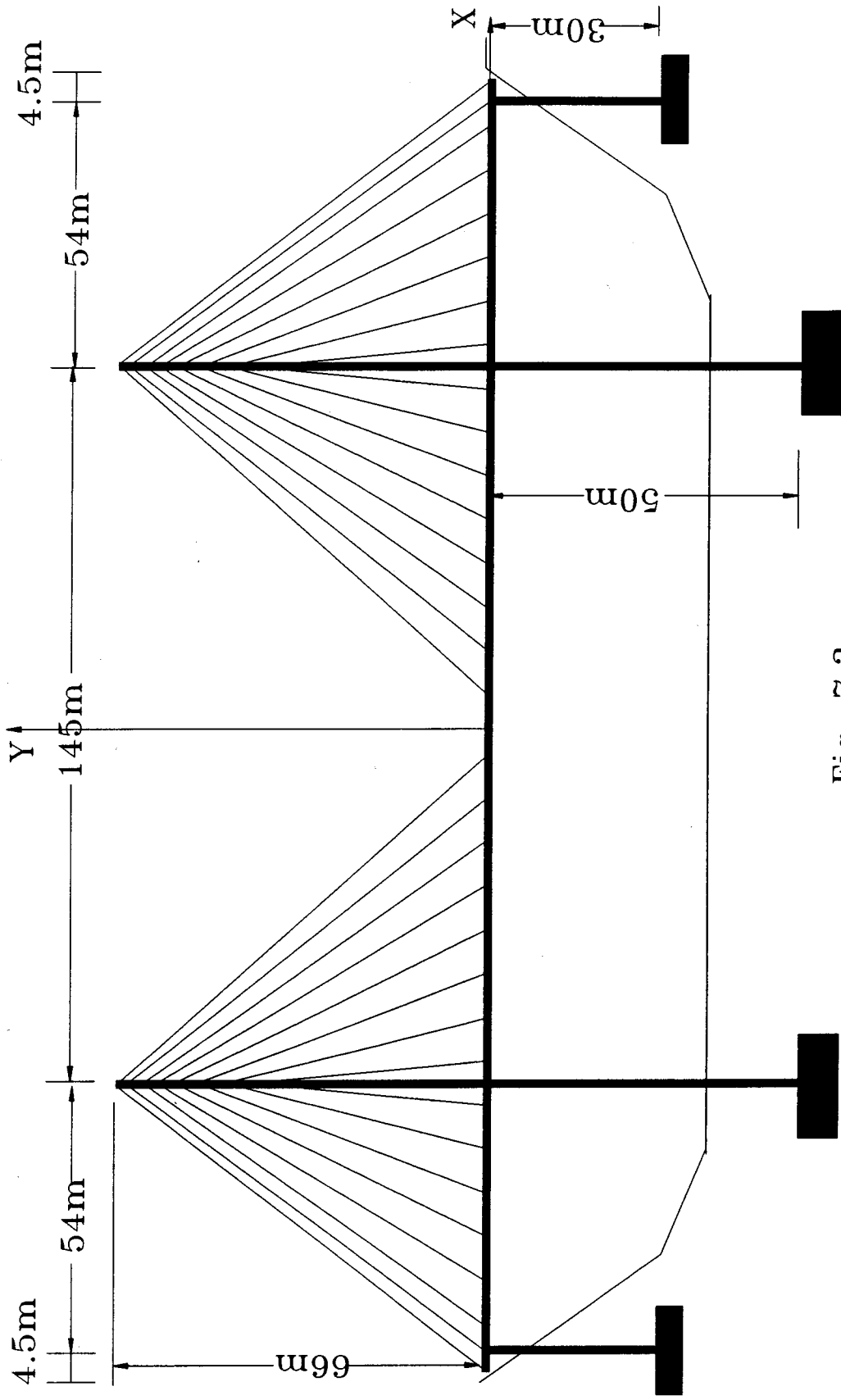


Fig. 7.3

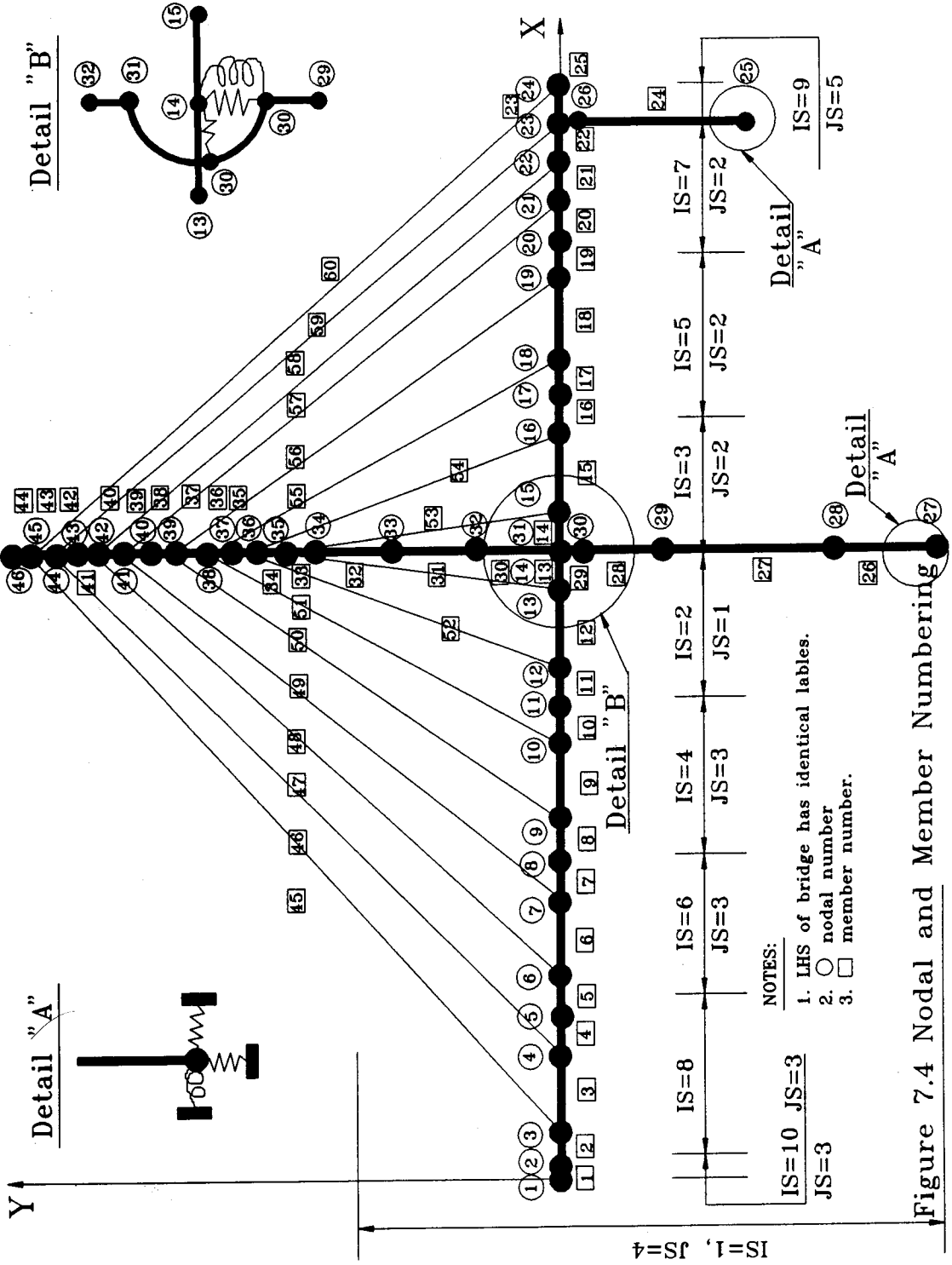


Figure 7.4 Nodal and Member Numbering

1. Use simplified structure in (a) with DL alone to compute tie-down force R1.
(See Section 4.7 and Fig. 4.9)

$$-R1 + R2 = 131 \times 136 = 17816$$

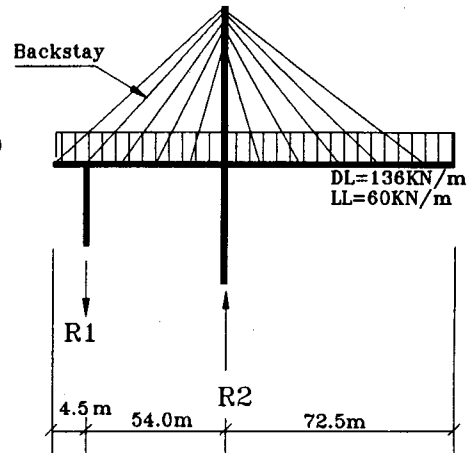
$$126.5R1 - 72.5R2 + (136 \times 131 \times 2) / 2 = 0$$

or,

$$R1 = 2309.481 \text{ KN}$$

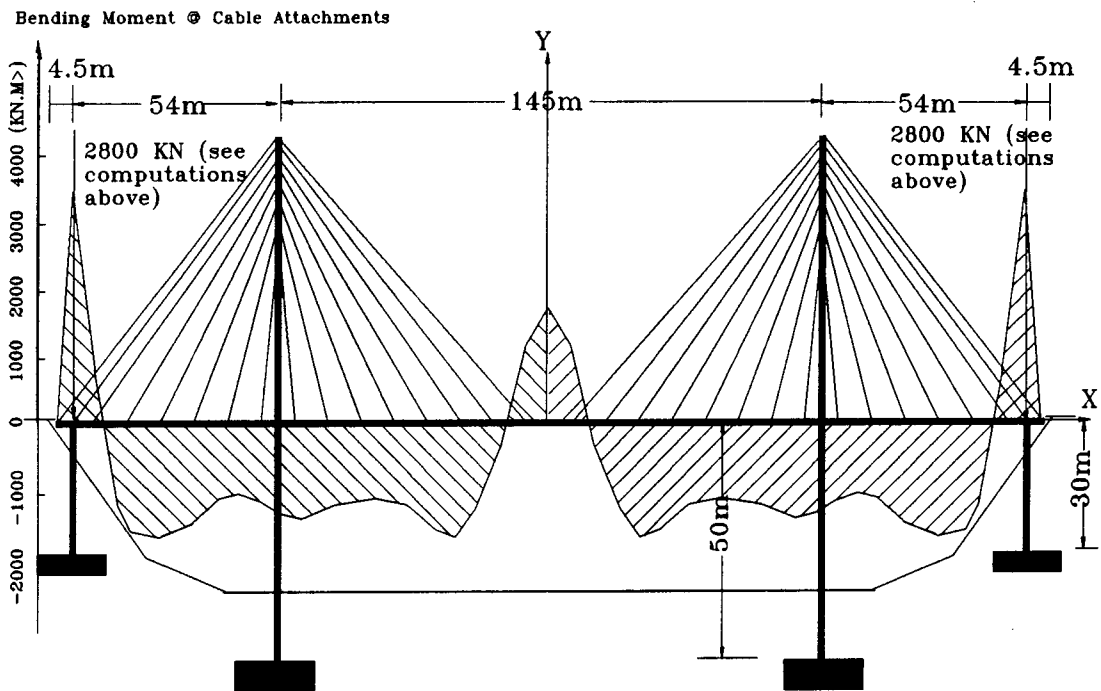
2. Run CASBA for DL=136, LL=60, and a range of values for R1 between 2000 and 3000 KN to fill the following Table.

R1(KN)	M _{DL} (KN.m)	M _{DL} + M _{LL} (KN.m)
3000	-65543	-65543+59360=-6183
2800	-53446	-53446+59360=5914
2400	-11295	-11295+59360=48065
2250	- 174	- 174+59360=59186
2000	24029	24029+59360=83389



3. Select R1 = 2800 KN to give 5914 KN.m of bending moment at the base of tower under combined actions of DL + LL.

(a) Selection of Tie-Down Force



(b) Internal Member-End Moments Specified for Reference Configuration

Figure 7.5 Specified Internal Bending Moment Distribution for Girder

Fig. 7-6 MAIN.DAT File

Note: For a description of data locations in this file see the User's Manual.

```
200000.0,160000.0,30000.0,0.000078,500.0,0,1,3,61,  
10,46,60,1030000.0,100.0,2050.0,  
10,46,60,1030000.0,100.0,2050.0,  
4,1,2,3,2,3,2,3,5,3,  
J001,0.0,0.0,  
J002,-500.0,0.0,  
J003,-5000.0,0.0,-1.2E9,  
J004,-14000.0,0.0,0.6E9,  
J005,-18500.0,0.0,  
J006,-23000.0,0.0,1.8E9,  
J007,-32000.0,0.0,1.6E9,  
J008,-36500.0,0.0,  
J009,-41000.0,0.0,1.1E9,  
J010,-50000.0,0.0,1.4E9,  
J011,-54500.0,0.0,  
J012,-59000.0,0.0,1.2E9,  
J013,-68000.0,0.0,1.5E9,  
J014,-72500.0,0.0,  
J015,-77000.0,0.0,1.3E9,  
J016,-86000.0,0.0,1.0E9,  
J017,-90500.0,0.0,  
J018,-95000.0,0.0,1.5E9,  
J019,-104000.0,0.0,1.6E9,  
J020,-108500.0,0.0,  
J021,-113000.0,0.0,1.8E9,  
J022,-122000.0,0.0,-0.8E9,  
J023,-126500.0,0.0,-3.5E9,  
J024,-131000.0,0.0,  
J025,-126500.0,-30000.0,0.0,2.0E17,2.0E17,2.0E17,  
J026,-126500.0,0.0,  
J027,-72500.0,-50000.0,0.0,2.0E17,2.0E17,2.0E17,  
J028,-72500.0,-49000.0,  
J029,-72500.0,-15000.0,  
J030,-72500.0,0.0,  
J031,-72500.0,0.0,  
J032,-72500.0,15000.0,  
J033,-72500.0,30000.0,  
J034,-72500.0,50000.0,  
J035,-72500.0,51000.0,  
J036,-72500.0,53000.0,  
J037,-72500.0,54000.0,  
J038,-72500.0,55000.0,  
J039,-72500.0,57000.0,  
J040,-72500.0,58000.0,  
J041,-72500.0,59000.0,
```

Fig. 7.6 (Contd...)

J042,-72500.0,61000.0,
J043,-72500.0,62000.0,
J044,-72500.0,63000.0,
J045,-72500.0,65000.0,
J046,-72500.0,66000.0,
M001,2.0E11,1.995E5,2.0E5,0.4E10,1.4E6,9.5E6,23,
M024,1.55E13,30.0E5,0.3E5,2.3E10,2.6E6,13.5E6,
M025,1.0E-6,2.0E17,1.0E-6
M026,8.8E13,8.8E6,0.3E5,8.5E10,9.5E6,150.0E6,3,
M029,1.0E-6,1.0E-6,1.0E-6,
M030,5.5E13,8.0E6,0.3E5,4.5E10,6.5E6,100.0E6,3,
M033,3.3E13,7.44E6,0.3E5,4.0E10,6.0E6,100.0E6,12,
M045,0.0,3000.0,1.6E5,0.0,0.0,3.5E6,16,
M001,136.0,22,
M023,136.0,1,1,0.28E7,0.0,
M024,0.0,3,
M027,226.0,2,
M029,0.0,1,
M030,186.0,15,
M045,0.0,16,
4,1,2,3,2,3,2,3,5,3,
J001,0.0,0.0,
J002,500.0,0.0,
J003,5000.0,0.0,-1.2E9,
J004,14000.0,0.0,0.6E9,
J005,18500.0,0.0,
J006,23000.0,0.0,1.8E9,
J007,32000.0,0.0,1.6E9,
J008,36500.0,0.0,
J009,41000.0,0.0,1.1E9,
J010,50000.0,0.0,1.4E9,
J011,54500.0,0.0,
J012,59000.0,0.0,1.2E9,
J013,68000.0,0.0,1.5E9,
J014,72500.0,0.0,
J015,77000.0,0.0,1.3E9,
J016,86000.0,0.0,1.0E9,
J017,90500.0,0.0,
J018,95000.0,0.0,1.5E9,
J019,104000.0,0.0,1.6E9,
J020,108500.0,0.0,
J021,113000.0,0.0,1.8E9,
J022,122000.0,0.0,-0.8E9,
J023,126500.0,0.0,-3.5E9,
J024,131000.0,0.0,
J025,126500.0,-30000.0,0.0,2.0E17,2.0E17,2.0E17,
J026,126500.0,0.0,

Fig. 7.6 (Contd...)

J027,72500.0,-50000.0,0.0,2.0E17,2.0E17,2.0E17,
J028,72500.0,-49000.0,
J029,72500.0,-15000.0,
J030,72500.0,0.0,
J031,72500.0,0.0,
J032,72500.0,15000.0,
J033,72500.0,30000.0,
J034,72500.0,50000.0,
J035,72500.0,51000.0,
J036,72500.0,53000.0,
J037,72500.0,54000.0,
J038,72500.0,55000.0,
J039,72500.0,57000.0,
J040,72500.0,58000.0,
J041,72500.0,59000.0,
J042,72500.0,61000.0,
J043,72500.0,62000.0,
J044,72500.0,63000.0,
J045,72500.0,65000.0,
J046,72500.0,66000.0,
M001,2.0E11,1.995E5,2.0E5,0.4E10,1.4E6,9.5E6,23,
M024,1.55E13,30.0E5,0.3E5,2.3E10,2.6E6,13.5E6,
M025,1.0E-6,2.0E17,1.0E-6
M026,8.8E13,8.8E6,0.3E5,8.5E10,9.5E6,150.0E6,3,
M029,1.0E-6,1.0E-6,1.0E-6,
M030,5.5E13,8.0E6,0.3E5,4.5E10,6.5E6,100.0E6,3,
M033,3.3E13,7.44E6,0.3E5,4.0E10,6.0E6,100.0E6,12,
M045,0.0,3000.0,1.6E5,0.0,0.0,3.5E6,16,
M001,136.0,22,
M023,136.0,1,1,0.28E7,0.0,
M024,0.0,3,
M027,226.0,2,
M029,0.0,1,
M030,186.0,25
M045,0.0,16
M001,0.0,2,
M003,0.0,1,1,1.0E6,0.0,
M004,0.0,57,
M001,0.0,60,
M001,0.0,11,
M012,0.0,1,1,1.0E6,0.0,
M013,0.0,48,
M001,0.0,60,

Fig. 7.7 ERECT.DAT File

Note: For an explanation of data locations in this file see User's Manual.

```
LC002,5   TOPPING REMOVAL
1,
1,22,30.0,90.0,0,
1,
1,22,30.0,90.0,0,
LC003,1   DECK-TOWER SPRING INSTALN.
1,
30,-800000.0,2.0E10,3,
1,
30,+800000.0,2.0E10,3,
LC004,2   BRCGS @ NN# 10 & 18
0,
2,
10,8000.0,160000.0,105.1,51800.0,1.0E6,2.0E6,
18,8000.0,160000.0,74.9,51800.0,1.0E6,2.0E6,
0,
2,
10,8000.0,160000.0,74.9,51800.0,1.0E6,2.0E6,
18,8000.0,160000.0,105.1,51800.0,1.0E6,2.0E6,
LC005,5   DERRICKS ON
2,
6,
6,0.0,0.0,0.0,0.0,1,200000.0,0.11,270.0,
5,0.0,0.0,0.0,0.0,1,310000.0,0.22,270.0,
21,0.0,0.0,0.0,0.0,1,225000.0,0.11,270.0,
22,0.0,0.0,0.0,0.0,1,410000.0,0.22,270.0,
2,0.0,0.0,0.0,0.0,1,045000.0,0.00,270.0,
23,0.0,0.0,0.0,0.0,1,045000.0,0.22,270.0,
2,
6,
6,0.0,0.0,0.0,0.0,1,200000.0,0.11,270.0,
5,0.0,0.0,0.0,0.0,1,310000.0,0.22,270.0,
21,0.0,0.0,0.0,0.0,1,225000.0,0.11,270.0,
22,0.0,0.0,0.0,0.0,1,410000.0,0.22,270.0,
2,0.0,0.0,0.0,0.0,1,045000.0,0.00,270.0,
23,0.0,0.0,0.0,0.0,1,045000.0,0.22,270.0,
LC006,5   UNGROUTING PC SLAB ON MEM# 1-4
3,
4,
1,8.5E10,1.12E5,1.6E5,380.0,
2,8.5E10,1.12E5,1.6E5,380.0,
3,8.5E10,1.12E5,1.6E5,380.0,
4,8.5E10,1.12E5,1.6E5,380.0,
3,
4,
```


Fig. 7.7 (Contd...)

1,8.5E10,1.12E5,1.6E5,380.0,
2,8.5E10,1.12E5,1.6E5,380.0,
3,8.5E10,1.12E5,1.6E5,380.0,
4,8.5E10,1.12E5,1.6E5,380.0,
LC007,5 PC DECK OFF MEM # 1-5
1,
1,4,80.0,90.0,0,
1,
1,4,80.0,90.0,0,
LC008,3 UNCOUPLING
LC009,5 REMOVING MEM # 1
4,
2,
4,
2,
LC010,5 UNGROUTING PC SLAB ON MEM# 23
3,
1,
23,8.5E10,1.12E5,1.6E5,380.0,
3,
1,
23,8.5E10,1.12E5,1.6E5,380.0,
LC011,5 PC DECK OFF MEM # 23
1,
23,23,80.0,90.0,0,
1,
23,23,80.0,90.0,0,
LC012,4 REMOVE CABLE # 60
1,
60,0.0,2,
1,
60,0.0,2,
LC013,5 SHIFT CABLE EQPT. TO 23
1,
23,23,0.0,0.0,2,45000.0,0.0,270.0,45000.0,1.0,90.0,
0,
0,
1,
23,23,0.0,0.0,2,45000.0,0.0,270.0,45000.0,1.0,90.0,
0,
0,
LC014,4 REMOVE CABLE # 59
1,
59,0.0,2,
1,
59,0.0,2,

Figure 7.8 OUTPUT File

Note: For a description of OUTPUT file see Appendix A.

```
***** LOAD CASE#      1*****
***** DEAD LOAD/LIVE LOAD *****
*****DEFLECTIONS (mm)*****LHS OF BRIDGE
NODAL #  X-DEFLECTION  Y-DEFLECTION
-----
  1      0.00          0.00
  2      0.00          0.00
  3      0.00          0.00
  4      0.00          0.00
  5      0.00          0.00
  6      0.00          0.00
  7      0.00          0.00
  8      0.00          0.00
  9      0.00          0.00
 10      0.00          0.00
 11      0.00          0.00
 12      0.00          0.00
 13      0.00          0.00
 14      0.00          0.00
 15      0.00          0.00
 16      0.00          0.00
 17      0.00          0.00
 18      0.00          0.00
 19      0.00          0.00
 20      0.00          0.00
 21      0.00          0.00
 22      0.00          0.00
 23      0.00          0.00
 24      0.00          0.00
 25      0.00          0.00
 26      0.00          0.00
 27      0.00          0.00
 28      0.00          0.00
 29      0.00          0.00
 30      0.00          0.00
 31      0.00          0.00
 32      0.00          0.00
 33      0.00          0.00
 34      0.00          0.00
 35      0.00          0.00
 36      0.00          0.00
 37      0.00          0.00
 38      0.00          0.00
 39      0.00          0.00
 40      0.00          0.00
```

Figure 7.8 (Contd...)

41	0.00	0.00
42	0.00	0.00
43	0.00	0.00
44	0.00	0.00
45	0.00	0.00
46	0.00	0.00
*****BENDING MOMENT (KN.M)(MEMBER-END)*****LHS OF BRIDGE		
MEMBER #	J-END	K-END

1	-2889.12	2899.32
2	-1200.00	2883.00
3	600.00	1200.00
4	-177.00	-600.00
5	1800.00	177.00
6	1600.00	-1800.00
7	-27.00	-1600.00
8	1100.00	27.00
9	1400.00	-1100.00
10	-77.00	-1400.00
11	1200.00	77.00
12	1500.00	-1200.00
13	23.00	-1500.00
14	1300.00	-23.00
15	1000.00	-1300.00
16	-127.00	-1000.00
17	1500.00	127.00
18	1600.00	-1500.00
19	323.00	-1600.00
20	1800.00	-323.00
21	-800.00	-1800.00
22	-3500.00	800.00
23	0.00	3500.00
24	0.00	0.00
25	0.00	0.00
26	-53446.19	52965.02
27	-52965.02	43822.91
28	-43822.91	29388.00
29	0.00	0.00
30	-29388.00	22170.54
31	-22170.54	14953.09
32	-14953.09	5329.81
33	-5329.81	4848.65
34	-4848.65	3878.48
35	-3878.48	3384.90
36	-3384.90	2891.33
37	-2891.33	1895.09
38	-1895.09	1439.95

Figure 7.8 (Contd...)

39	-1439.95	984.81
40	-984.81	455.89
41	-455.89	69.34
42	-69.34	-317.20
43	317.20	0.00
44	0.00	0.00
45	0.00	0.00
46	0.00	0.00
47	0.00	0.00
48	0.00	0.00
49	0.00	0.00
50	0.00	0.00
51	0.00	0.00
52	0.00	0.00
53	0.00	0.00
54	0.00	0.00
55	0.00	0.00
56	0.00	0.00
57	0.00	0.00
58	0.00	0.00
59	0.00	0.00
60	0.00	0.00
*****SHEAR FORCE (KN) (MEMBER-END)*****LHS OF BRIDGE		
MEMBER #	J-END	K-END

1	54.40	-13.60
2	680.00	-68.00
3	812.00	412.00
4	133.33	478.67
5	745.33	-133.33
6	589.78	634.22
7	-55.56	667.56
8	556.44	55.56
9	645.33	578.67
10	-22.22	634.22
11	589.78	22.22
12	645.33	578.67
13	-22.22	634.22
14	-589.78	-22.22
15	-578.67	-645.33
16	-55.56	-556.44
17	-667.56	55.56
18	-623.11	-600.89
19	-22.22	-589.78
20	-634.22	22.22
21	-323.11	-900.89
22	294.00	-906.00

Figure 7.8 (Contd...)

23	-1083.78	-2328.22
24	0.00	0.00
25	0.00	0.00
26	481.16	-481.16
27	481.16	-481.16
28	481.16	-481.16
29	0.00	0.00
30	-481.16	481.16
31	-481.16	481.16
32	-481.16	481.16
33	-481.16	481.16
34	-485.09	485.09
35	-493.58	493.58
36	-493.58	493.58
37	-498.12	498.12
38	-455.14	455.14
39	-455.14	455.14
40	-264.46	264.46
41	-386.54	386.54
42	-386.54	386.54
43	158.60	-158.60
44	0.00	0.00
45	0.00	0.00
46	0.00	0.00
47	0.00	0.00
48	0.00	0.00
49	0.00	0.00
50	0.00	0.00
51	0.00	0.00
52	0.00	0.00
53	0.00	0.00
54	0.00	0.00
55	0.00	0.00
56	0.00	0.00
57	0.00	0.00
58	0.00	0.00
59	0.00	0.00
60	0.00	0.00
*****AXIAL FORCE (KN) (MEMBER-END)*****LHS OF BRIDGE		
MEMBER #	J-END	K-END

1	481.16	-481.16
2	481.16	-481.16
3	1615.16	-1615.16
4	2813.64	-2813.64
5	2813.64	-2813.64
6	3933.12	-3933.12

Figure 7.8 (Contd...)

7	4796.20	-4796.20
8	4796.20	-4796.20
9	5423.50	-5423.50
10	5946.95	-5946.95
11	5946.95	-5946.95
12	6244.58	-6244.58
13	6357.48	-6357.48
14	-6357.48	6357.48
15	-6248.50	6248.50
16	-5959.37	5959.37
17	-5959.37	5959.37
18	-5440.46	5440.46
19	-4770.18	4770.18
20	-4770.18	4770.18
21	-3716.41	3716.41
22	-2719.02	2719.02
23	-975.40	975.40
24	0.00	0.00
25	0.00	0.00
26	-43966.00	43966.00
27	-43966.00	39672.00
28	-39672.00	32892.00
29	0.00	0.00
30	32892.00	-30102.00
31	30102.00	-27312.00
32	27312.00	-23592.00
33	23592.00	-23406.00
34	20891.33	-20519.33
35	18215.78	-18029.78
36	18029.78	-17843.78
37	15295.78	-14923.78
38	12575.78	-12389.78
39	12389.78	-12203.78
40	9411.33	-9039.33
41	6430.67	-6244.67
42	6244.67	-6058.67
43	2733.78	-2361.78
44	186.00	0.00
45	1574.30	-1574.30
46	1761.30	-1761.30
47	1776.63	-1776.63
48	1525.06	-1525.06
49	1296.91	-1296.91
50	1382.49	-1382.49
51	1205.75	-1205.75
52	1284.53	-1284.53
53	-1239.91	1239.91

Figure 7.8 (Contd...)

54	-1171.36	1171.36
55	-1370.48	1370.48
56	-1385.78	1385.78
57	-1861.98	1861.98
58	-1582.88	1582.88
59	-2679.23	2679.23
60	-1458.07	1458.07
***** LOAD CASE# 1*****		
***** DEAD LOAD/LIVE LOAD *****		
*****DEFLECTIONS (mm)*****RHS OF BRIDGE		
NODAL #	X-DEFLECTION	Y-DEFLECTION

1	0.00	0.00
2	0.00	0.00
3	0.00	0.00
4	0.00	0.00
5	0.00	0.00
6	0.00	0.00
7	0.00	0.00
8	0.00	0.00
9	0.00	0.00
10	0.00	0.00
11	0.00	0.00
12	0.00	0.00
13	0.00	0.00
14	0.00	0.00
15	0.00	0.00
16	0.00	0.00
17	0.00	0.00
18	0.00	0.00
19	0.00	0.00
20	0.00	0.00
21	0.00	0.00
22	0.00	0.00
23	0.00	0.00
24	0.00	0.00
25	0.00	0.00
26	0.00	0.00
27	0.00	0.00
28	0.00	0.00
29	0.00	0.00
30	0.00	0.00
31	0.00	0.00
32	0.00	0.00
33	0.00	0.00
34	0.00	0.00

Figure 7.8 (Contd...)

35	0.00	0.00
36	0.00	0.00
37	0.00	0.00
38	0.00	0.00
39	0.00	0.00
40	0.00	0.00
41	0.00	0.00
42	0.00	0.00
43	0.00	0.00
44	0.00	0.00
45	0.00	0.00
46	0.00	0.00
*****BENDING MOMENT (KN.M)(MEMBER-END)*****RHS OF BRIDGE		
MEMBER #	J-END	K-END

1	-2899.32	2889.12
2	-2883.00	1200.00
3	-1200.00	-600.00
4	600.00	177.00
5	-177.00	-1800.00
6	1800.00	-1600.00
7	1600.00	27.00
8	-27.00	-1100.00
9	1100.00	-1400.00
10	1400.00	77.00
11	-77.00	-1200.00
12	1200.00	-1500.00
13	1500.00	-23.00
14	23.00	-1300.00
15	1300.00	-1000.00
16	1000.00	127.00
17	-127.00	-1500.00
18	1500.00	-1600.00
19	1600.00	-323.00
20	323.00	-1800.00
21	1800.00	800.00
22	-800.00	3500.00
23	-3500.00	0.00
24	0.00	0.00
25	0.00	0.00
26	53446.19	-52965.02
27	52965.02	-43822.91
28	43822.91	-29388.00
29	0.00	0.00
30	29388.00	-22170.54
31	22170.54	-14953.09
32	14953.09	-5329.81

Figure 7.8 (contd...)

33	5329.81	-4848.65
34	4848.65	-3878.48
35	3878.48	-3384.90
36	3384.90	-2891.33
37	2891.33	-1895.09
38	1895.09	-1439.95
39	1439.95	-984.81
40	984.81	-455.89
41	455.89	-69.34
42	69.34	317.20
43	-317.20	0.00
44	0.00	0.00
45	0.00	0.00
46	0.00	0.00
47	0.00	0.00
48	0.00	0.00
49	0.00	0.00
50	0.00	0.00
51	0.00	0.00
52	0.00	0.00
53	0.00	0.00
54	0.00	0.00
55	0.00	0.00
56	0.00	0.00
57	0.00	0.00
58	0.00	0.00
59	0.00	0.00
60	0.00	0.00
*****SHEAR FORCE (KN) (MEMBER-END)*****RHS OF BRIDGE		
MEMBER #	J-END	K-END

1	13.60	-54.40
2	68.00	-680.00
3	-412.00	-812.00
4	-478.67	-133.33
5	133.33	-745.33
6	-634.22	-589.78
7	-667.56	55.56
8	-55.56	-556.44
9	-578.67	-645.33
10	-634.22	22.22
11	-22.22	-589.78
12	-578.67	-645.33
13	-634.22	22.22
14	22.22	589.78
15	645.33	578.67
16	556.44	55.56

Figure 7.8 (Contd...)

17	-55.56	667.56
18	600.89	623.11
19	589.78	22.22
20	-22.22	634.22
21	900.89	323.11
22	906.00	-294.00
23	2328.22	1083.78
24	0.00	0.00
25	0.00	0.00
26	-481.16	481.16
27	-481.16	481.16
28	-481.16	481.16
29	0.00	0.00
30	481.16	-481.16
31	481.16	-481.16
32	481.16	-481.16
33	481.16	-481.16
34	485.09	-485.09
35	493.58	-493.58
36	493.58	-493.58
37	498.12	-498.12
38	455.14	-455.14
39	455.14	-455.14
40	264.46	-264.46
41	386.54	-386.54
42	386.54	-386.54
43	-158.60	158.60
44	0.00	0.00
45	0.00	0.00
46	0.00	0.00
47	0.00	0.00
48	0.00	0.00
49	0.00	0.00
50	0.00	0.00
51	0.00	0.00
52	0.00	0.00
53	0.00	0.00
54	0.00	0.00
55	0.00	0.00
56	0.00	0.00
57	0.00	0.00
58	0.00	0.00
59	0.00	0.00
60	0.00	0.00
*****AXIAL FORCE (KN)	(MEMBER-END)	*****RHS OF BRIDGE
MEMBER #	J-END	K-END

Figure 7.8 (Contd...)

1	-481.16	481.16
2	-481.16	481.16
3	-1615.16	1615.16
4	-2813.64	2813.64
5	-2813.64	2813.64
6	-3933.12	3933.12
7	-4796.20	4796.20
8	-4796.20	4796.20
9	-5423.50	5423.50
10	-5946.95	5946.95
11	-5946.95	5946.95
12	-6244.58	6244.58
13	-6357.48	6357.48
14	6357.48	-6357.48
15	6248.50	-6248.50
16	5959.37	-5959.37
17	5959.37	-5959.37
18	5440.46	-5440.46
19	4770.18	-4770.18
20	4770.18	-4770.18
21	3716.41	-3716.41
22	2719.02	-2719.02
23	975.40	-975.40
24	0.00	0.00
25	0.00	0.00
26	-43966.00	43966.00
27	-43966.00	39672.00
28	-39672.00	32892.00
29	0.00	0.00
30	32892.00	-30102.00
31	30102.00	-27312.00
32	27312.00	-23592.00
33	23592.00	-23406.00
34	20891.33	-20519.33
35	18215.78	-18029.78
36	18029.78	-17843.78
37	15295.78	-14923.78
38	12575.78	-12389.78
39	12389.78	-12203.78
40	9411.33	-9039.33
41	6430.67	-6244.67
42	6244.67	-6058.67
43	2733.78	-2361.78
44	186.00	0.00
45	-1574.30	1574.30
46	-1761.30	1761.30
47	-1776.63	1776.63

Figure 7.8 (Contd...)

48	-1525.06	1525.06
49	-1296.91	1296.91
50	-1382.49	1382.49
51	-1205.75	1205.75
52	-1284.53	1284.53
53	1239.91	-1239.91
54	1171.36	-1171.36
55	1370.48	-1370.48
56	1385.78	-1385.78
57	1861.98	-1861.98
58	1582.88	-1582.88
59	2679.23	-2679.23
60	1458.07	-1458.07
***** LOAD CASE# 2*****		
***** ERECTION RESULTS *****		
*****DEFLECTIONS (mm)*****RHS OF BRIDGE		
NODAL #	X-DEFLECTION	Y-DEFLECTION

1	0.00	135.80
2	0.00	135.80
3	0.00	134.60
4	0.00	127.20
5	0.00	121.30
6	0.00	114.30
7	0.10	98.00
8	0.10	89.40
9	0.20	80.70
10	0.30	64.10
11	0.40	56.60
12	0.50	49.80
13	0.70	38.60
14	0.80	34.30
15	0.90	30.70
16	1.10	25.40
17	1.20	23.40
18	1.30	21.60
19	1.40	17.70
20	1.50	15.30
21	1.50	12.30
22	1.60	4.60
23	1.60	0.00
24	1.70	-5.00
25	0.00	0.00
26	0.00	0.00
27	0.00	0.00
28	0.00	0.00

Figure 7.8 (Contd...)

29	2.10	0.30
30	12.00	0.70
31	0.80	34.30
32	19.70	1.00
33	29.10	1.20
34	43.30	1.60
35	44.10	1.60
36	45.60	1.60
37	46.30	1.60
38	47.10	1.60
39	48.60	1.70
40	49.40	1.70
41	50.10	1.70
42	51.60	1.70
43	52.40	1.70
44	53.20	1.70
45	54.70	1.70
46	55.50	1.70
*****BENDING MOMENT (KN.M)(MEMBER-END)*****RHS OF BRIDGE		
MEMBER #	J-END	K-END

1	842.58	-850.52
2	855.36	-2166.56
3	2167.38	-3166.13
4	3165.59	-2140.11
5	2140.06	-3257.83
6	3258.41	-1923.25
7	1922.66	-110.82
8	110.75	-445.18
9	444.56	-27.52
10	28.00	1352.89
11	-1352.93	583.36
12	-584.68	371.16
13	-369.88	1401.51
14	281.90	-1401.48
15	-41.68	-282.70
16	382.02	42.58
17	-1340.85	-381.94
18	-2204.93	1341.21
19	-1458.72	2204.64
20	-2856.68	1458.75
21	-55.03	2857.19
22	2947.39	54.41
23	-0.01	-2947.46
24	0.00	0.00
25	0.00	0.00
26	-82367.54	83098.88

Figure 7.8 (Contd...)

27	-68397.10	82381.27
28	-46080.42	68407.97
29	0.00	0.00
30	46063.21	-34866.40
31	34864.95	-23642.24
32	23642.17	-8683.64
33	8681.03	-7932.50
34	7932.51	-6406.59
35	6406.58	-5628.54
36	5628.54	-4850.60
37	4850.60	-3290.00
38	3289.99	-2573.91
39	2573.91	-1857.95
40	1857.95	-895.94
41	895.93	-361.11
42	361.11	173.57
43	-173.57	0.00
44	0.00	0.00
45	0.00	0.00
46	0.00	0.00
47	0.00	0.00
48	0.00	0.00
49	0.00	0.00
50	0.00	0.00
51	0.00	0.00
52	0.00	0.00
53	0.00	0.00
54	0.00	0.00
55	0.00	0.00
56	0.00	0.00
57	0.00	0.00
58	0.00	0.00
59	0.00	0.00
60	0.00	0.00
*****SHEAR FORCE (KN) (MEMBER-END)*****RHS OF BRIDGE		
MEMBER #	J-END	K-END

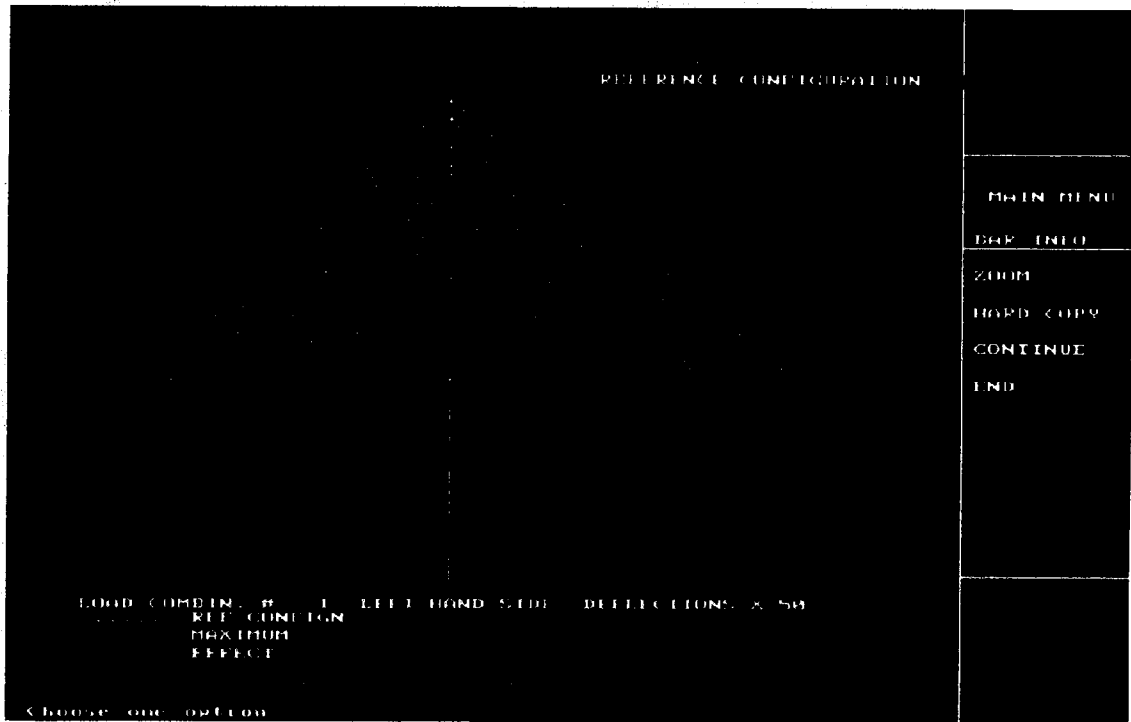
1	10.59	-42.39
2	52.88	-529.88
3	-366.03	-587.97
4	-466.39	-10.62
5	9.89	-486.89
6	-625.35	-328.65
7	-641.13	164.13
8	-164.18	-312.82
9	-523.34	-430.66
10	-545.36	68.36

Figure 7.8 (Contd....)

11	-67.48	-409.52
12	-453.28	-500.72
13	-467.75	-9.25
14	487.30	-10.30
15	513.04	440.96
16	144.15	332.86
17	621.34	-144.34
18	572.97	381.03
19	72.74	404.26
20	549.15	-72.15
21	165.65	788.35
22	-428.57	905.57
23	960.99	2451.01
24	0.00	0.00
25	0.00	0.00
26	731.34	-731.34
27	736.01	-736.01
28	744.25	-744.25
29	0.00	0.00
30	746.45	-746.45
31	748.18	-748.18
32	747.93	-747.93
33	748.54	-748.54
34	762.96	-762.96
35	778.04	-778.04
36	777.94	-777.94
37	780.30	-780.30
38	716.08	-716.08
39	715.96	-715.96
40	481.01	-481.01
41	534.82	-534.82
42	534.68	-534.68
43	-86.78	86.78
44	0.00	0.00
45	0.00	0.00
46	0.00	0.00
47	0.00	0.00
48	0.00	0.00
49	0.00	0.00
50	0.00	0.00
51	0.00	0.00
52	0.00	0.00
53	0.00	0.00
54	0.00	0.00
55	0.00	0.00
56	0.00	0.00
57	0.00	0.00

Figure 7.8 (Contd...)

MEMBER #	J-END	K-END
58	0.00	0.00
59	0.00	0.00
60	0.00	0.00
*****AXIAL FORCE (KN) (MEMBER-END)*****RHS OF BRIDGE		
MEMBER #	J-END	K-END
1	-731.09	731.09
2	-731.09	731.09
3	-1679.62	1679.62
4	-2677.36	2677.36
5	-2677.36	2677.36
6	-3597.12	3597.12
7	-4276.22	4276.22
8	-4276.22	4276.22
9	-4748.93	4748.93
10	-5158.35	5158.35
11	-5158.35	5158.35
12	-5386.01	5386.01
13	-5478.63	5478.63
14	-5478.63	5478.63
15	-5402.49	5402.49
16	-5191.70	5191.70
17	-5191.70	5191.70
18	-4786.81	4786.81
19	-4251.79	4251.79
20	-4251.79	4251.79
21	-3340.14	3340.14
22	-2476.32	2476.32
23	-859.95	859.95
24	126.43	-126.43
25	0.00	0.00
26	40044.57	-40044.57
27	35750.57	-40044.57
28	28970.57	-35750.57
29	0.00	0.00
30	28970.57	-26180.57
31	26180.57	-23390.57
32	23390.57	-19670.57
33	19670.57	-19484.57
34	17584.76	-17212.76
35	15501.80	-15315.80
36	15315.80	-15129.80
37	13151.21	-12779.21
38	10966.76	-10780.76
39	10780.76	-10594.76
40	8289.64	-7917.64
41	5736.52	-5550.52

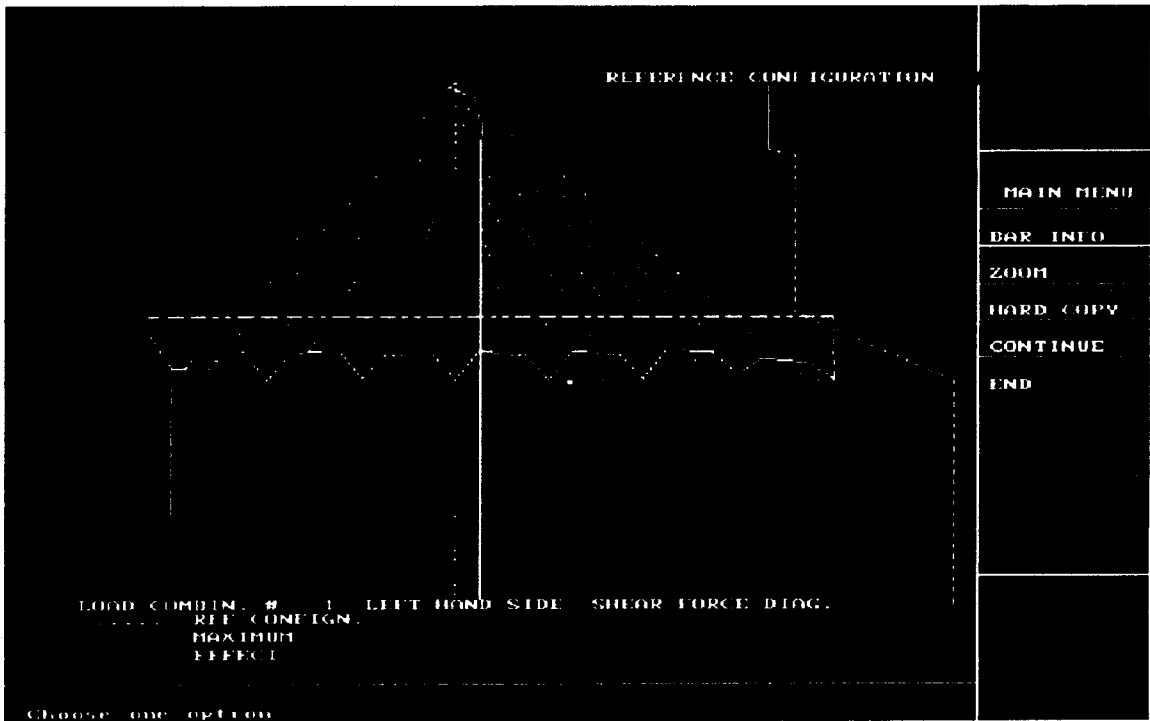


(a) Deflected Shape

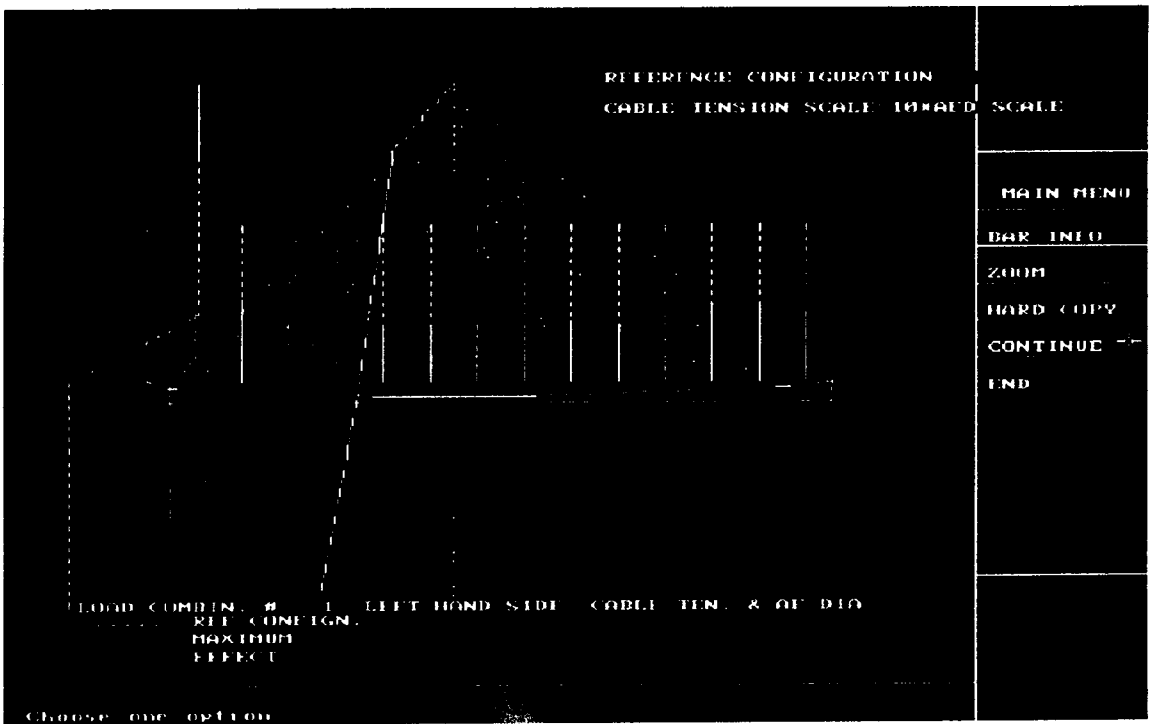


(b) Bending Moment Diagram

Figure 7.9 Reference Configuration

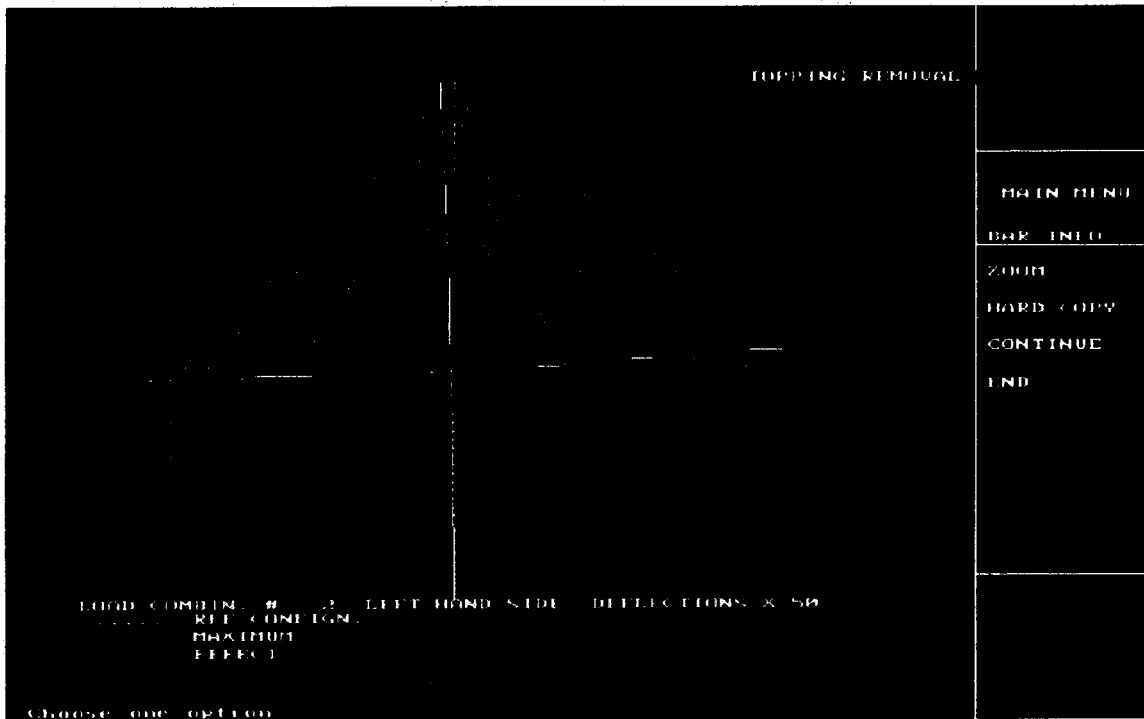


(c) Shear Force Diagram

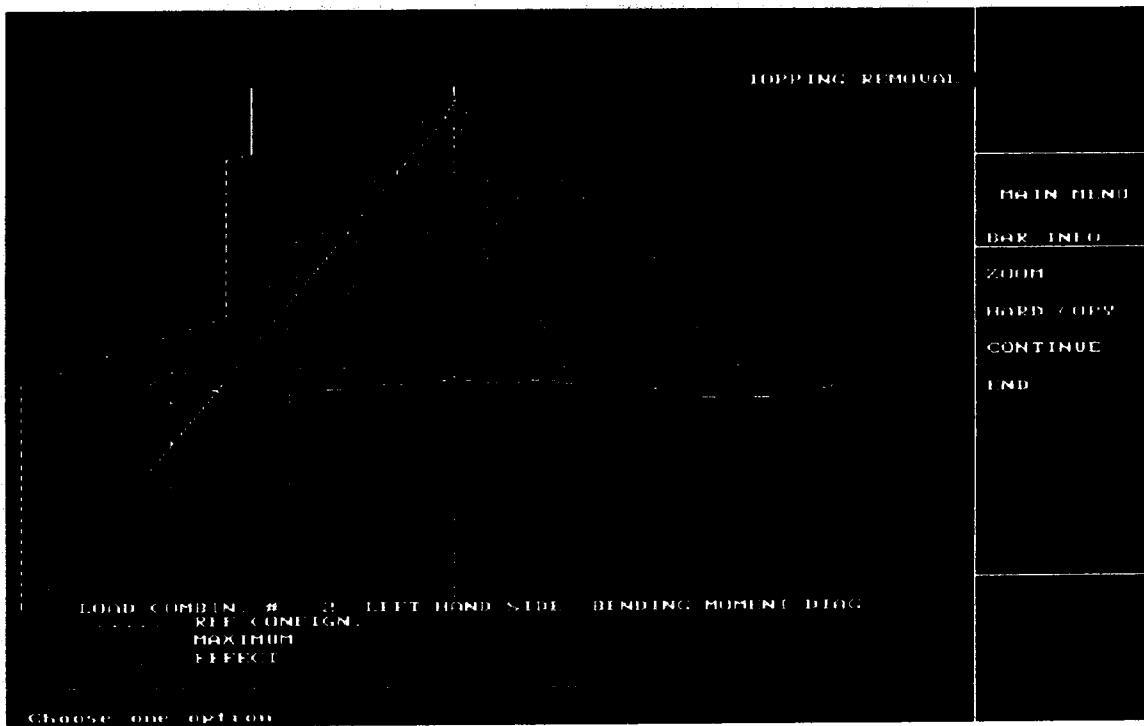


(d) Axial Force Diagram

Figure 7.9 Reference Configuration

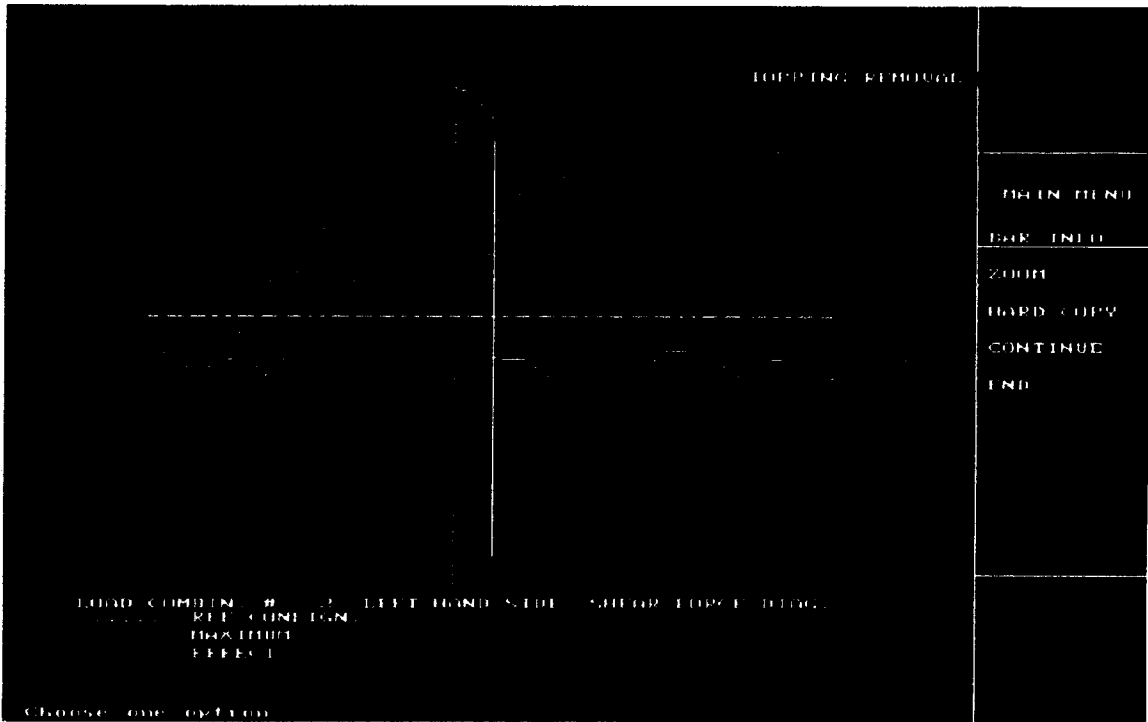


(a) Deflected Shape

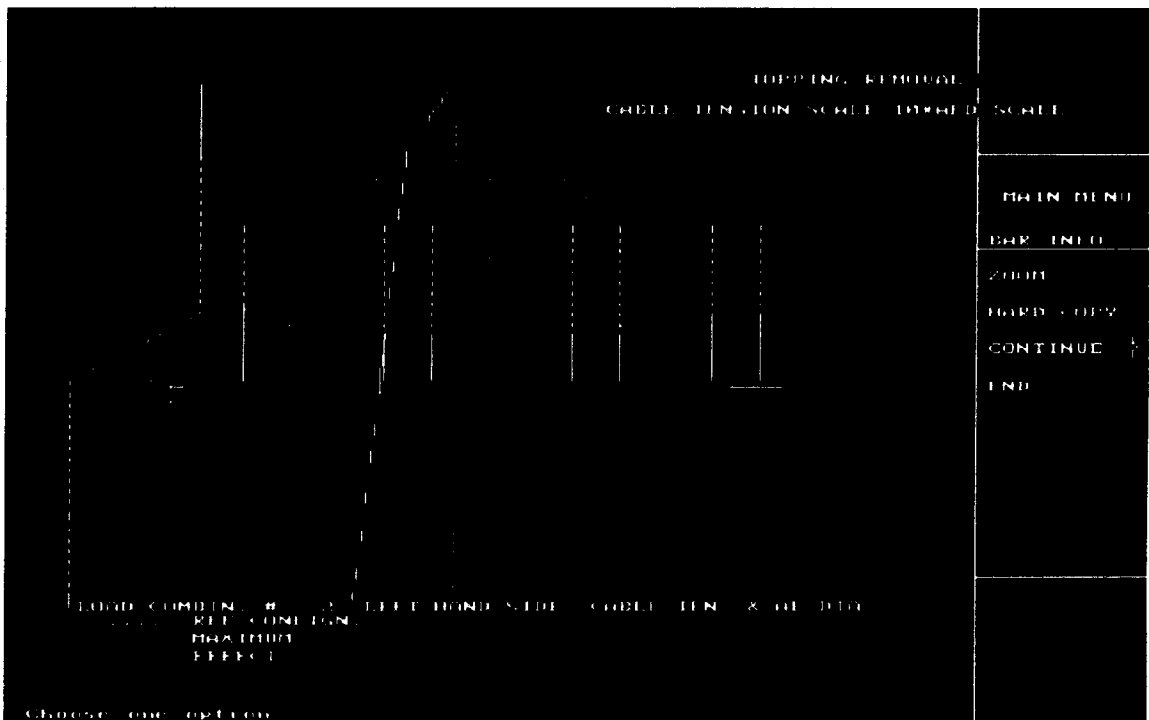


(b) Bending Moment Diagram

Figure 7.10

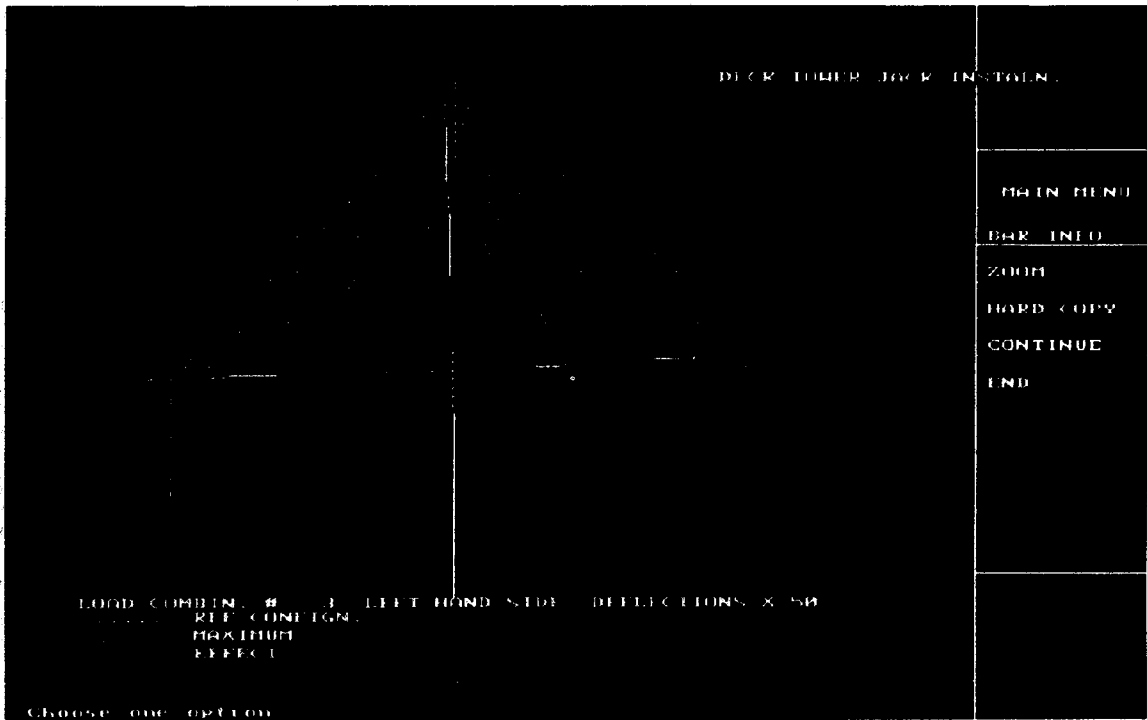


(c) Shear Force Diagram

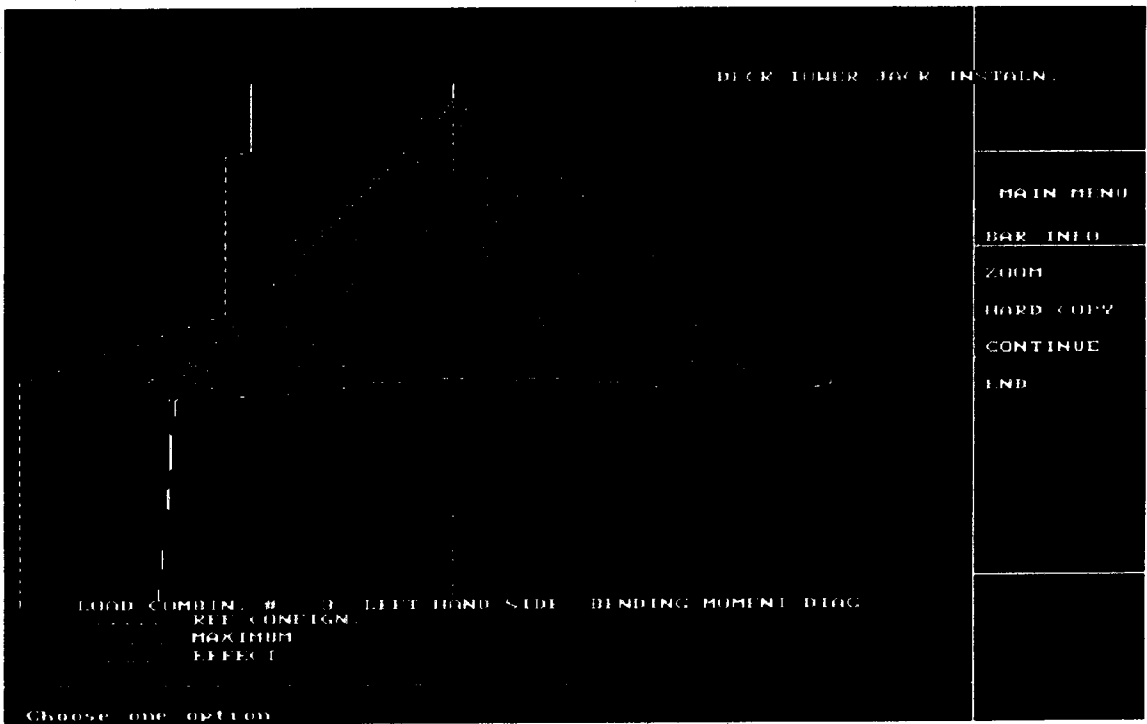


(d) Axial Force Diagram

Figure 7.10 Topping Removal

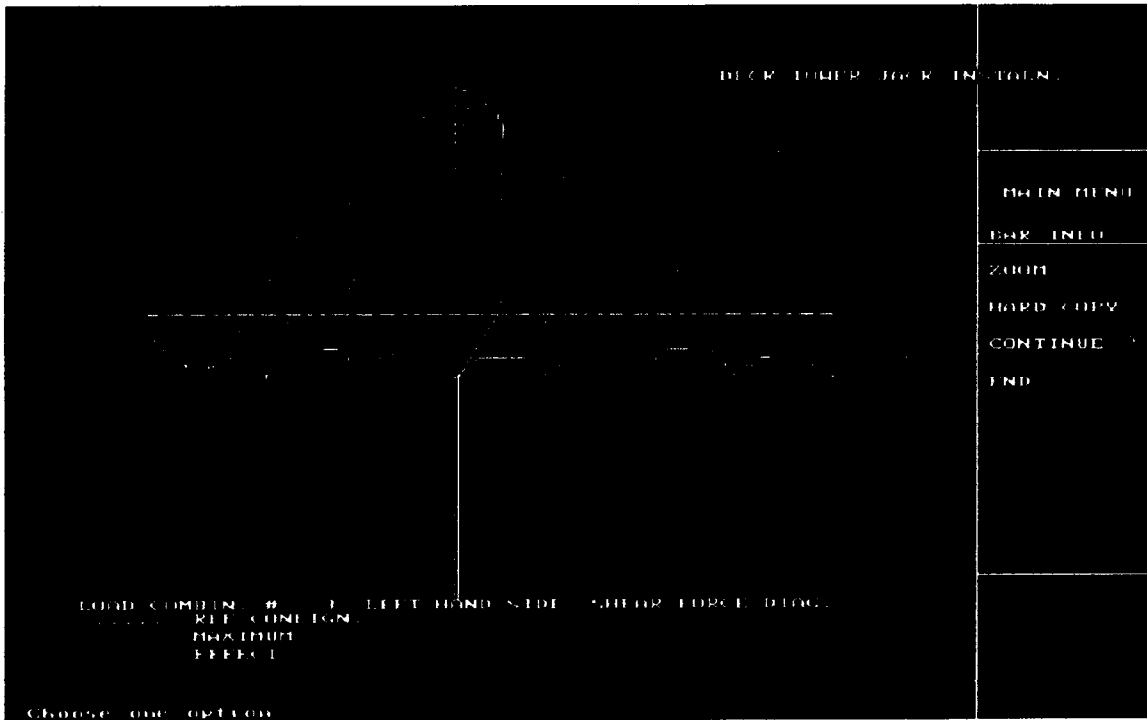


(a) Deflected Shape

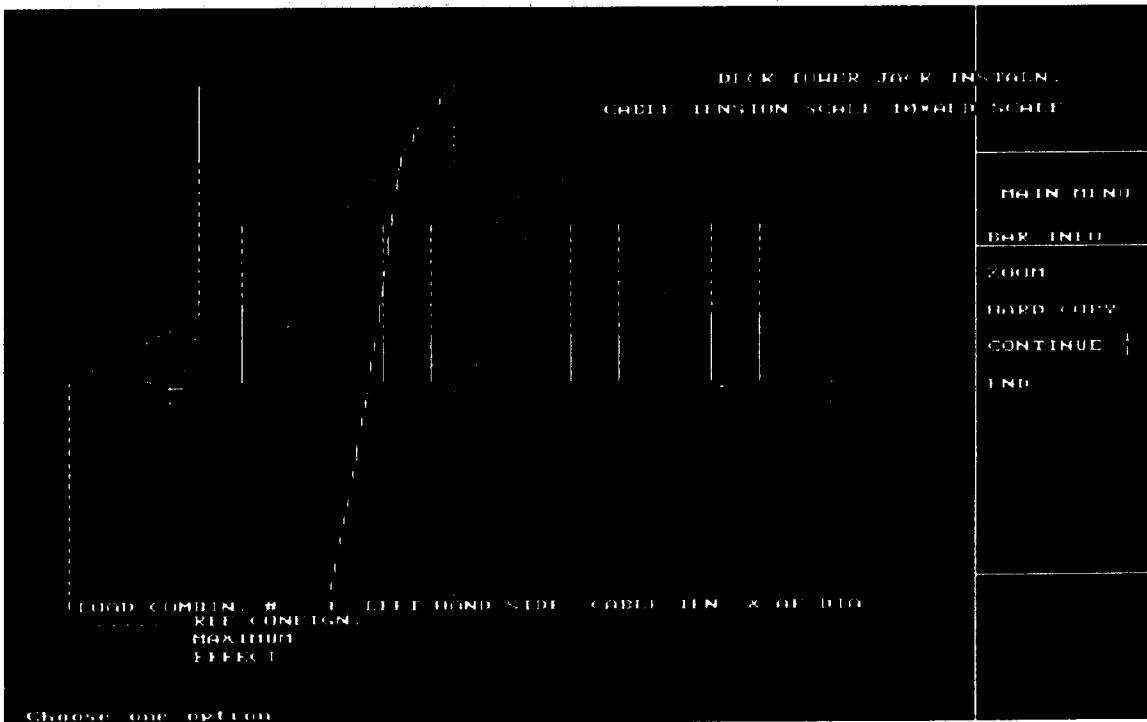


(b) Bending Moment Diagram

Figure 7.11



(c) Shear Force Diagram

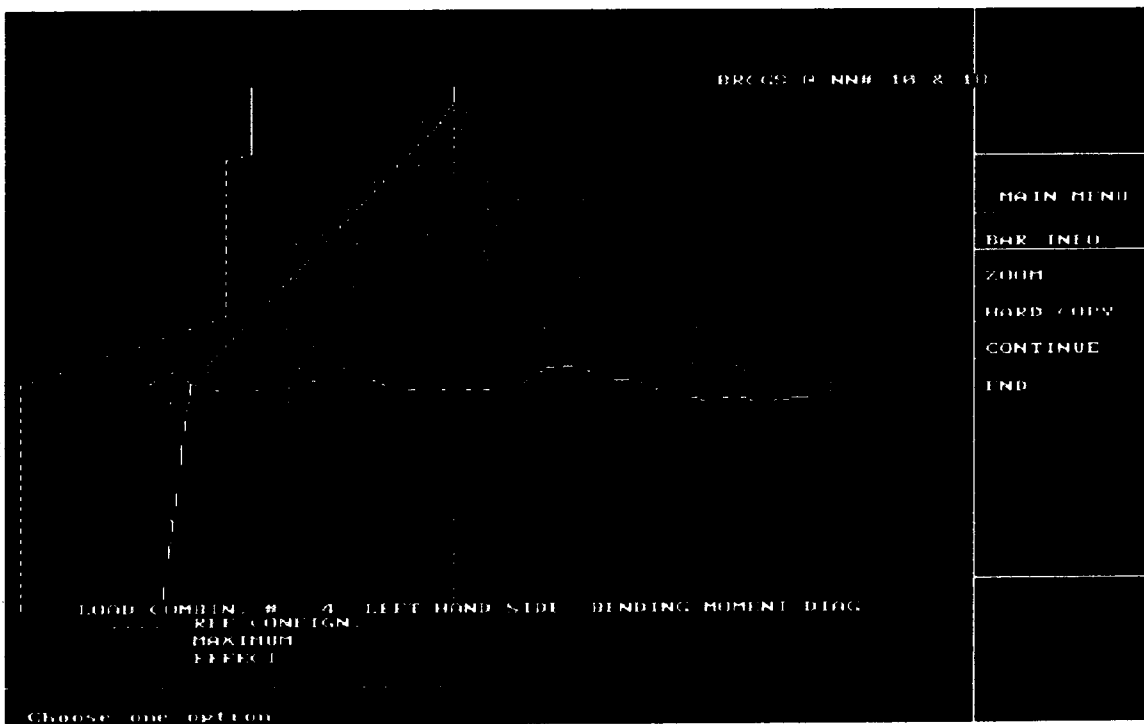


(d) Axial Force Diagram

Figure 7.11 Deck-Tower Jack Installation



(a) Deflected Shape

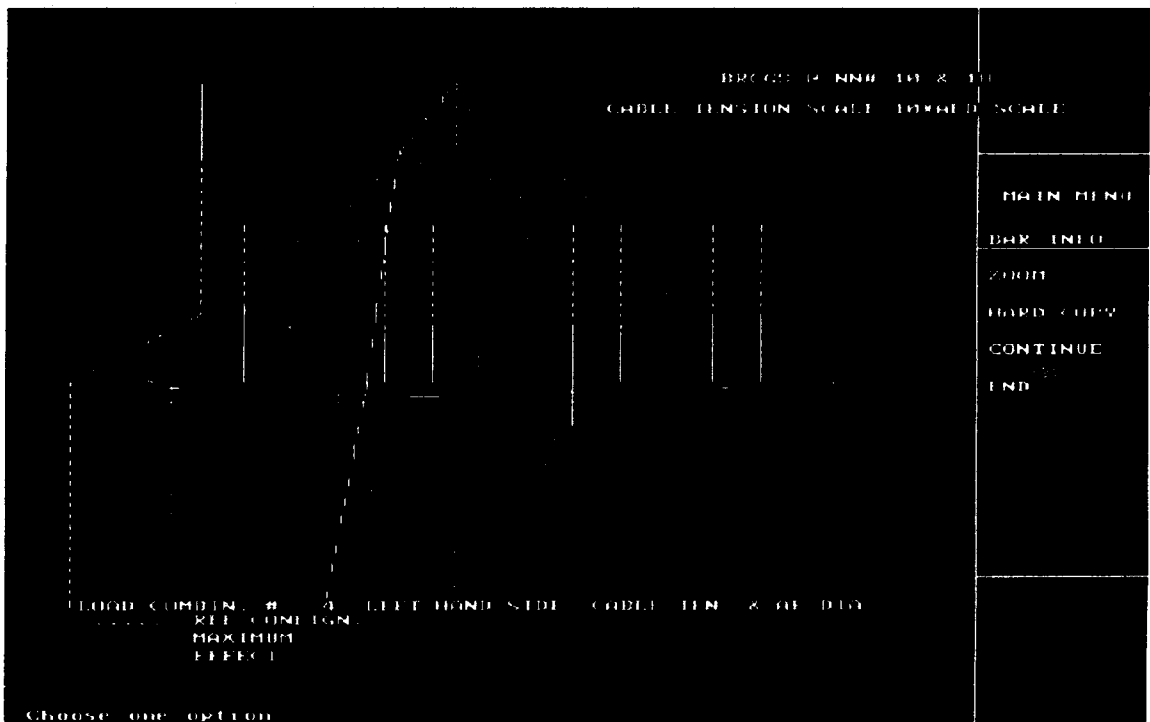


(b) Bending Moment Diagram

Figure 7.12

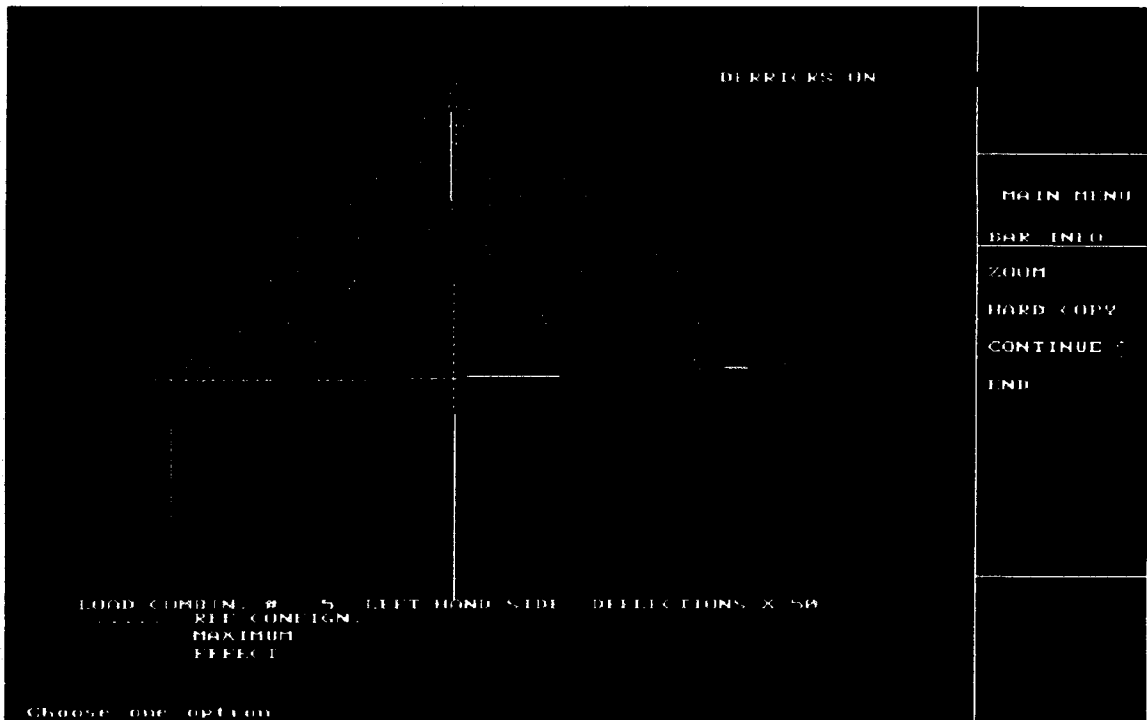


(c) Shear Force Diagram



(d) Axial Force Diagram

Figure 7.12 Installation of Bracing Sets @ NN 10 & 18



(a) Deflected Shape

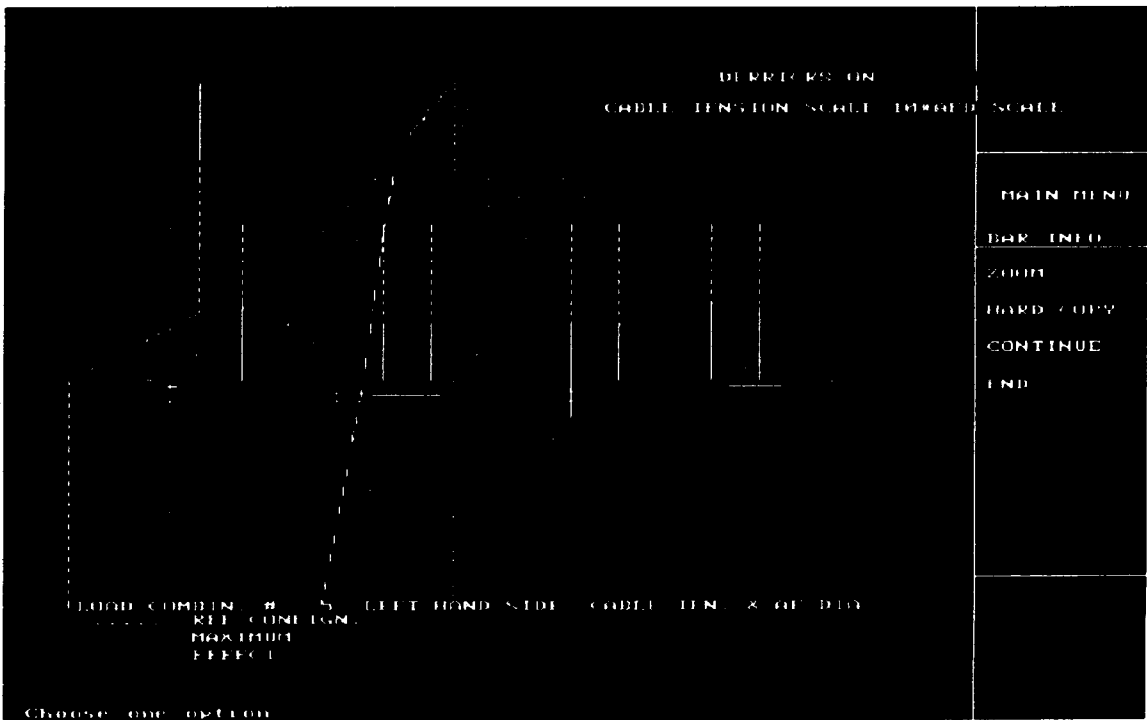


(b) Bending Moment Diagram

Figure 7.13

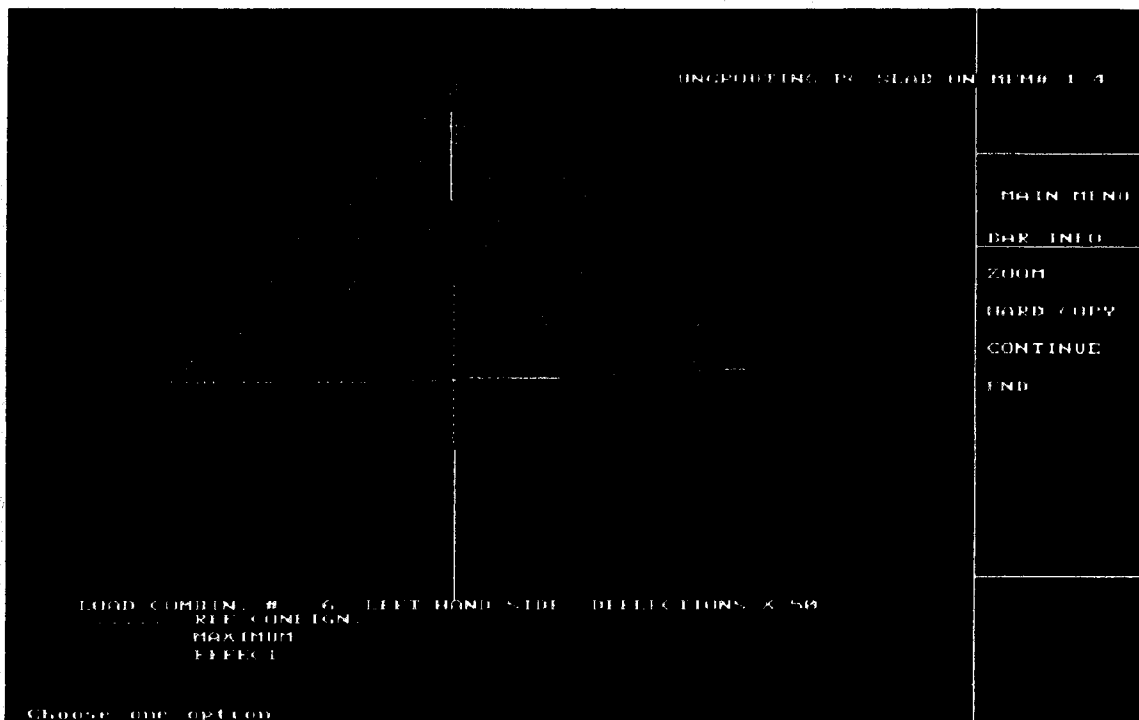


(c) Shear Force Diagram

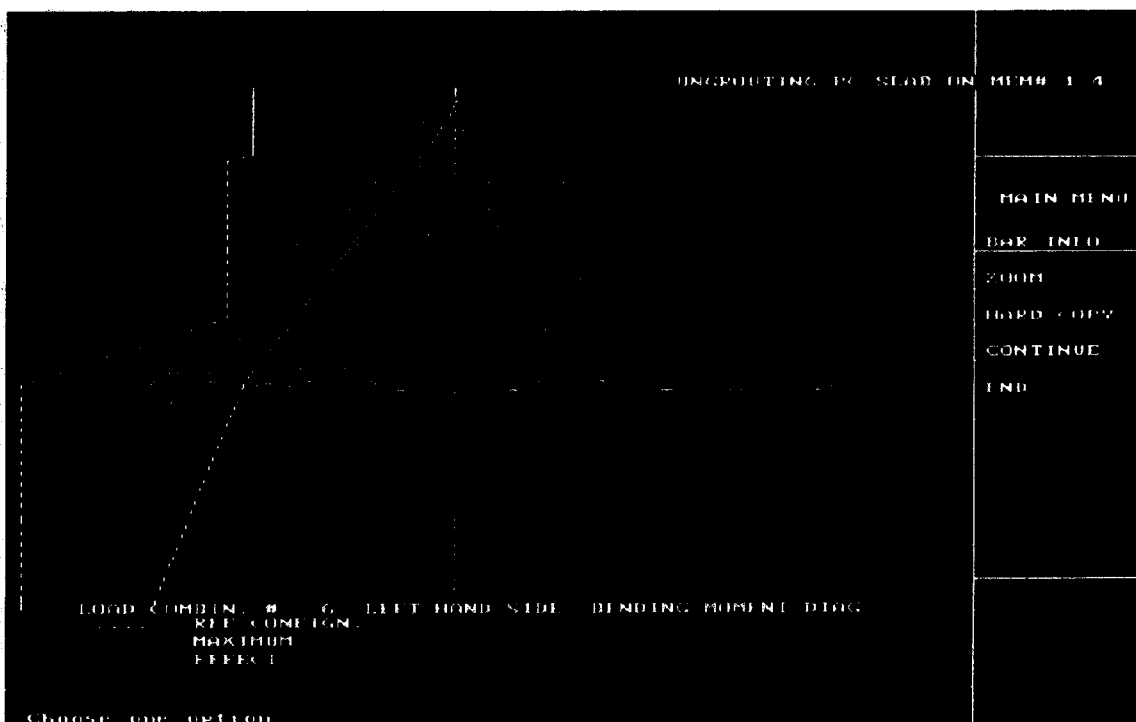


(d) Axial Force Diagram

Figure 7.13 Derricks on the Girder



(a) Deflected Shape

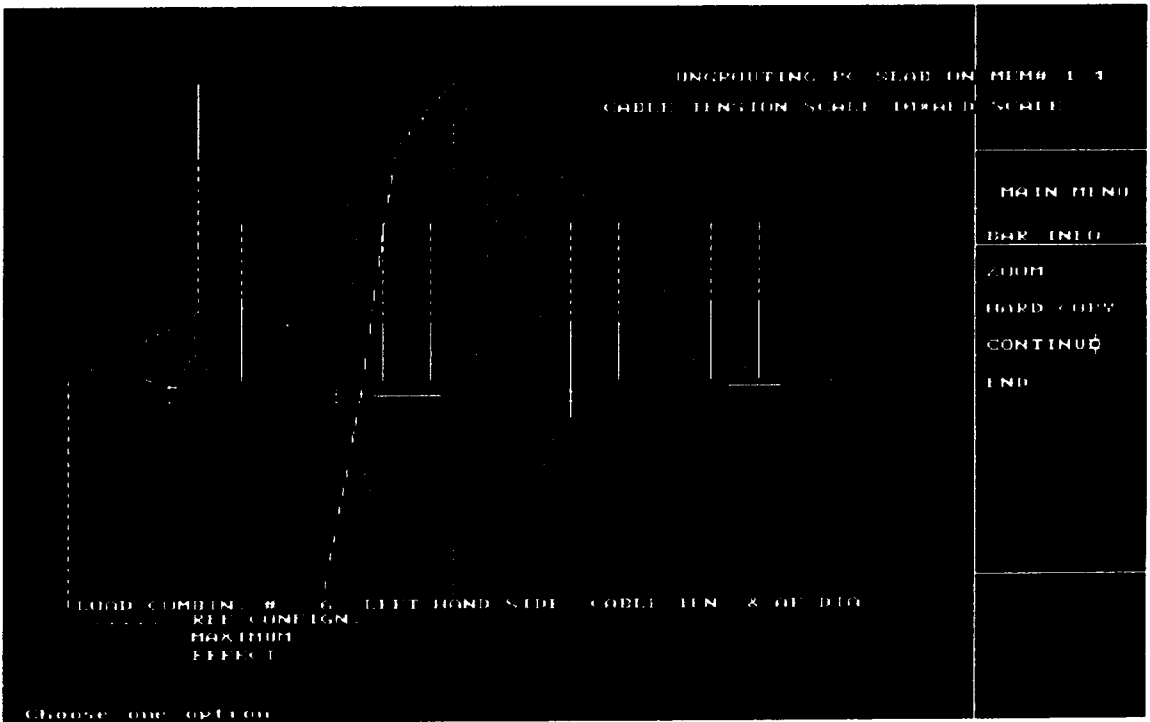


(b) Bending Moment Diagram

Figure 7.14

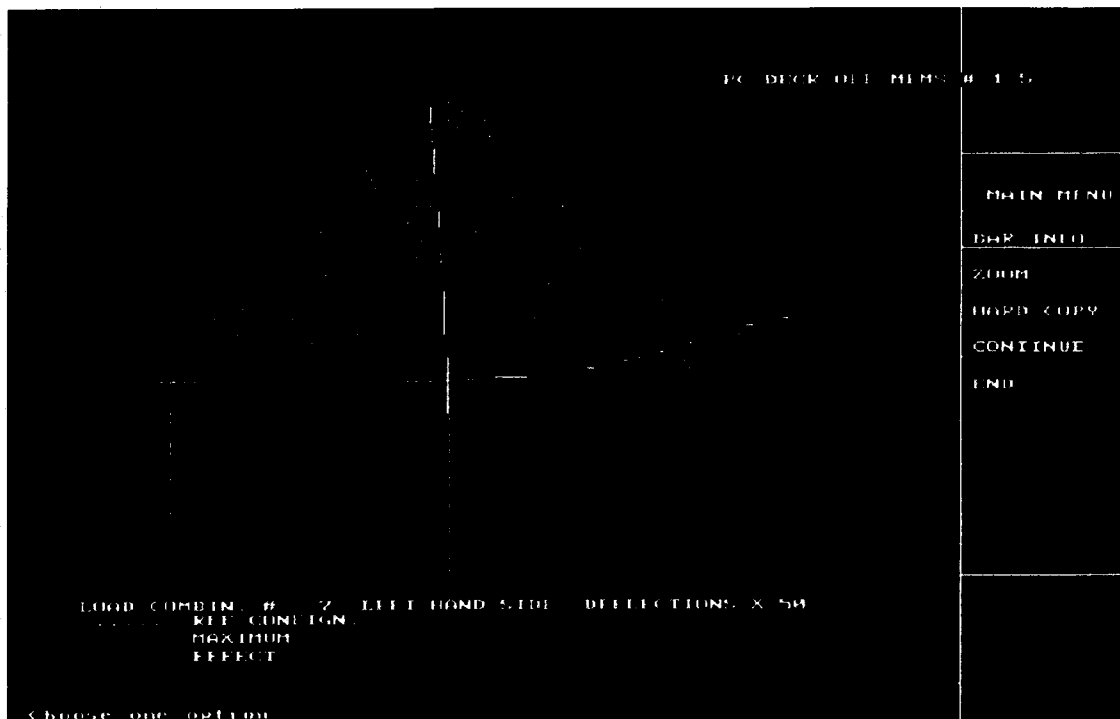


(c) Shear Force Diagram

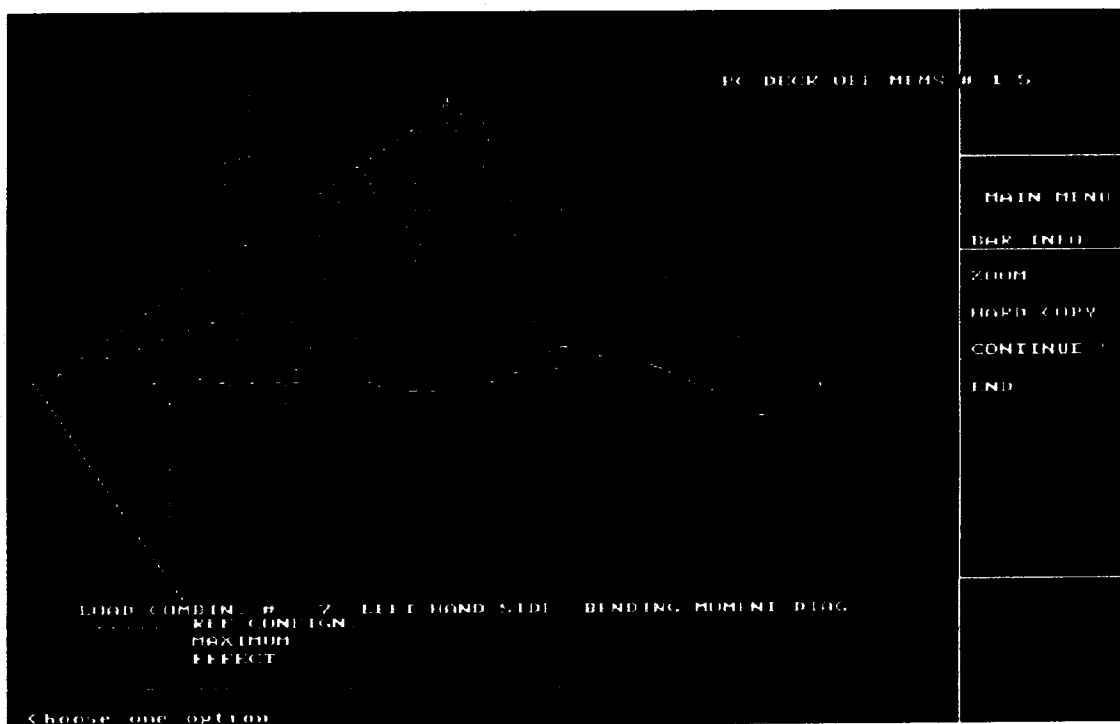


(d) Axial Force Diagram

Figure 7.14 Ungrouting of PC Slabs on Mems. 1-4



(a) Deflected Shape



(b) Bending Moment Diagram

Figure 7.15

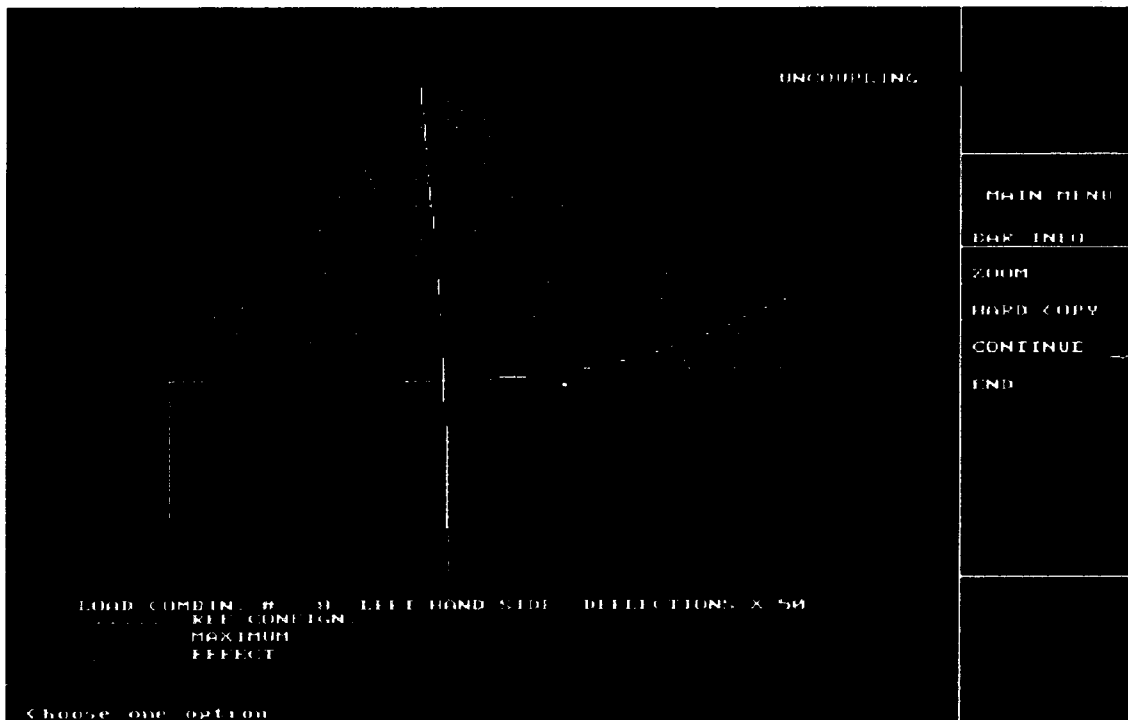


(c) Shear Force Diagram

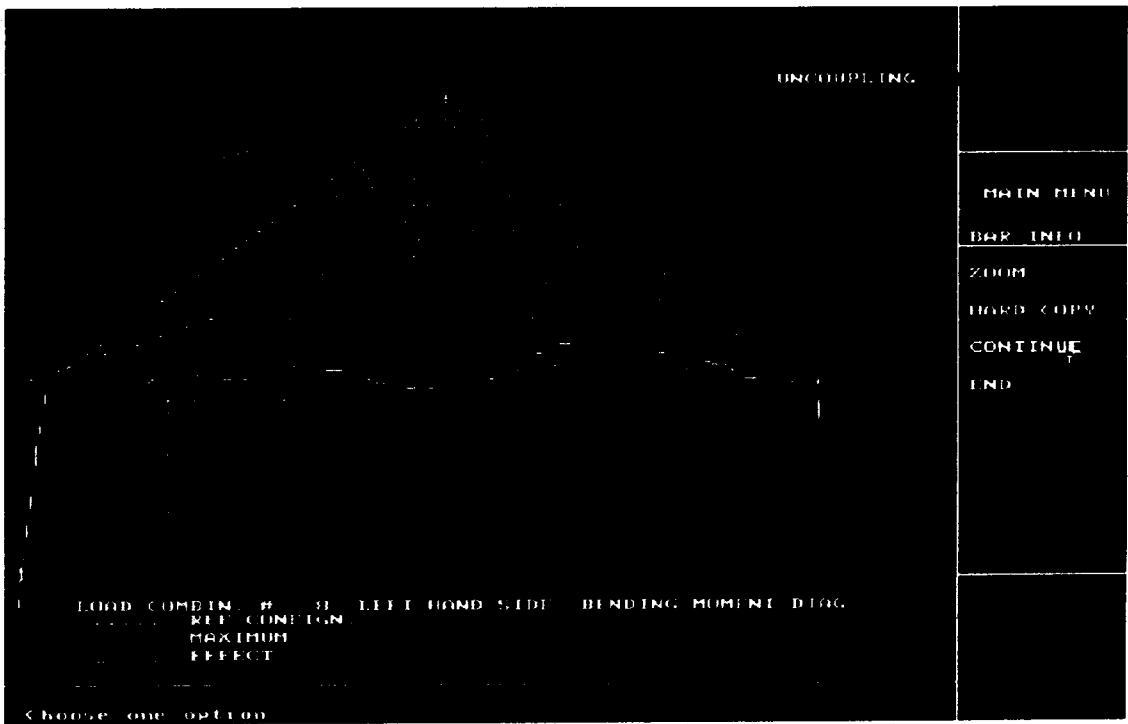


(d) Axial Force Diagram

Figure 7.15 Removal of PC Deck from Mem. 1-4

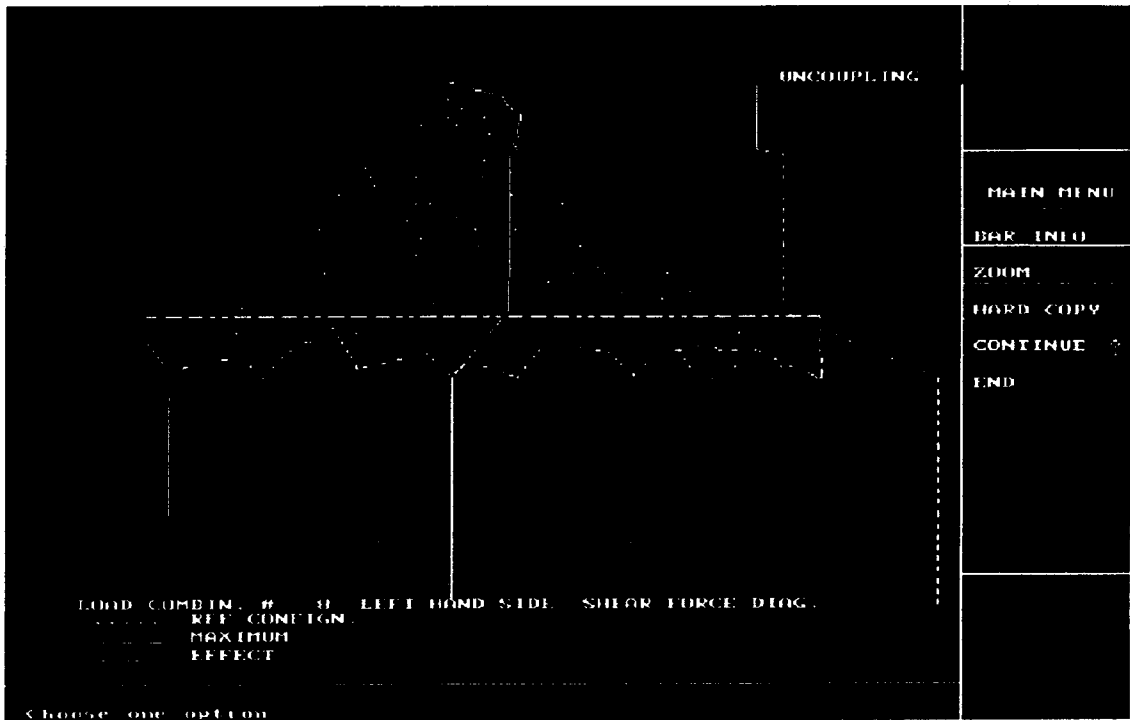


(a) Deflected Shape

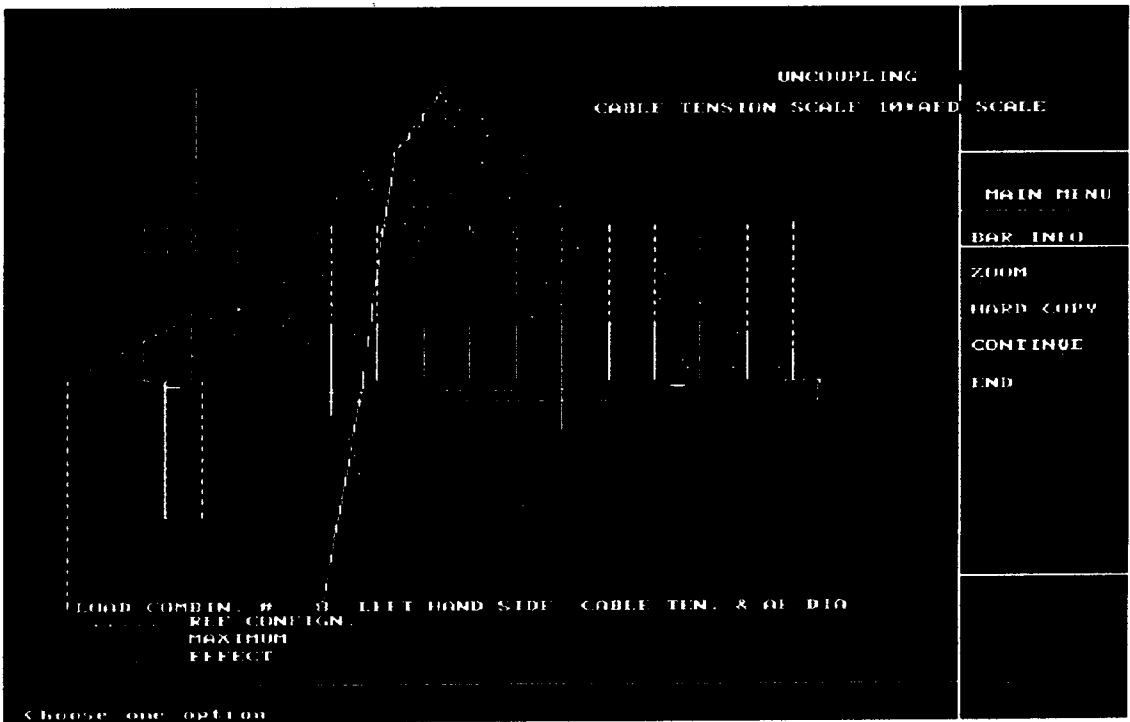


(b) Bending Moment Diagram

Figure 7.16

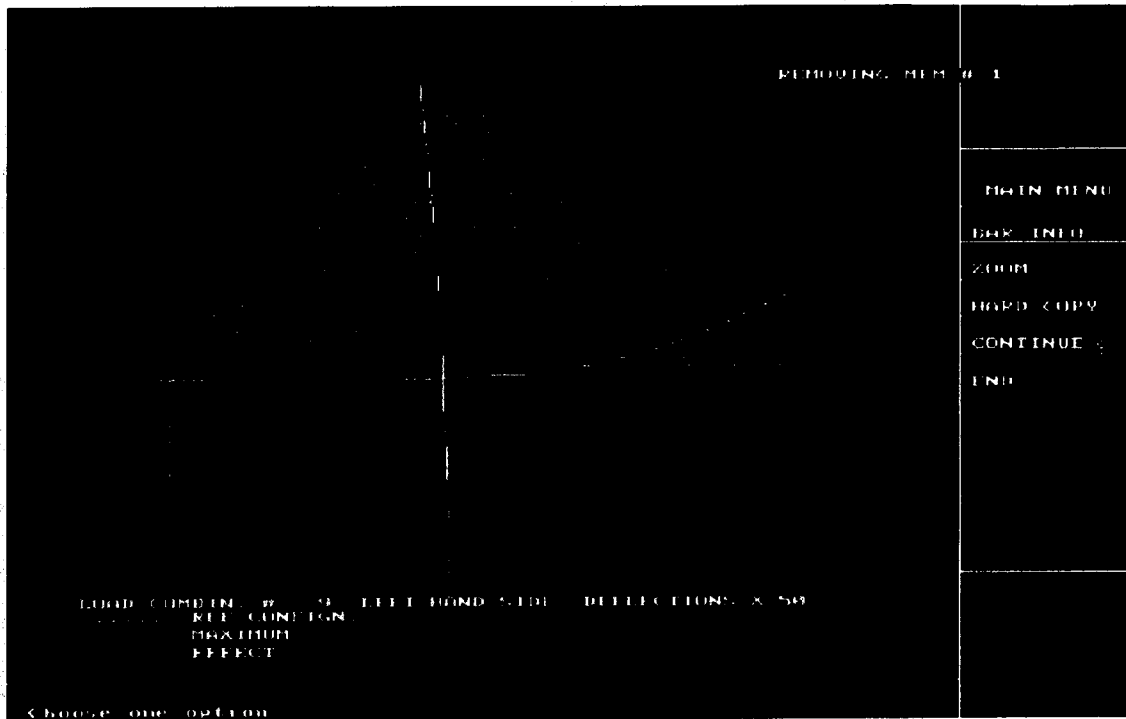


(c) Shear Force Diagram

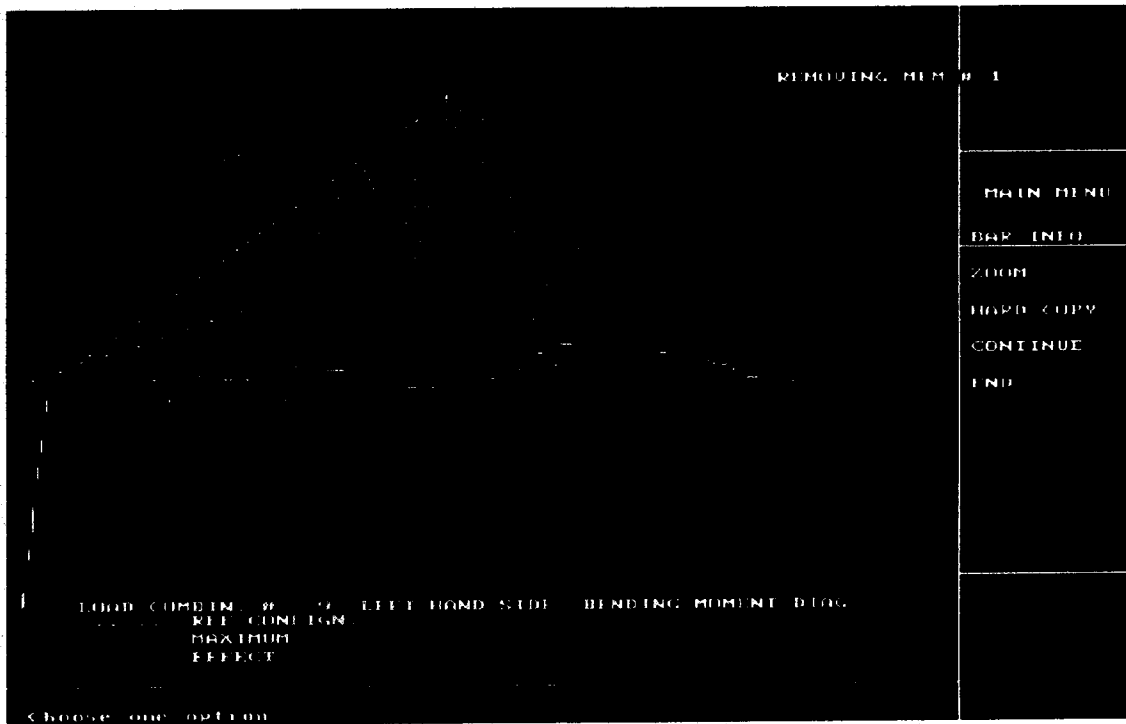


(d) Axial Force Diagram

Figure 7.16 Uncoupling of the Girder



(a) Deflected Shape

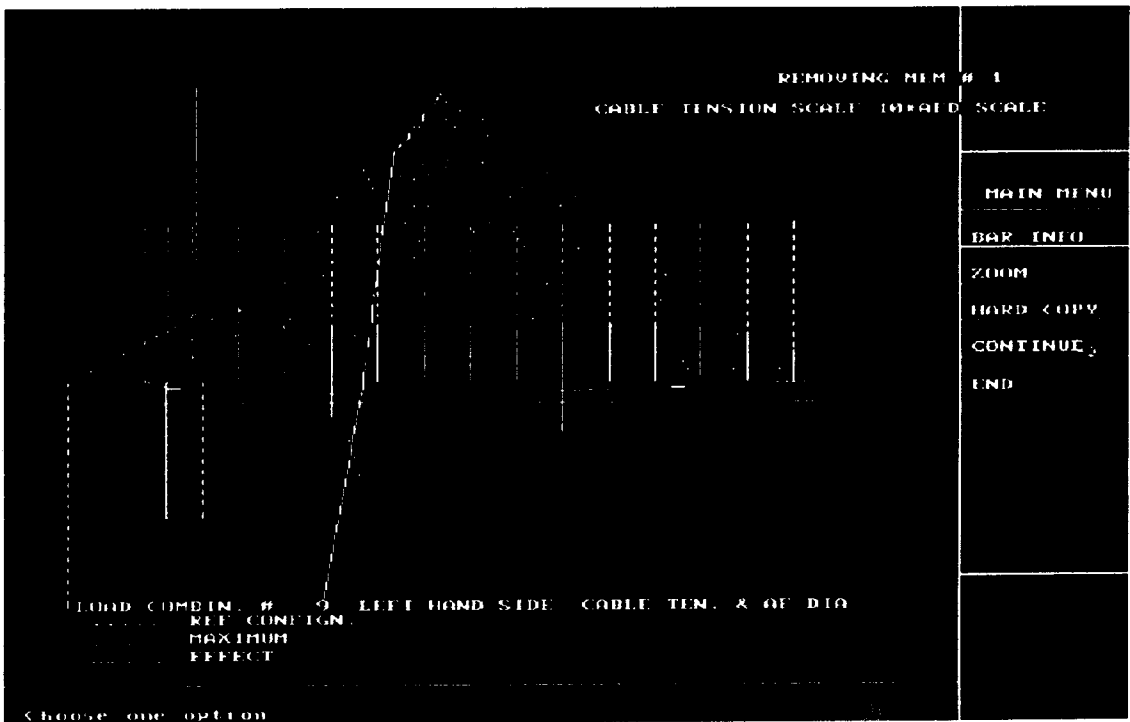


(b) Bending Moment Diagram

Figure 7.17

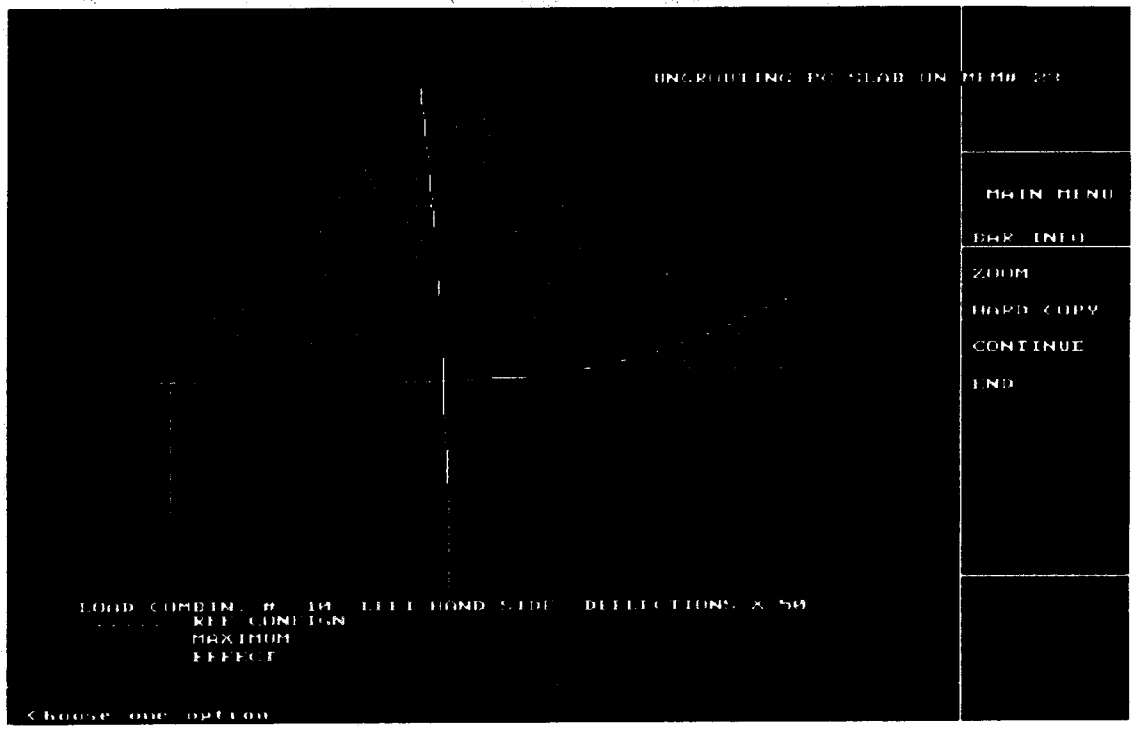


(c) Shear Force Diagram

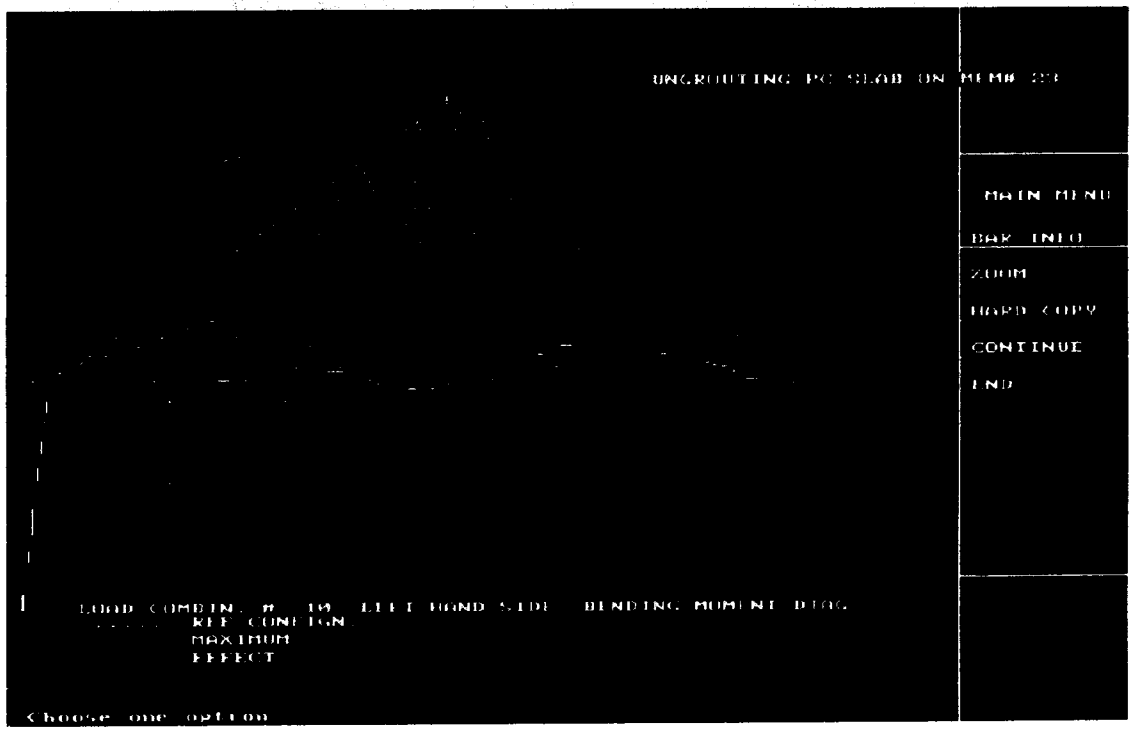


(d) Axial Force Diagram

Fig. 7.17 Removing Member #1

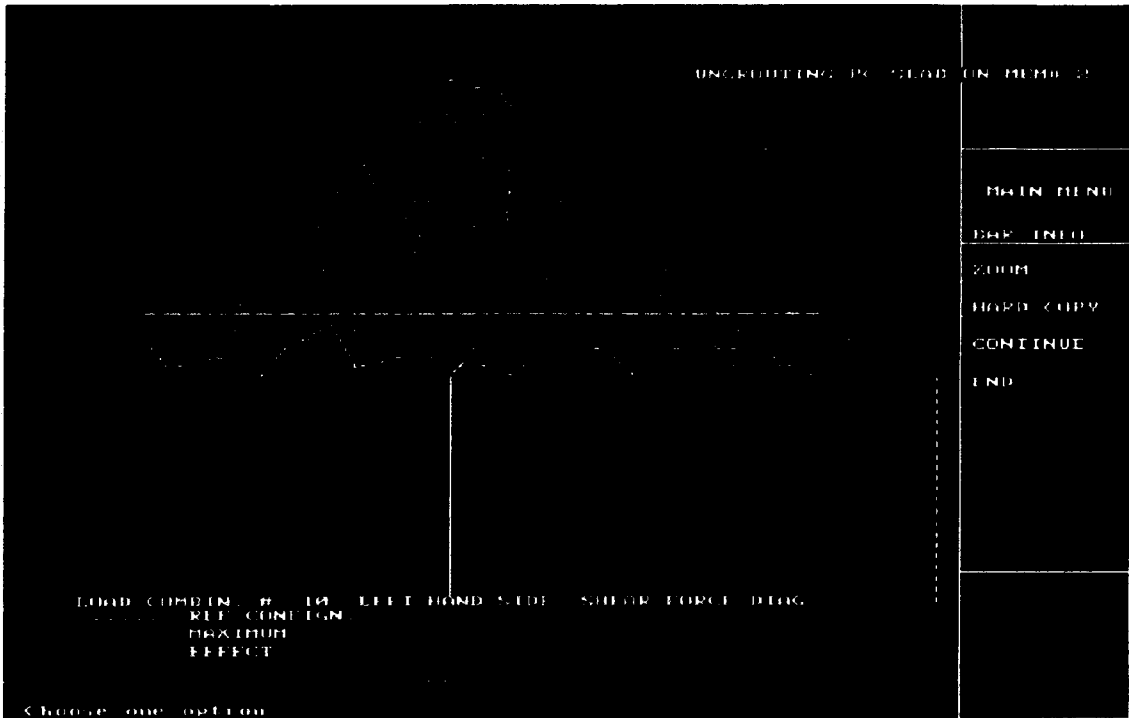


(a) Deflected Shape



(b) Bending Moment Diagram

Figure 7.18

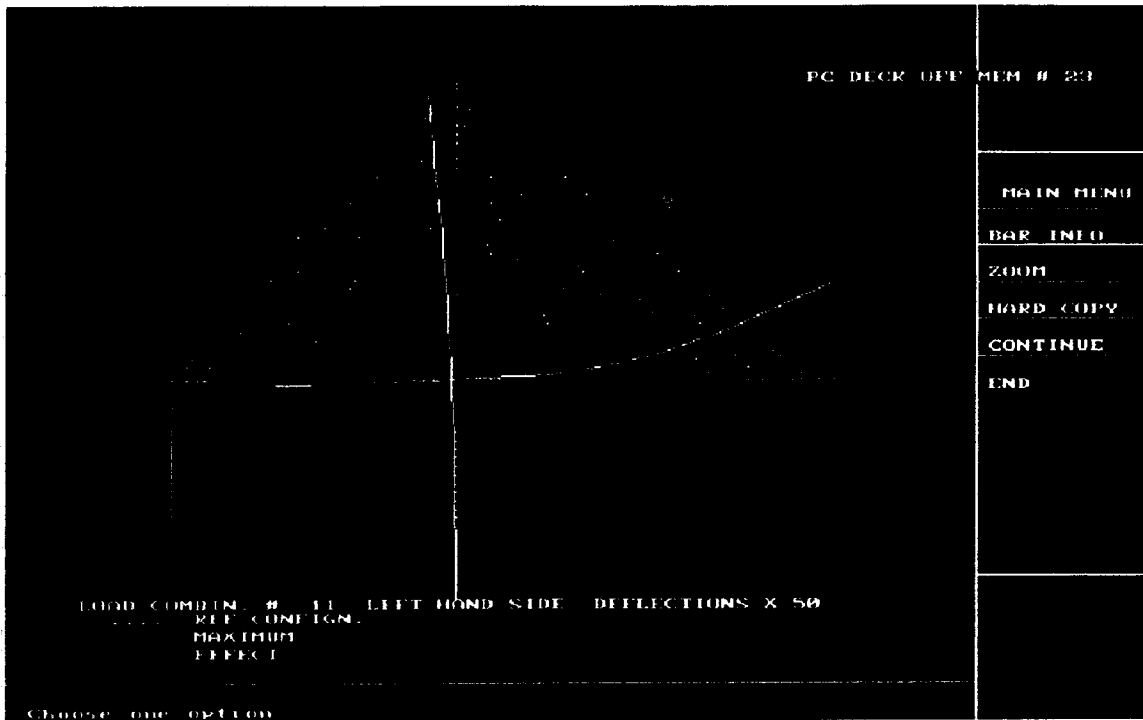


(c) Shear Force Diagram

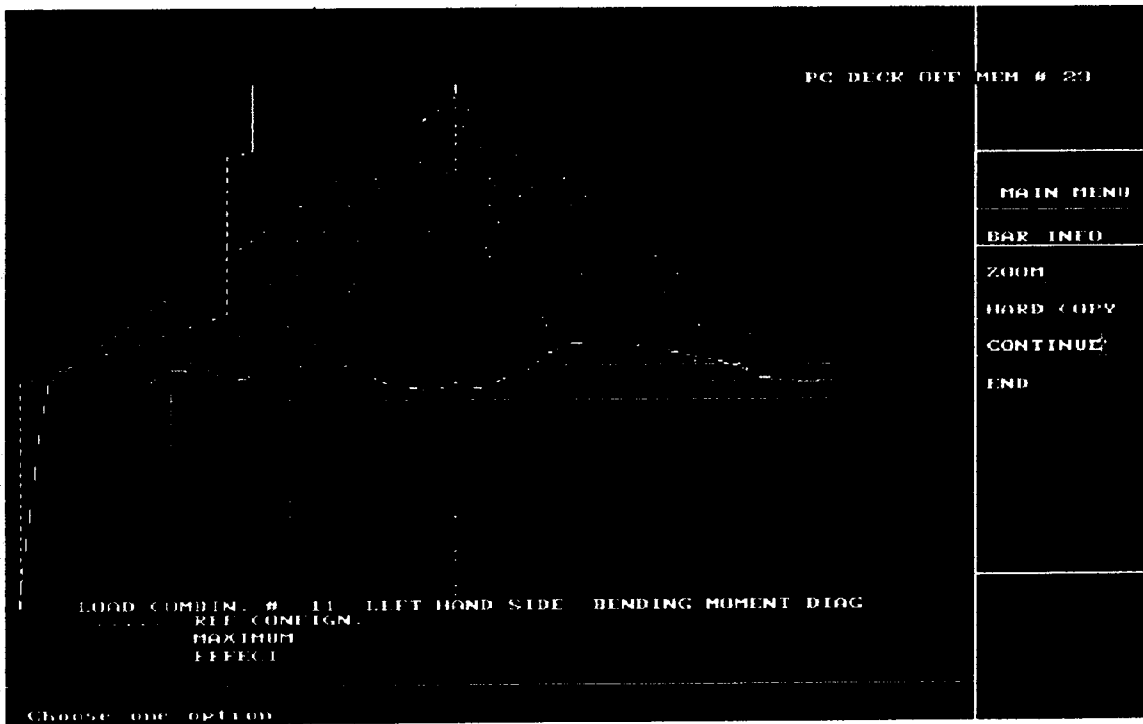


(d) Axial Force Diagram

Figure 7.18 Ungrouting PC slab on Member # 23

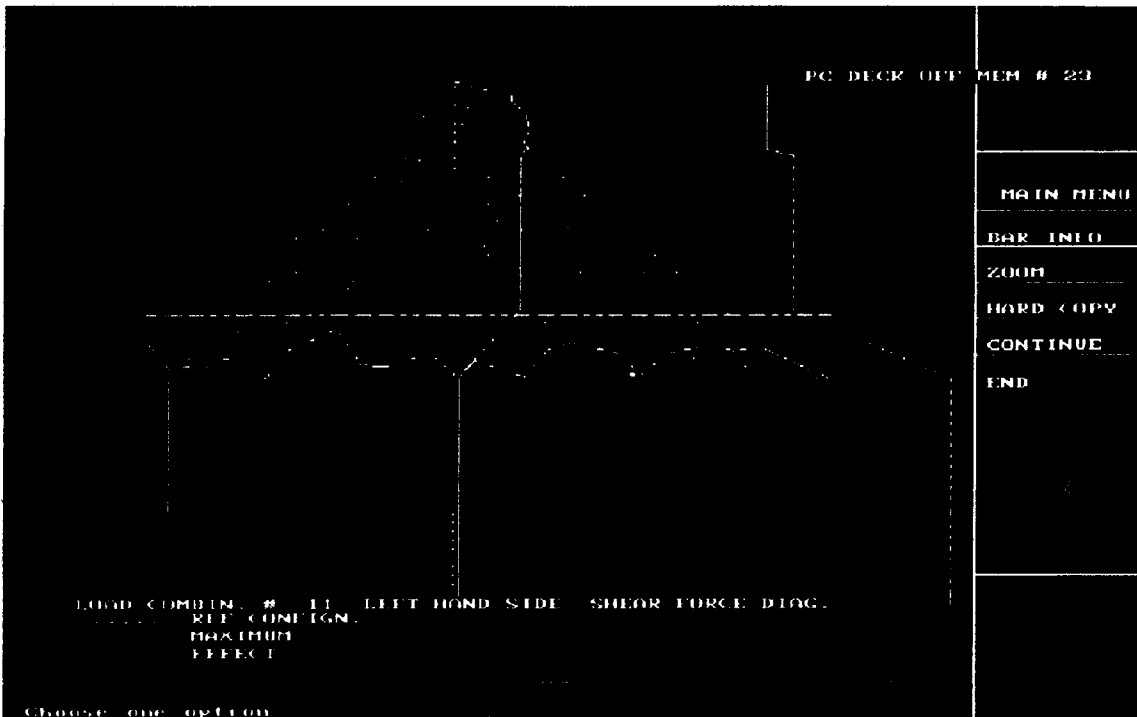


(a) Deflected Shape

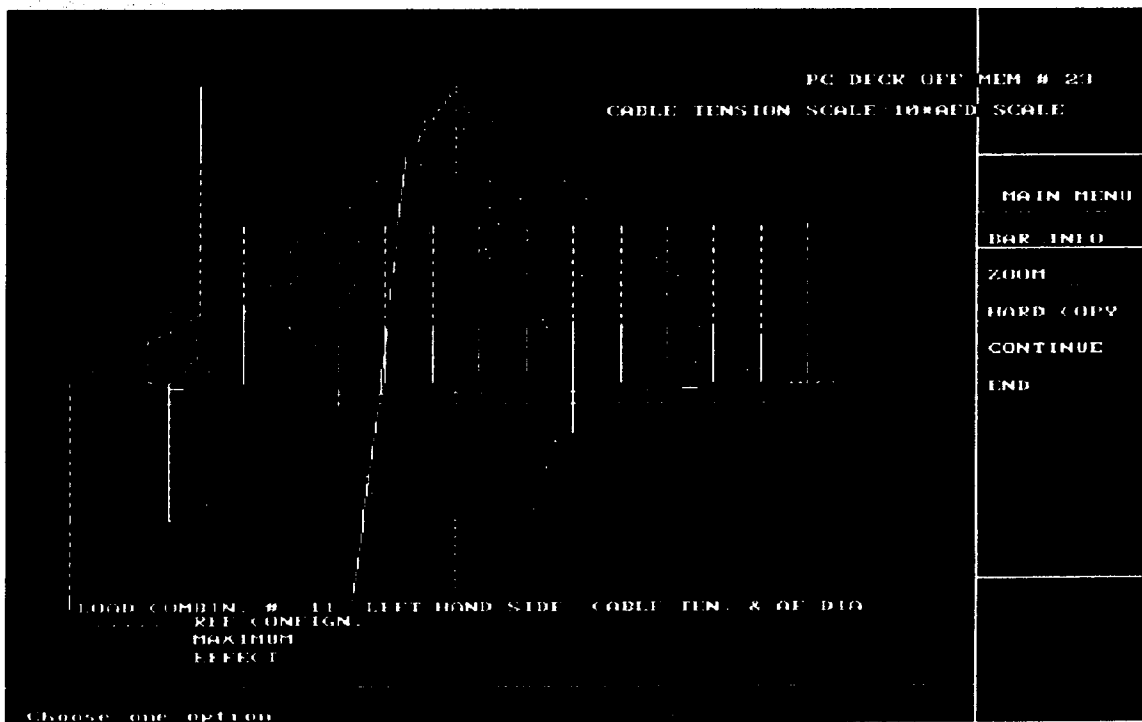


(b) Bending Moment Diagram

Figure 7.19

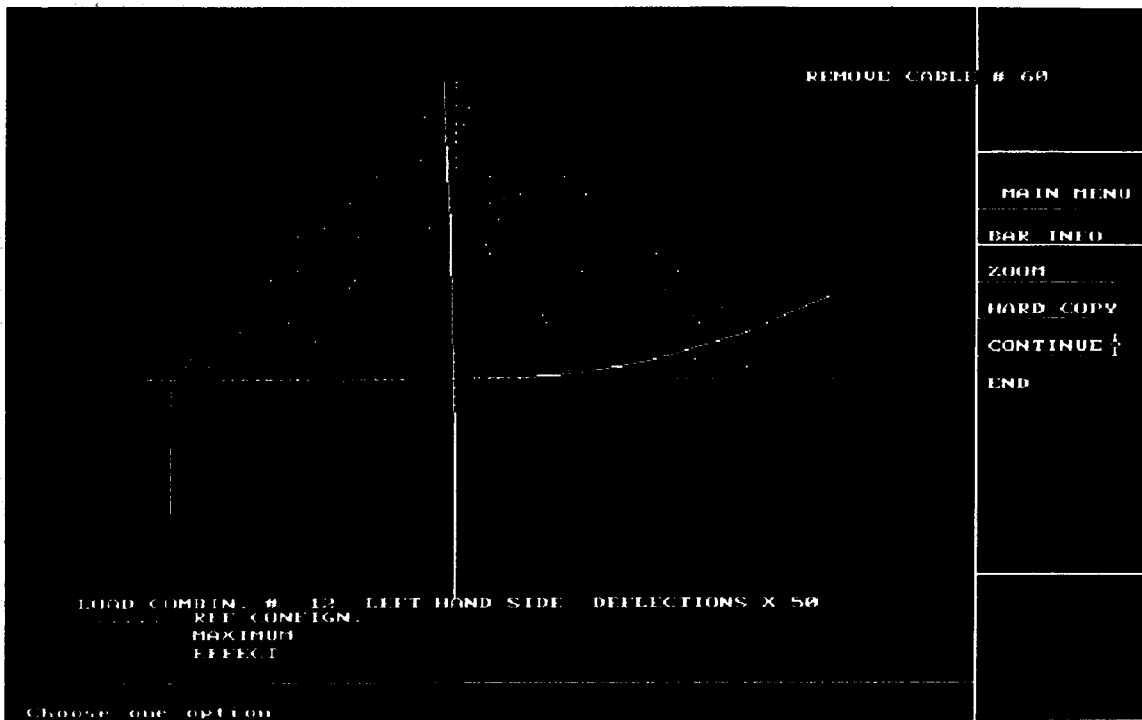


(c) Shear Force Diagram

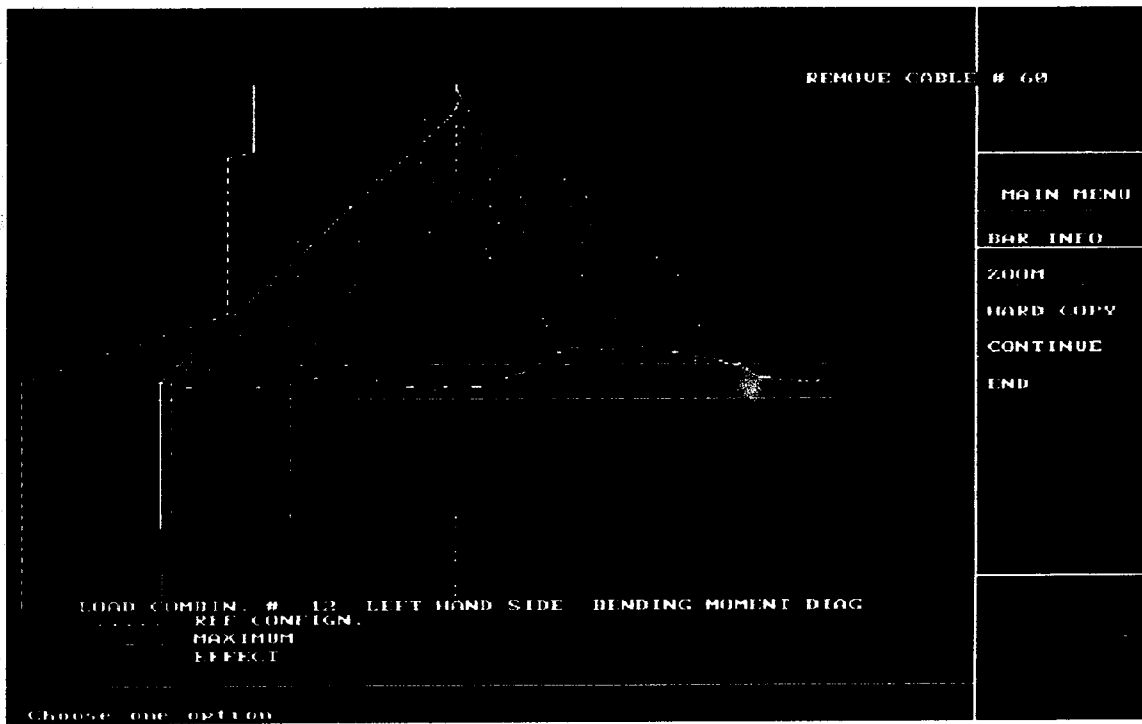


(d) Axial Force Diagram

Figure 7.19 Removal of PC Deck from Member # 23



(a) Deflected Shape

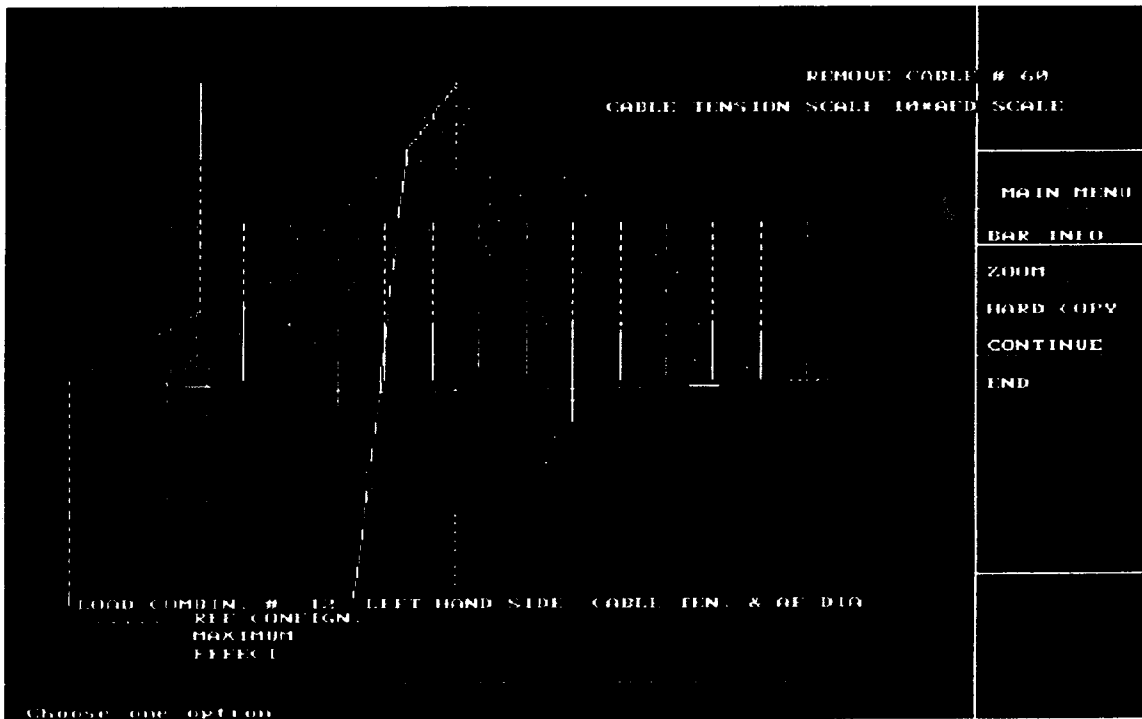


(b) Bending Moment Diagram

Figure 7.20



(c) Shear Force Diagram



(d) Axial Force Diagram

Figure 7.20 Removal of Cable # 60

CHAPTER 8 : SUMMARY, CONCLUSIONS AND RECOMMENDATIONS

8.1 Summary and Conclusions

The program developed in the present work is applicable to the erection and live load analyses of a cable-stayed bridge with a large number of stays supporting girders and deck elements on two central towers. The continuous structural change of a cable-stayed bridge during erection makes it desirable that special program be developed to determine consistent force and geometric configurations at each stage of erection and to ensure that these transient configurations finally evolve into the ultimate configuration specified by the designer for the completed bridge.

In order to achieve this central objective, the program developed, herein, uses the following techniques:

a) Definition of a Reference Configuration

The reference configuration is the state of internal and external forces plus the associated geometry under the dead load of the bridge. The designer is required to specify the reference configuration for the bridge before its erection analysis.

b) Disassembly (Backward) Analysis

In order to ensure that the intermediate configurations during erection will finally evolve into the reference configuration defined by the designer, the program begins erection analysis from the reference configuration and ends with the first segment of the bridge to be erected. This is referred to as a backward or disassembly analysis. Erection sequences are in the reverse order to the backward

analysis sequence, and erection loads are entered into the analysis with opposite signs with regard to their real directions. In this way a configuration (both force and geometric) is obtained for each stage of erection which is consistent with the reference configuration.

c) Substructure-Frontal Analysis

A special purpose analysis program has been developed to deal with the problem of structural changes during erection, without repeated renumbering of the nodes and members for each new partial structure. By combining the frontal method with the substructure technique, both of which reduce the high speed storage requirement, an economical method for the assembly, reduction and backsubstitution of the matrix equations of equilibrium has been developed for microcomputers, which makes use of the modular nature of a cable-stayed bridge to achieve greater economy and efficiency. No renumbering of nodes or members is required. Each segment of the girder with the supporting cables and tower piece is identified by a sequential number, called the substructure number. In a typical cable-stayed bridge only five substructure types are required to model the topography of all the substructure modules required for its assembly. These substructure types are central to the development of the substructure-frontal technique.

It is to be noted that although the above method has been applied to the analysis of cable-stayed bridges in the present work, it is generally applicable to any type of modular structure for which a limited number of substructure types may be identified.

Two types of nonlinearities have been considered in the development of the program. These are: cable nonlinearity due to its catenary shape, and P- Δ effects in the flexural elements.

The graphic capability of the program is intended to facilitate fast

decision making on the acceptability of the internal forces for the load combinations which occur during a proposed erection scheme. Lines representing cross-sectional capacities on the screen predict problematic segments of the bridge with the risk of overstressing.

It has been found that the substructure-frontal technique lends itself very well to microcomputer programming of framed structures with modular components. While it maintains the advantage of a low RAM requirement as the distinctive feature of the frontal technique, its application is greatly simplified by the elimination of the prefront procedure required by the latter.

Backward analysis has been used throughout this work. Although theoretically not required, it still appears to be the most effective way to ensure the consistency of the intermediate configurations of the structure during its erection, with the reference configuration which can be specified by the designer.

8.2 Recommendations

The objective of this work, which was started in 1986 on the suggestion of a local consulting engineer, has been to produce a computer code, which would run on an IBM-AT style computer, and which would be sufficiently 'user-friendly' so that it can be operated by the site engineer to provide back-up for the field monitoring of, and assist in the decisions which must be made during, the erection of cable-stayed bridges. While CASBA meets the basic requirements for this task, there are numerous ways by which it could be improved and expanded in order that it performs its function in a more versatile and effective manner. The following is the discussion of some of the improvements which it is recommended be

incorporated into further development of the program.

First, the program has been written using centreline coordinates of structural members. Yet the reference points for the girder in the field are generally related to an arbitrary 'work point' line. It would be more convenient for field erection if the program were altered such that girder nodes were defined on the work point line rather than on centroidal axes. In addition, the towers generally have substantial lateral dimensions in which case the cable anchorages are eccentric from the centroidal axes of the towers. The eccentric location of anchorages could be conveniently incorporated by including offsets from the tower centreline as a part of input data.

Second, the computation of stresses that arise in the girders and deck could be computed and output in a manner which is more directly related to the quantities which are of interest to the designer. Since the internal forces increase stepwise as the cross-section changes shape, the stresses should be computed by the superposition of incremental stresses due to incremental internal force changes acting on the effective section at the time the increment occurs. This should be incorporated into the computation of the stresses.

Third, the determination of capacities, and their graphical display, should be based upon moment-axial force interaction curves. While a comparison of the internal forces and the moment capacities displayed by the current program gives an indication of these areas where stress checks may be necessary, the numerical values are not very accurate because the interaction effects are not included.

Fourth, the application of the program should be more fully explored to a wider range of structural configurations and loading conditions. This

would include the erection of bridges in which the girders are prefabricated box-girder cross-sections and towers have a more general geometric configuration.. In addition, since the reference configuration moments are data which can be selected by the designer on the basis of the bending moment envelopes due to combined live load and dead load, a method of automatically generating these moment envelopes should be incorporated into the program. In addition, the initial computation of reference configuration forces should be expanded to include axial forces and arbitrary geometries.

Fifth, the effect of loadings such as temperature and wind, which can have a significant effect on partial structures in the erection sequence should be included. Creep strains could be included for the total structure. Even though, these strains should not be a factor in the erection sequence, they could be a factor in the selection of the internal forces of the reference configuration.

With respect to program strategy it may be possible to replace the linkage between global numbering and local substructure numbering with routines that construct the identification between the arrays from user defined data statements. If such a strategy could be developed it could make it much easier for the user to define alternative types of substructures and incorporate them into the program. Such a strategy should be investigated.

Finally, the rapid evolution of computer hardware and software, and the drastic reduction in cost of work-station facilities, has completely changed the computing environment during the course of this work. A new generation of interactive computer graphics software has arisen which facilitate the use of a window environment in which the analyst can design

his menus, graphical data generation and display. The user-friendliness of the program would benefit immensely by embedding it into such an environment.

REFERENCES

- Baron, F., and Lien, S. Y. 1971. Analytical Studies of the Southern Crossing Cable-Stayed Girder Bridges. Report No. UC SESM 71-10, Vol. I & II. Dept. of Civil Engineering, University of California, Berkeley, California.
- Baron, F., and Lien, S. Y. 1973. Analytical Studies of a Cable-Stayed Girder Bridge. Computers and Structures, Vol. 3, Pergoman Press, New York.
- Birkenmaier, M., and Narayanan, R. 1982. Fatigue Resistance of Large High Tensile Steel tendons. Proc. IABSE Colloq. on Fatigue of Steel and Concrete Structures, Luanne.
- Buchanon, G. R. 1970. Two-Dimensional Cable Analysis. ASCE Journal of Structural Engineering, 96 (7): 1581-87.
- Buchhaoldt, H. A. 1985. Cable Roof Structures. Cambridge University Press, Cambridge, England, p. xi.
- Carstraphen, F. C. 1919. A Simple Method of Computing Deflections of a Cable Span Carrying Multiple Loads Evenly Spaced. ASCE Transactions, 83: 1383-1408.
- Carstraphen, F. C. 1920. A Simple Method of Computing Deflections of a Cable Span Carrying Multiple Loads Evenly Spaced. ASCE Proceedings, 46 (5): 793-808.
- Dischinger, F. 1949. Hängebrücken für schwerste verkehrslasten. Der Bauingenieur: 65-107.
- Domingueze, R. F., and Smith, C. E. 1972. Dynamic Analysis of Cable Systems. ASCE Journal of Structural Engineering, 98 (8): 1817-1833.
- Douglass, M. McC., Lazar, B. E., and Troitsky, M. S. 1972. Load Balancing Analysis of Cable-Stayed Bridges. ASCE Journal of Structural Engineering, 98 (8): 1975-1740.
- Durkee, J. L. 1966. Advancements in Suspension Bridge Cable Construction. Proc. Int. Symposium on Suspension Bridges, Lisbon.
- Elwi, A. E. and Murray, D. W. 1985 Skyline Algorithms for Multilevel Substructure Analysis. International Journal For Numerical Methods in Engineering, Vol. 21: 465-479
- Fujisawa, N., and Tomo, H. 1985. Computer-Aided Cable Adjustment of Stayed Bridges. IABSE Proceedings, P-92/85 (4): 181-190.

- Gallagher, R. H. 1975. Finite Element Analysis Fundamentals. Prentice-Hall, Inc., Englewood, Cliffs. New Jersey.
- Gimsing, N. J. 1966. Anchored and Partially Anchored Stayed Bridges. Symposium on Suspension Bridges, Paper No. 30, Lisbon.
- Gimsing, N. J. 1983. Cable Supported Bridges: Concept and Design. John Wiley & Sons, New York, p. 242.
- Hegab, H. I. A. 1985. Energy Analysis of Cable-Stayed Bridges. ASCE Journal of Structural Engineering, 112 (5): 1182-1195.
- Hinton, E., and Owen, D. R. J. 1979. Finite Element Programming. Academic Press INC. (London), Second Printing.
- Jennings, A. 1962. The Free Cable. The Engineer, Dec. 28, 1962: 1111-1112.
- Kajita, T., and Cheung, Y. K. 1973. Finite Element Analysis of Cable-Stayed Bridges. IABSE Publication 33-II.
- Keifer, A. 1915. Ueber die Kettenlinie. Schweizerische Bauzeitung, Nov. 27, 1915.
- Khalil, M. S., Dilger, W. H., and Ghali, A. 1983. Time-Dependent Analysis of PC Cable-Stayed Bridges. ASCE Journal of Structural Engineering, 109(8): 1980-1995.
- Leonhardt, F., and Zellner, W. 1970. Cable-Stayed Bridges: Report on Latest Developments. Canadian Structural Engineering Conference, 1970, Toronto.
- Lin, T. Y. 1961. A New Concept for Prestressed Concrete. Construction Review, Sydney, Australia.
- Melan, J. 1888. Theorie der eisernen Bogenbrücken Und der Hängenbrücken in Handbuch de Ingenieur Wissenschaften, Leipzig, 2nd edition.
- Melan, J. 1906. Theorie der eisernen Bogenbrücken Und der Hängenbrücken in Handbuch de Ingenieur Wissenschaften, Leipzig, 3rd edition.
- Michalos, J., and Brinstiel, C. 1960. Movements of a Cable Due to Changes in Loading. ASCE Journal of Structural Engineering, 86 (12): 23-38.
- O'Brien, W. T., and Francis, A. J. 1964. Cable Movements Under Two-Dimensional Loads. ASCE Journal of Structural Engineering, 90 (3): 89-123.
- O'Brien, W. T. 1967. General Solution of Suspended Cable Problems. ASCE Journal of Structural Engineering, 93 (1): 1 - 26.

- Odenhausen, H. 1965. Static Principles of the Application of Steel Wire Ropes in Structural Engineering. Stahl, No. 2, 1965: 51 - 65.
- Okauchi, I., Yaba, A., and Ando, K., 1967. Studies on the Characteristics of a Cable-Stayed Bridge. Bulletin of the Faculty of Science and Engineering, Chuo University, Vol. 10.
- Phoenix, S. L., et al, 1986. Condition of Steel Cable after Period of Service. ASCE Journal of Structural Engineering, 112 (6): 1263 - 1279.
- Pigeaud, G. 1924. Etude sur le cables specialment sur les cables de ponts suspendus. Le Génie civil, 84 (15), April 12, 1924: 345-350.
- Podolny, W., Scalzi, J. B. 1976. Construction and Design of Cable-Stayed Bridges, John Wiley & Sons, New York. 1st edition.
- Podolny, W., Scalzi, J. B. 1987. Construction and Design of Cable-Stayed Bridges, John Wiley & Sons, New York. 2nd edition.
- Podolny, W. 1971. Static Analysis of Cable-Stayed Bridges. Ph. D. Thesis, University of Pittsburgh.
- Podolny, W., and Fleming, J. F. 1971. Cable-Stayed Bridges- A State-of-the-Art. Preprint Paper 1346, ASCE National Water Resources Engineering Meeting, Phoenix, Arizona, January 11-15, 1971.
- Pugsley, A. 1957. Theory of Suspension Bridges. Edward Arnold Publishers, London. pp. 1-10.
- Rankine, 1858. Applied Mechanics.
- Rankine, 1863. Civil Engineering.
- Roebing, J. A. 1855. Passage of the First Locomotive Over the Suspension Bridge Over the Falls of Niagara. Journal of the Franklin Institute.
- Scordelis, A. C., et al. 1989. Cable-Suspended Bridges - Past, Present, and Future. Lecture presented at ASCE Structures Congress, San Fransisco, May, 1989.
- Smith, B. S., 1967. The Single Plane Cable-Stayed Girder Bridge: A Method of Analysis Suitable for Computer Use. Proceedings of the Institution of Civil Engineers, Vol. 37 (May 1967): 183-194.
- Smith, B. S., 1968. A linear Method of Analysis for Double-Plane Cable-Stayed Girder Bridges. Proceedings of the Institution of Civil Engineers. Vol. 39 (January 1968): 85-94.
- Steinman, D. B. 1922. A Practical Treatise on Suspension Bridges. John Wiley and Sons, New York.

- Subcommittee on Cable-Stayed Bridges. 1977. Bibliography and Data on Cable-Stayed Bridges. ASCE Journal of Structural Engineering, 103 (10): 1971-2004.
- Syed, A. A. 1986. Dynamic Response of Sagged Cables. Computers and Structures, Vol. 23 (1): 51-57.
- Tang, M. C., 1971. Analysis of Cable-Stayed Girder Bridges. ASCE Journal of Structural Engineering, 97 (5): 1481-1495
- Task Committee on Cable-Suspended Structures. 1977. Tentative Recommendations for Cable-Stayed Bridge Structures. ASCE Journal of Structural Engineering, 103 (5): 929-939.
- Taylor, P. R. 1969. Cable-Stayed Bridges and Their Potential in Canada. Paper presented at 63rd Annual Meeting of EIC, Vancouver, B. C., September 1969.
- Taylor, P. R. 1987. Composite Cable-Stayed Bridges. AISC Engineering Journal, Fourth Quarter/ 1987: 157-163.
- Taylor, P. R., and Torrejon, J. E. 1987. Annacis Bridge. Concrete International, 9(7): 13-22.
- Troitsky, M. S., and Lazar, B. E. 1971. Model Analysis and design of Cable-Stayed Bridges. Proceedings of the Institution of Civil Engineers, March 1971.
- Troitsky, M. S. 1977. Cable-Stayed Bridges. Crosby Lockwood Staples Publishers, London, England, 1st. edition.
- Troitsky, M. S. 1988. Cable-Stayed Bridges. BSP Professional Books, London, England, 2nd edition.
- Tung, H. H., and Kudder, R. J. 1968. Analysis of Cables as Equivalent Two-Force Members, AISC Engineering Journal, January 1968: 12-14.
- Waldner, H. E., and Kulicki, J. M. 1988. Quincy Bayview Bridge - Construction Control. ASCE Proceedings of a Session Sponsored by the Structural Division, Nashville, Tennessee, May 9, 1988.
- Walmsley, T. 1924. The Length, Tension, and Sag of Stay-Ropes. Proceedings of the Institution of Civil Engineers, 1924 :4-11.
- Walther, R., et al. 1988. Cable-Stayed Bridges. Thomas Telford, London.
- Watson, S. C., and Stafford, D. 1988. Cables in Trouble. Civil Engineering, April 1988.

APPENDIX A : USER'S MANUAL

A.1 Introduction

CASBA uses two input files called MAIN.DAT and ERECT.DAT to produce two output files called OUTPUT and PRINT.PLT. This manual provides the basic information on how to prepare the data files and how to use the output files. All input data are entered in a free-field form and are separated by a comma.

A.2 File MAIN.DAT

A.2.1 Basic data for entire bridge

ECAB,DEN,ISYM,LCI,LCF,ISKIP

ECAB Modulus of elasticity of a straight piece of the cables in MPa.

DEN Density of the cable in N/mm^3 .

ISYM Symmetry flag,

Asymmetric bridge: ISYM=0

Symmetric bridge: ISYM=1

LCI Initial load case number,

Normal runs: LCI=1

Restart runs: LCI=Load case #

from which restart begins

Note: A normal run is any run which is not a restart run.

LCF Final load case number.

ISKIP Number of lines in ERECT.DAT file before load case LCI. This number is required only for restart runs. In normal runs it can

be any integer.

A.2.2 Basic data for left hand side of bridge

NSS(1),NND(1),NBR(1),BMRED(1),SFRED(1),AFRED(1)

NSS(1) Number of substructures on the left side of the bridge.

NND(1) Number of nodes on the left side of the bridge.

NBR(1) Number of members on the left side of the bridge.

BMRED(1) = $BMC / (1.25 * L)$ in which, BMC is the bending moment capacity of the left hand side tower, and L is the span of the side span.

SFRED(1) Same as BMRED(1) but for shear force capacity.

AFRED(1) Same as BMRED(1) but for axial force capacity.

A.2.3 Repeat Step A.2.2 for the right hand 'half' of the bridge, in which case subscripts in A.2.2 become 2.

A.2.4 Substructure types for left hand side of bridge

(IST(IS),IS=1,NSS(1))

IST(IS) Substructure type for substructure number IS.

A.2.5 Joint data for left hand side of bridge (one line for each joint) CJ,XDL,YDL,BMDL,SC(1),SC(2),SC(3)

CJ Joint number beginning with the letter J and then a 3 digit integer (eg. J007).

XDL X-Coordinate of node CJ in the reference configuration.

YDL Y-Coordinate of node CJ in the reference configuration.

BMDL Specified member-end moment (For cable attachments along the girder only)

- SC(1) Rotational spring coefficient between CJ and the ground (Default value is zero).
- SC(2) Vertical spring coefficient between CJ and the ground (Default value is zero).
- SC(3) Horizontal spring coefficient between CJ and the ground (Default value is zero).

A.2.6 Member data for left hand side of bridge (one line for NTYPE sequential members having same properties)

CM,GI,GA,GE,BM,SF,AF,NTYPE

- CM Member number, beginning with the letter M and then a three digit integer. (Ex. M001). (This is the member number of the first member in a group of members with same properties).
- GI Moment of inertia (mm^4) of member.(Rotational stiffness in the case of spring connections between girder and tower.)
- GA Cross-sectional area (mm^2) of member.(Stiffness in the vertical direction of spring connections between girder and tower.)
- GE Modulus of elasticity (MPa) of members.(Stiffness in the horizontal direction of spring connections between girder and tower.)
- BM Bending moment capacity (N.mm) of members.
- SF Shear force capacity (N) of members.
- AF Axial force capacity (N) of members.
- NTYPE Number of members in the group.

A.2.7 Repeat Steps A.2.4 to A.2.6 for the right hand 'half' of the bridge

A.2.8 Load data for right hand side of bridge (one line for NTYPE

sequential members having same loading conditions)

CM,UDL,NTYPE,NPL,(PLOAD(I),I=1,NPL),(XRP(I),I=1,NPL)

CM Member number, beginning with the letter M and then a three digit integer. (Ex. M001). (This is the member number of the first member in a group of members with similar loading conditions).

UDL Uniformly distributed load (N/mm or KN/m) for the group. (Always positive.)

NTYPE Number of members in the group.

NPL Number of point loads on member.

PLOAD(I) Point load I (N). (Always positive.)

XRP(I) Nondimensional distance of PLOAD(I) from J-end of member.

A.2.9 repeat Step A.2.8 for the left hand 'half' of the bridge

A.3 File ERECT.DAT

There are five basic disassembly operations which CASBA uses in the backward analysis in order to determine the geometric configurations and the internal force distributions of the partial structures encountered in the course of disassembly of a cable-stayed bridge. These are:

- a) Change of interconnection between the girder and the towers.(ICH = 1).
- b) Bracing installation, removal or modifications. (ICH = 2).
- c) Uncoupling of the girder. (ICH = 3).
- d) Cable removal and adjustment. (ICH = 4).
- e) Girder modifications. (ICH = 5).

Each of these operations is communicated to CASBA through a code number, ICH, and a few lines of data as described below. The data required for each category of variation is first given for the right hand 'half' of

the bridge and then repeated in the same order and with the same format for the left hand side.

A.3.1 CHANGE OF INTERCONNECTION BETWEEN GIRDER AND TOWERS

A.3.1.1 Heading (One record)

EXCL, ICH, LTYPE

EXCL Load case number, beginning with the letters LC and ending with a three digit integer which signifies the sequence of disassembly operations. (eg. LC002).

ICH Disassembly operation code. ICH = 1

LTYPE A message of up to 35 characters to be displayed on the screen to signify the type of disassembly operation.

A.3.1.2 Interconnection code for right hand side of bridge (One record)

INST Connection INST = 1
Disconnection INST = 2

A.3.1.3 If connection, (i.e. INST=1)

JNTN, DTF, DTC(2), IDT(2)

JNTN Joint number on the tower where the connection is being installed.

DTF Deck to tower initial force (N) at the time of connection. (Its sign is determined with reference to the global coordinates.)

DTC(2) Spring coefficient of the connection (N/mm).

IDT(2) Direction code IDT(2) = 2 if vertical
IDT(2) = 3 if horizontal

A.3.1.4 If disconnection, (i.e. INST=2)

JNTN, IDT(2)

JNTN Joint number on the tower where the connection is being installed.

IDT(2) Direction code
IDT(2) = 2 if vertical
IDT(2) = 3 if horizontal

A.3.1.5 Repeat Steps A.3.a.ii to A.3.a.iv for the left hand 'half' of the bridge

A.3.2 BRACING (INSTALLATION, REMOVAL OR MODIFICATION)

A.3.2.1 Heading (One record)

Same as A.3.1.1 but ICH = 2

A.3.2.2 Installation record for right hand side of bridge (One record)

IBR
IBR = 0 if installation
IBR = 1 if adjustment
IBR = 2 if elimination

A.3.2.3 If installation: (i.e. IBR=0)

NADBR (One record) Number of new bracing sets.

JNTN, AB, EB, ANB, BRSL(2, J), FBR, TCBRS(2, J) (One record for each new brace)

JNTN Joint number (It must be the K-end node number of the first member of a substructure.)

AB Area of the brace (mm^2).

EB Modulus of elasticity (MPa).

ANB Angle of bracing direction with global X-axis. (See Fig. 5.8).

BRSL(2, J) Length of the brace (mm)

FBR Initial tension (N)

TCBRS(2,J) Tension capacity of the brace

A.3.2.4 If tension adjustment: (i.e. IBR=1)

NBRC (One record) Number of braces being adjusted

JNTN, DELT (One record for each brace affected)

JNTN Joint number for brace being adjusted

DELT Amount of tension adjustment (N)

A.3.2.5 If elimination: (i.e. IBR=2)

NELBR, (JGBR(K), K=1, NELBR) (One record)

NELBR Number of braces to be eliminated

JGBR(K) Nodal number at the connection of brace K with girder

A.3.2.6 Repeat Steps A.3.2.2 to A.3.2.5 for the left hand 'half' of the bridge

A.3.3 UNCOUPLING OF GIRDER

A.3.3.1 Heading (One record)

Same as A.3.1.1 but ICH = 3

A.3.4 CABLE ADJUSTMENT AND REMOVAL

A.3.4.1 Heading (One record)

Same as A.3.1.1 but ICH = 4

A.3.4.2 NCAB Number of cables affected on the right hand 'half' of

the bridge

A.3.4.3 MEMN,CHANGE,ICHAN (One record for each affected cable on the right hand 'half' of the bridge)

MEMN	Global member number of the cable
CHANGE	Amount of change (in mm if change of length, in N if change of tension)
ICHAN	Modification flag.
	Change of length ICHAN =
	0 Change of tension ICHAN = 1
	Elimination ICHAN = 2

A.3.4.4 Repeat Steps A.3.4.2 and A.3.4.3 for the left hand 'half' of the bridge

A.3.5 GIRDER MODIFICATIONS

A.3.5.1 Heading (One record)

Same as A.3.1.1 but ICH = 5

A.3.5.2 Modification flag for the right hand 'half' of the bridge

ICODE	Typically repeated loading	ICODE = 1
	Irregular loading	ICODE = 2
	Cross-section modification	ICODE = 3
	Disassembly of a unit	ICODE = 4

A.3.5.3 If loading is typical, (i.e. ICODE=1)

NGM1,NGM2,UDL,AN1,ND,(PNL(I),XNR(I),ANN(I), I=1,ND)

NGM1 Member number from which loading begins
 NGM2 Member number at which loading ends
 UDL Magnitude of uniformly distributed load (N/mm)
 AN1 UDL angle of orientation with respect to X axis
 ND Number of point loads
 PNL(I) Magnitude of point load # I
 XNR(I) Nondimensional distance of point load I from J-end of member
 ANN(I) Angle of orientation of point load I with respect to X axis

A.3.5.4 If loading is irregular, (i.e. ICODE=2)

J2 Number of members loaded (One record for the right hand 'half' of
 the bridge)

MEMN,UDL,A1,A2,AN1,ND,(PNL(I),XNR(I),ANN(I),I=1,ND) (One record for each
 loaded member of the
 right hand 'half' of
 the bridge)

MEMN Member number
 UDL Magnitude of uniformly distributed load (N/mm)
 A1 Nondimensional distance between member's J-end and beginning of
 loading
 A2 Nondimensional distance from member's K-end and end of loading
 AN1 UDL angle of orientation with respect to X axis
 ND Number of point loads
 PNL(I) Amount of point load I (N)
 XNR(I) Nondimensional distance between point load I and member's J-end.
 ANN(I) Angle of orientation of point load I with respect to X axis

A.3.5.5 If cross-section modification,

J2 Number of members having cross-section modification (One record for the right hand 'half' of the bridge)

MEMN,ANEWI,ANEWA,ANEWE,ECCEN (One record for each affected member of the right hand 'half' of the bridge)

MEMN Member number

ANEWI Modified moment of inertia (mm^4)

ANEWA Modified cross-sectional area (mm^2)

ANEWE Modified modulus of elasticity (MPa)

ECCEN Shift in the centroidal axis due to cross-section modification

A.3.5.6 If disassembly,

LMEMN Last remaining member number

A.3.5.7 Repeat Steps A.3.e.ii and A.3.e.vi for the left hand 'half' of the bridge

A.4 File OUTPUT

The file OUTPUT contains the member-end forces in the member coordinates and the accumulated nodal displacements from the reference configuration in the global coordinates. The signs and directions conform with the general conventions described in Section 4.6. The displacement of each node is given in terms of the X and Y components of the displacement vector for that node.

A.5 File PRINT.PLT

The file PRINT.PLT is the graphics output of the screen displays selected for printer plotting. To print a hard copy of the display, a

translator utility, called JET.EXE, is used with the following parameters.

JET PRINT.PLT <par>

in which par is the printing quality parameter with these options.

- A Presentation quality (with the highest possible resolution)
- E Emphasized quality (with average resolution)
- R Draft quality (low resolution)

A.6 Hardware Requirements

Personal Computer	IBM PS/2 or compatible IBM AT or compatible
Graphics Card	IBM VGA or compatible IBM EGA or compatible Hercules Graphics card or compatible
Hard disk	A hard disk with at least 20 megabytes of free space
Memory	640 KB
Printer	Epson FX, LX, or LQ series or compatible
Optional	Math coprocessor (runs will be about three times faster)

A.7 Software Requirements

Operating System	DOS version 3.0 or higher
Text Editor	Any text editor
Fortran Compiler	Microsoft fortran compiler version 3.6 or higher
GKS Files	GKS version 2.0 or higher (supplied)

Batch files	COMLIGKS.BAT AND COMLICV.BAT (supplied)
Response file	LINKER (supplied)

A.8 System Configuration

AUTOEXEC.BAT Should include the following statements:

PATH C:\MSF

SET TMP=C:\MSF\TMP

SET LIB=C:\MSF\LIB;C:\GKS\LIB

SET GKSDIR=C:\GKS

CONFIG.SYS Should include the following statements:

FILES=20

BUFFERS=20

Directories

The compiler files in directory MSF and its subdirectories LIB, TMP and MOUSE1

The GKS files in directory GKS and its subdirectory LIB

CASBA files (ANALYSE1.FOR, ANALYSE2.FOR, ANALYSE3.FOR, ANALYSE4.FOR, ROOT.FOR, DRAW.FOR) in the current directory.

A.9 Source Code Alterations

If substructure types are altered, all the data statements listed in Table 7.7 must be modified to correspond to the nodal and member information of the new substructure types. (See Chapter 4 for a discription of each of the arays in Table 7.7). Moreover, if the maximum number of nodes in any of the substructure types exceeds 11, all the DIMENSION and COMMON statements containing arrays with 11 (number of nodes) and 33

(number of degrees of freedom) as one of their indices must be altered accordingly. A complete list of these statements appear in the beginning of MAIN program which is in the file ANALYSE1.FOR.

After any source code alteration the program should be recompiled by using COMLIGKS.BAT. For debugging through Microsoft Code View program use COMLICV.BAT.

APPENDIX B : CATENARY EQUATIONS OF A CABLE ELEMENT

B.1 The Inextensible Cable

From Fig. B.1a and by definition,

$$\theta = \tan^{-1} \frac{dy}{dx} \quad [\text{B.1}]$$

$$V = H \tan \theta = H \frac{dy}{dx} \quad [\text{B.2}]$$

From equilibrium of the cable element in Fig. B.1b,

$$\frac{d}{dx}(V)dx + wds = 0 \quad [\text{B.3}]$$

Substituting [B.2] in [B.3],

$$H \frac{d^2y}{dx^2} = -w \frac{ds}{dx} \quad [\text{B.4}]$$

From geometry,

$$ds = dx \sqrt{1 + \left(\frac{dy}{dx}\right)^2} \quad [\text{B.5}]$$

Substituting [B.5] into [B.4],

$$\frac{d^2y}{dx^2} = -\frac{w}{H} \sqrt{1 + \left(\frac{dy}{dx}\right)^2} \quad [\text{B.6}]$$

which is the governing differential equation of equilibrium.

To solve [B.6], let $\frac{dy}{dx} = z$. Then, after some simplifications [B.6]

becomes,

$$\frac{dz}{\sqrt{1+z^2}} = -\frac{w}{H} dx$$

Which after integration becomes,

$$z = \frac{dy}{dx} = -\sinh\left(\frac{wx}{H} - \phi\right) \quad [\text{B.7}]$$

in which ϕ is an integration constant.

Integrating [B.7] again,

$$y = -\frac{H}{w} \cosh\left(\frac{wx}{H} - \phi\right) + \frac{DH}{w} \cosh(-\phi) \quad [\text{B.8}]$$

In [B.8] $\frac{DH}{w} \cosh(-\phi)$ is another integration constant selected in this convenient form for evaluation.

The following sets of boundary conditions can be applied to [B.8] to evaluate the integration constants.

$$\text{i) } \begin{cases} x = 0 \\ y = 0 \end{cases}, \quad 0 = -\frac{H}{w} \cosh(-\phi) + \frac{DH}{w} \cosh(-\phi)$$

Hence $D = 1$ and,

$$y = -\frac{H}{w} \cosh\left(\frac{wx}{H} - \phi\right) + \frac{H}{w} \cosh(-\phi)$$

$$\text{ii) } \begin{cases} x = a \\ y = b \end{cases}, b = -\frac{H}{w} \cosh\left(\frac{wa}{H} - \phi\right) + \frac{H}{w} \cosh(-\phi) \quad [\text{B.9}]$$

Letting,

$$\lambda = \frac{wa}{2H} \quad [\text{B.10}]$$

and solving [B.9] for ϕ ,

$$\phi = \lambda + \sinh^{-1} \left[\frac{\frac{b\lambda}{a}}{\sinh \lambda} \right] \quad [\text{B.11}]$$

and,

$$y = \frac{H}{w} \left[\cosh \phi - \cosh \left(2\lambda \frac{x}{a} - \phi \right) \right] \quad [\text{B.12}]$$

which is the catenary equation of a cable subjected to end forces and its uniformly distributed weight.

The cable length may be computed from,

$$L_0 = \int_0^a \frac{ds}{dx} dx = \int_0^a \sqrt{1 + \left(\frac{dy}{dx}\right)^2} dx \quad [\text{B.13}]$$

Substituting $\frac{dy}{dx}$ from [B.7] into [B.13] and carrying out the integration, yields,

$$L_0 = \frac{2H}{w} \sinh \lambda \cdot \cosh(\lambda - \phi) \quad [\text{B.14}]$$

The vertical component of the internal force T may be computed from [B.2],

$$V = H \frac{dy}{dx} = -H \sinh \left(\frac{wx}{H} - \phi \right) \quad [\text{B.15}]$$

which after substitution of ϕ and $\cosh (\lambda - \phi)$ from [B.11] and [B.14], respectively, becomes,

$$V = H \left[\sinh \left(\lambda - \frac{wx}{H} \right) \frac{wL_0}{2H \sinh \lambda} + \frac{(b/a)\lambda}{\sinh \lambda} \cosh \left(\lambda - \frac{wx}{H} \right) \right] \quad [\text{B.16}]$$

The vertical components of T, V_A and V_B may be computed by substituting $x=0$ and $x=a$, respectively.

$$V_A = \frac{w}{2} (-L_0 + b \coth \lambda) \quad [\text{B.17}]$$

$$V_B = \frac{w}{2} (L_0 + b \coth \lambda) \quad [\text{B.18}]$$

Similarly the cable tension may be calculated from,

$$T = H \frac{ds}{dx} \quad [\text{B.19}]$$

in which,

$$\frac{ds}{dx} = \sqrt{1 + \left(\frac{dy}{dx} \right)^2} = \cosh \left(\frac{wx}{H} - \phi \right) \quad [\text{B.20}]$$

Substituting ϕ from [B.11] into [B.20],

$$T = H \left[\cosh \left(\frac{wx}{H} - \lambda \right) \left(\frac{wL}{2H \sinh \lambda} \right) - \sinh \left(\frac{wx}{H} - \lambda \right) \frac{(b/a)\lambda}{\sinh \lambda} \right]$$

[B.21]

The tangential end forces, T_A and T_B are computed by setting x in [B.21] to 0 and a , respectively, to yield

$$T_A = \frac{w}{2} (L_0 \coth \lambda + b) \quad [B.22]$$

$$T_B = \frac{w}{2} (L_0 \coth \lambda - b) \quad [B.23]$$

B.2 The Elastic Cable

For an elastic cable with the unstressed length of L_0 , the elastic extension may be computed from,

$$\Delta L = \int_0^{L_0} \frac{T}{AE} ds \quad [B.24]$$

Substituting [B.21] into [B.24] yields,

$$\Delta L = \frac{H}{AE} \int_0^a \left(\frac{ds}{dx} \right)^2 dx \quad [B.25]$$

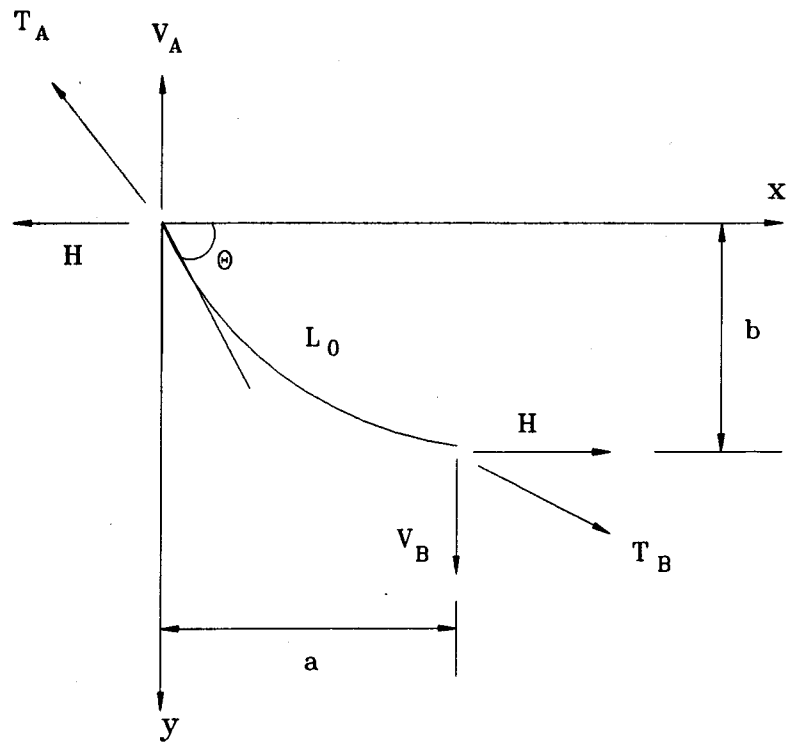
Using [B.20], [B.25] can be rewritten as,

$$\Delta L = \frac{H}{AE} \int_0^a \cosh^2 \left(\frac{wx}{H} - \phi \right) dx \quad [B.26]$$

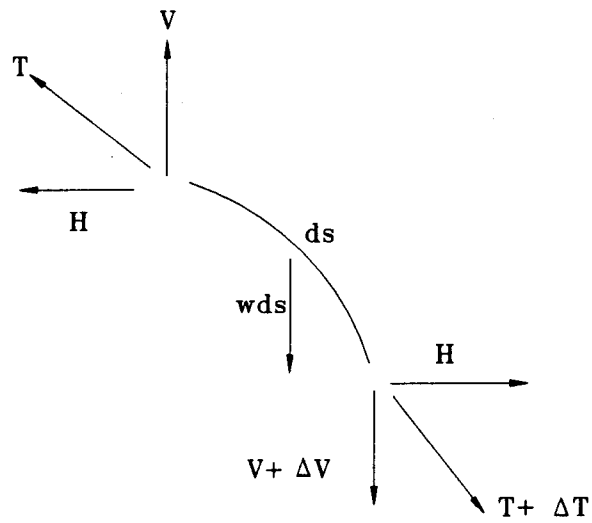
which after simplification and integration becomes,

$$\Delta L = \frac{HL_0^2}{aAE} \left[\lambda \coth \lambda + \frac{1}{2} \left(\frac{a}{L_0} \right)^2 - \frac{1}{2} \left(\frac{a}{L_0} \right)^2 \frac{\sinh 2\lambda}{2\lambda} \right] \quad [B.27]$$

Equations [B.12], [B.14], [B.17], [B.18] and [B.27] have been used in Chapter 3 to develop the catenary algorithms.



(a)



(b)

Fig. B.1 Catenary Cable Element

APPENDIX C: TREATMENT OF CENTROIDAL AXIS VARIATIONS IN CASBA

C.1 Introduction

In the cantilever method of erection of a cable-stayed bridge the girder elements for each module are erected first, then the concrete deck is placed. This substantial cross-sectional variation moves the centroidal axis of the girder elements by a considerable distance. In order to study the consequences of this change of centroidal axis on the force and displacement computations of the bridge, the structure shown in FIG. C.1 has been analysed with the following assumptions.

Model 1: The shift in the centroidal axis is disregarded.

Model 2: The actual shift in the centroidal axis is used in the calculations.

Model 3: The centroidal axis is assumed to be continuous but an external couple equal to the axial force times the vertical offset between the axes is applied to the composite element at the location of the change in cross-section. The results of analysis in terms of forces and displacements are shown in Table C.1.

The actual areas and moments of inertia shown in Fig. C.1 are used for the girder elements in all Models. The results of analysis in terms of forces and displacements are shown in Table C.1.

Note that in Model 2 a vertical beam element is used to simulate the effect of the offset between the centroidal axes of the two different cross-section. If the moment of inertia of this element is large this model will properly reproduce the kinematic constraint at the junction and can

therefore be considered to produce the correct results. Two different moments of inertia have been used for this element in order to determine the sensitivity of the analysis, giving rise to Models 2a and 2b.

A comparison of the results in Table C.1 indicates that:

- a) the results for Model 2 are insensitive to the moment of inertia of the offset beam.
- b) Model 3 produces results very close to those of Model 2 but permits the analysis to be carried out for a continuous centroidal axis.
- c) Model 1 produces results which are significantly in error.

Because of its simplicity Model 3 was selected for implementation in CASBA.

Table C.1

Loading: UDL=136 KN/M												
Node #	Vertical Deflections (mm)											
	2	3	4	5	6	7	8	9	10	11	D	
Model 1	-4.1	-26.2	-54.4	-83.4	-112.6	-142.3	-173.1	-205.1	-238.2	-272.9	-225.5	
Model 2a	-4.1	-26.1	-54.2	-83.1	-111.9	-141.4	-172.4	-205.5	-241.3	-278.5	-223.2	
Model 2b	-4.1	-26.1	-54.2	-83.1	-111.9	-141.4	-172.4	-205.6	-241.3	-278.4	-223.3	
Model 3	-4.1	-26.1	-54.3	-83.1	-111.9	-141.4	-172.2	-205.1	-240.3	-276.9	-223.4	

Member #	Bending Moment (KN.M) @ J-End of Girder Elements											Cable Tension (KN)					
	4	5	6	7	8	9	10	11	21	20	19	18					
Model 1	994.2	928.1	1152.5	1321.1	1388.9	1393.6	1379.3	1377.1	1855.8	1811.2	1767.7	1719.2					
Model 2a	942.4	886.9	1175	1482.1	1767.1	2039.8	1214.2	1376.8	1883.6	1822.5	1771.9	1711.4					
Model 2b	941.6	888.1	1179.4	1492.6	1779.8	2053.9	1218.8	1377.1	1882.8	1823.1	1772.9	1711.8					
Model 3	941.4	878.3	1154.3	1447.2	1722.7	2000.1	1210.1	1377.1	1884.3	1828.2	1767.6	1709.2					

Note: Model 2a uses I=1.5X10**10 and Model 2b uses I=1.5X10**12 for the moment of inertia of the offset beam at the change i

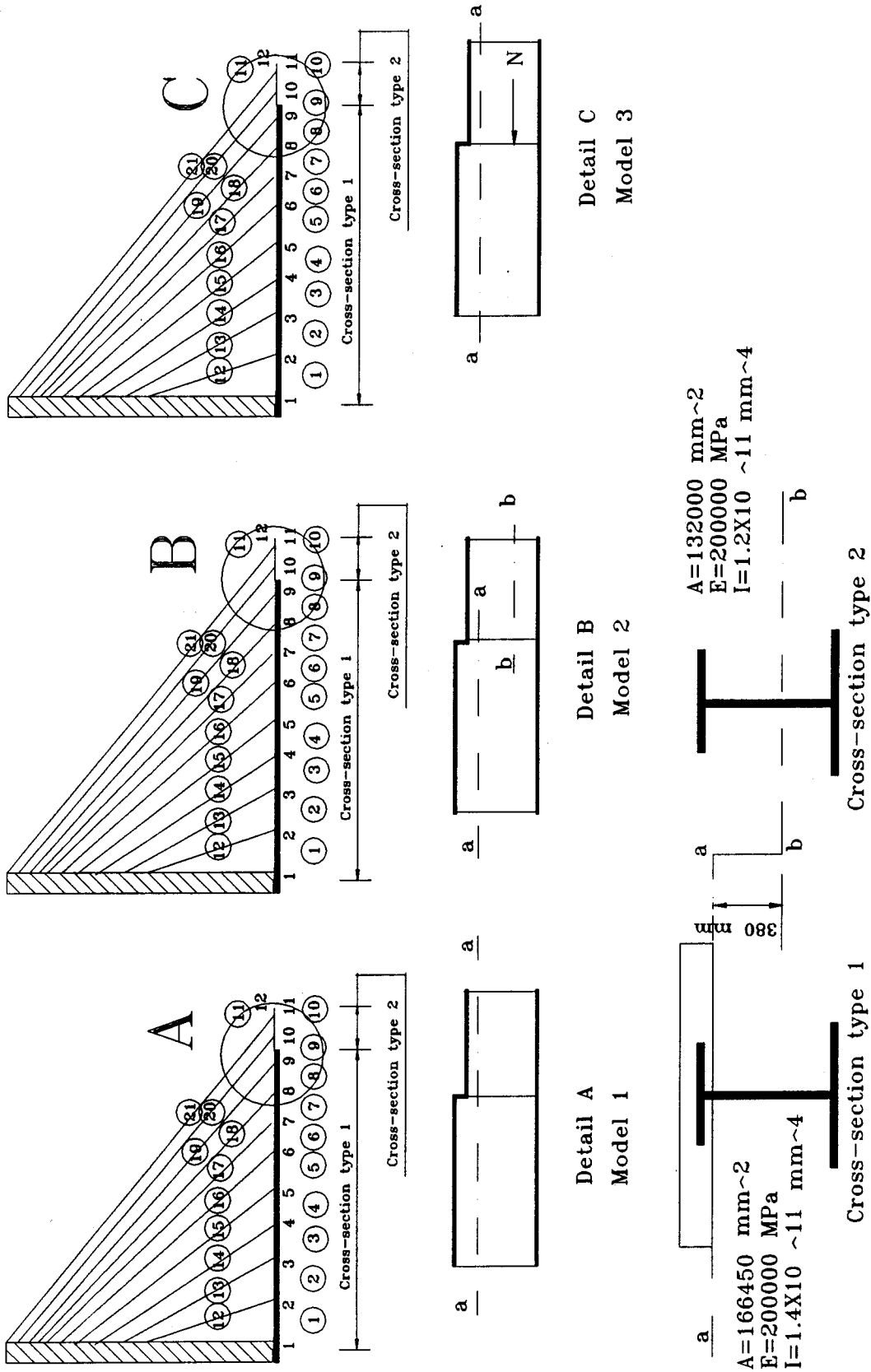


Fig. C.1